

Copyright

by

Jennifer Marie Knipe

2014

**The Dissertation Committee for Jennifer Marie Knipe Certifies that this is the approved
version of the following dissertation:**

**Multi-responsive microencapsulated nanogels for the oral delivery of small
interfering RNA**

Committee:

Nicholas A. Peppas, Supervisor

Donald Paul

Christopher Ellison

Lydia Contreras

Laura Suggs

**Multi-responsive microencapsulated nanogels for the oral delivery of small
interfering RNA**

by

Jennifer Marie Knipe, B.S.Ch.E.

Dissertation

Presented to the Faculty of the Graduate School of

The University of Texas at Austin

in Partial Fulfillment

of the Requirements

for the Degree of

Doctor of Philosophy

The University of Texas at Austin

December 2014

Dedication

This work is dedicated to my parents and sister

Acknowledgements

I thank Dr. Nicholas Peppas for the opportunity to learn from his immense technical and historical expertise in the field of biomaterials. I am extremely grateful for his guidance and instruction towards developing my thesis research as well as my professional career.

I thank my committee members not only for their willingness to serve on my committee, but also their technical knowledge and suggestions.

I thank my colleagues in the Peppas lab; I truly believe that I could not have had a better graduate research experience than I have had in this lab. Thanks to the post-doctoral researchers Dr. Brenda Carrillo-Conde, Dr. Mar Creixell, and Dr. Mary Caldorera-Moore, for their suggestions and help with my experiments. Thank you to the Peppamers who graduated during my tenure at UT, Dr. Margaret Phillips, Dr. David Kryscio, Dr. Cody Schoener, Dr. William Liechty, Dr. Diane Forbes, and Dr. Brandon Slaughter for being inspiring researchers and motivating me to succeed. A tremendous thank you to the Peppamers with whom I end my tenure in the lab: Amey Puranik, Stephanie Steichen, Jonathan Peters, Michael Koetting, Heidi Culver, Lindsey Sharpe, Sarena Horava, and David Spencer. I will always be grateful for the experimental assistance, lab maintenance, scientific intellect, motivation to be in lab by 8 AM, and most of all, the camaraderie of my fellow Peppamers. I also thank two undergraduate researchers who spent a significant amount of time working with me, Tu Pham and Frances Chen.

I thank my family, my parents Ernie and Rosie and my sister Sarah, for their endless encouragement, positive outlook, advice, and thoughtful care packages. Thank you to my roommate and fellow WVU alumnus, Michelle, whom I consider family after

more than four years of cohabitation, friendship, and helping each other navigate graduate school and adulthood in general. I thank my friends both near and far who have listened, advised, laughed, toasted, hypothesized, played flag football, and otherwise kept me going on a daily basis. I could not have accomplished this without each one of you!

Multi-responsive microencapsulated nanogels for the oral delivery of small interfering RNA

Jennifer Marie Knipe, Ph.D.

The University of Texas at Austin, 2014

Supervisor: Nicholas A. Peppas

Multi-responsive, anionic poly(methacrylic acid-co-*N*-vinyl-2-pyrrolidone) microscale hydrogels (microgels) encapsulating polycationic nanoscale hydrogels (nanogels) were synthesized with either degradable or nondegradable crosslinks. The pH-responsive volume phase transition of these formulations was consistent with the pH transition experienced during intestinal delivery, as the hydrogels swelled at pH values greater than pH 5.

The physicochemical characteristics of the nondegradable formulations were evaluated by microscopy, potentiometric titration, Fourier transform infrared spectroscopy, and thermal gravimetric analysis. The nondegradable formulations successfully loaded and released a model protein in physiological buffers, but the ability of the microgels to release the nanogels upon exposure to intestinal conditions was inadequate.

Therefore, microgels containing enzyme-degradable oligopeptide crosslinks were synthesized then characterized using Fourier transform infrared spectroscopy, electron microscopy, confocal microscopy, and ImageStream flow cytometry. Degradation of the microgels upon incubation in trypsin solutions, simulated gastric fluid, or simulated intestinal fluid was evaluated by measuring the change in relative turbidity over time.

Microgels were degraded specifically by the enzyme trypsin, and the rate of degradation was dependent upon the microgel to trypsin concentration ratio; for all ratios tested, degradation was complete within 4 hours.

The cytocompatibility of the enzyme-degraded microgels encapsulating nanogels was evaluated in both a human and a murine cell line; at microgel concentrations less than 0.4 mg/ml the cell viability was greater than 90%. Confocal microscopy was used to obtain Z-stack images of the cells following incubation with the microgels, confirming that nanogels were released from the degraded microgels and subsequently internalized by RAW 264.7 murine macrophage cells.

The microencapsulated nanogels were able to load siRNA via electrostatic complexation with loading efficiencies ranging from 60-80%. Incubation of loaded microgels in simulated intestinal fluid with reduced trypsin concentrations or in rat intestinal fluid resulted in successful degradation of the microgel matrix and release of a detectable amount of viable siRNA. The degraded microgels with nanogels transfected the two different cell lines with up to 20% silencing efficiency. Though the knockdown efficiency is not as high as that of nanogels alone, the microgel results are consistent and reproducible across two cell lines.

Table of Contents

List of Tables	xiv
List of Figures.....	xv
List of Illustrations.....	xxii
Chapter 1: Introduction	1
Chapter 2: Oral Delivery of Protein and Gene Therapeutics.....	6
2. 1 PHYSIOLOGICAL CONSIDERATIONS	6
2.2 HYDROGELS FOR ORAL DRUG DELIVERY	8
2.2.1 pH-Responsive Hydrogels	9
2.2.2 Biodegradable Hydrogels	12
2.2.3 Multi-responsive Hydrogels	15
REFERENCES.....	23
Chapter 3: RNA Background	33
3. 1 RNA Interference.....	33
3.1.1 Mechanism.....	33
3.1.2 Therapeutic Potential	34
3.2 Delivery of siRNA	38
3.2.1 Challenges to Delivery of siRNA	38
3.2.2 Cationic Polymer Systems.....	40
3.2.3 Theranostic Systems	43
3.2.4 Oral Delivery Systems	50
3.3 Conclusions.....	55
References	64
Chapter 4: Research Objectives	77
REFERENCES.....	81
Chapter 5: Non-degradable Crosslinked Microgels Encapsulating Polycationic Nanogels	82
5.1 INTRODUCTION	82

5.2 EXPERIMENTAL METHODS	83
5.2.1 Chemicals	83
5.2.2 Synthesis of P(MAA-co-NVP) Hydrogels	84
5.2.3 Characterization	85
5.2.3.1 Scanning Electron Microscopy	85
5.2.3.2 Fluorescent Microscopy	85
5.2.3.3 Fourier Transform Infrared Spectroscopy	85
5.2.3.4 Thermogravimetric Analysis	85
5.2.3.5 Swelling Studies	86
5.2.3.6 Potentiometric Titration	86
5.2.3.7 Cytotoxicity Study	87
5.2.3.8 Loading and Release Studies	87
5.3 RESULTS AND DISCUSSION	88
5.3.1 Microgel Morphology	88
5.3.2 FT-IR Spectroscopic Analysis	89
5.3.3 TGA Analysis	90
5.3.4 Swelling Studies	90
5.3.5 Potentiometric Titration	92
5.3.6 Cytotoxicity	93
5.3.7 Loading and Release of Model Therapeutic	94
5.4 CONCLUSIONS	96
5.5 TABLES	98
5.6 FIGURES	101
REFERENCES	109
Chapter 6: Multi-responsive and biodegradable crosslinked microgels	114
6.1 INTRODUCTION	114
6.2 EXPERIMENTAL METHODS	115
6.2.1 Chemicals	115
6.2.2 Synthesis and Purification	116
6.2.2.1 Synthesis of Linear Polymer	116

6.2.2.2 <i>Synthesis of Peptide Crosslinked Gels</i>	116
6.2.3 Characterization	117
6.2.3.1 <i>Potentiometric Titration</i>	117
6.2.3.2 <i>Fluorescamine Assay</i>	117
6.2.3.3 <i>Fourier Transform Infrared Spectroscopy</i>	118
6.2.3.4 <i>Scanning Electron Microscopy</i>	118
6.2.3.5 <i>Degradation Study</i>	118
6.2.3.7 <i>In vitro Cytotoxicity Study</i>	120
5.2.3.8 <i>Loading and Release Studies</i>	121
6.3 RESULTS AND DISCUSSION	121
6.3.1 Fluorescamine Assay	123
6.3.2 FTIR Spectroscopy	124
6.3.3 Degradation	125
6.3.4 Cytotoxicity	132
6.3.5 Loading and Release	132
6.4 CONCLUSIONS	134
6.5 TABLES	136
6.6 FIGURES	138
REFERENCES	152
Chapter 7: Biodegradable Microencapsulated Nanogels for Orally Delivered siRNA	156
7.1 INTRODUCTION	156
7.2 EXPERIMENTAL METHODS	158
7.2.1 Chemicals	158
7.2.2 Synthesis and Purification	158
7.2.2.1 <i>Synthesis of Linear Polymer</i>	158
7.2.2.2 <i>Synthesis of Peptide Crosslinked Gels</i>	159
7.2.3 Cell Culture	160
7.2.4 <i>In vitro Cytotoxicity Study</i>	160
7.2.5 siRNA Loading	161

7.2.6 Microgel Degradation and siRNA Stability.....	162
7.2.6.1 Microgel Degradation	162
7.2.6.2 Evaluation of siRNA Stability by Polyacrylamide Gel electrophoresis.....	163
7.2.7 Confocal Microscopy	164
7.2.8 ImageStream Flow Cytometry.....	166
7.2.9 Cell Transfection	166
7.3 RESULTS AND DISCUSSION	167
7.3.1 Incorporation of Polycationic Nanogels.....	168
7.3.2 Degradation of Microgels with Nanogels.....	169
7.3.3 Cytotoxicity of Degraded Microgels with Nanogels.....	173
7.3.4 siRNA Loading	176
7.3.5 Microgel Degradation and siRNA Stability.....	177
7.3.6 Confocal Microscopy to Verify InteRNAIization.....	180
7.3.7 Transfection of Murine Macrophage and Human Adenocarcinoma Cells	182
7.4 CONCLUSIONS	184
7.5 FIGURES	186
REFERENCES.....	209
Chapter 8: Conclusions and Recommendations for Future Research.....	212
8.1 CONCLUSIONS	212
8.2 RECOMMENDATIONS FOR FUTURE RESEARCH	216
REFERENCES.....	218
Appendix A: Emulsion Polymerization of Poly(methacrylic acid-co-N-vinyl-2- pyrrolidone) Particles	219
A.1 INTRODUCTION	219
A.2 EXPERIMENTAL METHODS.....	220
A.2.1 Chemicals.....	220
A.2.2 Emulsion Polymerization	220
A.2.3 Emulsion Characterization	221
A.3 RESULTS AND DISCUSSION	222

A.4 CONCLUSIONS	224
A.5 TABLES	225
A.5 FIGURES	226
REFERENCES.....	238
Appendix B: Abbreviations.....	239
C.1 PUBLICATIONS	242
C.2 PRESENTATIONS.....	242
C.3 COURSEWORK.....	244
References	245
Vita	274

List of Tables

Table 3.1:	Summary of inorganic theranostic particles used in gene therapy. ..59
Table 5.1:	P(MAA-co-NVP) hydrogel formulations with and without nanogels, with TEGDMA or PEGDMA crosslinking agents.98
Table 5.2:	Molar ratios of MAA and NVP in P(MAA-co-NVP) microgels determined by FTIR and potentiometric titration.99
Table 5.3:	Equilibrium weight swelling ratios and calculated swollen mesh size of P(MAA-co-NVP) 10 mm disks..100
Table 6.1:	Crosslinking reaction formulations and outcomes.....136
Table 6.2:	Linear parameters of the activity assay of 0.6 mg/ml trypsin incubated with various concentrations of P(MAA-co-NVP) microgels containing degradable crosslinks for 90 minutes.....137
Table A1:	Parameters varied to determine effect on emulsion stability225

List of Figures

Figure 2.1: Anatomy of the gastrointestinal tract.	21
Figure 2.2: The chemical structure of dextran, showing glucose subunits linked by α -1,6 glucosidic linkages.	22
Figure 3.1: Mechanism of RNAi with siRNA..	56
Figure 3.2: Barriers and challenges to the oral delivery of siRNA.....	57
Figure 3.3: Schematic of cellular uptake of siRNA delivery carrier, followed by endosomal escape and RNAi.	58
Figure 4.1: Schematic of the two-part microencapsulated-nanogel system for the oral delivery of siRNA to the intestine and to the cell cytosol.	79
Figure 4.2: Structures of monomers used in the anionic hydrogel synthesis.	80
Figure 5.1: Representative SEM micrographs of crushed P(MAA-co-NVP) microgels.....	101
Figure 5.2: Brightfield and fluorescent microscopy images of crushed P(MAA-co-NVP) microgels with PEGDMA crosslinks	102
Figure 5.3: FT-IR spectra of crosslinked P(MAA-co-NVP) copolymers with encapsulated nanogels at varying weight percentages (0-5 wt%) pressed in a KBr disk	103
Figure 5.4: TGA curves of P(MAA-co-NVP) copolymers with TEGDMA or PEGDMA crosslinks and 0-5 wt% encapsulated nanogels.	104
Figure 5.5: Weight swelling ratio of crosslinked P(MAA-co-NVP) hydrogel disks in response to dynamic change in buffer pH.....	105
Figure 5.6: Evaluation of cell viability after microgel exposure using an MTS cell proliferation assay	106

Figure 5.7: Loading efficiencies of P(MAA-co-NVP) microgels with PEGDMA crosslinker and 0 wt% or 5 wt% nanogels	107
Figure 5.8: Release of model therapeutics from P(MAA-co-NVP) microgels with PEGDMA crosslinker in pH 7.4 PBS buffer at 37°C over two hours.	108
Figure 6.1: Visual indication of hydrogel degradation in SIF, SGF, or PBS over a 4 hour incubation period.	139
Figure 6.2: P(MAA-co-NVP) microgels with peptide crosslinks in the dry state, crushed and sieved to <30 μ m..	140
Figure 6.3: FT-IR spectra of uncrosslinked P(MAA-co-NVP) lyophilized at pH 4 or pH 8 and peptide crosslinked P(MAA-co-NVP) at neutral pH.	141
Figure 6.4: FT-IR spectra of GRRRGK peptide, uncrosslinked P(MAA-co-NVP) lyophilized at pH 8, and peptide crosslinked P(MAA-co-NVP) at neutral.	142
Figure 6.5: FT-IR spectra of peptide crosslinked P(MAA-co-NVP) at neutral pH and peptide crosslinked P(MAA-co-NVP) degradation products following incubation with SGF, SIF, SIF without pancreatin, or a trypsin solution.....	143
Figure 6.6: SEM micrographs of microgels after 90 minutes incubation in SGF, SIF, and PBS.....	144
Figure 6.7: Relative turbidity over time of 2 mg/ml solutions of P(MAA-co-NVP) microgels with degradable crosslinks incubated in trypsin solutions ranging from 0-0.6 mg/ml trypsin in PBS.	145

Figure 6.8: Relative turbidity over time of 2 mg/ml solutions of P(MAA-co-NVP) microgels with degradable crosslinks incubated in PBS, 0.3 mg/ml trypsin in PBS, 0.6 mg/ml trypsin in PBS, rat gastric fluid, or rat intestinal fluid.	146
Figure 6.9: Activity assay of 0.6 mg/ml trypsin incubated with various concentrations of P(MAA-co-NVP) microgels containing degradable crosslinks for 90 minutes, and then deactivated with 0, 80, or 160 μ l DMEM.	147
Figure 6.10: Activity assay of various trypsin concentrations incubated without microgels, with 2 mg/ml P(MAA-co-NVP) microgels containing degradable crosslinks for 90 minutes, and after deactivation at 70°C for 5 minutes.	148
Figure 6.11: Activity assay of 0.6 mg/ml trypsin incubated with various concentrations of P(MAA-co-NVP) microgels containing degradable crosslinks for 90 minutes, and then deactivated with heat.....	149
Figure 6.12: Evaluation of degraded microgel exposure effect on cell metabolism using an MTS cell proliferation assay..	150
Figure 6.13: Loading efficiencies of degradable P(MAA-co-NVP) microgels with peptide crosslinker..	151
Figure 7.1: Image of P(MAA-co-NVP) microgel crosslinked by degradable peptide and encapsulating polycationic nanogels taken by confocal laser scanning microscopy.....	186
Figure 7.2: Orthogonal view of Z-stack image of P(MAA-co-NVP) microgel crosslinked by degradable peptide and encapsulating polycationic nanogels taken by confocal laser scanning microscopy.	187

Figure 7.3: Relative turbidity over time of various concentrations of P(MAA-co-NVP) microgels with degradable crosslinks encapsulating nanogels during incubation in 0.6 and 1.2 mg/ml trypsin in PBS.....	188
Figure 7.4: Relative turbidity over the first 20 minutes of incubation of trypsin with various concentrations of P(MAA-co-NVP) microgels with degradable crosslinks encapsulating nanogels.	189
Figure 7.5: The microgel:trypsin weight ratio versus initial rate of turbidity decrease was correlated with a linear fit.....	190
Figure 7.6: BAEE activity assay of 1.2 mg/ml trypsin and 0.6 mg/ml trypsin incubated with various concentrations of P(MAA-co-NVP) microgels containing degradable crosslinks for 90 minutes.....	191
Figure 7.7: Representative images obtained via ImageStream analysis of microgels encapsulating fluorescent nanogels incubated for 90 minutes in 1.2 mg/ml trypsin, 0.6 mg/ml trypsin, or pH 7.4 PBS.	192
Figure 7.8: Histogram plots of particle size as obtained by ImageStream analysis of microgels encapsulating fluorescent nanogels incubated for 90 minutes in 1.2 mg/ml trypsin, 0.6 mg/ml trypsin, or pH 7.4 PBS.	193
Figure 7.9: Representative images obtained via ImageStream analysis of microgels encapsulating fluorescent nanogels incubated for ~0 minutes in SGF, SIF, or 0.6 mg/ml trypsin.....	194
Figure 7.10: Histogram plots of particle size obtained by ImageStream analysis of microgels encapsulating fluorescent nanogels incubated for ~0 minutes in SGF, SIF, or 0.6 mg/ml trypsin.	195

Figure 7.11: Representative images obtained via ImageStream analysis of microgels encapsulating fluorescent nanogels incubated for 120 minutes in SGF, SIF, or 0.6 mg/ml trypsin.....	196
Figure 7.12: Histogram plots of particle size obtained by ImageStream analysis of microgels encapsulating fluorescent nanogels incubated for 120 minutes in SGF, SIF, or 0.6 mg/ml trypsin.	197
Figure 7.13: Median particle size values obtained by ImageStream analysis of microgels encapsulating fluorescent nanogels at various time points during the 120 minute degradation period.	198
Figure 7.14: Evaluation of degraded microgel and trypsin exposure effect on cell metabolism using a MTS cell proliferation assay and.LDH membrane integrity assay..	199
Figure 7.15: Evaluation of degraded microgel and trypsin exposure effect on cell metabolism using a MTS cell proliferation assay.....	200
Figure 7.16: Evaluation of degraded microgel and trypsin exposure effect on cell metabolism using a LDH membrane integrity assay..	201
Figure 7.17: Representative siRNA loading efficiencies of degradable P(MAA-co-NVP) microgels with peptide crosslinker and encapsulated polycationic nanogels..	202
Figure 7.18: PAGE evaluation of siRNA degradation after siRNA-loaded microgels were incubated in various solutions and buffers.....	203
Figure 7.19: PAGE evaluation of siRNA degradation after incubation in various solutions and buffers.....	204

Figure 7.20: Confocal laser scanning microscopy fluorescent and bright field images of RAW 264.7 cells incubated with nanogels and degraded microgels containing nanogels.	205
Figure 7.21: Confocal laser scanning microscopy fluorescent Z-stack orthogonal images of RAW 264.7 cells incubated with nanogels and degraded microgels containing nanogels.....	206
Figure 7.22: Confocal laser scanning microscopy fluorescent and bright field images of RAW 264.7 cells incubated with degraded microgels and nanogels	207
Figure 7.23: Gene knockdown by degraded and undegraded microgels containing nanogels, nanogels, commercially available Lipofectamine 2000, or naked siRNA.....	208
Figure A.1: Representative images of emulsions over time.....	226
Figure A.2: Absorbance spectra of emulsions over time	227
Figure A.3: TeRNAr phase plot of emulsions with 2 wt% Span 80/Tween 20 co-surfactant system.....	228
Figure A.4: Absorbance spectra of emulsions with 2 wt% Span 80/Tween 20 co-surfactant system.....	229
Figure A.5: TeRNAr phase plot of emulsions with 3 wt% Span 80/Tween 20 co-surfactant system.....	230
Figure A.6: Absorbance spectra of emulsions with 3 wt% Span 80/Tween 20 co-surfactant system.....	231
Figure A.7: TeRNAr phase plot of emulsions with 2 wt% Span 80/Tween 80 co-surfactant system.....	232

Figure A.8: Absorbance spectra of emulsions with 2 wt% Span 80/Tween 80 co-surfactant system.....	233
Figure A.9: TeRNAr phase plot of emulsions with 3 wt% Span 80/Tween 80 co-surfactant system.....	234
Figure A.10: Absorbance spectra of emulsions with 2 wt% Span 80/Tween 80 co-surfactant system.....	235
Figure A.11: SEM micrographs of particles from an unstable emulsion with low DN and a stable emulsion with high DN.....	236
Figure A.12: Z-average size and zeta potential measurements made using DLS of P(MAA-co-NVP) particles synthesized via a stable emulsion polymerization.	237

List of Illustrations

Scheme 6.1:	Peptide crosslinking reaction scheme..	138
-------------	--	-----

Chapter 1: Introduction

Gene therapy or the modification of gene expression to treat acquired or inherited disease, has potential to treat or cure a diverse array of chronic illnesses such as age-related macular degeneration, cardiovascular disease, and various cancers [1-3]. Since the seminal publication identifying gene silencing via RNA interference by Fire and Mello in 1998 [4], the ability of synthetic, small interfering RNAs (siRNA) to induce gene silencing in a therapeutic capacity has been well-documented. However, a marketable siRNA-based therapeutic has yet to be fully realized due to the challenges associated with delivery of this delicate molecule, including susceptibility to degradation and the necessity of cellular uptake for therapeutic efficacy.

Oral administration of such a therapeutic could overcome certain delivery challenges while being conducive to treating diseases of the gastrointestinal (GI) tract. Among the GI diseases that stand to benefit from an oral delivery formulation of siRNA for gene knockdown are inflammatory bowel disease (IBD) and celiac disease (CD). Both IBD [5] and CD [6, 7] are thought to stem from aberrant gene expression ultimately resulting in high levels of inflammatory cytokines and destruction of the intestinal epithelium.

One of the current IBD treatments on the market is an antibody that targets the inflammatory cytokine tumor necrosis factor- α (TNF- α), which is secreted in high levels by macrophage and dendritic cells in patients with IBD [5]. In a similar strategy, anti-TNF- α siRNA may be used to silence production of TNF- α and treat patients suffering from IBD [8-12] or CD. In this application, oral administration of the siRNA therapy would not only offer convenient administration for the patient, but local delivery to the

intestine may result higher efficacy compared to a systemic delivery route and also limit off-target effects.

The challenges associated with oral delivery of siRNA are not to be taken lightly. They include maintaining the stability of siRNA throughout the harsh pH and proteolytic environments in the GI tract [13], achieving intracellular delivery [14], and avoiding lysosomal degradation within the cell [15].

Many pH-responsive hydrogel nanoparticles have been thoughtfully designed as siRNA delivery vehicles to overcome some or all of these challenges. For example, the composition and architecture of poly[2-(diethylamino) ethyl methacrylate] (PDEAEMA) nanogels has been tuned to arrive at a formulation with desired pH response, excellent siRNA binding, acceptable cell uptake, and measurable gene silencing effect [16-20]. However, polycationic polymers such as these are charged and unstable in the low pH of the stomach, rendering them unsuitable for oral delivery applications.

Thus, researchers have turned toward two-component systems consisting of microparticles encapsulating nanoparticles to achieve oral delivery of siRNA [9, 10, 12, 21, 22]. Typically, the encapsulating material is designed to withstand the harsh environment of the upper GI tract while retaining the ability to release the nanoparticles for cellular uptake upon entry into the small intestine. The nanoparticles, in turn, are usually designed to facilitate complexation with siRNA, cellular uptake, and endosomal escape. In this manner it may be possible to develop a siRNA therapeutic delivery system that can overcome the oral delivery barriers and benefit patients suffering from incurable diseases of the GI tract.

REFERENCES

- [1] Atkinson, H. and Chalmers, R., *Delivering the goods: Viral and non-viral gene therapy systems and the inherent limits on cargo DNA and interNAL sequences*. Genetica, 2010. **138**(5): p. 485-498.
- [2] Robbins, P.D. and Ghivizzani, S.C., *Viral vectors for gene therapy*. Pharmacol. Ther., 1998. **80**: p. 35-47.
- [3] Forbes, D.C. and Peppas, N.A., *Oral delivery of small RNA and DNA*. J. Controlled Release, 2012. **162**(2): p. 438-445.
- [4] Fire, A., Xu, S.Q., Montgomery, M.K., Kostas, S.A., Driver, S.E., and Mello, C.C., *Potent and specific genetic interference by double-stranded RNA in caenorhabditis elegans*. Letters to Nature, 1998. **391**: p. 806-811.
- [5] Abraham, C. and Cho, J.H., *Inflammatory bowel disease*. N Engl J Med, 2009. **361**: p. 2066-2078.
- [6] Vader, W., *The hla-dq2 gene dose effect in celiac disease is directly related to the magnitude and breadth of gluten-specific t cell responses*. P Natl Acad Sci USA, 2003. **100**(21): p. 12390-12395.
- [7] Schuppan, D., *Current concepts of celiac disease pathogenesis*. Gastroenterology, 2000. **119**(1): p. 234-242.
- [8] Aouadi, M., Tesz, G.J., Nicoloro, S.M., Wang, M., Chouinard, M., Soto, E., Ostroff, G.R., and Czech, M.P., *Orally delivered siRNA targeting macrophage map4k4 suppresses systemic inflammation*. Nature, 2009. **458**(7242): p. 1180-1184.
- [9] Kriegel, C. and Amiji, M., *Oral TNF- α gene silencing using a polymeric microsphere-based delivery system for the treatment of inflammatory bowel disease*. J Controlled Release, 2011. **150**(1): p. 77-86.
- [10] Kriegel, C. and Amiji, M.M., *Dual TNF- α /cyclin d1 gene silencing with an oral polymeric microparticle system as a novel strategy for the treatment of inflammatory bowel disease*. Clin Trans Gastroenterol, 2011. **2**(3): p. e2.

- [11] Wilson, D.S., Dalmaso, G., Wang, L., Sitaraman, S.V., Merlin, D., and Murthy, N., *Orally delivered thioketal nanoparticles loaded with TNF- α -siRNA target inflammation and inhibit gene expression in the intestines*. Nat Mater, 2010. **9**: p. 923-928.
- [12] Laroui, H., Theiss, A.L., Yan, Y., Dalmaso, G., Nguyen, H.T.T., Sitaraman, S.V., and Merlin, D., *Functional TNF- α gene silencing mediated by polyethyleneimine/TNF- α siRNA nanocomplexes in inflamed colon*. Biomaterials, 2011. **32**(4): p. 1218-1228.
- [13] Bouchie, A., *Companies in footrace to deliver RNAi*. Nat Biotechnol, 2012. **30**(12): p. 1154-1157.
- [14] Whitehead, K.A., Langer, R., and Anderson, D.G., *Knocking down barriers: Advances in siRNA delivery*. Nat. Rev. Drug Discovery, 2009. **8**(2): p. 129-138.
- [15] Schiffelers, R.M., Woodle, M.C., and Scaria, P., *Pharmaceutical prospects for RNA interference*. Pharm Res, 2003. **21**: p. 1-7.
- [16] Forbes, D.C. and Peppas, N.A., *Polycationic nanoparticles for siRNA delivery: Comparing ARGET ATRP and UV-initiated formulations*. ACS Nano, 2014. **8**: p. 2908-2917.
- [17] Forbes, D.C. and Peppas, N.A., *Polymeric nanocarriers for siRNA delivery to murine macrophages*. Macromol Biosci, 2014. **14**(8): p. 1096-1105.
- [18] Liechty, W.B., Scheuerle, R.L., and Peppas, N.A., *Tunable, responsive nanogels containing t-butyl methacrylate and 2-(t-butylamino)ethyl methacrylate*. Polym, 2013. **54**(15): p. 3784-3795.
- [19] Fisher, O.Z. and Peppas, N.A., *Polybasic nanomatrices prepared by UV-initiated photopolymerization*. Macromolecules, 2009. **42**(9): p. 3391-3398.
- [20] Fisher, O.Z., Kim, T., Dietz, S.R., and Peppas, N.A., *Enhanced core hydrophobicity, functionalization and cell penetration of polybasic nanomatrices*. Pharm Res, 2009. **26**(1): p. 51-60.

- [21] Bhavsar, M.D. and Amiji, M.M., *Development of novel biodegradable polymeric nanoparticles-in-microsphere formulation for local plasmid DNA delivery in the gastrointestinal tract*. AAPS PharmSciTech, 2008. **9**(1): p. 288-294.
- [22] Bhavsar, M.D., Tiwari, S.B., and Amiji, M.M., *Formulation optimization for the nanoparticles-in-microsphere hybrid oral delivery system using factorial design*. J Controlled Release, 2006. **110**(2): p. 422-430.

Chapter 2: Oral Delivery of Protein and Gene Therapeutics

2.1 PHYSIOLOGICAL CONSIDERATIONS

Delicate therapeutics such as proteins, antibodies, and RNAs administered orally encounter harsh environments and delivery challenges along the oral delivery pathway [1], shown in Figure 2.1. When a therapeutic in an oral dosage form is ingested it first encounters the saliva within the mouth, which contains some enzymes but does not play a major role in digestion. Similarly, the primary function of the esophagus is transport from the mouth and buccal regions to the stomach rather than digestion [2].

Next, the therapeutic enters the gastrointestinal tract, which is comprised of the stomach, small intestine, and large intestine. Main functions of the stomach include storage and grinding of food into small particulates for release into the small intestine. The stomach is coated with a viscous layer of mucus to prevent harm from the variety of digestive enzymes, including pepsin and gastrin, and very low pH of the gastric fluid. The pH of the stomach has been measured between 1.4-2.1, and is generally accepted as 2.0 in a state of fasting [3]. The pH is largely dependent upon food consumption; it is quite low when the stomach is empty (pH 1-2) but can rise as high as 4-6 following a meal [4, 5]. The length of time spent in the stomach varies depending on type of food consumed, size of the food particles, and various other physiological conditions, but it can range from a few minutes to a couple hours [5]. In the fasting state, however, the entire emptying pattern, or migrating myoelectric complex (MMC), of the stomach into the small intestine is completed in about 2 hours [6].

From the stomach, the therapeutic enters the small intestine, which is divided into the duodenum, jejunum, and ileum. The small intestine is lined with villi that provide

access to blood and lymphatic vessels as well as increase surface area for absorption [7]. The epithelium of the small intestine is lined with four main cell types, including goblet cells that secrete mucus and enterocytes that are responsible for absorption [7, 8]. The mucus layer serves to trap and remove pathogens while lubricating the epithelium [9], and can be a significant barrier to penetration by therapeutics as the rate of turnover is constant [10], with shedding and clearance on the order of a few hours in rats [11]. Enterocytes are covered with a barrier of microvilli and negatively charged glycoprotein, known as the brush border, which is home to many digestive enzymes that can impede the delivery of delicate therapeutics [12, 13]. Additionally, the concentration of microflora increases from the proximal to distal intestine, as the pH increases from acidic to more neutral [14, 15]. These microflora produce a number of enzymes that pose a threat to delicate therapeutics such as proteins or RNAs. Transit time within the small intestine is approximately 3-4 hours, and is not greatly affected by variables such as particle size, density, or type of food consumed [16]. Supposing the therapeutic can withstand enzymatic degradation, delivery to the small intestine is convenient for adsorption and systemic delivery via the bloodstream.

Within the small intestine, the bacterial concentration increases sharply and remains high throughout the colon [14]. The pH throughout the colon ranges from 6-7.5, increasing from proximal to distal colon [15]. The ascending colon is characterized by antiperistalsis, which serves to retain and mix contents for 10-12 hours [17, 18]. Thus, the proximal colon provides a large window for therapeutic delivery making it a potential target site, though it is not as well-suited to absorption as the small intestine. The second portion is the transverse colon, where the content is divided by annular contractions and

moves slowly as water is reabsorbed, potentially trapping the therapeutic within viscous fecal content, making this region unsuitable for drug delivery [17]. Finally, the therapeutic enters the descending colon, which controls excretion of feces. The total retention time in the colon can be anywhere from 24-60 hours [17, 18]. Like the small intestine, epithelial cells of the large intestine produce a mucin layer that has a turnover rate of 16-24 hours to facilitate clearance of feces, but this also presents an additional delivery barrier [19].

2.2 HYDROGELS FOR ORAL DRUG DELIVERY

Hydrogels are three-dimensional, hydrophilic polymer networks with the ability to absorb large amounts of water or biological fluid. Hydrogels may be further stabilized by chemical or physical crosslinks, which render them insoluble and “permanent” [20, 21]. These crosslinked hydrogels are still able to swell with adsorption of water, which contributes to their high biocompatibility [20]. Thus, hydrogels have been used in biological applications such as tissue engineering, drug delivery, and diagnostic devices, among others [22].

In recent years, we have seen steady expansion of research utilizing “intelligent” or stimuli-responsive hydrogels, particularly in the fields of drug delivery and tissue engineering [23-27]. Stimuli-responsive hydrogels are crosslinked, hydrophilic polymer networks that undergo a physicochemical transition in response to a change in external stimuli such as pH, temperature, light, and analyte concentration, to name a few [27-29]. The response to stimuli may be a change in surface charge or hydrophobicity, change in phase volume of the gel, breaking of bonds resulting in degradation or gel-sol transition, or a combination of these [28, 30]. Gil and Hudson [31] reviewed an extensive list of

stimuli-responsive polymers, as well as bioconjugates made with the polymers, including the design criteria taken into consideration to achieve desired responses useful for biomedical applications.

For the purposes of oral drug delivery applications, pH responsive hydrogels such as acrylic acids have been of particular interest due to their ionization across a pH regime corresponding to that of the gastrointestinal tract. Also gaining momentum in the field is the use of multi-responsive hydrogels that respond to two or more environmental stimuli for increased specificity and control of drug release.

2.2.1 pH-Responsive Hydrogels

Stimuli-responsive hydrogels undergo physical or chemical changes in response to environmental triggers, such as variation in temperature or pH [32]. Hydrogels that contain acidic or basic pendant groups which can be ionized depending on the pH of surrounding solution are known as ionic hydrogels [33]. Poly(methacrylic acid) (PMAA), an anionic polymer, and poly(diethylaminoethyl methacrylate) (PDEAEMA), a cationic polymer, are among the most commonly studied ionic polymers [22]. Additionally, if the network contains two polymers that can form hydrogen bonds, such as carboxylic acid groups of MAA and ether groups of poly(ethylene glycol) (PEG), the hydrogel is known as a complexation hydrogel [34].

These stimuli-responsive hydrogels can be used as coatings or carriers. Enteric coatings can be made of pH-responsive hydrogels, usually acrylic- or cellulose-based, and are applied to prevent dissolution of the tablet, capsule, or particle until it reaches the small intestine [33]. The coating is typically applied by depositing a layer of linear polymer in aqueous solution then allowing the deposited layer to dry, forming a water-

soluble film coating [35, 36]. Dissolution of the coating is a function of pH; the polymers begin to swell and dissolve following gastric emptying into the upper small intestine, where the pH rises above 5 [37]. Eudragit® is one of the most common enteric coatings. The different formulations of Eudragit® are comprised of varying combinations methacrylic acid copolymers, resulting in formulation-dependent pH response ranging from 5.5-7.0 [38].

However, the pH range of the small intestine is similar to that of the colon, approximately 6-7.5 [15, 39], and varies among patients as well as between disease states, making delivery based on pH-specific dissolution within a narrow range difficult to achieve with consistency [33, 38]. Imperfect deposition, adhesion of coating layers, and instability over time can present problems with consistent dissolution and release from enteric coatings [40]. Additionally, the dissolution of enteric coatings is generally only modulated by polymer composition, addition of fillers, and/or deposition of multiple coating layers, resulting in several processing steps [41]. Hydrogels offer the ability to control diffusion throughout the material, vary crosslinking density and corresponding mesh size, or incorporate additional responsive moieties within a single synthesis step to better tune the release profile of the therapeutic.

Acrylic acids, including methacrylic acid, are especially well-suited to oral drug delivery applications as the pKa of these monomers falls within the pH gradient of the intestinal tract. With a pKa of 4.8-4.9 [42], methacrylic acid chains are protonated at low pH such as that of the stomach and hydrogen bonding takes place, maintaining the collapsed state of the gel and protecting any payload within. At pH values above the pKa,

MAA chains are ionized and ionic repulsion occurs, enhancing the imbibition of surrounding fluid by the hydrogel and facilitating release of the payload.

pH-Responsive hydrogel carriers can be loaded post-synthesis with a therapeutic such as a protein or drug by inducing swelling of the gel and allowing sufficient time for diffusion of the therapeutic into the gel, followed by subsequent collapse of the gel. Once administered, these loaded hydrogels swell as the pH of the physiological fluid changes, thereby allowing the therapeutic within to diffuse out through the increased mesh size of the network at the desired biological site [20].

Hydrogel carriers with a MAA backbone and grafted PEG chains were developed by Peppas and Klier in the late 1980s [43]. These P(MAA-g-EG) hydrogels were able to swell and absorb or release solute as a function of increased pH. Additionally, the equilibrium swelling and solute release characteristics of the hydrogel were shown to be dependent upon the complexation between MAA and PEG.

Later, Lowman and Peppas [44] published their studies on the effect of complexation on structure and physical properties of hydrogels. Dynamic and equilibrium swelling, molecular weight between crosslinks, and tensile strength were all found to be a function of solution pH, which in turn affected the complexation state of the hydrogel.

Consequently, sufficient evidence indicates that P(MAA-g-EG) would perform well as an oral delivery device for protein therapeutics. Indeed, P(MAA-g-EG) has been used as an oral delivery carrier with salmon calcitonin [45, 46] and insulin [34, 47-49]. The results were quite promising, and *in vivo* studies using P(MAA-g-EG) hydrogel particles to deliver insulin via an oral route were completed in rats [47, 50-53].

This complexation hydrogel was a springboard for other anionic hydrogel materials designed to facilitate oral delivery of therapeutics. In an effort to reduce premature swelling while enhancing release of proteins at high pH, hydrogel microparticles comprised of MAA copolymerized with *N*-vinyl-2-pyrrolidone (NVP) were developed [54]. These hydrogel particles were effective at loading insulin, protecting the therapeutic in gastric conditions, and releasing on a time scale relevant to that needed for delivery to the upper small intestine [55]. Additionally, the material was well-tolerated by cells, causing minimal toxicity at all concentrations tested [56].

Anionic hydrogels continue to be widely investigated as oral drug delivery carriers, and much of the research is devoted to overcoming limitations such insufficient loading and release of large, oppositely charged, or hydrophobic molecules and increasing mucoadhesive properties [26, 57-61]. As an alternative to anionic hydrogels and their inherent shortcomings, biodegradable and multi-responsive hydrogel formulations are of great importance to the development of the field of hydrogel-based drug delivery.

2.2.2 Biodegradable Hydrogels

A chief limitation of pH responsive hydrogels used in drug delivery is their inability to be degraded biologically [29]. Biodegradable synthetic polymers for drug delivery applications include polyglycolides, polylactides, poly(ϵ -caprolactone), and polyanhydrides [62]. However, natural polymers such as polysaccharides are also frequently used due to their wide availability, biocompatibility, chemically reactive functional groups and facile modification [63]. Polysaccharides commonly used in hydrogel synthesis include alginate, collagen, chitosan, and dextran [64, 65].

The polysaccharide dextran is instrumental in colon-targeted drug delivery as it is degraded by enzymes produced by bacteria belonging to the *Bacteroides* genus [66], which are significantly more abundant within the colon than other portions of the GI tract. In fact, bacterial concentration in the colon is $\sim 10^{11}$ cfu/ml, with *Bacteroides* bacteria making up a large portion [14]. Dextranases produced by these bacteria hydrolyze the glucosidic linkages in dextran chains [67], pictured in Figure 2.2.

Dextran has been used as a prodrug for colonic delivery of therapeutics for decades, and incorporation into hydrogel networks followed suit. In 1995, Hennink et al. [68] published a new procedure for methacrylation of dextran which allowed greater control over the degree of substitution as well as resulted in yields of 70-90%. The methacrylated dextran was then polymerized to form dextran hydrogels, which were loaded with Immunoglobulin G to evaluate degradation of the gel and release of the protein over time [69]. It was found that incorporation of spacers containing hydroxyethyl groups could be used to tailor the degradation time of the hydrogel in physiological conditions, which was on the order of 1-2 months. Release of the protein was strongly dependent on the composition of the hydrogel, and took over a month to reach 100% release, if at all.

Hovgaard and Brøndsted [70] studied the degradation of dextran hydrogels of different molecular weights *in vitro* in a dextranase solution, as well as *in vivo* in rats. Increasing the molecular weight of the dextran resulted in hydrogels with a lower degree of equilibrium swelling and higher mechanical strength. Release of hydrocortisone was greatly improved in the presence of dextranase; 100% release was achieved in approximately 2 hours.

Proteolytic degradation of hydrogels comprised of polypeptides is also a popular targeted degradation mechanism. Enzymatic degradation of peptides and proteins is highly selective and biocompatible, making it an attractive mechanism to tailor hydrogels for targeted delivery to sites of specific enzymatic activity or overexpression, such as the small intestine, mucosa, or even regions of diseased tissue [71, 72]. The lumen of the small intestine, for example, contains gram quantities of pancreatic peptidases, which consist of the serine proteases α -chymotrypsin, trypsin, elastase, and carboxypeptidases [73]. Additionally, there is evidence indicating high levels of serine protease activity in the intestine and fecal content of patients suffering with certain types of inflammatory bowel disease or irritable bowel syndrome [74, 75].

Enzyme-degradable oligopeptide crosslinkers are quite prevalent in tissue engineering applications [76-78]. Though their use in drug delivery devices has also been reported, instances are far fewer. Kopeček et al. [79] published a number of studies during the 1980s-1990s describing the synthesis, characterization, and degradation of hydrogels degradable by various enzymes, including chymotrypsin. The hydrogel was composed of *N*-(2-hydroxypropyl) methacrylamide crosslinked with oligopeptide sequences of varying length and composition. Results showed that the rate of enzymatic degradation was dependent upon the structure and length of the peptide sequence, as well as degree of swelling of the gels. The study was expanded upon by investigation of the release of macromolecules and drugs from the degradable hydrogels [80]. Though complete degradation took hundreds of hours, 100% release of the molecules was achieved in less than 24 hours.

A separate study described controlled release of a therapeutic by enzyme-responsive swelling of a hydrogel [81]. The PEG-acrylamide hydrogel contained an enzyme cleavable linker that leaves the gel with a cationic charge following enzyme hydrolysis, causing the gel to swell and release dextran molecules. The hydrogel particles were most responsive to the enzymes elastase and thermolysin, and degradation and release were evaluated over the course of an hour.

Nanoparticles incorporating a peptide crosslinker degradable by the enzyme cathepsin B have also been synthesized as an intravenously injectable delivery system [71]. The particles were loaded with DNA or antibody prior to incubation in a solution of cathepsin B to measure the release of each therapeutic. The nanoparticles showed signs of degradation in as little as 30 minutes after addition of the enzyme, and were fully degraded within 24-48 hours. Though a small amount of the DNA or antibody was released prior to exposure to the enzyme, most of the therapeutic was released upon degradation.

Polysaccharide- and oligopeptide-based crosslinking agents have many appealing attributes for drug delivery, such as release of payloads on a relevant time scale, complete degradation allowing release of large molecules, and site-specific enzymatic degradation.

2.2.3 Multi-responsive Hydrogels

Hydrogels with specific, tunable, and even reversible responses to environmental stimuli have been known for decades as excellent candidates for drug delivery [29, 82] and regenerative medicine [24, 25] applications. The Peppas lab and many others have dedicated careers to developing complexation and responsive hydrogels suitable for

delivery of delicate therapeutics [26, 54, 83-85]. Likewise, innumerable researchers have used chitosan [86, 87], poly(*N*-isopropyl acrylamide) [88] and various other natural and synthetic responsive polymers [89] in the areas of tissue engineering and regenerative medicine for many years.

However, the need for a material with both broad utility and increased specificity to the application is ever-present. The fourth generation of biomaterials, known as ‘smart’ or biomimetic materials that respond to the host environment, is evolving into sophisticated materials that respond to multiple stimuli in order to better mimic biological processes [90]. Multi-responsive hydrogels are a prime example of these advanced systems. These composite, interpenetrating polymer network (IPN) or supramolecular hydrogels respond to two or more environmental stimuli, including pH, temperature, photons, enzymatic, redox potential, electric or magnetic field, or analyte concentration. The output of these functional materials is contraction, swelling, degradation, color change, etc., and the exact response may be manipulated by tuning the polymer chemistry [28, 30]. This has tremendous advantages in terms of physiological compatibility and biomimetic properties [91-93], targeted drug delivery [94], controlled release [95], and directed cell growth [96, 97].

A multi-responsive hydrogel system can be designed to deliver a therapeutic in response to specific analyte presence. As shown by Gu et al. [95], such a system can have important implications as a closed-loop treatment for diabetes. Uniform chitosan microgels containing insulin and glucose oxidase and catalase nanocapsules were formed by a facile electrospray procedure. In the presence of hyperglycemic glucose concentrations, the microgels swelled significantly as the enzymatic nanocapsules

converted glucose to gluconic acid, enabling the protonation and swelling of chitosan chains in the increasingly acidic solution. In these conditions, insulin was released steadily over about three hours and was even shown to decrease blood glucose level in diabetic mice. The built-in delivery trigger via enzymatic nanocapsules certainly enhances the specificity of the response and has great potential for closed-loop delivery, but likely would not prevent the microgels from swelling in acidic conditions without the presence of glucose.

Other researchers have developed multi-responsive hydrogel systems that require the presence of both stimuli to elicit a response in the material. For example, to achieve release of lipid microspheres from an IPN of gelatin and dextran, the presence of both dextranase and α -chymotrypsin was required [98]. Upon exposure to just one of the enzymes, release of the microspheres was negligible. The requirement of both enzymes for release imparts the system with a very high level of delivery specificity, which could potentially be tuned to target diseased regions that express a particular combination of enzymes.

Hydrogels incorporating multiple responses can also be useful in encapsulating and delivering multiple drugs with different properties. Lv et al. [99] proposed selective release of one of multiple encapsulated molecules in response to a specific stimulus, i.e. releasing one payload in response to pH and one in response to chemical reduction. This was achieved by using a redox and pH sensitive polymer, polyaniline, to create nanocontainers that encapsulated the first molecule of interest. The nanocontainers were then decorated with gold nanoparticles that could be loaded with a second molecule. The molecule contained in the polymer shell was shown to be released only as a function of

increasing pH, while the second molecule loaded onto the gold nanoparticles was released only as a function of concentration of reducing agent. Though the authors proposed this selective release system for anti-corrosion applications, it could easily be translated to biomedical applications such as drug delivery given the dynamic physiological pH environments and reductive intracellular environments.

With respect to oral drug delivery, multi-responsive hydrogels that are both pH-responsive and enzymatically biodegradable are of abundant utility as they can capitalize on both the drastic change in pH in transition from the stomach to the intestine as well as the local concentration of enzymes in specific regions of the intestine. Biodegradable amino acids with free carboxylic acid groups such as poly(aspartic acid) (PASP) and poly(glutamic acid) (PGA) have been used by many researchers to develop smart hydrogels, since they have both a pH and biodegradable response [100]. Interestingly, Jiang et al. [101] found that the acid groups of PASP can be used to complex with gelatin to tune the response to stimuli as well as interactions with therapeutics. In the case of PASP prepared alone, loading and release of a model drug was highly dependent on pH and ionic strength of the environment whereas it was faster, more predictable, and more consistent across pH and ionic strengths when PASP was complexed with gelatin.

Gao et al. [102] developed copolymer hydrogels containing pH-sensitive poly(acrylic acid) derivatives (PAAD) of varying hydrophobicity and biodegradable PGA for the oral delivery of insulin. PGA is a polypeptide with a molecule weight that is easily controlled, and it is known to be biocompatible and biodegradable. The copolymer hydrogels were found to have a swelling response at pH 4-5 regardless of PAAD hydrophobicity, which is desirable for oral delivery applications, while the extent of

swelling was reduced with the incorporation of more hydrophobic PAAD. The hydrogels exhibited some degradation upon exposure to simulated gastric fluid (SGF) containing pepsin, but the weight degradation was significantly more rapid upon exposure to simulated intestinal fluid (SIF) containing pancreatin enzymes. Additionally, release of insulin was significantly greater in SIF than SGF.

Casadei et al. [103] developed a pH- and enzymatically-responsive hydrogel using biodegradable methacrylated dextran crosslinks and the pH-responsive succinic acid derivative of the polyaminoacid known as methacrylated α,β -poly(N-2-hydroxyethyl)-DL-aspartamide. This hydrogel was designed for colonic delivery of an antiangiogenic drug for the treatment of colon-rectal cancer. Upon exposure to simulated gastrointestinal fluids, the hydrogel swelled minimally in simulated SGF but swelled dramatically in SIF. Following 24 hours of incubation with enzymes dextranase or esterase, however, the hydrogels showed loss of mass in conjunction with increased weight swelling, indicating partial degradation. This system also demonstrated increased drug release in the presence of SIF containing enzymes compared to SIF without enzymes.

Another study utilized a different polysaccharide, konjac glucomannan (KGM), with methacrylic acid to synthesize an IPN hydrogel that was both pH responsive and degradable [104]. The IPNs underwent a phase transition beginning at pH 5 regardless of MAA mass ratio, but the degree of swelling was generally increased with higher incorporation of MAA at pH 7.4. Inversely, IPNs with greater mass ratio of KGM generally experienced greater mass loss over time upon exposure to the enzyme mannanase. Interestingly, IPNs incubated with just pH 7.4 buffer or buffer with

pancreatin experienced little to no mass loss over time, indicating that the KGM was degraded solely by mannanase. Drug release was controlled by both pH and enzyme exposure, with greatest release measured in pH 7.4 buffer containing enzymes. This can likely be attributed to the effect of pH of enzyme activity.

Similarly, Yang et al. [105] developed IPN hydrogels using pH-responsive chitosan derivatives and biodegradable alginate to achieve comparable pH-responsive drug release behavior. However, this system experienced an undesirable “burst” release of drug at low pH and the biodegradation of the material was not specifically studied, though it was hypothesized to contribute to the increased drug release at high pH.

These are only a few of the many strategies employed to achieve oral delivery of delicate therapeutics to the intestine via hydrogels. As there are advantages to each approach, a delivery vehicle which incorporates elements of each strategy might be able to consistently deliver a therapeutic to a specific portion of the intestine while maintaining its bioactivity.

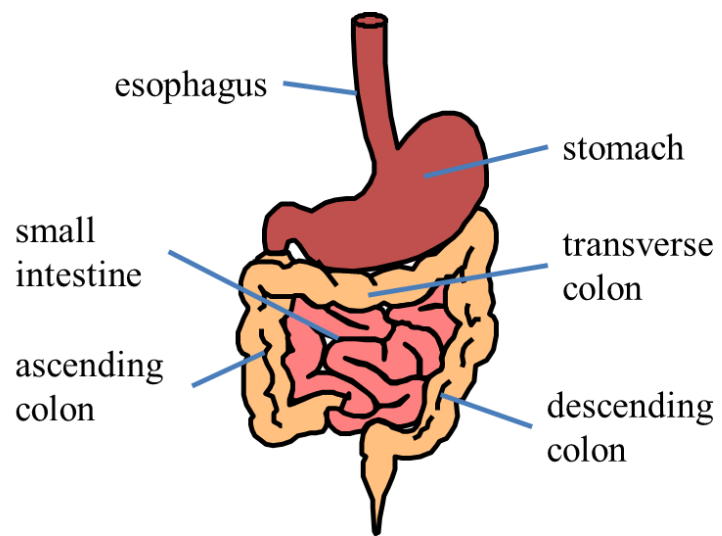


Figure 2.1: Anatomy of the gastrointestinal tract.

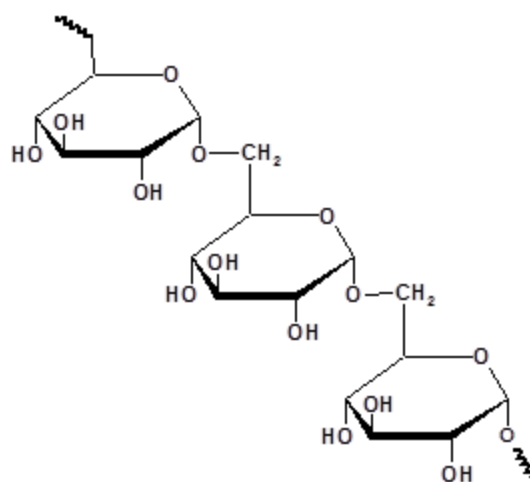


Figure 2.2: The chemical structure of dextran, showing glucose subunits linked by α -1,6 glucosidic linkages.

REFERENCES

- [1] Blanchette, J., Kavimandan, N., and Peppas, N., *Principles of transmucosal delivery of therapeutic agents*. Biomed Pharmacother, 2004. **58**(3): p. 142-151.
- [2] Squier, C.A. and Kremer, M.J., *Biology of oral mucosa and esophagus*. J Natl Cancer Inst Monogr, 2001. **29**: p. 7-15.
- [3] Dressman, J.B., Berardi, R.R., Dermentzoglou, L.C., Russell, T.L., Schmaltz, S.P., Barnett, J.L., and Jarvenpaa, K.M., *Upper gastrointestinal ph in young, healthy man and women*. Pharm Res, 1990. **7**: p. 756-761.
- [4] Russell, T.L., Berardi, R.R., Barnett, J.L., Dermentzoglou, L.C., Jarvenpaa, K.M., Schmaltz, S.P., and Dressman, J.B., *Upper gastrointestinal ph in seventy-nine healthy, elderly, north american men and women*. Pharm Res, 1993. **10**: p. 187-196.
- [5] Deshpande, A.A., Rhodes, C.T., Shah, N.H., and Malick, A.W., *Controlled-release drug delivery systems for prolonged gastric residence: An overview*. Drug Dev Ind Pharm, 1996. **22**: p. 531-539.
- [6] Oberle, R.L. and Amidon, G.L., *The influence of variable gastric emptying and intestinal transit rates on the plasma level curve of cimetidine; an explanation for the double peak phenomenon*. J Pharmacokinet Biopharm, 1987. **15**: p. 529-544.
- [7] Haeberlin, B. and Friend, D.R., *Anatomy and physiology of the gastrointestinal tract: Implications for colonic drug delivery*, in *Oral colon-specific drug delivery*, D.R. Friend, Editor. 1992, CRC Press, Inc.: Boca Raton, FL. p. 1-43.
- [8] Barker, N., van de Wetering, M., and Clevers, H., *The intestinal stem cell*. Gene Dev, 2008. **22**(14): p. 1856-1864.
- [9] Ensign, L.M., Cone, R., and Hanes, J., *Oral drug delivery with polymeric nanoparticles: The gastrointestinal mucus barriers*. Adv Drug Deliver Rev, 2012. **64**(6): p. 557-570.
- [10] Cone, R.A., *Barrier properties of mucus*. Adv Drug Deliver Rev, 2009. **61**(2): p. 75-85.
- [11] Lehr, C.-M., Poelma, F.G.J., Junginger, H.E., and Tukker, J.J., *An estimate of turnover time of intestinal mucus gel layer in the rat in situ loop*. Int J Pharm, 1991. **70**: p. 235-240.

- [12] Houghton, S.E. and McCarthy, C.F., *The isolation, partial characterization, and subfractionation of human intestinal brush borders*. Gut, 1973. **14**: p. 529-534.
- [13] Weinbaum, S., Tarbell, J.M., and Damiano, E.R., *The structure and function of the endothelial glycocalyx layer*. Annu Rev Biomed Eng, 2007. **9**(1): p. 121-167.
- [14] Simon, G.L. and Gorbach, S.L., *The human intestinal microflora*. Digest Dis Sci, 1986. **31**: p. 147S-162S.
- [15] Nugent, S.G., Kumar, D., Rampton, D.S., and Evans, D.F., *Intestinal luminal pH in inflammatory bowel disease: Possible determinants and implications for therapy with aminosalicylates and other drugs*. Gut, 2001. **48**: p. 571-577.
- [16] Davis, S.S., Hardy, J.G., and Fara, J.W., *Transit of pharmaceutical dosage forms through the small intestine*. Gut, 1986. **27**: p. 886-892.
- [17] Barrow, L., Spiller, R.C., and Wilson, C.G., *Pathological influences on colonic motility: Implications for drug delivery*. Adv Drug Deliver Rev, 1991. **7**: p. 201-218.
- [18] Cummings, J.H. and Macfarlane, G.T., *The control and consequences of bacterial fermentation in the human colon*. J Appl Bacteriol, 1991. **70**: p. 443-459.
- [19] Mersny, R.J., *Drug absorption in the colon: A critical review*, in *Oral colon-specific drug delivery*, D.R. Friend, Editor. 1992, CRC Press, Inc.: Boca Raton, FL. p. 45-84.
- [20] Peppas, N.A., Bures, P., Leobandung, W., and Ichikawa, H., *Hydrogels in pharmaceutical formulations*. Eur J Pharm Biopharm, 2000. **50**: p. 27-46.
- [21] Hoffman, A.S., *Hydrogels for biomedical applications*. Adv Drug Deliver Rev, 2002. **43**: p. 3-12.
- [22] Peppas, N.A., Hilt, J.Z., Khademhosseini, A., and Langer, R., *Hydrogels in biology and medicine: From molecular principles to bionanotechnology*. Adv Mater, 2006. **18**(11): p. 1345-1360.
- [23] Lee, S.C., Kwon, I.K., and Park, K., *Hydrogels for delivery of bioactive agents: A historical perspective*. Adv Drug Deliver Rev, 2013. **65**(1): p. 17-20.
- [24] Annabi, N., Tamayol, A., Uquillas, J.A., Akbari, M., Bertassoni, L.E., Cha, C., Camci-Unal, G., Dokmeci, M.R., Peppas, N.A., and Khademhosseini, A., *25th*

- anniversary article: Rational design and applications of hydrogels in regenerative medicine.* Adv Mater, 2014. **26**(1): p. 85-124.
- [25] Slaughter, B.V., Khurshid, S.S., Fisher, O.Z., Khademhosseini, A., and Peppas, N.A., *Hydrogels in regenerative medicine.* Adv Mater, 2009. **21**(32-33): p. 3307-3329.
- [26] Sharpe, L.A., Daily, A.M., Horava, S.D., and Peppas, N.A., *Therapeutic applications of hydrogels in oral drug delivery.* Expert Opin Drug Deliv, 2014. **11**(6): p. 901-915.
- [27] Caldorera-Moore, M. and Peppas, N.A., *Micro- and nanotechnologies for intelligent and responsive biomaterial-based medical systems.* Adv Drug Deliver Rev, 2009. **61**(15): p. 1391-1401.
- [28] Hoffman, A.S., *Environmentally sensitive polymers and hydrogels.* MRS Bulletin, 1991. **16**: p. 42-46.
- [29] Qiu, Y. and Park, K., *Environment-sensitive hydrogels for drug delivery.* Adv Drug Deliver Rev, 2001. **53**(3): p. 321-339.
- [30] Peppas, N.A., *Hydrogels and drug delivery.* Curr Opin Colloid Interface Sci, 1997. **2**(5): p. 531-537.
- [31] Gil, E. and Hudson, S., *Stimuli-responsive polymers and their bioconjugates.* Prog Polym Sci, 2004. **29**(12): p. 1173-1222.
- [32] Liechty, W.B., Kryscio, D.R., Slaughter, B.V., and Peppas, N.A., *Polymers for drug delivery systems.* Annu Rev Chem Biomol Eng, 2010. **1**(1): p. 149-173.
- [33] Peppas, N.A., Wood, K.M., and Blanchette, J.O., *Hydrogels for oral delivery of therapeutic proteins.* Expert Opin. Biol. Ther., 2004. **4**: p. 1-7.
- [34] Foss, A.C., Goto, T., Morishita, M., and Peppas, N.A., *Development of acrylic-based copolymers for oral insulin delivery.* Eur J Pharm Biopharm, 2004. **57**(2): p. 163-169.
- [35] Patell, M.K., *Enteric coated tablet and process for making.* 1988, Bristol-Myers Company: United States.
- [36] Wurster, D.E. and Lindlof, J.A., *Apparatus for the encapsulation of discrete particles.* 1965, Wisconsin Alumni Research Foundation: United States. p. 5.

- [37] Friend, D.R., *New oral delivery systems for treatment of inflammatory bowel disease*. Adv Drug Deliver Rev, 2005. **57**(2): p. 247-265.
- [38] Khan, M.Z.I., Prebeg, Z., and Kurjakovic, N., *A ph-dependent colon targeted oral delivery system using methacrylic acid copolymers i. Manipulation of drug release using eudragit l100-55 and eudragit s100 combinations*. J Controlled Release, 1999. **58**: p. 215-222.
- [39] Thelen, K., Coboeken, K., Willmann, S., Burghaus, R., Dressman, J.B., and Lippert, J., *Evolution of a detailed physiological model to simulate the gastrointestinal transit and absorption process in humans, part 1: Oral solutions*. J Pharm Sci, 2011: p. n/a-n/a.
- [40] Thoma, K. and Bechtold, K., *Enteric coated hard gelatin capsules*, Capsugel, Editor. p. 1-17.
- [41] Colombo, P., Conte, U., Gazzaniga, A., Maggi, L., Sangalli, M.E., Peppas, N.A., and Manna, A.L., *Drug release modulation by physical restrictions of matrix swelling*. Int J Pharm, 1990. **63**: p. 43-48.
- [42] Blanchette, J. and Peppas, N.A., *Oral chemotherapeutic delivery: Design and cellular response*. Ann Biomed Eng, 2005. **33**(2): p. 142-149.
- [43] Peppas, N.A. and Klier, J., *Controlled release by using poly(methacrylic acid-g-ethylene glycol) hydrogels*. J Controlled Release, 1991. **16**: p. 203-214.
- [44] Lowman, A.M. and Peppas, N.A., *Analysis of the complexation/decomplexation phenomena in graft copolymer networks*. Macromolecules, 1997. **30**: p. 4959-4965.
- [45] Torres-Lugo, M. and Peppas, N.A., *Preparation and characterization of p(maa-g-eg) nanospheres for protein delivery applications*. J Nanopart Res, 2002. **4**: p. 73-81.
- [46] Torres-Lugo, M. and Peppas, N.A., *Molecular design and in vitro studies of novel ph-sensitive hydrogels for the oral delivery of calcitonin*. Macromolecules, 1999. **32**: p. 6646-6651.
- [47] Lowman, A.M., Morishita, M., Kajita, M., Nagai, T., and Peppas, D.N.A., *Oral delivery of insulin using ph-responsive complexation gels*. J Pharm Sci, 1999. **88**: p. 933-937.

- [48] Kavimandan, N., Losi, E., and Peppas, N., *Novel delivery system based on complexation hydrogels as delivery vehicles for insulin–transferrin conjugates*. Biomaterials, 2006. **27**(20): p. 3846-3854.
- [49] Yamagata, T., Morishita, M., Kavimandan, N.J., Nakamura, K., Fukuoka, Y., Takayama, K., and Peppas, N.A., *Characterization of insulin protection properties of complexation hydrogels in gastric and intestinal enzyme fluids*. J Controlled Release, 2006. **112**(3): p. 343-349.
- [50] Morishita, M., Goto, T., Nakamura, K., Lowman, A.M., Takayama, K., and Peppas, N.A., *Novel oral insulin delivery systems based on complexation polymer hydrogels: Single and multiple administration studies in type 1 and 2 diabetic rats*. J Controlled Release, 2006. **110**(3): p. 587-594.
- [51] Morishita, M., Goto, T., Peppas, N.A., Joseph, J.I., Torjman, M.C., Munsick, C., Nakamura, K., Yamagata, T., Takayama, K., and Lowman, A.M., *Mucosal insulin delivery systems based on complexation polymer hydrogels: Effect of particle size on insulin enteral absorption*. J Controlled Release, 2004. **97**(1): p. 115-124.
- [52] Nakamura, K., Murray, R.J., Joseph, J.I., Peppas, N.A., Morishita, M., and Lowman, A.M., *Oral insulin delivery using p(maa-g-eg) hydrogels: Effects of network morphology on insulin delivery characteristics*. J Controlled Release, 2004. **95**(3): p. 589-599.
- [53] Tuesca, A., Nakamura, K., Morishita, M., Joseph, J., Peppas, N., and Lowman, A., *Complexation hydrogels for oral insulin delivery: Effects of polymer dosing on in vivo efficacy*. J Pharm Sci, 2008. **97**(7): p. 2607-2618.
- [54] Carr, D.A. and Peppas, N.A., *Molecular structure of physiologically-responsive hydrogels controls diffusive behavior*. Macromol Biosci, 2009. **9**: p. 497-505.
- [55] Carr, D.A., Gomez-Burgaz, M., Boudes, M.C., and Peppas, D.N.A., *Complexation hydrogels for the oral delivery of growth hormone and salmon calcitonin*. Ind Eng Chem Res, 2010. **49**: p. 11991-11995.
- [56] Carr, D.A. and Peppas, N.A., *Assessment of poly(methacrylic acid-co-n-vinyl pyrrolidone) as a carrier for the oral delivery of therapeutic proteins using caco-2 and ht29-mtx cell lines*. J Biomed Mater Res A, 2009. **92A**: p. 504-512.
- [57] Koetting, M.C. and Peppas, N.A., *pH-responsive poly(itaconic acid-co-n-vinylpyrrolidone) hydrogels with reduced ionic strength loading solutions offer*

- improved oral delivery potential for high isoelectric point-exhibiting therapeutic proteins.* Int J Pharm, 2014. **471**(1-2): p. 83-91.
- [58] Schoener, C.A., Hutson, H.N., and Peppas, N.A., *pH-responsive hydrogels with dispersed hydrophobic nanoparticles for the oral delivery of chemotherapeutics.* J Biomed Mater Res A, 2013. **101A**(8): p. 2229-2236.
- [59] Wood, K.M., Stone, G.M., and Peppas, N.A., *Wheat germ agglutinin functionalized complexation hydrogels for oral insulin delivery.* Biomacromolecules, 2008. **9**: p. 1293-1298.
- [60] Serra, L., Domenech, J., and Peppas, N., *Design of poly(ethylene glycol)-tethered copolymers as novel mucoadhesive drug delivery systems.* Eur J Pharm Biopharm, 2006. **63**(1): p. 11-18.
- [61] Kamei, N., Morishita, M., Chiba, H., Kavimandan, N.J., Peppas, N.A., and Takayama, K., *Complexation hydrogels for intestinal delivery of interferon β and calcitonin.* J Controlled Release, 2009. **134**(2): p. 98-102.
- [62] Edlund, U. and Albertsson, A.-C., *Degradable polymer microspheres for controlled drug delivery.* Adv Polym Sci, 2002. **157**: p. 67-112.
- [63] Sinha, V.R. and Kumria, R., *Polysaccharides in colon-specific drug delivery.* Int J Pharm, 2001. **224**: p. 19-38.
- [64] Cheng, Y., Nada, A.A., Valmikinathan, C.M., Lee, P., Liang, D., Yu, X., and Kumbar, S.G., *In situ gelling polysaccharide-based hydrogel for cell and drug delivery in tissue engineering.* J Appl Polym Sci, 2014. **131**: p. 39934-39945.
- [65] Smeds, K.A. and Grinstaff, M.W., *Photocrosslinkable polysaccharides for in situ hydrogel formation.* Journal of Biomedical Materials Research, 2001. **54**: p. 115-121.
- [66] Sery, T.W. and Hehre, E.J., *Degradation of dextrans by enzymes of intestinal bacteria.* J Bacteriol, 1956. **71**: p. 373-380.
- [67] McLeod, A.D., *Dextran prodrugs for colon-specific drug delivery*, in *Oral colon-specific drug delivery*, D.R. Friend, Editor. 1992, CRC Press, Inc.: Boca Raton, FL. p. 213-231.
- [68] Dijk-Wolthuis, W.N.E.v., Franssen, O., Talsma, H., Steenberg, M.J.v., Bosch, J.J.K.-v.d., and Hennink, W.E., *Synthesis, characterization, and polymerization of*

- glycidyl methacrylate derivatized dextran*. *Macromolecules*, 1995. **28**: p. 6317-6322.
- [69] Dijk-Wolthuis, W.N.E.v., Franssen, O., Talsma, H., Steenbergen, M.J.v., Bosch, J.J.K.-v.d., and Hennink, W.E., *Degradation and release behavior of dextran-based hydrogels*. *Macromolecules*, 1997. **30**: p. 4639-4645.
- [70] Hovgaard, L. and Brondsted, H., *Dextran hydrogels for colon-specific drug delivery*. *J Controlled Release*, 1995. **36**: p. 159-166.
- [71] Glangchai, L.C., Caldorera-Moore, M., Shi, L., and Roy, K., *Nanoimprint lithography based fabrication of shape-specific, enzymatically-triggered smart nanoparticles*. *J Controlled Release*, 2008. **125**(3): p. 263-272.
- [72] Guo, D.-S., Wang, K., Wang, Y.-X., and Liu, Y., *Cholinesterase-responsive supramolecular vesicle*. *J Am Chem Soc*, 2012. **134**(24): p. 10244-10250.
- [73] Vlieghe, P., Lisowski, V., Martinez, J., and Khrestchatisky, M., *Synthetic therapeutic peptides: Science and market*. *Drug Discovery Today*, 2010. **15**(1-2): p. 40-56.
- [74] MacDonald, T.T. and Pender, S.L.F., *Proteolytic enzymes in inflammatory bowel disease*. *Inflamm Bowel Dis*, 1998. **4**: p. 157-164.
- [75] Gecse, K., Roka, R., Ferrier, L., Leveque, M., Eutamene, H., Cartier, C., Ait-Belgnaoui, A., Rosztoczy, A., Izbeki, F., Fioramonti, J., Wittmann, T., and Bueno, L., *Increased faecal serine protease activity in diarrhoeic ibs patients: A colonic luminal factor impairing colonic permeability and sensitivity*. *Gut*, 2008. **57**(5): p. 591-599.
- [76] West, J.L. and Hubbell, J.A., *Polymeric biomaterials with degradation sites for proteases involved in cell migration*. *Macromolecules*, 1999. **32**: p. 241-244.
- [77] Kim, S. and Healy, K.E., *Synthesis of injectable poly(n-isopropylacrylamide-co-acrylic acid) hydrogels with proteolytically degradable crosslinks*. *Biomacromolecules*, 2003. **4**: p. 1214-1223.
- [78] Nguyen, L.H., Kudva, A.K., Guckert, N.L., Linse, K.D., and Roy, K., *Unique biomaterial compositions direct bone marrow stem cells into specific chondrocytic phenotypes corresponding to the various zones of articular cartilage*. *Biomaterials*, 2011. **32**(5): p. 1327-1338.

- [79] Ulbrich, K., Strohalm, J., and Kopecek, J., *Polymers containing enzymatically degradable bonds. Iv. Hydrophilic gels cleavable by chymotrypsin*. Biomaterials, 1982. **3**: p. 150-154.
- [80] Subr, V., Duncan, R., and Kopecek, J., *Release of macromolecules from hydrophilic gels containing enzymatically degradable bonds*. J. Biomater. Sci. Polymer Edn, 1990. **1**: p. 261-278.
- [81] Thornton, P.D., Mart, R.J., and Ulijn, R.V., *Enzyme-responsive polymer hydrogel particles for controlled release*. Adv Mater, 2007. **19**(9): p. 1252-1256.
- [82] Hoffman, A.S., *Stimuli-responsive polymers: Biomedical applications and challenges for clinical translation*. Adv Drug Deliver Rev, 2013. **65**(1): p. 10-16.
- [83] Peppas, N.A., Bures, P., Leobandung, W., and Ichikawa, H., *Hydrogels in pharmaceutical formulations*. Eur J Pharm Biopharm, 2000. **50**: p. 27-46.
- [84] Siegel, R.A., *Stimuli sensitive polymers and self regulated drug delivery systems: A very partial review*. J Controlled Release, 2014.
- [85] Kost, J. and Langer, R., *Responsive polymeric delivery systems*. Adv Drug Deliver Rev, 2012. **64**: p. 327-341.
- [86] Martins, A.M., Alves, C.M., Kurtis Kasper, F., Mikos, A.G., and Reis, R.L., *Responsive and in situ-forming chitosan scaffolds for bone tissue engineering applications: An overview of the last decade*. J Mater Chem, 2010. **20**(9): p. 1638.
- [87] Muzzarelli, R.A.A., Greco, F., Busilacchi, A., Sollazzo, V., and Gigante, A., *Chitosan, hyaluronan and chondroitin sulfate in tissue engineering for cartilage regeneration: A review*. Carbohydrate Polymers, 2012. **89**(3): p. 723-739.
- [88] Egami, M., Haraguchi, Y., Shimizu, T., Yamato, M., and Okano, T., *Latest status of the clinical and industrial applications of cell sheet engineering and regenerative medicine*. Archives of Pharmacal Research, 2013. **37**(1): p. 96-106.
- [89] Pérez, R.A., Won, J.-E., Knowles, J.C., and Kim, H.-W., *Naturally and synthetic smart composite biomaterials for tissue regeneration*. Adv Drug Deliver Rev, 2013. **65**(4): p. 471-496.
- [90] Holzapfel, B.M., Reichert, J.C., Schantz, J.-T., Gbureck, U., Rackwitz, L., Nöth, U., Jakob, F., Rudert, M., Groll, J., and Hutmacher, D.W., *How smart do biomaterials need to be? A translational science and clinical point of view*. Adv Drug Deliver Rev, 2013. **65**(4): p. 581-603.

- [91] Quadir, M.A., Martin, M., and Hammond, P.T., *Clickable synthetic polypeptides—routes to new highly adaptive biomaterials*. Chem Mater, 2014. **26**(1): p. 461-476.
- [92] Yang, Y. and Urban, M.W., *Self-healing polymeric materials*. Chem Soc Rev, 2013. **42**(17): p. 7446.
- [93] Galaev, I.Y. and Mattiasson, B., *'Smart' polymers and what they could do in biotechnology and medicine*. Trends Biotechnol, 1999. **17**: p. 335-340.
- [94] Cheng, R., Meng, F., Deng, C., Klok, H.-A., and Zhong, Z., *Dual and multi-stimuli responsive polymeric nanoparticles for programmed site-specific drug delivery*. Biomaterials, 2013. **34**(14): p. 3647-3657.
- [95] Gu, Z., Dang, T.T., Ma, M., Tang, B.C., Cheng, H., Jiang, S., Dong, Y., Zhang, Y., and Anderson, D.G., *Glucose-responsive microgels integrated with enzyme nanocapsules for closed-loop insulin delivery*. ACS Nano, 2013. **7**: p. 6758-6766.
- [96] Kharkar, P.M., Kiick, K.L., and Kloxin, A.M., *Designing degradable hydrogels for orthogonal control of cell microenvironments*. Chem Soc Rev, 2013. **42**(17): p. 7335.
- [97] Temtem, M., Barroso, T., Casimiro, T., Mano, J.F., and Aguiar-Ricardo, A., *Dual stimuli responsive poly(n-isopropylacrylamide) coated chitosan scaffolds for controlled release prepared from a non residue technology*. J Supercrit Fluids, 2012. **66**: p. 398-404.
- [98] Kurisawa, M. and Yui, N., *Dual-stimuli-responsive drug release from interpenetrating polymer network-structured hydrogels of gelatin and dextran*. J Controlled Release, 1998. **54**: p. 191-200.
- [99] Lv, L.-P., Landfester, K., and Crespy, D., *Stimuli-selective delivery of two payloads from dual responsive nanocontainers*. Chem Mater, 2014. **26**(11): p. 3351-3353.
- [100] Gyenes, T., Torma, V., Gyarmati, B., and Zrínyi, M., *Synthesis and swelling properties of novel ph-sensitive poly(aspartic acid) gels*. Acta Biomater, 2008. **4**(3): p. 733-744.
- [101] Jiang, H.L. and Zhu, K.J., *Comparison of poly(aspartic acid) hydrogel and poly(aspartic acid)/gelatin complex for entrapment and ph-sensitive release of protein drugs*. J Appl Polym Sci, 2006. **99**(5): p. 2320-2329.

- [102] Gao, X., He, C., Xiao, C., Zhuang, X., and Chen, X., *Biodegradable ph-responsive polyacrylic acid derivative hydrogels with tunable swelling behavior for oral delivery of insulin*. Polym, 2013. **54**(7): p. 1786-1793.
- [103] Casadei, M.A., Pitarresi, G., Calabrese, R., Paolicelli, P., and Giammona, G., *Biodegradable and ph-sensitive hydrogels for potential colon-specific drug delivery: Characterization and in vitro release studies*. Biomacromolecules, 2008. **9**: p. 43-49.
- [104] Xu, Q., Huang, W., Jiang, L., Lei, Z., Li, X., and Deng, H., *Kgm and pmaa based ph-sensitive interpenetrating polymer network hydrogel for controlled drug release*. Carbohydrate Polymers, 2013. **97**(2): p. 565-570.
- [105] Yang, J., Chen, J., Pan, D., Wan, Y., and Wang, Z., *Ph-sensitive interpenetrating network hydrogels based on chitosan derivatives and alginate for oral drug delivery*. Carbohydrate Polymers, 2013. **92**(1): p. 719-725.

Chapter 3: RNA Background¹

In 1998, Fire and Mello published a seminal paper [1] describing the potent, specific, and heritable gene silencing effect of double-stranded RNAs. Their discovery of this endogenous gene silencing pathway, termed RNA interference (RNAi), earned them the Nobel Prize of Medicine in 2006. Shortly following the initial discovery, it was found that RNAi could be initiated by synthetic small interfering RNA (siRNA) in mammalian cells [2]. Together, these discoveries were heralded as a major development in medicine with great potential for clinical applications.

3.1 RNA INTERFERENCE

3.1.1 Mechanism

The molecules known as small interfering RNAs (siRNAs) are fragmented pieces of double-stranded RNA about 21-23 nucleotides in length that induce RNAi by facilitating the selective cleavage of perfectly complementary messenger RNA (mRNA) strands, depicted in Figure 3.1 [3]. Following introduction in the cell cytosol, siRNA is loaded with protein Argonaute-2 (AGO-2) into the RNA-induced silencing complex (RISC) [4]. There, AGO-2 cleaves the sense-strand of the siRNA, activating the RISC [5]. The anti-sense strand serves to guide the activated RISC to seek out and pair with complementary mRNA [6, 7]. Finally, AGO-2 is responsible for the cleaving of the mRNA strand, inhibiting translation of mRNA into protein and thereby silencing that specific gene [8]. The activated RISC then continues to cleave many other strands of

¹ Portions adapted from Knipe, J.M., Peters, J.T., and Peppas, N.A., *Theranostic agents for intracellular gene delivery with spatiotemporal imaging*. Nano Today, 2013. **8**(1): p. 21-38. Knipe specifically contributed the gold nanoparticle and quantum dot sections, Peters specifically contributed the magnetic nanoparticle section, and Peppas oversaw the project.

complementary mRNA, exemplifying the potency of RNAi [9]. In fact, the therapeutic effect of siRNA has been observed for up to a week in rapidly dividing cells, and on the order of weeks in non-dividing cells [10].

3.1.2 Therapeutic Potential

The therapeutic potential of RNAi was immediately identified and articles suggesting the possible impact of RNAi as a treatment for various disease targets began appearing in rapid succession [11-13]. Novina et al. [14] demonstrated in 2002 the ability of siRNA to silence a principle receptor for HIV-1 on HeLa-derived cells, thereby inhibiting cellular entry of the virus. While siRNA targeted to a gene within the virus was also shown to inhibit virus replication in HeLa-derived cells, the researchers found that transfection efficiency and expression reduction was much lower in primary cell lines such as a more therapeutically relevant T-cell line. In a similar approach, Gitlin et al. [15] showed the ability of two virus-specific siRNAs to suppress replication and provide immunity from a different RNA virus, poliovirus, in HeLa cells. Both of these studies provided proof-of-concept of siRNA as a treatment for a viral disease, but also identified the need for an improved transfection mechanism for primary cell targets.

One of the first reports of RNAi *in vivo* also appeared in 2002, when McCaffrey et al. [16] delivered naked firefly luciferase siRNA or unrelated siRNA using a luciferase-expression plasmid to the liver of mice. By monitoring luciferase expression via whole-body imaging, the researchers showed that the inhibition of luciferase expression was specifically achieved only by the luciferase-specific siRNA, reducing expression by an average of 81%. Additionally, the researchers demonstrated therapeutic potential by targeting human hepatitis C virus expressed within mice. In this case, the

siRNA was successful in reducing virus expression by 75%, suggesting feasibility as a therapeutic. However, the authors acknowledged that delivery of siRNA was a “major obstacle” and could perhaps take advantage of viral and non-viral gene vectors for improved therapeutic effect.

Less than a year later, Sørensen et al. [17] published their results on the ability of synthetic siRNAs to knockdown tumor necrosis factor- α (TNF- α) expression in adult mice. Not only was anti-TNF- α siRNA capable of reducing target protein expression in murine macrophage cells, but it also reduced expression in mice and protected them from lipopolysaccharide-induced sepsis as indicated by a higher survival rate compared to mice treated with inactive siRNA. This was a key advancement, demonstrating that siRNAs have the ability to reduce expression of pathogenic proteins *in vitro* and *in vivo*, opening the door for numerous protein expression targets. However, the authors noted that the therapeutic effect of a single dose of siRNA was only about 4-6 days.

In the decade or so since, the volume of siRNA research has grown tremendously, therapeutic targets for treatment of diseases including cancer, neurological diseases, and infectious diseases, continue to be identified [18-20], and companies are racing to develop siRNA products and bring them to market [21, 22]. It is noteworthy that thus far the primary modes of administration of siRNA therapies are topical, local injection, and systemic administration to the eye, skin, kidneys, liver, spleen, or tumors [23]. A successful mechanism for oral delivery of siRNA has yet to be developed, though such a formulation would be especially conducive to treating diseases of the gastrointestinal (GI) tract like inflammatory bowel disease (IBD) or celiac disease.

Inflammatory bowel disease (IBD) can be classified into two routes of pathogenesis known as ulcerative colitis and Crohn's disease, which collectively affect 1.5 million people and cost more than \$6.3 billion annually in the United States [24]. Though the exact cause of IBD is unknown, it is thought to be an aberrant immune response to microflora in the gut within a genetically susceptible host [25]. The resultant inflammation affects the colon and rectum in patients with ulcerative colitis, but can be present anywhere along the GI tract in patients with Crohn's disease [26]. Symptoms of IBD can include diarrhea, abdominal pain, rectal bleeding, weight loss, malnutrition, and fatigue, and usually manifest in early adulthood or between the ages of 50-70 [27].

There is no cure for IBD, but treatment options do exist and are dependent upon the severity and location of the inflammation. Adjunctive agents, diet, and surgery can be used to manage symptoms and combat complications such as osteoporosis and cancer, but these do not treat the underlying inflammation [26]. 5-Aminosalicylate-based compounds and corticosteroids have been used to treat mild to severe IBD, but come with a range of uncomfortable to serious side effects such as headache, nausea, diarrhea, osteoporosis, hypertension, and diabetes due to their lack of specificity to the inflammation site [24, 26, 28]. When these treatments are no longer effective, the patient may resort to weekly injections of an immunomodulatory drug, but several weeks of treatment are needed before results are observed and the patient is prone to serious infection [26].

AlteRNAtively, IBD can be treated by targeting the cytokines which signal the inflammatory response. In particular, tumor necrosis factor- α (TNF- α) is secreted in high levels by macrophage and dendritic cells in patients with IBD [25]. The anti-TNF- α

monoclonal antibody treatment infliximab has been demonstrated as an effective treatment in studies where the therapeutic was administered by infusion three times over a six week period [26, 27]. However, the mechanism and long-term efficacy of this drug is unknown, and it is quite expensive [26]. In a similar strategy, anti-TNF- α siRNA may be used to silence production of TNF- α and treat patients suffering from IBD [29-33].

Celiac disease is a second condition of the GI tract that may benefit from oral delivery of siRNAs. Celiac disease is an autoimmune disease of the small intestine, in which T-cells initiate an inappropriate immune response to ingested gluten protein in genetically susceptible people, destroying the villi and crypts of the small intestine [34]. The disease is associated with human leukocyte antigen (HLA) DQ2 and DQ8, which are expressed on macrophages and dendritic cells and serve to bind and present the gluten peptides to T cells which initiate a Th-2 (autoimmune) or Th-1 (inflammation) response [35, 36].

Celiac patients suffer from symptoms such as abdominal pain, diarrhea, and weight loss, and if untreated the condition can lead to other diseases like diabetes, iron deficiency anemia, or autoimmune disorders [36, 37]. In most cases, a gluten-free diet (GFD) is sufficient to reduce or eliminate symptoms and reverse damage [34]. However, inadvertent exposure to gluten occurs in up to 30% of patients, resulting in nonresponsive celiac disease [37]. Additionally, patients on a GFD may still present symptoms as a result of associated or secondary conditions [37].

Like IBD, celiac disease is associated with high expression of cytokines such as TNF- α [36] and interferon- γ [35]. Orally delivered siRNA could be used to silence

expression of these cytokines, providing an alternative treatment to patients who are nonresponsive or unable to achieve a sufficient GFD.

Thus, the therapeutic potential of siRNA has been well established and various worthwhile oral delivery targets do exist. As many researchers have noted since the identification of RNAi as a therapeutic mechanism, the principal challenge lies in delivering genetic material within a cell to initiate the gene silencing machinery.

3.2 DELIVERY OF siRNA

As applications for siRNA-mediated gene silencing are ever-growing, there is a need to develop effective carriers that can withstand various administration methods and overcome physiological barriers to deliver siRNA within cells. It is generally accepted that the single biggest obstacle to effective and marketable siRNA therapies is delivery [19, 20], and consequently any success with *in vivo* trials has been limited.

3.2.1 Challenges to Delivery of siRNA

The many barriers to effective delivery of siRNA are shown schematically in Figure 3.2. The first challenge in delivery of siRNAs is their lack of stability; unmodified siRNA are highly susceptible to degradation by endogenous enzymes along the GI tract as well as renal clearance, resulting in a half-life on the order of minutes in serum [38]. Additionally, unmodified siRNA duplexes are especially labile in acidic conditions such as gastric conditions or the environment within lysosomes and endosomes [21].

After reaching the site of delivery whether by direct, systemic, or oral administration, biologically active siRNA must cross the cell membrane into the cell cytoplasm for RNAi to transpire, depicted schematically in Figure 3.3. Besides low bioavailability due to degradation, siRNA are large molecules (~13 kDa) with a net

negative charge, making transport into the cell cytoplasm a formidable prospect [23]. The negatively charged mucus lining the GI tract, shown in Figure 3.2, is particularly challenging to cellular uptake. The siRNA typically enter the cell by an active transport mechanism such as endocytosis. Even after cellular uptake, though, delivery challenges exist. The therapeutic must escape the endosome to the cytoplasm, where it can avoid lysosomal degradation and proceed with RNAi [39].

Chemical modifications to siRNA such as phosphorothioate modifications or replacement of sugars have been shown to increase serum stability, cellular uptake, and cytosolic release of siRNA [21, 40, 41]. For example, Soutscheck et al. [40] delivered modified siRNA that was conjugated with cholesterol via tail-vein injection in mice to achieve knockdown of the apolipoprotein B mRNA. Results indicated that cholesterol conjugation was necessary to achieve delivery of active siRNA and consequent knockdown of mRNA expression via the systemic administration route, likely because the conjugated cholesterol mediated cell uptake. This study was promising in that modified siRNAs could achieve silencing of an endogenous gene by systemic administration, but it left room for further modifications and improvements to increase efficacy, as high dosages were required. It is possible that once the siRNA was taken up into the cell it became trapped and degraded in an endosomal compartment.

Therefore, transfection vectors, either viral or nonviral, have become widely used in conjunction with chemical modifications to improve siRNA stability and delivery into the cell cytosol. Viral vectors, though extremely effective with long-lasting effect, can present deleterious or even fatal side effects such as endogenous virus recombination, oncogenic effects, and unanticipated immune response [42]. In addition to those risks, a

stoichiometric excess of siRNA within the cell could saturate the RNAi mechanism and interrupt normal cell function and processes, leading to unexpected side effects [20]. Nonviral vectors such as nanometer-scale liposomes and polymeric hydrogels avoid these undesirable effects while enhancing intracellular delivery of siRNA by increasing half-life circulation, facilitating cellular uptake and endosomal escape, and employing functionalization and targeting schemes [3, 43]. Polymer nanoparticles are particularly advantageous because they offer increased protection of the therapeutic, greater control over size, structure, and surface charge, they can be functionalized with poly(ethylene glycol) (PEG) or targeting ligands to increase bioavailability and cellular uptake, and synthesis is scalable [23, 38].

3.2.2 Cationic Polymer Systems

The surface charge of a synthetic vector greatly affects its interaction with both therapeutic molecules and surrounding cells [23]. The primary advantage of cationic surfaces is their ability to form condensed complexes with siRNA due to electrostatic interactions [44]. Cationic surfaces are also known to induce increased cellular uptake due to ionic interaction with the negatively charged cell surface [45]. Hence, most synthetic vectors are comprised of cationic lipids or polymers to capitalize on these surface properties with the goal of enhancing cellular uptake of siRNA.

Polycationic nanoparticles provide one additional advantage- due to the high charge density on the repeat units of the polymer, they can induce what is known as the “proton sponge effect” [46]. It is generally accepted that polycationic nanoparticles are taken up into endosomal compartments that are gradually acidified; as the pH lowers, the cationic repeat units become protonated, inducing a flux of ions into the compartment,

which is known as the “proton sponge effect”. Eventually, the difference in osmotic pressure results in endosomal rupture, releasing the siRNA payload into the cell cytosol.

Various cationic polymers have been used to design nanoparticles for gene delivery, some of the most common being polyethyleneimine (PEI), poly(L-lysine) (PLL), chitosan, and poly[2-(diethyleamino)ethyl methacrylate] (PDEAEMA) [47-51]. Recently, a novel UV-initiated emulsion synthesis of polycationic 2-(diethylamino)ethyl methacrylate nanoparticles crosslinked with tetra(ethylene glycol) dimethacrylate (TEGDMA) and grafted with PEG was developed by Fisher and Peppas [52]. PDEAEMA undergoes a phase transition near the physiologically relevant pH of 7.4, making it of great utility for drug delivery applications. It was determined that crosslinking density could be utilized to control the network mesh size and affect the loading of insulin and gold colloids. Consequently, higher crosslinking density also improved biocompatibility.

Fisher et al. [53] improved upon the original PDEAEMA nanogel formulation by incorporating hydrophobic comonomers into the synthesis. They demonstrated the ability to tune the loading of protein with the hydrophobic comonomer, as well as functionalize primary amines with a targeting moiety via a zero-length linkage. Polycationic nanoparticles loaded with fluorescently-labeled albumin were shown to be taken up by two different cell lines. Considering the pH responsive behavior, size, and ability of these particles to be uptaken by cells, they had excellent potential as intracellular delivery vehicles.

Liechty et al. [54] continued to develop and tune the pH-responsive properties of the PDEAEMA copolymer nanogels by comparing the effects of tert-butyl methacrylate

(TBMA) versus 2-(tert-butylamino)ethyl methacrylate (TBAEMA) as comonomers. The nanoparticles had a mean calculated dry diameter of approximately 50-65 nm and a hydrated diameter of approximately 90 nm regardless of copolymer composition. Interestingly, though, the copolymer composition could be used to tune the relative swelling volume as a function of pH, with the more hydrophobic TBMA formulations having a depressed pH phase transition point as a function of TBMA content.

Expanding on the effect of polymer composition on physicochemical properties, Forbes and Peppas [55] investigated the effect of polymerization method on molecular structure. As components of the molecular structure such as hydrophobic clustering and cross-linking density can affect drug delivery performance, the authors compared the composition and structure of PDEAEMA nanogels prepared by UV-initiated polymerization versus activator regenerated by electron transfer (ARGET) atom transfer radical polymerization (ATRP). They found that the heterogeneity of nanoparticles was decreased by the ARGET-ATRP method, as evidenced by narrower molecular weight distribution and sharper temperature transitions.

Forbes et al. [56] also compared the drug delivery properties of the polycationic nanogels prepared by the two synthesis methods. The ability to load a hydrophobic drug was comparable, but the biocompatibility and drug release was increased in the UV-initiated formulations. However, the differing structural properties of the UV-initiated and ARGET-ATRP nanogels made little impact when evaluated as carriers for siRNA delivery [57]. The siRNA binding, biocompatibility, and cellular uptake were not significantly different between nanogels synthesized by the two methods. As the ARGET-ATRP nanogels presented promising gene knockdown results, further

investigation was conducted using the ARGET-ATRP formulation with the greatest TBMA content to evaluate various transfection conditions to optimize cellular uptake of the particles and gene silencing effect in murine macrophage cells [58]. Cellular uptake of the nanogels was confirmed by confocal microscopy and was determined to be a function of both nanogel concentration and incubation time. Knockdown experiments using AllStars death siRNA also showed the dependence of gene silencing on both nanogel and siRNA concentration.

Over the past 6 years, the composition and architecture of the PDEAEMA nanogels has been tuned to arrive at a formulation with desired pH response, excellent siRNA binding, acceptable cell uptake, and measurable gene silencing effect. However, drawbacks to cationic polymer nanoparticle delivery vehicles include their inherent toxicity and unspecific reactions with proteins and molecules systemically [50, 59]. Additionally, polycationic polymers are charged and unstable in the low pH regime, such as that in the stomach, making them unsuitable for oral delivery applications. There is a need to further modify this delivery system to make it suitable for oral delivery application without appreciable toxic effect. Also of interest is incorporation of a tracking modality to better monitor and study systemic distribution, cellular uptake, and clearance from the body.

3.2.3 Theranostic Systems

A biomaterial or device that not only delivers a therapeutic but also possesses a targeting or imaging modality is known as a “theranostic” agent and could have monumental utility in siRNA delivery. Such theranostic agents enable improved disease treatment due to targeted delivery and the ability monitor particle localization in a

noninvasive manner [60]. Theranostic agents are typically comprised of nanoscale inorganic particles, such as gold or iron oxide, modified with a lipid or polymeric coating and targeting moiety, and finally loaded with a therapeutic agent. Many theranostic, inorganic-based particles for the delivery and spatiotemporal tracking of oligonucleotide transfection and gene therapy are summarized in Table 3.1.

Gold nanoparticles have been used to study aspects of gene delivery such as serum stability and Dicer recognition, essential components of RNAi [61]. Mirkin et al. developed gold nanoparticles functionalized with fluorescein-labeled siRNAs. Since the gold quenches the fluorescent signal from the fluorescein, the fluorescence intensity will increase upon degradation and cleavage of the siRNA from the gold nanoparticle. The siRNA-Au-NP, with various commonly used types of siRNA, were incubated with either Dicer to test specific cleavage or FBS to test nonspecific degradation. A greater increase in fluorescence intensity demonstrated that Dicer has a preference for siRNA with a 3' overhang, though these siRNA were also more 10-15-fold more susceptible to nonspecific degradation. The serum stability of chemically modified siRNAs was then tested, and the results showed that these modifications can decrease nonspecific degradation by ~40%, but Dicer recognition was decreased by ~60%. Finally, the researchers found that serum stability depended upon the orientation of the siRNA on the nanoparticle; siRNA with the more thermally stable base pair distal to the nanoparticle experienced greatly reduced nonspecific degradation while maintaining comparable Dicer recognition. As might be expected, increased serum stability enhanced cellular uptake by 300% and resulted in ~85% GFP knockdown.

Research has been done in the area of targeted intracellular delivery of siRNA using hyaluronic acid (HA) to induce HA-mediated endocytosis [62]. Cysteamine-modified gold nanoparticles (AuCM) were coated with siRNA, PEI, and HA by layer-by-layer assembly. Addition of each layer was confirmed by TEM, atomic force microscopy, UV-Vis, and zeta-potential measurements. The AuCM/siRNA/PEI/HA complexes were stable in serum-containing media up to 24 hours, presenting no aggregation or precipitation. Cellular uptake of the complexes was visualized by TEM after 24 hours of incubation with B16F1 cells; the complexes were distributed throughout the cytoplasm with no large aggregates present. An MTS cell viability assay showed cell viability of at least 90% for the AuCM/siRNA/PEI/HA complexes as well as the various controls. Anti-luciferase siRNA was used to determine a gene silencing efficiency of ~50% for AuCM/siRNA/PEI/HA complexes in 10 vol% serum. In 50 vol% serum, silencing efficiency of the AuCM/siRNA/PEI/HA complexes improved to 70-80%, which may be attributed to the stability of this formulation in serum. This highlights the large effect protein adsorption and serum stability may have on intracellular uptake. Anti-VEGF siRNA was also tested, and RT-PCR showed ~70% reduction in gene expression, which outperformed the 20% reduction by siVEGF/Lipofectamine 2000. Dark field microscopy confirmed that cells with HA receptors did uptake AuCM/siRNA/PEI/HA complexes, but the same cells pretreated with HA did not, demonstrating effective targeting of the HA receptors by the complexes. Gene knockdown results corresponded with cellular uptake; gene silencing in the presence of free HA was significantly lower than that without free HA. Finally, the target-specific systemic delivery of the AuCM/siRNA/PEI/HA complex with anti-ApoB siRNA to the liver was tested. Following injection into the tail-vein of

Balb/c mice, most of the complexes accumulated in the liver and spleen, as determined by inductively coupled plasma-atomic emission spectroscopy. The ApoB mRNA in the liver was reduced to ~20%, demonstrating effective target-delivery and gene down regulation.

Quantum dots (QDs) have been considered as potential gene delivery devices due to their convenient size and inherent stability against photobleaching while imaging, making them an effective theranostic agent. QDs have also enabled imaging of individual molecules within the cell environment, which can be particularly useful in gene silencing therapies. One of the earliest reports appeared in 2005, in which QDs were used to monitor siRNA transfection [63]. A conventional transfection agent, Lipofectamine 2000 (Invitrogen), was loaded with both CdSe-core ZnS-shell QDs and siRNA targeting the Lamin A/C gene. Fibroblast cells were then transfected with the loaded liposomes for 5 hours. Following transfection, siRNA uptake and silencing efficacy was measured by flow cytometry, western blotting, and immunofluorescence staining. Cells transfected with QDs and siRNA showed a strong correlation between gene silencing and fluorescence. Additionally, cells transfected with QDs and siRNA underwent ~90% gene knockdown, while cells transfected with siRNA alone experienced only ~20-30% gene knockdown [63]. This paper demonstrated that not only are QDs a suitable probe to track siRNA delivery, but that they may also increase gene silencing efficiency. This study became a springboard for further investigation of QD-mediated siRNA delivery.

Other research groups have terminated QDs with a positively charged molecule or coating such as chitosan [64] or other cationic polymers [65, 66] in an effort to achieve effective cellular transfection and gene knockdown with low cytotoxic effect from the

particles. One of the first reports utilized the endosome-disrupting polymer PEI, grafted with PEG to mitigate the cytotoxic effects associated with PEI [65]. (PEI-g-PEG) was attached to CdSe/CdS/ZnS QDs by a ligand exchange reaction, resulting in a hydrodynamic size of 21-22 nm. It was noted that the PEG grafted nanoparticles were quite stable in acidic conditions as well as biological media. Confocal microscopy was used to image the modified QDs, and it was observed that cellular uptake via endocytosis or macropinocytosis began as early as 1-2 hours into incubation. It was also noted that the amount of grafted PEG greatly influenced cellular uptake and intracellular distribution. QDs with four grafted PEG chains were apparently trapped in organelles, while QDs with only two grafted PEG chains had apparently escaped endosomal compartments and were released into the cytoplasm, as is necessary for effective siRNA delivery. However, QDs with four PEG chains displayed less cytotoxicity, as determined by a standard MTT assay. The ability to tune endosomal escape and cytotoxicity by grafted PEG chains gives a greater degree of control over the properties of the QD nanoparticle, though an optimal formulation was not reported.

In a more recent report, L-arginine (L-Arg)-modified CdSe/ZnSe quantum dots, with or without β -cyclodextrin (β -CD), were used as siRNA delivery devices to silence the gene HPV18 E6 [67]. L-Arg provided a positive surface charge onto which negatively charged siRNA could be electrostatically bound, and β -CD had been shown to induce greater biocompatibility and lower cytotoxicity. HeLa cells were transfected with the QD/siRNA complexes for 24 hours, and cell viability remained >70% for QD concentrations less than 70 μ g/mL over this period of time. Confocal microscopy was used to track the QD/siRNA location in real time. Fluorescence intensity measured by

flow cytometry was used to quantify cellular uptake. A gene silencing efficiency of nearly 80%, as well as 80% protein suppression was achieved using the QD/siRNA complexes, as determined by reverse transcription- polymerase chain reaction (RT-PCR) and western blotting, respectively. These values were greater than that of commercial transfection agents also tested [67].

Further expanding the dexterity of quantum dots, fluorescent resonance energy transfer (FRET) may be utilized to gather information regarding spatial conformation of QDs and siRNA within the cell. FRET is the transfer of energy from a donor fluorophore to an acceptor fluorophore across nanometer-scale distances, resulting in a lower fluorescence intensity for the donor and a higher fluorescence intensity for the acceptor [68]. FRET has been employed with QDs to observe the intracellular delivery of siRNA [69, 70] and DNA [71-73], though most studies utilize QDs as an imaging modality in addition to a polymeric or lipid-based transfection agent [74, 75].

In one study, electrostatic binding of FITC-labeled siRNA to amphiphilic polymer-encapsulated QDs was perceived by the quenching of the FITC signal via FRET induced by the excited QDs [70]. Time-lapse confocal microscopy was used to monitor the QD-siRNA intracellular interaction; at approximately 1.5 hours after transfection, the particles were present inside the cell and decomplexation between the QD and siRNA was indicated by the appearance of a signal in the FITC channel. At 5 hours post-transfection, siRNA was dispersed throughout the cell. Increased death in cells transfected with HER2 siRNA compared to those transfected with random or no siRNA was indicative of endosomal escape and gene knockdown by RNAi, but was not conclusive. The amphiphilic polymer coating outperformed a conventional polymer, PEI,

and was comparable to the commercial transfection agent Lipofectamine in terms of gene silencing efficiency. The nanocomplex carrier has the added benefit of less cytotoxic effect than these other carriers [70]. Similarly, Lee et al. employed FRET to track the delivery of cyanine-labeled siRNAs electrostatically bound to the QD-PEI complexes [69]. The QD-PEI complexes displayed knockdown of the VEGF gene comparable to that of commercially available Lipofectamine.

Theranostic inorganic nanoparticles are effective vectors for gene delivery, even outperforming standard transfection vectors in some instances, while providing mechanisms for targeting, imaging and tracking of gene delivery. In recent years, gold, magnetic, and quantum dot nanoparticles have proven themselves superior in their ability to execute controlled and targeted delivery. Advances in imaging technology have established the capability to image spatiotemporal gene transfection at the single-molecule level with the aid of these theranostic particles. These small successes have opened up new doors for the development of gene therapy options, yet the goal for highly efficient, specific *in vivo* delivery and tracking of oligonucleotides has still not been fully recognized.

Recent research has focused on increasing transfection efficiency *in vitro* while minimizing cytotoxicity. In order to successfully administer genetic therapies, the coatings that were successful *in vitro* need to be combined with common *in vivo* targeting mechanisms. Some work has looked to combining these areas of research; however, the success has been limited to unique disease models, such as cancer. Disease models without unique anatomies need to be pursued in order to test the limits of nanoparticle-mediated gene delivery.

The success of nanoparticle theranostics will depend on the target diseases and the genes used to treat them. The correct combination of nanoparticle, coating, and targeting mechanism will need to be tailored to each disease/gene combination. Substantial progress has been made toward improving cytotoxicity and transfection efficiency, and future work needs to focus on treatment of specific disease models *in vivo*, as well as the development of real-time *in vivo* imaging capability. Further, specific targeting mechanisms and minimum dosage levels must be determined in order for theranostic gene delivery to become a treatment standard.

3.2.4 Oral Delivery Systems

siRNA as a therapeutic has been a major area of research for well over a decade now, but the prevalent method of delivery is still by local injection or intravenous administration. In fact, of the thirty recent or active clinical trials involving siRNA therapy, at least twenty of the studies utilized these methods of administration and none administered the treatment orally [76]. The advantages of oral delivery, especially for the treatment of diseases of the GI tract, include elimination of systemic effects, increased patient compliance and comfort, and reduction of associated costs [77]. Though there have been only small number of groups investigating oral delivery of siRNA, several reviews highlighting the great potential as well as challenges of oral siRNA delivery have been published in recent years [78-80].

It is important to note that nearly all siRNA oral delivery strategies target TNF- α , a cytokine that signals the inflammatory response. High levels of TNF- α are associated with diseases of the GI tract such as Crohn's disease, ulcerative colitis, and celiac disease, making it a logical target for gene knockdown by orally delivered siRNA [81].

The first study aimed at developing an orally administered carrier for siRNA delivery was published in 2009, in which β 1,3-D-glucan microshells were incubated with RNA-PEI complexes to form a cationic core, which was then loaded with Endo-Porter, a peptide to facilitate intracellular delivery, followed by fluorescently-labeled siRNAs targeting TNF- α , and finally an additional incubation period with PEI to trap the cargo [29]. Uptake of the β -1,3-D-glucan-encapsulated siRNA particles (GeRPs) by macrophages was observed *in vitro* using confocal microscopy, and 70-80% knockdown of target mRNA was measured after transfection. GeRPs with specific and scrambled siRNA sequences were then administered orally to mice; target mRNA expression was reduced by 70% and TNF- α expression was reduced by 80% compared to the scrambled sequence of RNA. At the dosage administered, this oral delivery formulation was up to 250 times more potent *in vivo* than systemic delivery formulations that had been reported. However, the GeRPs were also found in other tissues throughout the body, indicating migration of macrophages containing the siRNA therapy and lack of tissue-specific targeting, which is not desirable.

Amiji et al.[82, 83] developed a hybrid nanoparticle-in-microsphere (NiMOS) oral delivery system to the intestinal mucosa in which FITC-gelatin nanoparticles were embedded in a poly(ϵ -caprolactone) (PCL) matrix of less than 2-5 μ m in diameter. This system has been used to encapsulate reporter plasmid DNA [82] and TNF- α specific as well as scrambled siRNA [30, 31] and has been administered orally to rats or Balb/c mice, respectively. In the case of the NiMOS containing TNF- α siRNA given to mice with induced colitis symptoms, the group receiving the formulation had the lowest TNF- α mRNA and protein expression compared to the controls at both 10 and 14 days after

administration. Though the NiMOS particles performed well *in vivo*, *in vitro* studies showed that some therapeutic was released prematurely (~20%) and performance of NiMOS through pH variation is unknown.

In 2010, results were published describing thioketal nanoparticles (TKNs) loaded with siRNA against TNF- α for oral delivery to the intestines [32]. These particles were designed to be degraded by reactive oxygen species produced by phagocytes at the site of inflammation. It was shown that the TKNs localized delivery of siRNA to the colon of mice with induced colitis symptoms, and that TNF- α mRNA was reduced 10-fold by TNF- α -TKNs compared to the controls. The therapeutic effect of this siRNA carrier, however, is limited to diseases where intestinal inflammation is present.

In 2011, Laroui et al. [33] published a report on branched PEI that was complexed with TNF- α siRNA, loaded into polylactide, and covered with polyvinyl alcohol in a multi-step synthesis process. The particles were then encapsulated in alginate or chitosan and administered orally to C57BL/6 mice. After four days of administration inflammation was induced in the mice by injection of lipopolysaccharide (LPS). Results indicated that the siRNA-loaded particles outperformed Lipofectamine *in vitro*, and *in vivo* the particles were targeted to the colon and effectively reduced LPS-induced TNF- α production. Though the efficacy of this system is promising, the synthesis of these multi-layered particles is laborious.

In the past couple years, a number of papers describing the development of an oral delivery system for siRNA have come out of the Yin laboratory. Trimethyl chitosan-cysteine conjugates (TMC-Cys) were initially synthesized using 10, 100, or 200 kDa chitosan to evaluate performance as a drug carrier with plasmids encoding enhanced

green fluorescent protein (pEGFP) [84]. It was thought that the trimethyl and cysteine groups would improve interactions between chitosan and the epithelial mucosa during oral delivery to facilitate cellular uptake. Following formation of nanocomplexes via electrostatic interaction between the plasmid and TMC-Cys, the nanocomplexes were incubated with HEK293 cells. It was observed that release of the plasmid was increased in the presence of glutathione as it is capable of reducing disulfide bonds between the thiolated chitosan chains, a positive result as glutathione is present within cellular endosomes. Cell uptake and transfection by the plasmid were confirmed by increased GFP expression of the cells and were dependent upon the molecular weight of the TMC conjugates, with higher molecular weight chitosan performing better.

As this system was promising with plasmid DNA, the researchers explored its capability to deliver siRNA, a much smaller molecule [85]. It was determined that TMC-Cys conjugates electrostatically complexed with siRNA targeting interleukin 6 (IL-6) had increased stability and intestinal permeation when physically crosslinked via ionic gelation with sodium tripolyphosphate. Intestinal permeation is critical for a system administered orally to have systemic effect. This formulation was also shown to significantly reduce expression of IL-6 in RAW 264.7 murine macrophage cells compared to other TMC nanocomplex formulations.

Next, the molecular weight of the TMC-Cys conjugates was further increased to 100, 200, or 500 kDa chitosan, and nanoparticles were prepared complexation with siRNA targeting TNF- α followed by ionic gelation with sodium tripolyphosphate [86]. Nanoparticles were administered to mice via a single oral gavage or an intraperitoneal injection, and interestingly the expression of TNF- α was significantly reduced using the

200 kDa molecular weight formulation administered orally as compared to intraperitoneal administration.

Finally, 200 kDa TMC-Cys conjugate nanoparticles were modified with mannose in an effort to improve intracellular uptake via interaction with mannose receptors on M cell surfaces [87]. These mannose-modified nanoparticles complexed with siRNA targeting TNF- α were effective in reducing serum levels of TNF- α over 4 hours compared to a scrambled siRNA sequence, and the effect was potent at various nanoparticle dosages. However, there was no comparison between mannose-modified and unmodified TMC-Cys nanocomplexes to confirm increased cellular uptake by virtue of the mannose molecule. Studies using uptake pathway inhibitors suggested that the mannose receptors mediated endocytosis of the nanoparticles, but were inconclusive. Nonetheless, the researchers have made great strides in developing a nanoparticle siRNA carrier that can overcome some of the challenges of oral delivery.

Chitosan/siRNA nanoparticles were employed by a separate group of researchers for oral delivery to the gastrointestinal tract. Ballarín-González et al. [88] prepared nanoparticles by complexation between chitosan and fluorescently labeled anti-TNF- α siRNA, then administered them to mice by oral gavage. Though the design of the two-component carrier is quite simplistic, the authors report siRNA stability at the higher chitosan to siRNA ratios in simulated gastric and intestinal fluids as evaluated by native polyacrylamide gel electrophoresis. Northern blot analysis from various gastrointestinal and other tissues indicated systemic distribution of siRNA following oral administration, as stable siRNA was accumulating in the liver, spleen, and kidney just 1 hour after gavage. However, the extent of accumulation in each location was a function of the

chitosan to siRNA ratio, most likely due to the influence of the chitosan on stability and cellular interactions. This study is remarkable for a couple reasons, first that oral delivery of intact siRNA was achieved with simple siRNA-chitosan complexes, and second that systemic distribution of siRNA is possible via oral administration.

3.3 CONCLUSIONS

RNAi has exciting potential as a gene therapy for many diseases, particularly diseases of the GI tract, but there are many extracellular and intracellular barriers to oral siRNA delivery. Additionally, oral delivery is advantageous in terms of cost and patient compliance. The current strategies for oral delivery of siRNA to the intestine are relatively few in number, but are effective in some capacity though they leave much room for improvement, particularly in terms of increasing cellular uptake, maintaining siRNA integrity, and increasing dosage efficacy. Consequently, there is great need to design an improved polymer carrier which can not only protect siRNA from harsh gastric conditions and target delivery specifically to the intestine, but can also facilitate cell-specific uptake and endosomal escape into the cytoplasm where RNAi occurs.

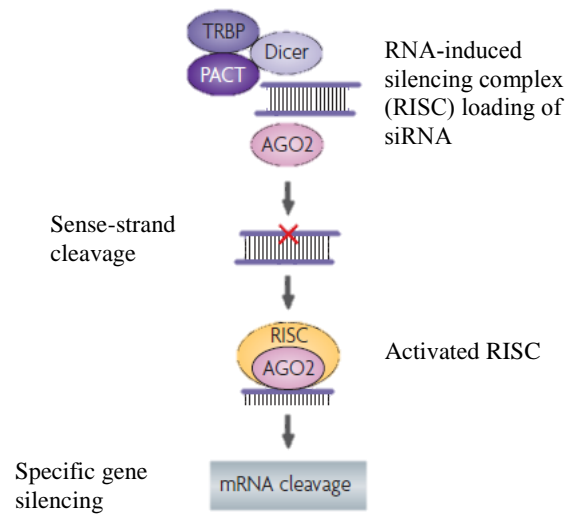
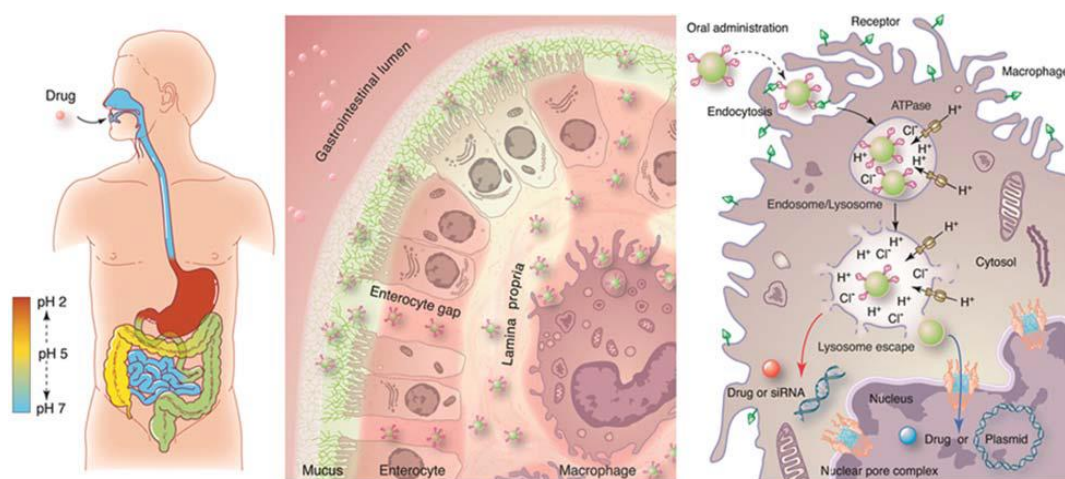


Figure 3.1: Mechanism of RNAi with siRNA. Adapted from [3].



Organism level
Harsh GI environment
(dynamic pH gradient)
Residence time

Tissue level
Mucus penetration
Stability in the area of
inflammation

Cell level
Cell uptake by endocytosis
Endosomal escape
Enzymatic degradation

Figure 3.2: Barriers and challenges to the oral delivery of siRNA. Adapted from [81].

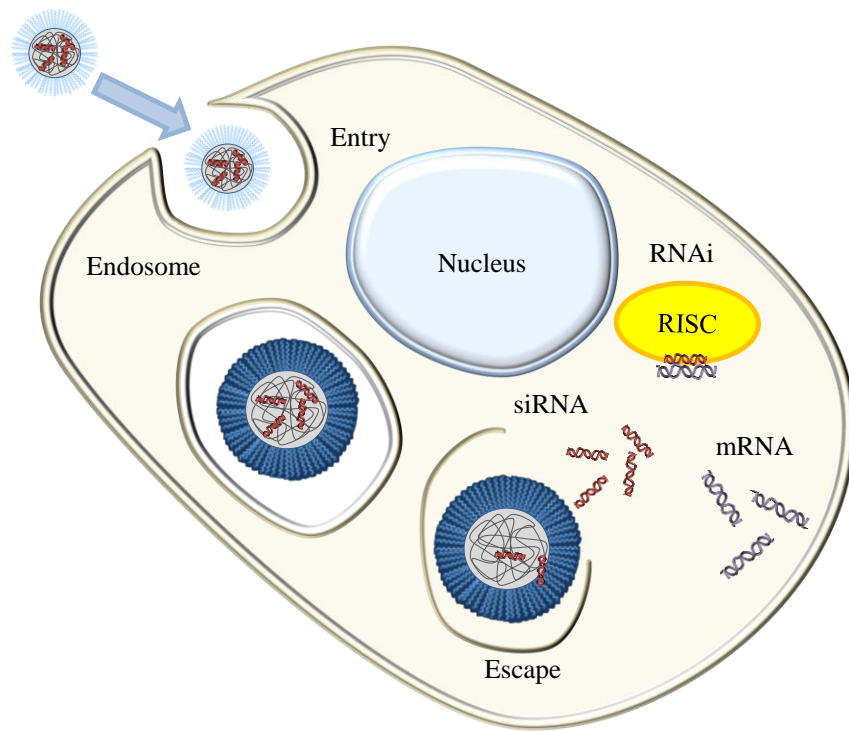


Figure 3.3: Schematic of cellular uptake of siRNA delivery carrier, followed by endosomal escape and RNAi.

Table 3.1: Summary of inorganic theranostic particles used in gene therapy [121].

Particle Type	Imaging	Delivery/ release method	Coating	<i>In vitro or in vivo</i>	Gene Therapy	Ref.
MNP	Fluoresence	Magnetofection	Acidic/Neutral PEI	<i>In vitro</i>	DNA	[89]
MNP	Fluoresence	Magnetofection	Chitosan	<i>In vitro</i>	DNA	[90]
MNP	Fluoresence	Magnetofection	PEI	<i>In vitro</i>	DNA/siRNA	[91]
MNP	Fluoresence	Magnetofection	PPI dendrimer	<i>In vitro/In vivo</i>	siRNA	[92]
MNP	Fluoresence	Magnetofection	PAMAM dendrimer	<i>In vitro</i>	asODN	[93]
MNP	Fluoresence	Magnetofection	Chitosan/PEI/PEG	<i>In vitro</i>	DNA	[94]
MNP	Fluoresence	Magnetofection	ODN	<i>In vitro</i>	DNA	[95]
MNP	Fluoresence	Magnetofection	PEI/DNA	<i>In vitro</i>	DNA	[96]
MNP	MRI/ Fluoresence	Magnetofection	Dextran	<i>In vitro</i>	shRNA	[97]
MNP	Fluoresence	Magnetofection	Cationic Lipid	<i>In vivo</i>	siRNA/DNA	[98]
MNP	Fluoresence	Magnetofection	Cationic Lipid/PEI	<i>In vitro</i>	pDNA	[99]
MNP	Fluoresence	Magnetofection	Cationic Lipid	<i>In vitro</i>	DNA	[100]
MNP	Fluoresence	Magnetofection	Clustered MNPs	PEI <i>In vitro</i>	siRNA	[101]
MNP	Fluoresence	Magnetofection	deacylated PEI	<i>In vitro</i>	pDNA	[102]
MNP	Fluoresence	Magnetofection	DNA	<i>In vitro</i>	DNA	[103]
MNP	Fluoresence	Magnetofection	DNA	<i>In vitro</i>	DNA	[104]

Table 3.1: Summary of inorganic theranostic particles used in gene therapy [121] (cont.).

Particle Type	Imaging	Delivery/ release method	Coating	<i>In vitro or in vivo</i>	Gene Therapy	Ref.
MNP	Fluorescence	Magnetofection	Cationic Lipospheres	<i>In vitro</i>	siRNA	[105]
AuNR	SERS, Fluorescence microscopy, Maestro	N/A	PEG	<i>In vivo</i> (mouse)	N/A	[106]
AuNP	SERS, Dark-field microscopy, TEM	Electrostatic	PEI/chitosan	<i>In vitro</i>	shRNA	[107]
AuNS	Fluorescence microscopy, Flow cytometry	Laser-induced		<i>In vitro</i>	ssDNA	[108]
AuNS	Fluorescence microscopy, Dark-field microscopy	Laser-induced	L-lysine	<i>In vitro</i>	siRNA, ssDNA	[109]

Table 3.1: Summary of inorganic theranostic particles used in gene therapy [121] (cont.).

Particle Type	Imaging	Delivery/ release method	Coating	<i>In vitro or in vivo</i>	Gene Therapy	Ref.
AuNS	Fluorescence microscopy, TEM	Laser-induced	PEG, lipid bilayer, Tat peptide	<i>In vitro</i>	siRNA	[110]
AuNP	Fluorescence microscopy	Dicer cleavage		<i>In vitro</i>	siRNA	[61]
AuNP	Light microscopy	Dicer cleavage		<i>In vitro</i>	miRNA	[111]
AuNP	TEM, Dark-field microscopy	Electrostatic	PEI, Hyaluronic acid	<i>In vitro</i>	siRNA	[62]
AuNR	Dark-field microscopy	Electrostatic	Polyelectrolytes	<i>In vitro</i>	siRNA	[112]
AuNP	TEM, Fluorescent microscopy	N/A	N/A	<i>In vitro</i>	N/A	[113]
AuNP	TEM, Fluorescent microscopy	N/A	N/A	<i>In vitro</i>	N/A	[114]

Table 3.1: Summary of inorganic theranostic particles used in gene therapy [121] (cont.).

Particle Type	Imaging	Delivery/ release method	Coating	<i>In vitro or in vivo</i>	Gene Therapy	Ref.
AuNS	TEM, Contrast microscopy	N/A	DMSA	<i>In vitro</i>	N/A	[115]
QD	Flow cytometry		Lipofectamine 2000	<i>In vitro</i>	siRNA	[63]
QD	Flow cytometry	Disulfide reduction	F3 peptide	<i>In vitro</i>	siRNA	[116]
QD	Fluorescent imaging, TEM	Disulfide reduction	Lipofectamine, RGD and Tat peptides	<i>In vitro</i>	siRNA	[117]
QD	Time-lapse fluorescent imaging			<i>In vitro</i>	ASON	[118]
QD	Confocal microscopy	Electrostatic	PEI-g-PEG	<i>In vitro</i>		[65]
QD	Flow cytometry, Fluorescent imaging	Electrostatic	PEG-amine	<i>In vitro</i>	siRNA	[119]

Table 3.1: Summary of inorganic theranostic particles used in gene therapy [121] (cont.).

Particle Type	Imaging	Delivery/ release method	Coating	<i>In vitro or in vivo</i>	Gene Therapy	Ref.
QD	Confocal laser scanning microscopy, TEM	Electrostatic	2-vinylpyridine	<i>In vitro</i>	siRNA	[120]
QD	Confocal microscopy, Flow cytometry	Electrostatic	L-arginine, cyclodextrin	β - <i>In vitro</i>	siRNA	[67]
QD	FRET, Time-lapse confocal microscopy	Electrostatic	Amphiphilic polymer	<i>In vitro</i>	siRNA	[70]
QD	FRET, Time-lapse confocal microscopy	Electrostatic	PEI	<i>In vitro</i>	siRNA	[69]
QD	FRET, Time-lapse confocal microscopy	Electrostatic	Polycation	<i>In vitro</i>	pDNA	[71]

REFERENCES

- [1] Fire, A., Xu, S.Q., Montgomery, M.K., Kostas, S.A., Driver, S.E., and Mello, C.C., *Potent and specific genetic interference by double-stranded RNA in caenorhabditis elegans*. Letters to Nature, 1998. **391**: p. 806-811.
- [2] Elbashir, S.M., Harborth, J., Lendeckel, W., Yalcin, A., Weber, K., and Tuschl, T., *Duplexes of 21-nucleotide RNAs mediate RNA interference in cultured mammalian cells*. Nature 2001. **411**: p. 494-498.
- [3] Kim, D.H. and Rossi, J.J., *Strategies for silencing human disease using RNA interference*. Nature Reviews Genetics, 2007. **8**(3): p. 173-184.
- [4] Rand, T.A., *Biochemical identification of argonaute 2 as the sole protein required for RNA-induced silencing complex activity*. P Natl Acad Sci USA, 2004. **101**(40): p. 14385-14389.
- [5] Rand, T.A., Petersen, S., Du, F., and Wang, X., *Argonaute2 cleaves the anti-guide strand of siRNA during risc activation*. Cell, 2005. **123**(4): p. 621-629.
- [6] Ameres, S.L., Martinez, J., and Schroeder, R., *Molecular basis for target RNA recognition and cleavage by human risc*. Cell, 2007. **130**(1): p. 101-112.
- [7] Martinez, J., Patkaniowska, A., Urlaub, H., Luhrmann, R., and Tuschl, T., *Single-stranded antisense siRNAs guide target RNA cleavage in RNAi*. Cell, 2002. **110**: p. 563-574.
- [8] Liu, J., *Argonaute2 is the catalytic engine of mammalian RNAi*. Science, 2004. **305**(5689): p. 1437-1441.
- [9] Hutvagner, G., *A microRNA in a multiple-turnover RNAi enzyme complex*. Science, 2002. **297**(5589): p. 2056-2060.
- [10] Bartlett, D.W., *Insights into the kinetics of siRNA-mediated gene silencing from live-cell and live-animal bioluminescent imaging*. Nucleic Acids Res, 2006. **34**(1): p. 322-333.

- [11] Silva, J.M., Hammond, S.M., and Hannon, G.J., *Rna interference: A promising approach to antiviral therapy?* Trends Mol Med, 2002. **8**: p. 505-508.
- [12] Shuey, D.J., McCallus, D.E., and Giordano, T., *Rnai: Gene-silencing in therapeutic intervention.* Drug Discovery Today, 2002. **7**: p. 1040-1046.
- [13] Agami, R., *Rnai and related mechanisms and their potential use for therapy.* Current Opinion in Chemical Biology, 2002. **6**: p. 829-834.
- [14] Novina, C.D., Murray, M.F., Dykxhoorn, D.M., Beresford, P.J., Riess, J., Lee, S.-K., Collman, R.G., Lieberman, J., Shankar, P., and Sharp, P.A., *SiRNA-directed inhibition of hiv-1 infection.* Nature Medicine, 2002.
- [15] Gitlin, L., Karelsky, S., and Andino, R., *Short interfering RNA confers intracellular antiviral immunity in human cells.* Nature, 2002. **418**: p. 430-434.
- [16] McCaffrey, A.P., Meuse, L., Pham, T.-T.T., Conklin, D.S., Hannon, G.J., and Kay, M.A., *Rna interference in adult mice.* Nature, 2002. **418**: p. 38-39.
- [17] Sørensen, D.R., Leirdal, M., and Sioud, M., *Gene silencing by systemic delivery of synthetic siRNAs in adult mice.* JouRNAI of Molecular Biology, 2003. **327**(4): p. 761-766.
- [18] Takeshita, F. and Ochiya, T., *Therapeutic potential of RNA interference against cancer.* Cancer Science, 2006. **97**(8): p. 689-696.
- [19] Ryther, R.C.C., Flynt, A.S., Phillips, J.A., and Patton, J.G., *SiRNA therapeutics: Big potential from small RNAs.* Gene Ther, 2004. **12**(1): p. 5-11.
- [20] Stevenson, M., *Therapeutic potential of RNA interference.* New England JouRNAI of Medicine, 2004. **351**: p. 1772-1777.
- [21] Bouchie, A., *Companies in footrace to deliver RNAi.* Nat Biotechnol, 2012. **30**(12): p. 1154-1157.

- [22] Moran, N., *First gene therapy approved*. Nat Biotechnol, 2012. **30**(12): p. 1153-1153.
- [23] Whitehead, K.A., Langer, R., and Anderson, D.G., *Knocking down barriers: Advances in siRNA delivery*. Nat. Rev. Drug Discovery, 2009. **8**(2): p. 129-138.
- [24] Yuan, F., Thiele, G.M., and Wang, D., *Nanomedicine development for autoimmune diseases*. Drug Dev Res, 2011. **72**(8): p. 703-716.
- [25] Abraham, C. and Cho, J.H., *Inflammatory bowel disease*. N Engl J Med, 2009. **361**: p. 2066-2078.
- [26] Podolsky, D.K., *Inflammatory bowel disease*. N Engl J Med, 2002. **347**: p. 417-429.
- [27] Boirivant, M. and Cossu, A., *Inflammatory bowel disease*. Oral Dis, 2012. **18**(1): p. 1-15.
- [28] Loftus, E.V., Kane, S.V., and Bjorkman, D., *Short-term adverse effects of 5-aminosalicylic acid agents in the treatment of ulcerative colitis*. Aliment Pharm Therap, 2004. **19**(2): p. 179-189.
- [29] Aouadi, M., Tesz, G.J., Nicoloso, S.M., Wang, M., Chouinard, M., Soto, E., Ostroff, G.R., and Czech, M.P., *Orally delivered siRNA targeting macrophage map4k4 suppresses systemic inflammation*. Nature, 2009. **458**(7242): p. 1180-1184.
- [30] Kriegel, C. and Amiji, M., *Oral TNF- α gene silencing using a polymeric microsphere-based delivery system for the treatment of inflammatory bowel disease*. J Controlled Release, 2011. **150**(1): p. 77-86.
- [31] Kriegel, C. and Amiji, M.M., *Dual TNF- α /cyclin d1 gene silencing with an oral polymeric microparticle system as a novel strategy for the treatment of inflammatory bowel disease*. Clin Trans Gastroenterol, 2011. **2**(3): p. e2.
- [32] Wilson, D.S., Dalmasso, G., Wang, L., Sitaraman, S.V., Merlin, D., and Murthy, N., *Orally delivered thioketal nanoparticles loaded with TNF- α -siRNA target inflammation and inhibit gene expression in the intestines*. Nat Mater, 2010. **9**: p. 923-928.

- [33] Laroui, H., Theiss, A.L., Yan, Y., Dalmasso, G., Nguyen, H.T.T., Sitaraman, S.V., and Merlin, D., *Functional TNF- α gene silencing mediated by polyethyleneimine/TNF- α siRNA nanocomplexes in inflamed colon*. Biomaterials, 2011. **32**(4): p. 1218-1228.
- [34] Fasano, A. and Catassi, C., *Current approaches to diagnosis and treatment of celiac disease: An evolving spectrum*. Gastroenterology, 2001. **120**(3): p. 636-651.
- [35] Vader, W., *The hla-dq2 gene dose effect in celiac disease is directly related to the magnitude and breadth of gluten-specific t cell responses*. P Natl Acad Sci USA, 2003. **100**(21): p. 12390-12395.
- [36] Schuppan, D., *Current concepts of celiac disease pathogenesis*. Gastroenterology, 2000. **119**(1): p. 234-242.
- [37] Evans, K.E. and Sanders, D.S., *Celiac disease*. Gastroenterol Clin N, 2012. **41**(3): p. 639-650.
- [38] Fattal, E. and Bochot, A., *State of the art and perspectives for the delivery of antisense oligonucleotides and siRNA by polymeric nanocarriers*. Int. J. Pharm., 2008. **364**(2): p. 237-248.
- [39] Schiffelers, R.M., Woodle, M.C., and Scaria, P., *Pharmaceutical prospects for RNA interference*. Pharm Res, 2003. **21**: p. 1-7.
- [40] Soutschek, J., Akinc, A., Bramlage, B., Charisse, K., Constien, R., Donoghue, M., Elbashir, S., Geick, A., Hadwiger, P., Harborth, J., John, M., Kesavan, V., Lavine, G., Pandey, R.K., Racie, T., Rajeev, K.G., Rohl, I., Toudjarska, I., Wang, G., Wuschko, S., Bumcrot, D., Koteliensky, V., Limmer, S., Manoharan, M., and Vornlocher, H.-P., *Therapeutic silencing of an endogenous gene by systemic administration of modified siRNAs*. Nature, 2004. **432**: p. 173-178.
- [41] Dorsett, Y. and Tuschl, T., *SiRNAs: Applications in functional genomics and potential as therapeutics*. Nat Rev Drug Discovery, 2004. **3**(4): p. 318-329.

- [42] Niidome, T. and Huang, L., *Gene therapy progress and prospects: Nonviral vectors*. Gene Ther., 2002. **9**(24): p. 1647-1652.
- [43] Pecot, C.V., Calin, G.A., Coleman, R.L., Lopez-Berestein, G., and Sood, A.K., *Rna interference in the clinic: Challenges and future directions*. Nat Rev Cancer, 2010. **11**(1): p. 59-67.
- [44] Aigner, A., *Applications of RNA interference: Current state and prospects for siRNA-based strategies in vivo*. Appl Microbiol Biot, 2007. **76**(1): p. 9-21.
- [45] Khalil, I.A., *Uptake pathways and subsequent intracellular trafficking in nonviral gene delivery*. Pharmacological Reviews, 2006. **58**(1): p. 32-45.
- [46] Akinc, A., Thomas, M., Klibanov, A.M., and Langer, R., *Exploring polyethylenimine-mediated DNA transfection and the proton sponge hypothesis*. The JouRNAI of Gene Medicine, 2005. **7**(5): p. 657-663.
- [47] BOUSSIF, O., LEZOUALC'H, F., ZANTA, M.A., MERGNY, M.D., SCHERMAN, D., DEMENEIX, B., and BEHR, J.-P., *A versatile vector for gene and oligonucleotide transfer into cells in culture and in vivo: Polyethylenimine*. P Natl Acad Sci USA, 1995. **92**: p. 7297-7301.
- [48] Wu, G.Y. and Wu, C.H., *Receptor-mediated in vitro gene transformation by a soluble DNA carrier system*. The JouRNAI of Biological Chemistry, 1987. **262**: p. 4429-4432.
- [49] Smedt, S.C.D., Demeester, J., and Hennink, W.E., *Cationic polymer based gene delivery systems*. Pharm Res, 2000. **17**: p. 113-126.
- [50] Merdan, T., Kopecek, J., and Kissel, T., *Prospects for cationic polymers in gene and oligonucleotide therapy against cancer*. Adv Drug Deliver Rev, 2002. **54**: p. 715-758.
- [51] Zhang, S., Zhao, B., Jiang, H., Wang, B., and Ma, B., *Cationic lipids and polymers mediated vectors for delivery of siRNA*. J Controlled Release, 2007. **123**(1): p. 1-10.

- [52] Fisher, O.Z. and Peppas, N.A., *Polybasic nanomatrices prepared by uv-initiated photopolymerization*. *Macromolecules*, 2009. **42**(9): p. 3391-3398.
- [53] Fisher, O.Z., Kim, T., Dietz, S.R., and Peppas, N.A., *Enhanced core hydrophobicity, functionalization and cell penetration of polybasic nanomatrices*. *Pharm Res*, 2009. **26**(1): p. 51-60.
- [54] Liechty, W.B., Scheuerle, R.L., and Peppas, N.A., *Tunable, responsive nanogels containing t-butyl methacrylate and 2-(t-butylamino)ethyl methacrylate*. *Polym*, 2013. **54**(15): p. 3784-3795.
- [55] Forbes, D.C. and Peppas, N.A., *Differences in molecular structure in cross-linked polycationic nanoparticles synthesized using ARGET ATRP or UV-initiated polymerization*. *Polym*, 2013. **54**(17): p. 4486-4492.
- [56] Forbes, D.C., Creixell, M., Frizzell, H., and Peppas, N.A., *Polycationic nanoparticles synthesized using ARGET ATRP for drug delivery*. *Eur J Pharm Biopharm*, 2013. **84**(3): p. 472-478.
- [57] Forbes, D.C. and Peppas, N.A., *Polycationic nanoparticles for siRNA delivery: Comparing ARGET ATRP and UV-initiated formulations*. *ACS Nano*, 2014. **8**: p. 2908-2917.
- [58] Forbes, D.C. and Peppas, N.A., *Polymeric nanocarriers for siRNA delivery to murine macrophages*. *Macromol Biosci*, 2014. **14**(8): p. 1096-1105.
- [59] Lv, H., Zhang, S., Wang, B., Cui, S., and Yan, J., *Toxicity of cationic lipids and cationic polymers in gene delivery*. *J Controlled Release*, 2006. **114**(1): p. 100-109.
- [60] Caldorera-Moore, M.E., Liechty, W.B., and Peppas, N.A., *Responsive theranostic systems: Integration of diagnostic imaging agents and responsive controlled release drug delivery carriers*. *Acc. Chem. Res.*, 2011. **44**: p. 1061-1070.
- [61] Patel, P.C., Hao, L., Au Yeung, W.S., and Mirkin, C.A., *Duplex end breathing determines serum stability and intracellular potency of siRNA-augmented nanoparticles*. *Mol. Pharm.*, 2011. **8**(4): p. 1285-1291.

- [62] Lee, M.-Y., Park, S.-J., Park, K., Kim, K.S., Lee, H., and Hahn, S.K., *Target-specific gene silencing of layer-by-layer assembled gold-cysteamine/siRNA/pe/-ha nanocomplex*. ACS Nano, 2011. **5**: p. 6138-6147.
- [63] Chen, A.A., Derfus, A.M., Khetani, S.R., and Bhatia, S.N., *Quantum dots to monitor RNAi delivery and improve gene silencing*. Nucleic Acids Res., 2005. **33**(22): p. e190-e190.
- [64] Tan, W.B., Jiang, S., and Zhang, Y., *Quantum-dot based nanoparticles for targeted silencing of her2/neu gene via RNA interference*. Biomaterials, 2007. **28**(8): p. 1565-1571.
- [65] Duan, H. and Nie, S., *Cell-penetrating quantum dots based on multivalent and endosome-disrupting surface coatings*. J. Am. Chem. Soc., 2007. **129**: p. 3333-3338.
- [66] Yezhelyev, M.V., Qi, L., O'Regan, R.M., Nie, S., and Gao, X., *Proton-sponge coated quantum dots for siRNA delivery*. J. Am. Chem. Soc., 2008. **130**: p. 9006-9012.
- [67] Li, J.-M., Zhao, M.-X., Su, H., Wang, Y.-Y., Tan, C.-P., Ji, L.-N., and Mao, Z.-W., *Multifunctional quantum-dot-based siRNA delivery for hpv18 e6 gene silence and intracellular imaging*. Biomaterials, 2011. **32**(31): p. 7978-7987.
- [68] Selvin, P.R., *The renaissance of fluorescence resonance energy transfer*. Nat. Struct. Mol. Biol., 2000. **7**: p. 730-734.
- [69] Lee, H., Kim, I.-K., and Park, T.G., *Intracellular trafficking and unpacking of siRNA/quantum dot-pei complexes modified with and without cell penetrating peptide: Confocal and flow cytometric fret analysis*. Bioconjugate Chem., 2010. **21**: p. 289-295.
- [70] Qi, L. and Gao, X., *Quantum dot-amphipol nanocomplex for intracellular delivery of real-time imaging of siRNA*. ACS Nano, 2008. **2**: p. 1403-1410.

- [71] Shaheen, S.M., Akita, H., Yamashita, A., Katoono, R., Yui, N., Biju, V., Ishikawa, M., and Harashima, H., *Quantitative analysis of condensation/decondensation status of pdna in the nuclear sub-domains by qd-fret*. Nucleic Acids Res., 2011. **39**(7): p. e48-e48.
- [72] Ho, Y.-P., Chen, H.H., Leong, K.W., and Wang, T.-H., *Evaluating the intracellular stability and unpacking of DNA nanocomplexes by quantum dots-fret*. J. Controlled Release, 2006. **116**(1): p. 83-89.
- [73] Biju, V., Anas, A., Akita, H., Shibu, E.S., Itoh, T., Harashima, H., and Ishikawa, M., *Fret from quantum dots to photodecompose undesired acceptors and report the condensation and decondensation of plasmid DNA*. ACS Nano, 2012. **6**: p. 3776-3788.
- [74] Wu, Y., Ho, Y.-P., Mao, Y., Wang, X., Yu, B., Leong, K.W., and Lee, L.J., *Uptake and intracellular fate of multifunctional nanoparticles: A comparison between lipoplexes and polyplexes via quantum dot mediated förster resonance energy transfer*. Mol. Pharm., 2011. **8**(5): p. 1662-1668.
- [75] Zhang, B., Zhang, Y., Mallapragada, S.K., and Clapp, A.R., *Sensing polymer/DNA polyplex dissociation using quantum dot fluorophores*. ACS Nano, 2011. **5**: p. 129-138.
- [76] *Clinicaltrials.Gov*. 2012.
- [77] Peppas, N.A., Bures, P., Leobandung, W., and Ichikawa, H., *Hydrogels in pharmaceutical formulations*. Eur J Pharm Biopharm, 2000. **50**: p. 27-46.
- [78] Xu, J., Ganesh, S., and Amiji, M., *Non-condensing polymeric nanoparticles for targeted gene and siRNA delivery*. Int J Pharm, 2012. **427**(1): p. 21-34.
- [79] Forbes, D.C. and Peppas, N.A., *Oral delivery of small RNA and DNA*. J. Controlled Release, 2012. **162**(2): p. 438-445.
- [80] Kriegel, C., Attarwala, H., and Amiji, M., *Multi-compartmental oral delivery systems for nucleic acid therapy in the gastrointestinal tract*. Adv Drug Deliver Rev, 2013. **65**(6): p. 891-901.

- [81] Xiao, B. and Merlin, D., *Oral colon-specific therapeutic approaches toward treatment of inflammatory bowel disease*. Expert Opin Drug Deliv, 2012. **9**: p. 1393-1407.
- [82] Bhavsar, M.D. and Amiji, M.M., *Development of novel biodegradable polymeric nanoparticles-in-microsphere formulation for local plasmid DNA delivery in the gastrointestinal tract*. AAPS PharmSciTech, 2008. **9**(1): p. 288-294.
- [83] Bhavsar, M.D., Tiwari, S.B., and Amiji, M.M., *Formulation optimization for the nanoparticles-in-microsphere hybrid oral delivery system using factorial design*. J Controlled Release, 2006. **110**(2): p. 422-430.
- [84] Zhao, X., Yin, L., Ding, J., Tang, C., Gu, S., Yin, C., and Mao, Y., *Thiolated trimethyl chitosan nanocomplexes as gene carriers with high in vitro and in vivo transfection efficiency*. J Controlled Release, 2010. **144**(1): p. 46-54.
- [85] Zhang, J., He, C., Tang, C., and Yin, C., *TeRNary polymeric nanoparticles for oral siRNA delivery*. Pharm Res, 2013. **30**(5): p. 1228-1239.
- [86] He, C., Yin, L., Tang, C., and Yin, C., *Trimethyl chitosan-cysteine nanoparticles for systemic delivery of TNF- α siRNA via oral and intraperitoneal routes*. Pharm Res, 2013. **30**(10): p. 2596-2606.
- [87] He, C., Yin, L., Tang, C., and Yin, C., *Multifunctional polymeric nanoparticles for oral delivery of TNF- α siRNA to macrophages*. Biomaterials, 2013. **34**(11): p. 2843-2854.
- [88] Ballarín-González, B., Dagnaes-Hansen, F., Fenton, R.A., Gao, S., Hein, S., Dong, M., Kjems, J., and Howard, K.A., *Protection and systemic translocation of siRNA following oral administration of chitosan/siRNA nanoparticles*. Mol Ther Nucleic Acids, 2013. **2**(3): p. e76.
- [89] Al-Deen, F.N., Ho, J., Selomulya, C., Ma, C., and Coppel, R., *Superparamagnetic nanoparticles for effective delivery of malaria DNA vaccine*. Langmuir, 2011. **27**(7): p. 3703-3712.

- [90] Kumar, A., Jena, P.K., Behera, S., Lockey, R.F., Mohapatra, S., and Mohapatra, S., *Multifunctional magnetic nanoparticles for targeted delivery*. Nanomedicine: Nanotechnology, Biology and Medicine, 2010. **6**(1): p. 64-69.
- [91] Zhang, H., Lee, M.-Y., Hogg, M.G., Dordick, J.S., and Sharfstein, S.T., *Gene delivery in three-dimensional cell cultures by superparamagnetic nanoparticles*. ACS Nano, 2010. **4**(8): p. 4733-4743.
- [92] Taratula, O., *Multifunctional nanomedicine platform for cancer specific delivery of siRNA by superparamagnetic iron oxide nanoparticles-dendrimer complexes*. Current Drug Delivery, 2011. **2011**(8): p. 59-69.
- [93] Pan, B., Cui, D., Sheng, Y., Ozkan, C., Gao, F., He, R., Li, Q., Xu, P., and Huang, T., *Dendrimer-modified magnetic nanoparticles enhance efficiency of gene delivery system*. Cancer Research, 2007. **67**(17): p. 8156-8163.
- [94] Kievit, F.M., Veisheh, O., Fang, C., Bhattarai, N., Lee, D., Ellenbogen, R.G., and Zhang, M., *Chlorotoxin labeled magnetic nanovectors for targeted gene delivery to glioma*. ACS Nano, 2010. **4**(8): p. 4587-4594.
- [95] Cutler, J.I., Zheng, D., Xu, X., Giljohann, D.A., and Mirkin, C.A., *Polyvalent oligonucleotide iron oxide nanoparticle "click" conjugates*. Nano Letters, 2010. **10**(4): p. 1477-1480.
- [96] Arsianti, M., Lim, M., Marquis, C.P., and Amal, R., *Polyethylenimine based magnetic iron-oxide vector: The effect of vector component assembly on cellular entry mechanism, intracellular localization, and cellular viability*. Biomacromolecules, 2010. **11**(9): p. 2521-2531.
- [97] Kumar, M., Yigit, M., Dai, G., Moore, A., and Medarova, Z., *Image-guided breast tumor therapy using a small interfering RNA nanodrug*. Cancer Research, 2010. **70**(19): p. 7553-7561.
- [98] Namiki, Y., Namiki, T., Yoshida, H., Ishii, Y., Tsubota, A., Koido, S., Nariai, K., Mitsunaga, M., Yanagisawa, S., Kashiwagi, H., Mabashi, Y., Yumoto, Y., Hoshina, S., Fujise, K., and Tada, N., *A novel magnetic crystal-lipid*

- nanostructure for magnetically guided in vivo gene delivery*. Nat Nano, 2009. **4**(9): p. 598-606.
- [99] Pan, X., Guan, J., Yoo, J.-W., Epstein, A.J., Lee, L.J., and Lee, R.J., *Cationic lipid-coated magnetic nanoparticles associated with transferrin for gene delivery*. InterNAtional JouRNAI of Pharmaceutics, 2008. **358**(1-2): p. 263-270.
- [100] Biswas, S., Gordon, L.E., Clark, G.J., and Nantz, M.H., *Click assembly of magnetic nanovectors for gene delivery*. Biomaterials, 2011. **32**(10): p. 2683-2688.
- [101] Park, J.S., Na, K., Woo, D.G., Yang, H.N., Kim, J.M., Kim, J.H., Chung, H.-M., and Park, K.-H., *Non-viral gene delivery of DNA polyplexed with nanoparticles transfected into human mesenchymal stem cells*. Biomaterials, 2010. **31**(1): p. 124-132.
- [102] Kami, D., Takeda, S., Makino, H., Toyoda, M., Itakura, Y., Gojo, S., Kyo, S., Umezawa, A., and Watanabe, M., *Efficient transfection method using deacylated polyethylenimine-coated magnetic nanoparticles*. JouRNAI of Artificial Organs, 2011. **14**(3): p. 215-222.
- [103] Geinguenaud, F., Souissi, I., Fagard, R., Motte, L., and Lalatonne, Y., *Electrostatic assembly of a DNA superparamagnetic nano-tool for simultaneous intracellular delivery and in situ monitoring*. Nanomedicine: Nanotechnology, Biology and Medicine, (0).
- [104] Zhou, Y., Tang, Z., Shi, C., Shi, S., Qian, Z., and Zhou, S., *Polyethylenimine functionalized magnetic nanoparticles as a potential non-viral vector for gene delivery*. JouRNAI of Materials Science: Materials in Medicine: p. 1-12.
- [105] del Pino, P., Munoz-Javier, A., Vlaskou, D., Rivera Gil, P., Plank, C., and Parak, W.J., *Gene silencing mediated by magnetic lipospheres tagged with small interfering RNA*. Nano Letters, 2010. **10**(10): p. 3914-3921.
- [106] Qian, J., Jiang, L., Cai, F., Wang, D., and He, S., *Fluorescence-surface enhanced raman scattering co-functionalized gold nanorods as near-infrared probes for purely optical in vivo imaging*. Biomaterials, 2011. **32**(6): p. 1601-1610.

- [107] Jeong, S., Choi, S.Y., Park, J., Seo, J.-H., Park, J., Cho, K., Joo, S.-W., and Lee, S.Y., *Low-toxicity chitosan gold nanoparticles for small hairpin RNA delivery in human lung adenocarcinoma cells*. J. Mater. Chem., 2011. **21**(36): p. 13853.
- [108] Huschka, R., Neumann, O., Barhoumi, A., and Halas, N.J., *Visualizing light-triggered release of molecules inside living cells*. Nano Lett., 2010. **10**(10): p. 4117-4122.
- [109] Huschka, R., Barhoumi, A., Liu, Q., Roth, J.A., Ji, L., and Halas, N.J., *Gene silencing by gold nanoshell-mediated delivery and laser-triggered release of antisense oligonucleotide and siRNA*. ACS Nano, 2012. **6**: p. 7681-7691.
- [110] Braun, G.B., Pallaoro, A., Wu, G., Missirlis, D., Zasadzinski, J.A., Tirrell, M., and Reigh, N.O., *Laser-activated gene silencing via gold nanoshell-siRNA conjugates*. ACS Nano, 2009. **3**: p. 2007-2015.
- [111] Hao, L., Patel, P.C., Alhasan, A.H., Giljohann, D.A., and Mirkin, C.A., *Nucleic acid-gold nanoparticle conjugates as mimics of microRNA*. Small, 2011. **7**(22): p. 3158-3162.
- [112] Reynolds, J.L., Law, W.C., Mahajan, S.D., Aalinkeel, R., Nair, B., Sykes, D.E., Yong, K.-T., Hui, R., Prasad, P.N., and Schwartz, S.A., *Nanoparticle based galectin-1 gene silencing, implications in methamphetamine regulation of hiv-1 infection in monocyte derived macrophages*. J. Neuroimmune Pharmacol., 2012. **7**(3): p. 673-685.
- [113] Ng, C.-T., Dheen, S.T., Yip, W.-C.G., Ong, C.-N., Bay, B.-H., and Lanry Yung, L.-Y., *The induction of epigenetic regulation of pros1 gene in lung fibroblasts by gold nanoparticles and implications for potential lung injury*. Biomaterials, 2011. **32**(30): p. 7609-7615.
- [114] Kim, E.Y., Schulz, R., Swantek, P., Kunstman, K., Malim, M.H., and Wolinsky, S.M., *Gold nanoparticle-mediated gene delivery induces widespread changes in the expression of innate immunity genes*. Gene Ther., 2011. **19**(3): p. 347-353.

- [115] Liang, Z., Liu, Y., Li, X., Wu, Q., Yu, J., Luo, S., Lai, L., and Liu, S., *Surface-modified gold nanoshells for enhanced cellular uptake*. J Biomed Mater Res A, 2011. **98A**(4): p. 479-487.
- [116] Derfus, A.M., Chen, A.A., Min, D., Ruoslahti, E., and Bhatia, S.N., *Targeted quantum dot conjugates for siRNA delivery*. Bioconjugate Chem., 2007. **18**: p. 1391-1396.
- [117] Jung, J., Solanki, A., Memoli, K.A., Kamei, K.-i., Kim, H., Drahl, M.A., Williams, L.J., Tseng, H.-R., and Lee, K., *Selective inhibition of human brain tumor cells through multifunctional quantum-dot-based siRNA delivery*. Angew. Chem., Int. Ed. Engl., 2010. **49**(1): p. 103-107.
- [118] Li, Y., Duan, X., Jing, L., Yang, C., Qiao, R., and Gao, M., *Quantum dot-antisense oligonucleotide conjugates for multifunctional gene transfection, mRNA regulation, and tracking of biological processes*. Biomaterials, 2011. **32**(7): p. 1923-1931.
- [119] Li, S., Liu, Z., Ji, F., Xiao, Z., Wang, M., Peng, Y., Zhang, Y., Liu, L., Liang, Z., and Li, F., *Delivery of quantum dot-siRNA nanoplexes in sk-n-sh cells for bace1 gene silencing and intracellular imaging*. Mol. Ther. Nucleic Acids, 2012. **1**(4): p. e20.
- [120] Klein, S., Zolk, O., Fromm, M.F., Schrödl, F., Neuhuber, W., and Kryschi, C., *Functionalized silicon quantum dots tailored for targeted siRNA delivery*. Biochem. Biophys. Res. Commun., 2009. **387**(1): p. 164-168.
- [121] Knipe, J.M., Peters, J.T., and Peppas, N.A., *Theranostic agents for intracellular gene delivery with spatiotemporal imaging*. Nano Today, 2013. **8**(1): p. 21-38.

Chapter 4: Research Objectives

A multi-component hydrogel system is needed to harness the potential of siRNA as a gene silencing therapeutic while overcoming the challenges of oral delivery of siRNA. A combination of “intelligent” pH-responsive behavior of ionic polymers, mechanical integrity and hydrophilicity of hydrogel networks, and targeted oral delivery strategies was employed to create a novel, two-component oral delivery strategy for siRNA. The objectives of this research were to:

1. Design, synthesize, and characterize microgel matrices that are capable of encapsulating and protecting polycationic nanogels upon exposure to gastric conditions;
2. Impart multi-responsive behavior in the microencapsulation system in the form of swelling and/or degradation in response to pH and/or enzyme concentration, which is capable of triggering release of polycationic nanogels in intestinal conditions; and
3. Achieve loading and intracellular delivery of stable siRNA that is capable of inducing gene knockdown in an *in vitro* cell model.

The multi-component system was a collaborative effort comprised of a polyanionic microgel matrix encapsulating polycationic nanogels. The synthesis and characterization of the encapsulated polycationic nanoparticles prepared by copolymerization of 2-(diethylamino)ethyl methacrylate with tert-butyl methacrylate and grafted with poly(ethylene glycol) were investigated in great detail by Drs. William B. Liechty and Diane C. Forbes within the Peppas laboratory. These researchers demonstrated the effect of molecular structure and physicochemical properties on the

ability of the nanogels to complex with siRNA, cross the cell membrane, promote endosomal escape, and induce gene silencing [1-5].

The focus of the body of work herein is the development of a microgel matrix designed to protect polycationic nanogels and siRNA through gastric conditions and release the nanogels upon exposure to intestinal conditions for cellular internalization and siRNA delivery, depicted schematically in Figure 4.1. The polyanionic microgels were synthesized using methacrylic acid (MAA) copolymerized with *N*-vinylpyrrolidone (NVP) and covalently crosslinked with poly(ethylene glycol) dimethacrylate (PEGDMA), tetra(ethylene glycol) dimethacrylate (TEGDMA), or a biodegradable crosslinking agent. Structures of the monomers are shown in Figure 4.2. Synthesis and characterization of the microgel systems were completed for formulations with varying amounts of incorporated polycationic nanoparticles and different crosslinking agents. Formulations capable of releasing nanogels were evaluated *in vitro* to evaluate simulated oral delivery performance, cytocompatibility, and cell uptake and gene silencing ability.

The following specific aims were addressed within this research:

Specific Aim 1: Develop, characterize, and compare varying formulations of microencapsulation systems;

Specific Aim 2: Incorporate a biodegradable crosslinking agent into the matrix network;

Specific Aim 3: Evaluate and optimize release of polycationic nanoparticles from the system in response to pH and/or simulated gastrointestinal conditions; and

Specific Aim 4: Investigate siRNA gene silencing efficiency of the best performing microencapsulation system using cell models.

Two-Part Oral Delivery Scheme

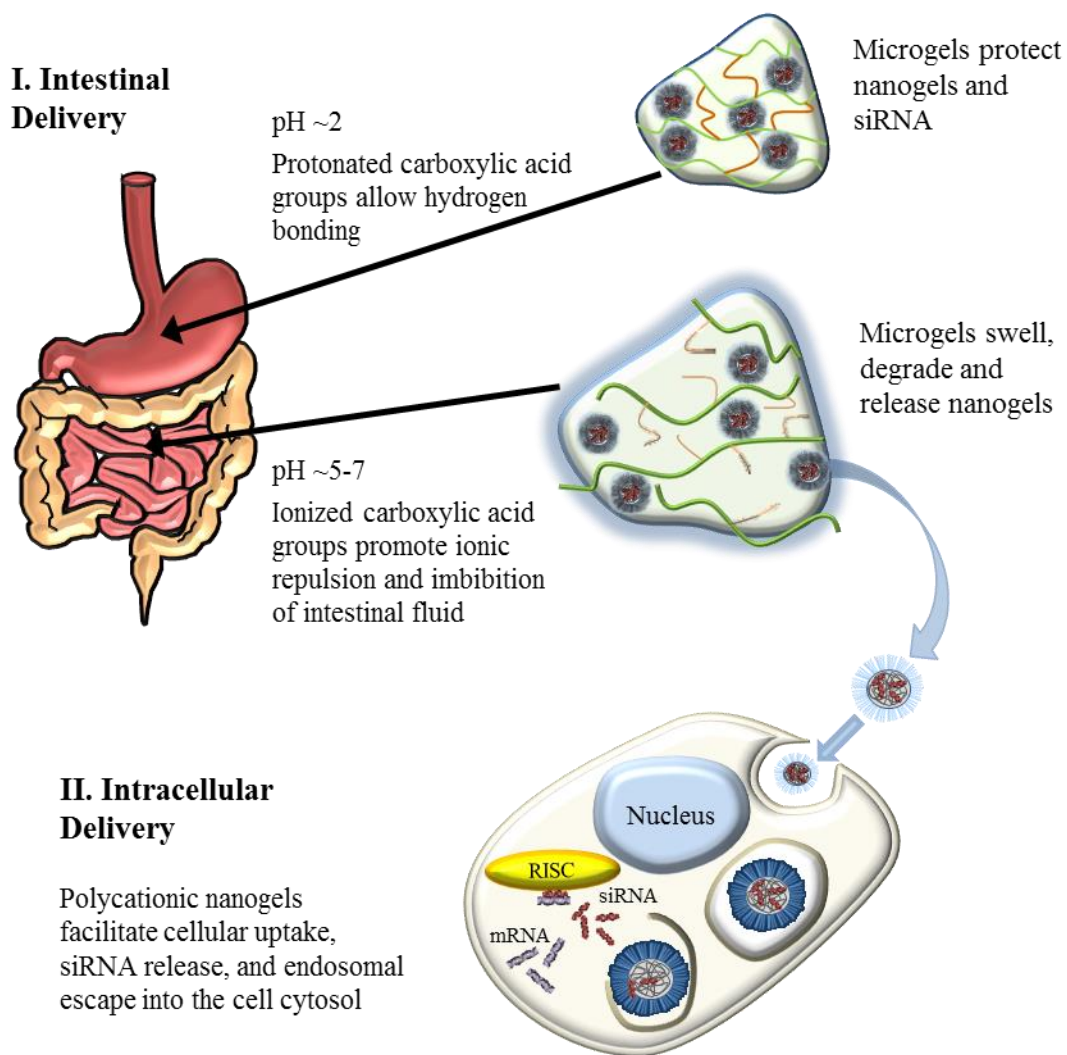


Figure 4.1: Schematic of the two-part microencapsulated-nanogel system for the oral delivery of siRNA I) to the intestine and II) to the cell cytosol.

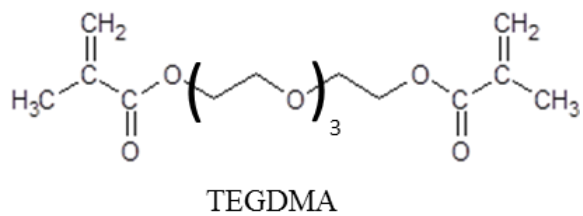
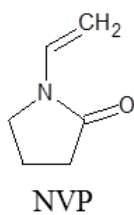
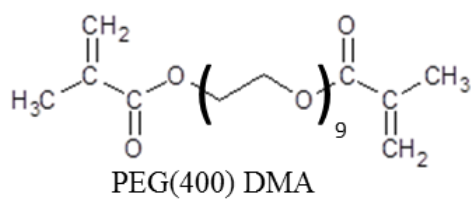
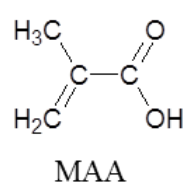


Figure 4.2: Structures of monomers used in the anionic hydrogel synthesis.

REFERENCES

- [1] Liechty, W.B., Scheuerle, R.L., and Peppas, N.A., Tunable, responsive nanogels containing *t*-butyl methacrylate and 2-(*t*-butylamino)ethyl methacrylate. *Polym*, 2013. 54(15): p. 3784-3795.
- [2] Forbes, D.C., Creixell, M., Frizzell, H., and Peppas, N.A., Polycationic nanoparticles synthesized using ARGET ATRP for drug delivery. *Eur J Pharm Biopharm*, 2013. 84(3): p. 472-478.
- [3] Forbes, D.C. and Peppas, N.A., Differences in molecular structure in cross-linked polycationic nanoparticles synthesized using ARGET ATRP or UV-initiated polymerization. *Polym*, 2013. 54(17): p. 4486-4492.
- [4] Forbes, D.C. and Peppas, N.A., Polymeric nanocarriers for siRNA delivery to murine macrophages. *Macromol Biosci*, 2014. 14(8): p. 1096-1105.
- [5] Forbes, D.C. and Peppas, N.A., Polycationic nanoparticles for siRNA delivery: Comparing ARGET ATRP and UV-initiated formulations. *ACS Nano*, 2014. 8: p. 2908-2917.

Chapter 5: Non-degradable Crosslinked Microgels Encapsulating Polycationic Nanogels²

5.1 INTRODUCTION

Stimuli responsive hydrogels are three-dimensional, crosslinked polymer networks that respond in an intelligent manner to environmental changes such as pH, temperature, or analyte concentration while maintaining structural integrity [1, 2]. Stimuli responsive hydrogels may exhibit change in shape, surface characteristics, solubility, permeability, mechanical strength, or molecular self-assembly [2, 3]. The specific response of the polymer network may be controlled by incorporation of functionalities such as chain side groups, branches, and crosslinks [1].

In the case of pH responsive hydrogels, the polymer network contains weak acid or base pendant groups that become ionized as a function of pH, ionic strength, and ionic composition, among other factors [4]. Additionally, changes in the pH of the environment will affect the porosity of the hydrogel; polyanionic hydrogels will be deswollen at low pH and swollen at high pH while the opposite is true for polycationic hydrogels [5]. These polymers are categorized as polyelectrolytes when they contain many ionizable pendant groups [6].

These hydrogels have been studied for a number of applications, including controlled drug delivery [5-10], biosensors [11-13], tissue engineering [14, 15], catalysis [16, 17], and separations [18, 19]. Such polyelectrolytes may be used within separation processes [10] as semipermeable membranes for counter-ions [1] or to separate and

² Knipe, J., Chen, F. and Peppas, N. *Multiresponsive polyanionic microgels with inverse pH responsive behavior by encapsulation of polycationic nanogels*. J. Appl. Polym. Sci., 2014. 131: p. 40098. Knipe was the primary contributor, while Chen contributed to certain experiments and Peppas oversaw the project.

recover target proteins by phase separation or sorption by electrostatic or hydrophilic interactions [20-22].

Recent developments with “intelligent” hydrogels have focused on the combination of multiple responsive properties to achieve a unique physiochemical response for specific applications [23-26]. In many instances, this hybrid is achieved by incorporating nanoparticles within polyelectrolytes [17, 27]. These hybrid morphologies, such as multilayer and core-shell particles, are promising tools for drug delivery, theranostics, and binding and immobilization of proteins [28-32].

In this study, we show the facile synthesis and characterization of polycationic nanogels encapsulated within polyanionic microgels. Previously within our lab, hydrophilic microgels with domains of hydrophobic nanogels were developed for the delivery of hydrophobic chemotherapeutics [27]. Building upon this idea, polycationic nanogels were incorporated into the polymerization of polyanionic microgels to achieve a system encompassing inverse pH responsive behavior. Basic polymer characterization, including scanning electron microscopy (SEM), Fourier transform infrared spectroscopy (FTIR), and thermal gravimetric analysis (TGA) was completed. Additionally, the pH response was evaluated by dynamic and equilibrium swelling experiments as a function of pH as well as potentiometric titration. A cell proliferation assay and protein/small molecule loading and release were determined for drug delivery or protein separation applications.

5.2 EXPERIMENTAL METHODS

5.2.1 Chemicals

Methacrylic acid (MAA), *N*-vinyl-2-pyrrolidone (NVP), and tetra(ethylene glycol) dimethacrylate (TEGDMA) were obtained from Sigma-Aldrich (St. Louis, MO).

Poly(ethylene glycol) (400) dimethacrylate (PEGDMA) was purchased from Polysciences, Inc. (Warrington, PA). Irgacure 184[®] (1-hydroxy-cyclohexyl-phenylketone) was purchased from Sigma-Aldrich. All reagents were used as received. Polycationic nanogels were synthesized as described previously [8, 33].

5.2.2 Synthesis of P(MAA-*co*-NVP) Hydrogels

P(MAA-*co*-NVP) hydrogels were synthesized by photoinitiated, free-radical polymerization. MAA and NVP were added at a 1:1 molar ratio to a 1:1 (w/w) deionized water and ethanol solution to yield a 1:1 (w/w) total monomer to solvent ratio. Polycationic nanogels were added to the solution at 0, 1, 2, or 5 wt% with respect to total monomer weight. One of two crosslinking agents, TEGDMA or PEGDMA, was added at 1 mol% of the total monomer molar content. Photoinitiator Irgacure 184[®] was added at 1 wt% with respect to total monomer weight.

The mixture was homogenized by sonication, then loaded into a sealed glove box (MBraun, Garching, Germany). The solution was purged with nitrogen for 10 minutes, then pipetted between glass slides (150 x 150 x 3 mm³) separated by a Teflon spacer (0.7 mm). The plates were exposed to UV light (Dymax 2000-EC Light Curing System, Torrington, CT) at 70% intensity and allowed to polymerize for 30 minutes. Following polymerization, the film was removed from the slides and purified from unreacted reagents in deionized water for 7 days with daily water changes. The purified film was dried under vacuum at 30°C for two days. The dried film was crushed into particles less than 75 µm in size using a mortar and pestle and stored in a dessicator at room temperature.

5.2.3 Characterization

5.2.3.1 Scanning Electron Microscopy

SEM samples were prepared by dusting carbon tape-covered aluminum stubs with vacuum-dried, crushed microgels. The samples were coated with 12-15 nm of Pt/Pd coating using a Cressington 208 Benchtop sputter coater (Watford, England). Scanning electron microscopy images were obtained using an FEI Quanta 650 FEG scanning electron microscope (Hillsboro, OR).

5.2.3.2 Fluorescent Microscopy

Polycationic nanogels were reacted with 4-chloro-7-nitrobenzofurazan (NBD-Cl, 98%) (Sigma-Aldrich), which generates a fluorescent product upon reaction with amines present on the surface of the nanogels. Nanogel presence within the microgels was then confirmed using a Zeiss Axiovert 200 M fluorescence microscope (Thornwood, NY).

5.2.3.3 Fourier Transform Infrared Spectroscopy

Fourier transform infrared spectroscopy (FTIR) spectra for each sample were obtained using a Thermo Mattson Infinity Gold spectrometer (Thermo Fisher Scientific Inc., Waltham, MA). Samples were pressed in KBr (Sigma-Aldrich) disks. For all formulations background spectra was subtracted from the sample spectra. Copolymer compositions were calculated using a standard band of 650 cm^{-1} according to the calculation procedure reported previously [34]. Characteristic absorption bands of 1290 cm^{-1} and 2983 cm^{-1} were used as analytical bands for NVP and MAA, respectively.

5.2.3.4 Thermogravimetric Analysis

Thermogravimetric analysis (TGA) was performed using a Mettler-Toledo TGA/DSC 1 (Columbus, OH). Samples were loaded in aluminum oxide crucibles.

Temperature increased from 40-600°C at a rate of 10°C/minute under nitrogen flowing at 50 ml/min.

5.2.3.5 Swelling Studies

Dynamic swelling studies were carried out in 0.1 M 3,3-dimethylglutaric acid/NaOH buffers ranging in pH from 3.2-7.6; pH 1.2 and 2.2 buffers were achieved using 3,3-dimethylglutaric acid/HCl and were stable during the relevant timescale. All buffers had an ionic strength of 0.1 M by addition of NaCl and were heated to 37°C. Hydrogel disks of 10 mm in diameter were stepped through each buffer from lowest to highest pH, spending 10 minutes in each buffer. The weights of the disks were measured between each buffer.

Equilibrium swelling studies were completed using a 0.1 N HCl solution and pH 7.4 phosphate buffered saline (PBS) solution. Hydrogel disks of 10 mm in diameter were placed in 37°C low pH solution for 24 hours, weighed in air and a nonsolvent, heptane, then placed in 37°C high pH buffer for 24 hours. At the conclusion of the study, the disks were again weighed in air and heptane.

5.2.3.6 Potentiometric Titration

To determine the MAA content of the hydrogels, a 3.5 mg/ml solution of microgels in deionized water was titrated to pH 11.5 using 0.2 N NaOH (standardized with potassium hydrogen phthalate) at 25°C with constant stirring. pH was measured with a Mettler-Toledo SevenEasy™ (Columbus, OH) pH probe and was recorded when the pH reached a steady value (± 0.01 pH units in three consecutive measurements over 5 minutes). The equivalence point was used in conjunction with a charge balance to determine the amount of MAA present in each formulation.

5.2.3.7 Cytotoxicity Study

The cytotoxic effect of the microgels was evaluated using a CellTiter 96® Aqueous One Solution Cell Proliferation Assay (Promega, Madison, WI). Microgel concentrations ranged from 1.25-10 mg/ml in DMEM without phenol red; studies were completed with human colon adenocarcinoma Caco-2, mucus-secreting HT29-MTX, and murine fibroblast L929 cells. Cells were incubated with microgels for two hours at 37°C and 5% CO₂, and then the microgel solution was removed. MTS assay was added to the wells and incubated for 90 minutes at the same conditions before absorbance measurements were made at 490 nm using a Bio-Tek Synergy™ HT multi-mode plate reader (Winooski, VT).

Caco-2 and L929 cells were obtained from American Type Culture Collection (ATCC, Rockwell, MD) and HT29-MTX cells, a sub-population of HT29 cells that were adapted to 10⁻⁶ M methotrexate (MTX) [35], were a gift from Dr. Thecla Lesuffleur, INSERM, Paris, France. All cell lines were cultured in Dulbecco's modified Eagle medium (DMEM) (Mediatech, Herndon, VA) supplemented with 10% heat-inactivated fetal bovine serum (Cambrex, East Rutherford, NJ), 1% non-essential amino acids (Mediatech), 100 U/ml penicillin, and 100 µg/ml streptomycin (Mediatech).

5.2.3.8 Loading and Release Studies

Microgels were loaded by equilibrium partitioning post-synthesis with two models, bovine serum albumin (BSA) (Sigma-Aldrich) and FITC-dextran (MW 3,000-5,000, Sigma-Aldrich). Microgels were incubated at 37°C overnight in a 0.5 mg/mL BSA or FITC-dextran solution of pH ~5.5 at a ratio of 7:1 microgel:therapeutic by weight. The microgels were then collapsed by addition of 1 N HCl, followed by a wash with 0.2 N HCl and recovery by vacuum filtration. The microgels were lyophilized and stored in a

dessicator. Protein loading was evaluated with a MicroBCA assay (Pierce-Thermo, Rockford, IL)) and FITC-dextran loading by fluorescence.

Release studies were completed in pH 7.4 PBS buffer at 37°C at a microgel concentration of 0.6 mg/mL buffer. Samples were taken at 0, 5, 10, 15, 30, 60, and 120 minutes. Protein or FITC-dextran concentration was evaluated in the same manner as the loading study.

5.3 RESULTS AND DISCUSSION

Eight different formulations were synthesized, as listed in Table 5.1. Nanogel weight percent is the feed percentage. The formulations will be referred to henceforth by their descriptive name in Table 5.1. All films had an opaque appearance and were glassy and brittle when dry at room temperature.

5.3.1 Microgel Morphology

Hydrogel films were dried and crushed into microgels resembling a fine, white powder. SEM images of dried microgels, as seen in Figure 5.1, showed the wide polydispersity of size and morphology attributed to the crushing of the hydrogel film. At least two dimensions of the microgels are less than 75 μm as ensured by the sieving process, but other dimension of the microgel may vary due to the inability to control particle size and shape during the crushing of the film. In comparing Figure 5.1A and 5.1D, there is no observable distinction of the nanogels within the microgel. There is also no noticeable difference in morphology between the TEGDMA and PEGDMA crosslinking agents, shown in Figure 5.1A and 5.1C, respectively.

To confirm the nanogels remain within the microgels throughout synthesis and purification, the nanogels were labeled with NBD-Cl, which binds to primary amines present on the surface of the nanogels. Upon reaction with the amine the NBD-Cl

becomes a fluorescent compound ($\gamma_{\text{ex}}=464$ nm, $\gamma_{\text{em}}=512$ nm), effectively labeling the nanogels [36]. Fluorescent microscopy was used to evaluate the fluorescence of microgels containing 0 and 5 wt% nanogels before and after reaction with NBD-Cl. As shown in Figure 5.2, microgels containing no particles exhibited only a background level of fluorescence, while there was a definite increase in the fluorescence intensity of microgels containing 5 wt% nanogels after reacting with NBD-Cl.

5.3.2 FT-IR Spectroscopic Analysis

The FTIR spectra for all formulations are shown in Figure 5.3. The characteristic IR band of the nanogels was indistinguishable as it was masked by the wide band in the 2800-3100 cm^{-1} range attributed to the stretching mode of hydrogen-bonded carboxylic acid dimers [37]. However, several important bands appear in the 1200-2000 cm^{-1} range, shown in Figure 5.3. In the carbonyl stretching region, the band at 1700 cm^{-1} is attributed to the carbonyl of the carboxylic acid, and the band at 1725 cm^{-1} is indicative of complexation between the hydroxyl group of the acid and carbonyl of the PNVP [37]. Similarly, the stretching band at 1680 cm^{-1} is attributed to the carbonyl of PNVP and is shifted to 1640 cm^{-1} when hydrogen bonding is present [38]. The band at 1290 cm^{-1} is ring C-N stretching coupled with ring CH_2 wagging in PNVP [38].

Using the reported reactivity ratios of $r_1=0.56$ and $r_2=0.04$ for MAA and NVP respectively [39], an equimolar feed ratio of MAA:NVP should result in an approximately alternating structure of 60:40 MAA:NVP as calculated by the copolymer equation. Copolymer molar compositions were calculated based on peak absorbance relative to a standard band absorbance [34]. Using this method, the calculated molar ratios were comparable to the theoretical compositions, as shown in Table 5.2. As the copolymer equation does not take into account the effect of the crosslinking agent, the

calculated values are reasonable. The incorporation of nanogels into the feed appears to have little to no effect on reactivity.

5.3.3 TGA Analysis

The TGA results from the TEGDMA microgels are shown in Figure 5.4A and the PEGDMA microgels in Figure 5.4B. TGA indicated that all formulations have a similar degradation profile, suggesting the same degradation mechanism. The first stage of degradation, beginning at about 60°C and accounting for approximately 6% weight loss, may be attributed to the loss of water and smaller molecules or oligomers [40]. The second stage of degradation begins at about 160-175°C and accounts for up to 5% weight loss. This loss is likely anhydride formation and some decarboxylation within the MAA, resulting in release of water and carbon dioxide [41]. It is interesting to note that this loss occurs at higher temperatures relative to that of pure PMAA, as has been observed by Polacco et al. with PMAA/PVP complexes [42]. The nanogels undergo significant degradation in this region, which may also contribute to the weight loss. The transition occurred approximately 10°C earlier in gels with PEGDMA crosslinker than in gels with TEGDMA crosslinker. The crosslinker likely affects intramolecular bonding within the gel, causing variances in stability as a function of temperature. All formulations showed massive degradation from 300-500°C, with a maximum at about 430°C. This is a result of the decomposition of the polymer backbone primarily into monomer units, but also some oligomers [40, 42].

5.3.4 Swelling Studies

Dynamic swelling studies were conducted to evaluate the hydrogels' response to pH variation on a short time scale (10 min/buffer). Weight swelling ratios were calculated

using Equation 1, where W_D is the dry weight of the hydrogel disk and W_S is the swollen weight.

$$q = \frac{W_S}{W_D} \quad (5.1)$$

As shown in Figures 5.5A and 5.5B, all formulations exhibit an increase in weight swelling ratio at pH values greater than ~ 5 , which is expected as the pKa of methacrylic acid is approximately 4.8 [43]. Beyond the pKa of MAA, the carboxylic acid groups are ionized, and ionic repulsion drives the swelling of the hydrogel to weight swelling ratios ranging from 1.3-1.6. It was especially important to confirm that the hydrogels do not swell prematurely at low pH, which is a concern as the nanogels are ionized at low pH.

The pH response of formulations with TEGDMA crosslinker, shown in Figure 5.5A, is affected by the incorporation of nanogels as demonstrated by greater swelling ratios at low pH in formulations with higher nanogel content. This is because the nanogels are ionized at low pH and swelling facilitated by ionic repulsion allows increased imbibition of solution, resulting in increased weight swelling ratios. Around pH 5, however, the 2 wt% TEGDMA gels reach greater swelling ratios than the 5 wt% TEGDMA gels as the cationic nanogels collapse upon exposure to high pH solution, resulting in a decrease in weight swelling ratio that is more apparent with greater nanogel content.

On the other hand, formulations with PEGDMA crosslinker are not as sensitive to the nanogel incorporation and the weight swelling ratios are similar regardless of nanogel content, shown in Figure 5.5B. In the case of the PEDGMA gels, the longer crosslinker allows the network to be swollen to the point where any weight loss resulting from the collapse of nanogels is negligible. This characteristic may have unique applications in oral drug delivery as it allows nanogel incorporation while minimizing pH-dependent swelling variations.

Equilibrium swelling studies were conducted to obtain the maximum weight swelling ratio of the gels and calculate the swollen mesh size. All formulations had a weight swelling ratio of ~1.3 in the 0.1 N HCl buffer (data not shown). For many formulations, including all of the TEGDMA gels, swollen weights at pH 7.4 could not be measured due to the fragility and destruction of the gels prior to reaching equilibrium. For those that reached equilibrium swelling, the mesh size was calculated using the Peppas-Merrill equation. Weight swelling ratios at pH 7.4 for the PEGDMA gels, as well as the calculated swollen mesh size, are reported in Table 5.3. The swollen mesh sizes ranged from ~21-35 nm for the PEGDMA gels. The equilibrium weight swelling ratios of the PEGDMA gels are much greater than the dynamic swelling weight ratios at pH 7.4, indicating some tortuosity present in the hydrogel that retards swelling on a short time scale. This may be due to regions of crystallinity or the glassiness of the hydrogel in a dried state.

5.3.5 Potentiometric Titration

Potentiometric titration studies were completed with crushed microgels to determine the actual MAA incorporation in each formulation and whether the crosslinking agent or addition of nanogels had any effect. As shown in Table 5.2, formulations with the TEGDMA crosslinker had 46-50 mol% MAA which was the inverse of what was calculated from the FTIR spectra. However, the lower relative content of MAA explains why these formulations exhibit some swelling at a low pH as observed in the dynamic swelling studies, since the hydrophilicity of the NVP dominates. On the other hand, formulations with the PEGDMA crosslinker had 53-66 mol% MAA, which was in close agreement with what was calculated from the FTIR spectra though a bit higher for formulations that contained nanogels. The higher relative amount of MAA

in the PEGDMA gels explains the dynamic swelling profile of these gels; the swelling response is controlled by the ionization of MAA rather than the hydrophilicity of NVP. As in the case of the FTIR analysis, the amount of crosslinker and nanogels incorporated was not taken into account so some error is expected. Additionally, the polycationic nanogels are ionized at pH values less than ~6, but the charge of this species was ignored due to the low relative content.

5.3.6 Cytotoxicity

Cytotoxicity studies were performed with various microgel concentrations to find the maximum concentration that Caco-2 and murine fibroblast L929 cells (data not shown) could withstand without disruption to metabolic activity. Figures 5.6A and 5.6B shows Caco-2 cell viability relative to a positive control without microgels. Viability greater than 80% (black line) is considered acceptable in our evaluation. For all formulations, concentrations greater than 1.25 mg/ml caused significant disruption to cell metabolic activity. This may reflect a chemical impediment of cellular activity due to a reduction in pH resulting from higher concentrations of charged functional groups, or a physical impediment of cellular activity due to the density of the sedimenting particles covering the cell monolayer. The trend suggests that higher incorporation of nanogels may cause loss of cell viability; this is in agreement with reports of toxicity associated with cationic polymers [44]. This leads us to believe that the charged functional groups within the polymer play a role in the cytotoxicity results, but at low concentrations this effect is not very pronounced. Additionally, for drug delivery applications it is not likely that local concentrations higher than 1.25 mg/ml would exist.

5.3.7 Loading and Release of Model Therapeutic

Two formulations were chosen to proceed with loading and release studies based on results from the aforementioned characterization studies. The PEGDMA hydrogels with 0 wt% and 5 wt% nanogels were used to evaluate potential influence of nanogel presence on ability to load and release model therapeutics. It was hypothesized that in a loading buffer of pH ~5.5, the P(MAA-co-NVP) matrix and nanogels should both undergo swelling due to partial ionization. In that case, there is a possibility that the therapeutic could partition into the nanogels, which would remain collapsed at a high pH ~7.4 and fail to release the therapeutic. This could have applications in both drug delivery and protein separations.

The first therapeutic tested was BSA, a large (66.5 kDa) model protein. Loading efficiency was calculated by Equation 2 and weight efficiency was calculated by Equation 3, where c_o is the initial protein concentration, c_f is the final protein concentration, $mass_o$ is the initial mass of protein in solution, $mass_f$ is the final mass of protein in solution, and $mass_p$ is the mass of polymer in solution.

$$\text{Loading Efficiency} = \frac{c_o - c_f}{c_o} * 100 \quad (5.2)$$

$$\text{Weight Loading Efficiency} = \frac{mass_o - mass_f}{mass_o - mass_f + mass_p} * 100 \quad (5.3)$$

As shown in Figure 5.7, the weight loading efficiencies were very similar regardless of nanogel content. Though the loading and weight efficiencies of BSA were lower than desired at ~40-45% and ~5.5-5.6% respectively, they were comparable to those reported for similar hydrogel systems with large proteins [45].

The release of BSA from microgels was calculated relative to the total weight of therapeutic based on the weight loading efficiency for each formulation. For both

formulations, a burst release was observed in pH 7.4 buffer, reaching a maximum of ~50-60% in approximately 20 minutes as shown in Figure 5.8A. We can infer that the therapeutic was not loaded into the nanogels in the 5 wt% formulation, since we would expect to see lower release relative to that of the 0 wt% formulation as the nanogels would remain collapsed at pH 7.4. This disproves the hypothesis that the nanogels could be loaded simultaneously at pH 5.5, but there is a possibility that the loading procedure could be modified to achieve simultaneous loading of nanogels and microgels in the 5 wt% formulation.

With respect to the 0 wt% formulation, the percent release of BSA was low compared to reported release of other proteins from comparable systems [45]. This is likely due to a combination of the large size of BSA restricting diffusion along with some surface loading rather than partitioning within the hydrogel. A small amount of the protein is likely removed from the particle surface during the wash steps following the loading procedure, which would result in artificially high loading efficiencies and seemingly low percent release. Charge repulsion between the protein and microgel may also factor into the low release percentages; at pH 7.4 both the BSA and microgels carry a negative charge, which may impede diffusion of BSA from the microgel.

To determine if the size of the therapeutic was affecting partition loading and release, a smaller model therapeutic, FITC-dextran (3-5 kDa) was also evaluated. The loading efficiencies were higher for this model, at around ~65-67% loading efficiency as shown in Figure 5.7, while the weight loading efficiencies were nearly the same as BSA at ~5.3-5.6%. Again there was little difference between the 0 wt% and 5 wt% formulations. These efficiencies were comparable to a similar system loaded with a smaller protein [46].

As in the case of BSA, both the 0wt% and 5 wt% formulations showed similar release profiles and percentages, disproving the hypothesis that the nanogels would be loaded with model therapeutic. The release of FITC-dextran in pH 7.4 buffer, shown in Figure 5.8B, was unexpectedly low at 20-25% release for the 0 wt% formulation. It was anticipated that the 0 wt% nanogel formulation would exhibit a much higher percent release than the 5 wt% nanogel formulation, since the therapeutic could have been contained within the nanogels in the 5 wt% formulation, but the data did not support this. This suggests that the model therapeutic is not partitioning into the nanogels, or that the therapeutic diffused from the nanogels as the microgels collapsed in the acidified environment. Since accurate fluorescence measurements could not be obtained after collapsing the particles by acidification of the solution, it is possible that some of the loaded FITC-dextran was forced out of the microgels as the structure collapsed and the actual loading efficiencies were lower, causing depressed release efficiencies. It is also possible that hydrogen bonding between the microgel and polysaccharide chains inhibited adequate loading and release.

5.4 CONCLUSIONS

Formulations with two different crosslinking agents and varying cationic nanogel content were synthesized by UV-initiated bulk free radical polymerization. The microgels have similar morphology across formulations and retain the nanogels through synthesis and purification, as shown by fluorescent microscopy. Copolymer composition based upon feed ratio and FTIR is in good agreement at approximately 60:40 MAA:NVP and does not vary across formulations. However, the swelling behaviors of the gels do indicate some differences, with the TEGDMA hydrogels experiencing higher weight swelling ratios with increased nanogel content while the swelling of the PEGDMA gels

are not dependent upon nanogel content, which is favorable for drug delivery applications. Two model therapeutics were loaded into the PEGDMA microgels, but the release of the models was lower than expected in both cases and nanogel content did not affect loading or release efficiency. It is likely that the release is poor due to surface loading rather than equilibrium partitioning with in microgels.

5.5 TABLES

Formulation	Nanogel	Crosslinker
Nanogel %, Crosslinker	weight%	
0 wt%, TEGDMA	0	TEGDMA
1 wt%, TEGDMA	1	TEGDMA
2 wt%, TEGDMA	2	TEGDMA
5 wt%, TEGDMA	5	TEGDMA
0 wt%, PEGDMA	0	PEGDMA
1 wt%, PEGDMA	1	PEGDMA
2 wt%, PEGDMA	2	PEGDMA
5 wt%, PEGDMA	5	PEGDMA

Table 5.1: P(MAA-co-NVP) hydrogel formulations with and without nanogels, with TEGDMA or PEGDMA crosslinking agents.

	MAA		NVP	
	FTIR	Titration	FTIR	Titration
0%, TEGDMA	53%	47%	47%	53%
1%, TEGDMA	55%	50%	45%	50%
2%, TEGDMA	53%	46%	47%	54%
5%, TEGDMA	53%	48%	47%	52%
0%, PEGDMA	53%	53%	47%	47%
1%, PEGDMA	55%	61%	45%	39%
2%, PEGDMA	58%	66%	42%	34%
5%, PEGDMA	56%	62%	44%	38%

Table 5.2: Molar ratios of MAA and NVP in P(MAA-co-NVP) microgels determined by FTIR and potentiometric titration.

Formulation	q_{pH 7.4} (g/g)	Swollen mesh size (nm)
0 wt% PNP, PEGDMA	N/A ^a	N/A ^a
1 wt% PNP, PEGDMA	14.3	25-35
2 wt% PNP, PEGDMA	14.7	25-35
5 wt% PNP, PEGDMA	11.7	21

Table 5.3: Equilibrium weight swelling ratios and calculated swollen mesh size of P(MAA-co-NVP) 10 mm disks. ^aCould not be determined due to disk rupture.

5.6 FIGURES

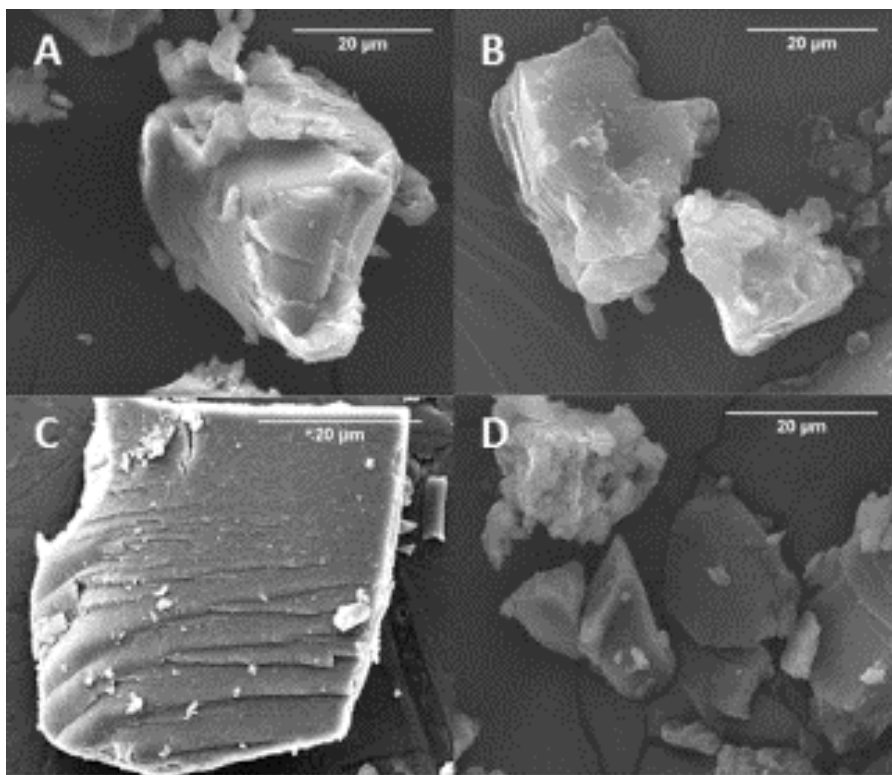


Figure 5.1: Representative SEM micrographs of crushed P(MAA-co-NVP) microgels. Gels were crushed and sieved to $<75\text{ }\mu\text{m}$. A) A) 0 wt% nanogels, TEGDMA crosslink; B) 5 wt% nanogels, TEGDMA crosslink; C) 0 wt% nanogels, PEGDMA crosslink; D) 5 wt% nanogels, PEGDMA crosslink. (Scale bar = $20\text{ }\mu\text{m}$)

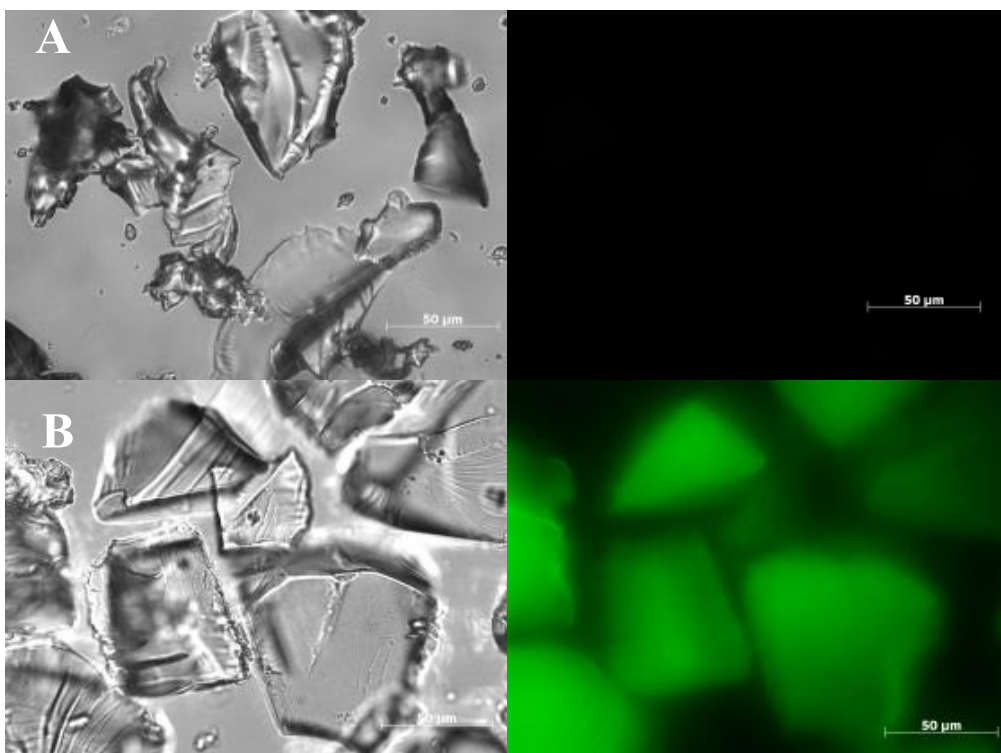


Figure 5.2: Brightfield (left) and fluorescent microscopy (right) images of crushed P(MAA-co-NVP) microgels with PEGDMA crosslinks. A) Film with no nanogels reacted with NBD-Cl; B) Film with 5 wt% nanogels reacted with NBD-Cl. (Scale bars = 50 μm)

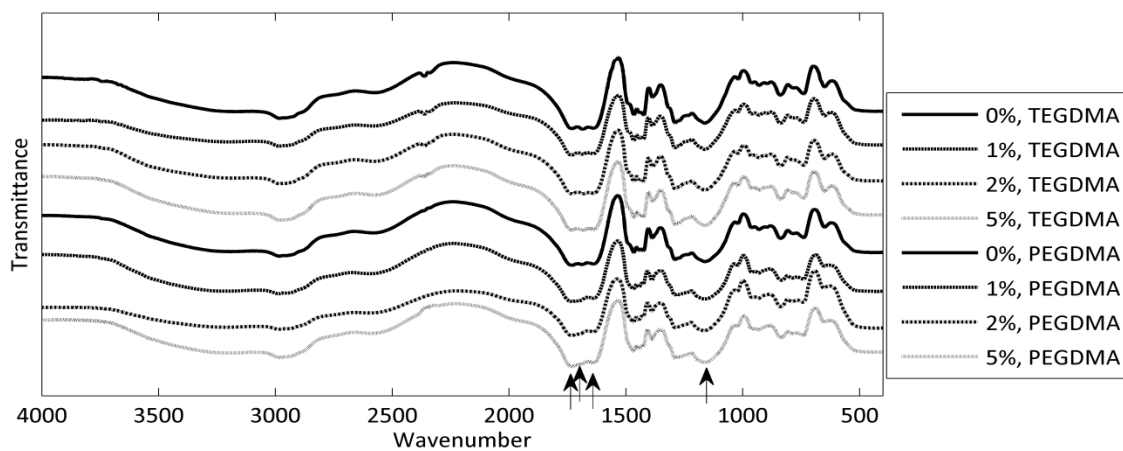


Figure 5.3: FT-IR spectra of crosslinked P(MAA-co-NVP) copolymers with encapsulated nanogels at varying weight percentages (0-5 wt%) pressed in a KBr disk . Crosslinking was achieved with either poly(ethylene glycol) (400) dimethacrylate or tetra(ethylene glycol) dimethacrylate at 1 mol%.

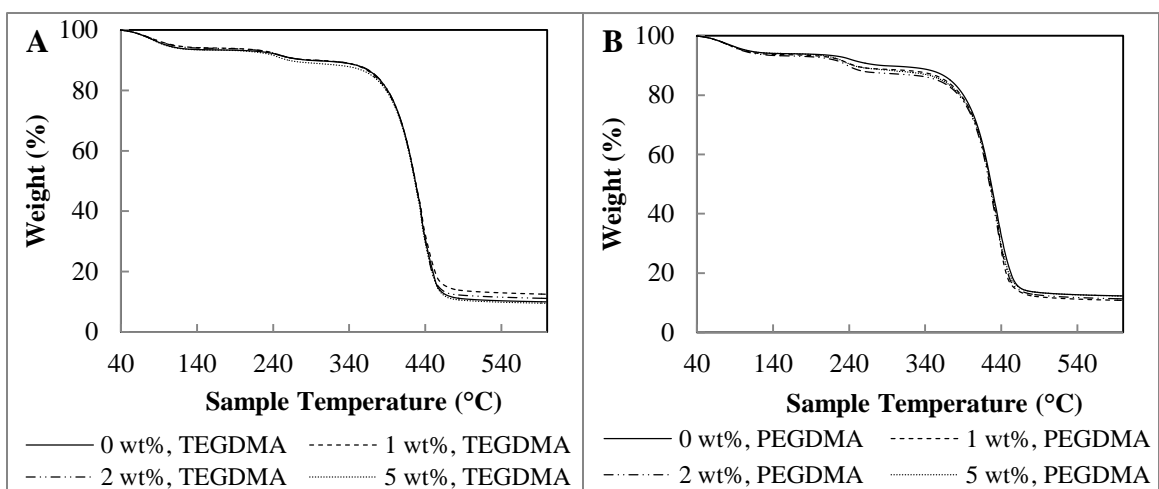


Figure 5.4: TGA curves of P(MAA-co-NVP) copolymers with TEGDMA (A) or PEGDMA (B) crosslinks and 0-5 wt% encapsulated nanogels. 15 mg samples were run at 10°C/min from 40-600°C under nitrogen gas.

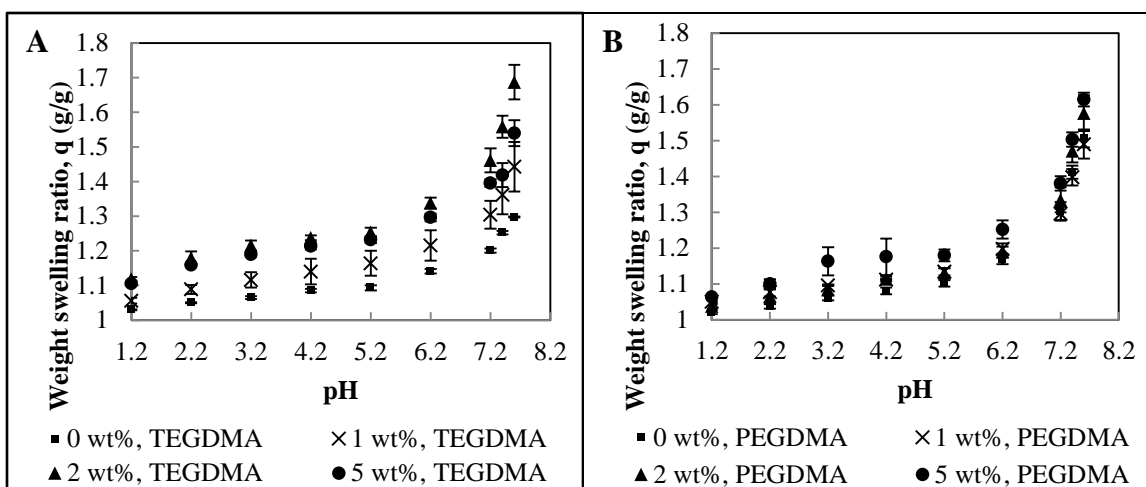


Figure 5.5: Weight swelling ratio of crosslinked P(MAA-co-NVP) hydrogel disks in response to dynamic change in buffer pH. Hydrogels were crosslinked with TEGDMA (left) or PEGDMA (right) and contained 0-5 wt% nanogels. Studies were completed in DMGA/NaOH or HCl buffer with 0.1M NaCl at 37°C (N=3).

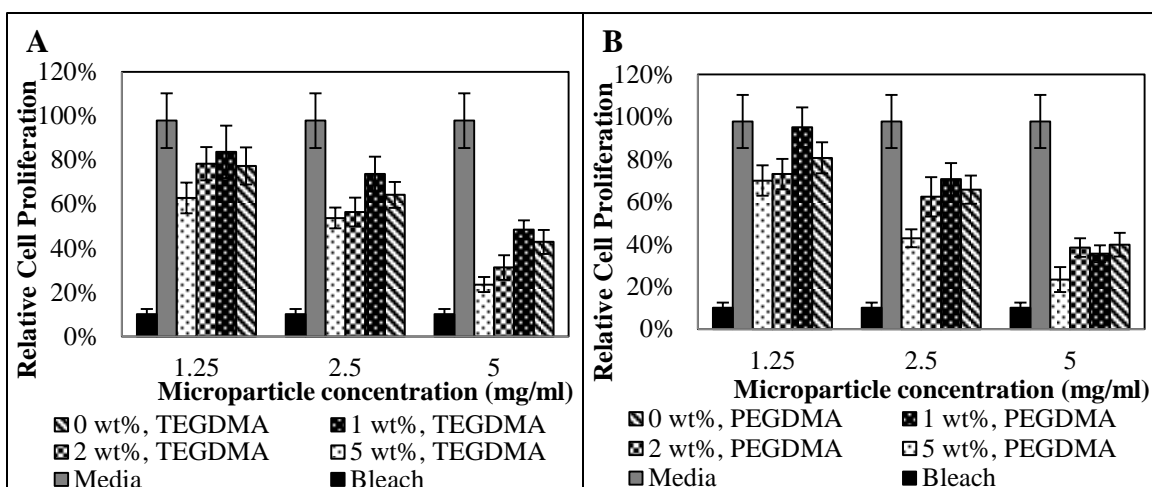


Figure 5.6: Evaluation of cell viability after microgel exposure using an MTS cell proliferation assay (Promega). Caco-2 human colorectal adenocarcinoma cells were incubated with microgel solutions ranging from 1.25-5 mg/mL in culture media for 2 hours. Following removal of the microgels, the MTS assay was allowed to incubate for 90 minutes. Percent viable cells is relative to the positive control (culture media only, gray bar). Microgels were crosslinked with TEGDMA (left) or PEGDMA (right) and contained 0-5 wt% nanogels. (N=3).

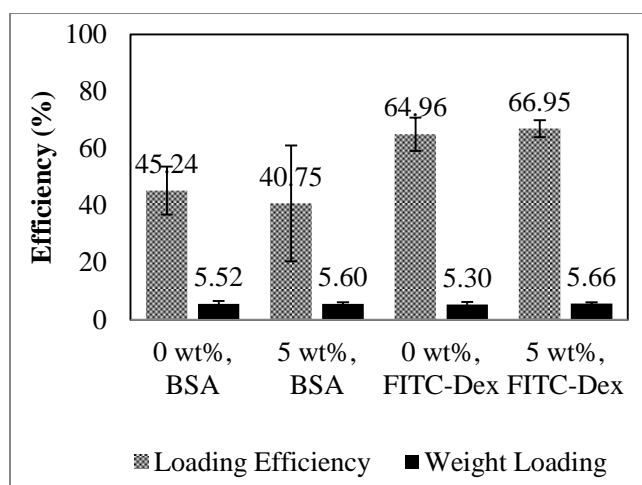


Figure 5.7: Loading efficiencies of P(MAA-co-NVP) microgels with PEGDMA crosslinker and 0 wt% or 5 wt% nanogels. Bovine serum albumin (BSA, MW 66.5 kDa) and FITC-dextran (FITC-Dex, MW 3-5 kDa) were loaded into the microgels. Loading efficiency was based on amount of protein or dextran loaded into microgels relative to initial amount in solution. Weight loading efficiency is weight of loaded protein or dextran relative to total weight of microgel and protein or dextran. Microgels were loaded over 24 hours (N=3).

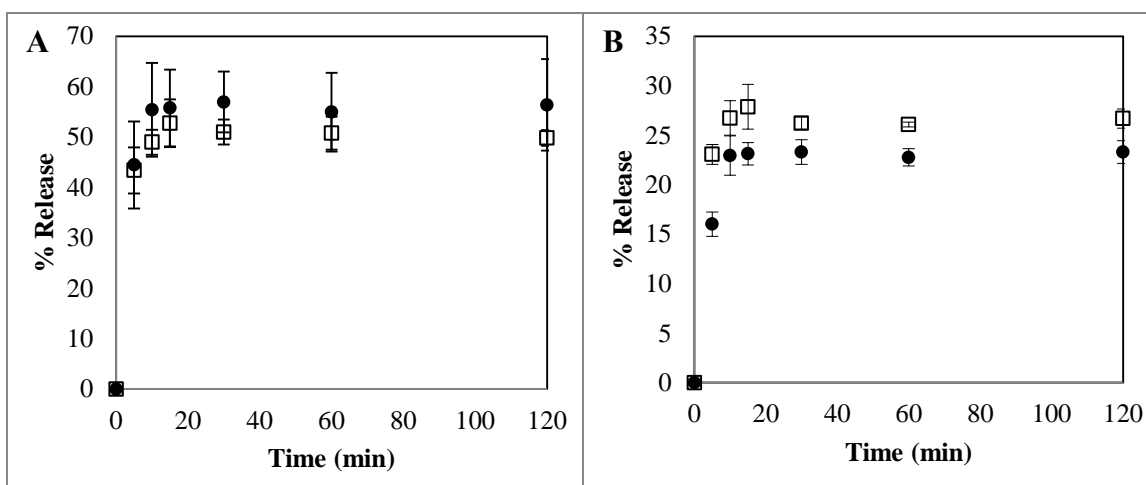


Figure 5.8: Release of model therapeutics from P(MAA-co-NVP) microgels with PEGDMA crosslinker in pH 7.4 PBS buffer at 37°C over two hours. Microgels encapsulated either 0 wt% (●) or 5 wt% (□) nanogels. A) Release of bovine serum albumin (MW 66 kDa) ; B) release of FITC-dextran (MW 3-5 kDa).

REFERENCES

- [1] Peppas, N.A., Hilt, J.Z., Khademhosseini, A., and Langer, R., *Hydrogels in biology and medicine: From molecular principles to bionanotechnology*. Adv Mater, 2006. **18**(11): p. 1345-1360.
- [2] Peppas, N.A., Bures, P., Leobandung, W., and Ichikawa, H., *Hydrogels in pharmaceutical formulations*. Eur J Pharm Biopharm, 2000. **50**: p. 27-46.
- [3] Jeong, B. and Gutowska, A., *Lessons from nature: Stimuli-responsive polymers and their biomedical applications*. Trends Biotechnol, 2002. **20**(7): p. 305-311.
- [4] Firestone, B.A. and Siegel, R.A., *Kinetics and mechanisms of water sorption in hydrophobic, ionizable copolymer gels*. J Appl Polym Sci, 1991. **43**(5): p. 901-914.
- [5] Kost, J. and Langer, R., *Responsive polymeric delivery systems*. Adv Drug Deliver Rev, 2012. **64**: p. 327-341.
- [6] Qiu, Y. and Park, K., *Environment-sensitive hydrogels for drug delivery*. Adv Drug Deliver Rev, 2012. **64**: p. 49-60.
- [7] Hoffman, A.S., *Stimuli-responsive polymers: Biomedical applications and challenges for clinical translation*. Adv Drug Deliver Rev, 2013. **65**(1): p. 10-16.
- [8] Liechty, W.B., Scheuerle, R.L., and Peppas, N.A., *Tunable, responsive nanogels containing t-butyl methacrylate and 2-(t-butylamino)ethyl methacrylate*. Polym, 2013. **54**(15): p. 3784-3795.
- [9] Gran, M.L., *Metal-polymer nanoparticulate systems for exteRNAlly-controlled delivery*, in *Chemical Engineering*. 2010, The University of Texas at Austin: Austin.
- [10] Bajpai, A.K., Shukla, S.K., Bhanu, S., and Kankane, S., *Responsive polymers in controlled drug delivery*. Prog Polym Sci, 2008. **33**(11): p. 1088-1118.
- [11] Tokareva, I., Minko, S., Fendler, J.H., and Hutter, E., *Nanosensors based on responsive polymer brushes and gold nanoparticle enhanced transmission surface plasmon resonance spectroscopy*. J Am Chem Soc, 2004. **126**: p. 15950-15951.

- [12] Stuart, M.A.C., Huck, W.T.S., Genzer, J., Müller, M., Ober, C., Stamm, M., Sukhorukov, G.B., Szleifer, I., Tsukruk, V.V., Urban, M., Winnik, F., Zauscher, S., Luzinov, I., and Minko, S., *Emerging applications of stimuli-responsive polymer materials*. Nat Mater, 2010. **9**: p. 101-113.
- [13] Peppas, N.A. and Byrne, M.E., *New biomaterials for intelligent biosensing, recognitive drug delivery and therapeutics*. Bull. Gattefossé, 2003. **96**: p. 23-25.
- [14] Martins, A.M., Alves, C.M., Kurtis Kasper, F., Mikos, A.G., and Reis, R.L., *Responsive and in situ-forming chitosan scaffolds for bone tissue engineering applications: An overview of the last decade*. J Mater Chem, 2010. **20**(9): p. 1638.
- [15] Han, L.-H., Lai, J.H., Yu, S., and Yang, F., *Dynamic tissue engineering scaffolds with stimuli-responsive macroporosity formation*. Biomaterials, 2013. **34**(17): p. 4251-4258.
- [16] Gao, T., Ye, Q., Pei, X., Xia, Y., and Zhou, F., *Grafting polymer brushes on graphene oxide for controlling surface charge states and templated synthesis of metal nanoparticles*. J Appl Polym Sci, 2013. **127**(4): p. 3074-3083.
- [17] Xiao, L., Isner, A.B., Hilt, J.Z., and Bhattacharyya, D., *Temperature responsive hydrogel with reactive nanoparticles*. J Appl Polym Sci, 2013. **128**(3): p. 1804-1814.
- [18] Marambio, O.G., Pizarro, G.d.C., Jeria-Orell, M., and Geckeler, K.E., *Swelling behavior and metal ion retention from aqueous solution of hydrogels based on *N*-vinyl-2-pyrrolidone and *N*-hydroxymethylacrylamide*. J Appl Polym Sci, 2009. **113**(3): p. 1792-1802.
- [19] Tokarev, I. and Minko, S., *Stimuli-responsive porous hydrogels at interfaces for molecular filtration, separation, controlled release, and gating in capsules and membranes*. Adv Mater, 2010. **22**(31): p. 3446-3462.
- [20] Kayitmazer, A.B., Seeman, D., Minsky, B.B., Dubin, P.L., and Xu, Y., *Protein–polyelectrolyte interactions*. Soft Matter, 2013. **9**(9): p. 2553.
- [21] GeRNAndt, J. and Hansson, P., *Core–shell separation of a hydrogel in a large solution of proteins*. Soft Matter, 2012. **8**(42): p. 10905.

- [22] Yigit, C., Welsch, N., Ballauff, M., and Dzubiella, J., *Protein sorption to charged microgels: Characterizing binding isotherms and driving forces*. Langmuir, 2012. **28**(40): p. 14373-14385.
- [23] Liu, J., Chen, G., Guo, M., and Jiang, M., *Dual stimuli-responsive supramolecular hydrogel based on hybrid inclusion complex (hic)*. Macromolecules, 2010. **43**(19): p. 8086-8093.
- [24] Motornov, M., Roiter, Y., Tokarev, I., and Minko, S., *Stimuli-responsive nanoparticles, nanogels and capsules for integrated multifunctional intelligent systems*. Prog Polym Sci, 2010. **35**(1-2): p. 174-211.
- [25] White, E.M., Yatvin, J., Grubbs, J.B., Bilbrey, J.A., and Locklin, J., *Advances in smart materials: Stimuli-responsive hydrogel thin films*. J Polym Sci, Part B: Polym Phys, 2013. **51**(14): p. 1084-1099.
- [26] Fleige, E., Quadir, M.A., and Haag, R., *Stimuli-responsive polymeric nanocarriers for the controlled transport of active compounds: Concepts and applications*. Adv Drug Deliver Rev, 2012. **64**(9): p. 866-884.
- [27] Schoener, C.A., Hutson, H.N., and Peppas, N.A., *pH-responsive hydrogels with dispersed hydrophobic nanoparticles for the oral delivery of chemotherapeutics*. J Biomed Mater Res A, 2013. **101A**(8): p. 2229-2236.
- [28] Welsch, N., Becker, A.L., Dzubiella, J., and Ballauff, M., *Core-shell microgels as "smart" carriers for enzymes*. Soft Matter, 2012. **8**(5): p. 1428.
- [29] Chapel, J.P. and Berret, J.F., *Versatile electrostatic assembly of nanoparticles and polyelectrolytes: Coating, clustering and layer-by-layer processes*. Curr Opin Colloid Interface Sci, 2012. **17**(2): p. 97-105.
- [30] Knipe, J.M., Peters, J.T., and Peppas, N.A., *Theranostic agents for intracellular gene delivery with spatiotemporal imaging*. Nano Today, 2013. **8**(1): p. 21-38.
- [31] Satarkar, N.S., Biswal, D., and Hilt, J.Z., *Hydrogel nanocomposites: A review of applications as remote controlled biomaterials*. Soft Matter, 2010. **6**(11): p. 2364.

- [32] Döring, A., Birnbaum, W., and Kuckling, D., *Responsive hydrogels – structurally and dimensionally optimized smart frameworks for applications in catalysis, micro-system technology and material science*. Chem Soc Rev, 2013. **42**(17): p. 7391.
- [33] Forbes, D.C., Creixell, M., Frizzell, H., and Peppas, N.A., *Polycationic nanoparticles synthesized using ARGET ATRP for drug delivery*. Eur J Pharm Biopharm, 2013. **84**(3): p. 472-478.
- [34] Pekel, N., Sahiner, N., Guven, O., and Rzaev, Z.M.O., *Synthesis and characterization of n-vinylimidazole-ethyl methacrylate copolymers and determination of monomer reactivity ratios*. Eur Polym J, 2001. **37**: p. 2443-2451.
- [35] Lesuffleur, T., Porchet, N., Aubert, J.-P., Swallow, D., Gum, J.R., S.Kim, Y., Real, F.X., and Zweibaum, A., *Differential expression of the human mucin genes muc1 to muc5 in relation to growth and differentiation of different mucus-secreting ht-29 cell populations*. J Cell Sci, 1993. **106**: p. 771-783.
- [36] Ghosh, P.B. and Whitehouse, M.W., *7-chloro-4-nitrobenzo-2-oxa-1,3-diazole: A new fluorogenic reagent for amino acids and other amines*. Biochem. J. , 1968. **108**: p. 155.
- [37] Lee, J.Y., Painter, P.C., and Coleman, M.M., *Hydrogen bonding in polymer blends. 4. Blends involving polymers containing methacrylic acid and vinylpyridine groups*. Macromolecules, 1988. **21**: p. 954-960.
- [38] Zhu, X., Lu, P., Chen, W., and Dong, J., *Studies of uv crosslinked poly(n-vinylpyrrolidone) hydrogels by ftir, raman and solid-state nmr spectroscopies*. Polym, 2010. **51**(14): p. 3054-3063.
- [39] Bianco, G. and Gehlen, M.H., *Synthesis of poly(n-vinyl-2-pyrrolidone) and copolymers with methacrylic acid initiated by the photo-fenton reaction*. J Photochem Photobiol A, 2002. **149**: p. 115-119.
- [40] Loría-Bastarrachea, M.I., Herrera-Kao, W., Cauich-Rodríguez, J.V., Cervantes-Uc, J.M., Vázquez-Torres, H., and Ávila-Ortega, A., *A tg/ftir study on the thermal degradation of poly(vinyl pyrrolidone)*. J Therm Anal Calorim, 2010. **104**(2): p. 737-742.

- [41] Ho, B.-C., Lee, Y.-D., and Chin, W.-K., *Thermal degradation of polymethacrylic acid*. J Polym Sci, Part A: Polym. Chem, 1992. **30**: p. 2389-2397.
- [42] Polacco, G., Cascone, M.G., Petarca, L., and Peretti, A., *Thermal behaviour of poly(methacrylic acid)/poly(n-vinyl-2-pyrrolidone) complexes*. Eur Polym J, 2000. **36**: p. 2541-2544.
- [43] Blanchette, J. and Peppas, N.A., *Oral chemotherapeutic delivery: Design and cellular response*. Ann Biomed Eng, 2005. **33**(2): p. 142-149.
- [44] Fischer, D., Li, Y., Ahlemeyer, B., Krieglstein, J., and Kissel, T., *In vitro cytotoxicity testing of polycations: Influence of polymer structure on cell viability and hemolysis*. Biomaterials, 2003. **24**: p. 1121-1131.
- [45] Carr, D.A., Gomez-Burgaz, M., Boudes, M.C., and Peppas, D.N.A., *Complexation hydrogels for the oral delivery of growth hormone and salmon calcitonin*. Ind Eng Chem Res, 2010. **49**: p. 11991-11995.
- [46] Carr, D.A. and Peppas, N.A., *Assessment of poly(methacrylic acid-co-n-vinyl pyrrolidone) as a carrier for the oral delivery of therapeutic proteins using caco-2 and ht29-mtx cell lines*. J Biomed Mater Res A, 2009. **92A**: p. 504-512.

Chapter 6: Multi-responsive and biodegradable crosslinked microgels

6.1 INTRODUCTION

Multi-responsive hydrogels, or hydrophilic, crosslinked polymer networks that undergo physicochemical changes in response to multiple environmental stimuli, offer the specificity of highly tunable stimuli-responsive systems combined with excellent biocompatibility [1-4]. As the next generation of biomaterials, these “intelligent” systems are better able to mimic biological processes [5]. This capability could be instrumental in achieving various biomedical advances, including tissue regeneration and oral delivery of delicate therapeutics.

Hydrogels with pH-responsive behavior are among the most widely utilized “intelligent” hydrogel systems for oral drug delivery applications. Polyanionic hydrogels such as poly(methacrylic acid) (PMAA) exhibit complexation via hydrogen bonding at low pH conditions, such as that of gastric fluid, and undergo increased swelling due to ionization of the carboxylic groups at neutral pH conditions, such as that of the intestine [6]. Thus, many researchers have utilized PMAA copolymers as oral drug delivery carriers for their ability to protect a loaded therapeutic from denaturation and proteolytic degradation as it travels through gastric conditions yet swell and release the therapeutic at the site of absorption in the small intestine [7-12].

Though enzymatic attack on a therapeutic as it travels through the gastrointestinal tract is undesirable, the power of enzymes may be harnessed to facilitate delivery of a therapeutic from its carrier at a specific site [13, 14]. A relatively small number of researchers have investigated the use of hydrogels with enzyme-degradable peptide components for the purpose of drug delivery to the small intestine [13, 15, 16], where enzymes such as trypsin, chymotrypsin, and cathepsin- β are prevalent [17]. In particular,

peptide crosslinks are an appealing route to achieve enzyme-specific degradation of the network and subsequent drug delivery [13, 15, 16, 18, 19].

Here, a poly(methacrylic acid-co-*N*-vinylpyrrolidone) (P(MAA-co-NVP)) polymer backbone is used to impart hydrophilic and pH-responsive behavior that may inhibit or enhance proteolytic degradation as a function of pH-responsive swelling. The polymer backbone is crosslinked by a facile bioconjugation reaction with an oligopeptide rich in arginine and lysine groups specifically targeted for degradation by the enzyme trypsin. Synthesis, degradation, cytocompatibility, and therapeutic loading and release of the pH- and enzyme-responsive, biodegradable P(MAA-co-NVP) with peptide crosslinks are detailed herein.

6.2 EXPERIMENTAL METHODS

6.2.1 Chemicals

Methacrylic acid (MAA), *N*-vinyl-2-pyrrolidone (NVP), and Irgacure 184[®] (1-hydroxy-cyclohexyl-phenylketone) were obtained from Sigma-Aldrich (St. Louis, MO). 1-ethyl-3-(3-dimethylaminopropyl) carbodiimide hydrochloride (EDC) was obtained from Sigma-Aldrich. *N*-hydroxysuccinimide (NHS) was obtained from Pierce Biotechnology, Inc. (Rockford, IL). The custom sequence oligopeptide GRRRGK was synthesized by CHI Scientific (Maynard, MA). All reagents were used as received. Fluorescamine was purchased from Acros Organics (Geel, Belgium). Purified pepsin from porcine gastric mucosa (≥ 2500 U/mg) and pancreatin from porcine pancreas (4x USP specifications) were purchased from Sigma-Aldrich. Trypsin-EDTA solution (1X) and N_{α} -benzoyl-L-arginine ethyl ester hydrochloride (BAEE) trypsin substrate were obtained from Sigma-Aldrich. Recombinant human insulin (≥ 27.5 IU/mg) was obtained

from Sigma-Aldrich. All other solvents and buffers were purchased from Fisher Scientific (Waltham, MA).

6.2.2 Synthesis and Purification

6.2.2.1 Synthesis of Linear Polymer

P(MAA-co-NVP) linear polymer was synthesized by photoinitiated, free-radical polymerization. MAA and NVP were added at a 1:1 molar ratio to a 1:1 (w/w) deionized water and ethanol solution to yield a 1:3 (w/w) total monomer to solvent ratio. Photoinitiator Irgacure 184[®] was added at 1 wt% with respect to total monomer weight.

The mixture was homogenized by sonication then the round bottom flask was sealed with a rubber septum. The solution was purged with nitrogen for 20 minutes, then the reaction was initiated with a Dymax BlueWave[®] 200 UV point source (Dymax, Torrington, CT) at 100mW/cm² intensity and allowed to polymerize for 30 minutes while stirring.

Following polymerization, the linear polymer was purified from unreacted monomer by addition of 1 N hydrochloric acid (HCl) to precipitate polymer, centrifugation, and resuspension in deionized water. After 3 wash cycles, the polymer solution was frozen in liquid nitrogen (LN₂) and lyophilized for at least 24 hours.

6.2.2.2 Synthesis of Peptide Crosslinked Gels

Linear P(MAA-co-NVP) was dissolved in a 1:1 (v/v) water:ethanol solution at a concentration of 50 mg/ml. EDC was dissolved in ethanol at a concentration of 50 mg/ml and NHS was dissolved in ethanol at a concentration of 16 mg/ml. The EDC and NHS solutions were added to the polymer solution at a ratio of 6:3:1 polymer:EDC:NHS by weight. The mixture was vortexed briefly, then allowed to react for ~3 min with shaking. The pH was raised to ~8 by the addition of 1 N sodium hydroxide (NaOH), and then a

volume of 100 mg/ml peptide in ethanol solution was added to achieve a 2:1 weight ratio of polymer:peptide. The mixture was allowed to react overnight with shaking then purified by 3 wash cycles with water and centrifugation at 10,000 x g for 5 minutes. Following the washes, the polymer was frozen in LN₂ and lyophilized for at least 24 hours.

After lyophilization, the polymer was milled into a fine power by crushing with mortar and pestle. The powder was sifted to the size ranges of 30-75 µm and less than 30 µm by ultraprecision ASTM sieves (Precision Eforming, Cortland, NY).

6.2.3 Characterization

6.2.3.1 Potentiometric Titration

To determine the MAA content of the linear polymer, a 3.5 mg/ml solution of microgels in deionized water was titrated to pH 11.5 using 0.2 N NaOH (standardized with potassium hydrogen phthalate) at 25°C with constant stirring. pH was measured with a Mettler-Toledo SevenEasy™ (Columbus, OH) pH probe and was recorded when the pH reached a steady value (± 0.01 pH units in three consecutive measurements over 5 minutes). The equivalence point was used in conjunction with a charge balance to determine the amount of MAA present in each formulation.

6.3.2.2 Fluorescamine Assay

The fluorescamine solution was prepared fresh before each test. 3 mg of fluorescamine (Sigma-Aldrich) was dissolved in 10 ml filtered acetone. SuperNAtant from the EDC-NHS reactions were mixed in a range of dilutions with phosphate buffered saline (PBS) and the fluorescamine solution with agitation. After reacting at room temperature with shaking for 15 min, 200 µl of each sample was transferred in triplicate

to a black 96-well plate and the fluorescence at 360 ex/460 em was measured using a Bio-Tek Synergy™ HT multi-mode plate reader(Winooski, VT), sensitivity=85.

6.2.3.3 Fourier Transform Infrared Spectroscopy

Fourier transform infrared spectroscopy (FTIR) spectra were obtained using a Thermo Mattson Infinity Gold spectrometer (Thermo Fisher Scientific Inc., Waltham, MA). The incubation buffer of degraded samples was exchanged with water using 30,000 MWCO centrifugal filters (Millipore, Billerica, MA) over 5 washes. Samples were lyophilized and then pressed in KBr (Sigma-Aldrich) disks. For each sample, 512 scans were performed with a resolution of 4 cm⁻¹ and gain of 1.0, and background spectra of a KBr blank disk was subtracted from the sample spectra.

6.2.3.4 Scanning Electron Microscopy

Scanning electron microscopy (SEM) samples were prepared by dusting carbon tape-covered aluminum stubs with lyophilized, crushed microgels. The samples were coated with 5 or 10 nm of Pt/Pd coating using a Cressington 208 Benchtop sputter coater (Watford, England). Scanning electron microscopy images were obtained using an FEI Quanta 650 FEG scanning electron microscope (Hillsboro, OR) and a Zeiss Supra 40V scanning electron microscope (Jena, Germany).

6.2.3.5 Degradation Study

Microgels were degraded at various trypsin concentrations in 1X phosphate buffered saline solution (pH 7.4), simulated gastric fluid, simulated intestinal fluid, rat gastric fluid or rat intestinal fluid.

Simulated gastric fluid (SGF) and simulated intestinal fluid (SIF) were prepared according to USP 29 [20]. Briefly, the SGF was prepared by dissolving 2 g of sodium chloride and 3.2 g of purified pepsin from porcine stomach mucosa was dissolved in

~800 ml deionized water. 7 ml of HCl was added, then enough water to make up to 1 L and the pH adjusted to 1.2. SIF was prepared by dissolving 6.8 g monobasic potassium phosphate in 250 ml deionized water, then 77 ml of 0.2 N NaOH was added while stirring. 500 ml additional water was added then 10 g pancreatin was mixed into the solution. The pH was adjusted to 6.8 using 0.2 N NaOH or HCl then the solution was made up to 1 L with water.

Gastrointestinal fluids were harvested from Sprague Dawley juvenile male rats (250-300 g) according to a protocol published by Yamagata et al. with some modifications [21]. Briefly, after sacrificing the rat the stomach was excised and ligated at both ends. A needle was inserted to inject 5 ml of pH 1.2 HCl-NaCl buffer (same as SGF minus pepsin) and the gastric contents were collected in a 50 ml centrifuge tube. Similarly, a ~20 cm section of the upper small intestine was cannulated and flushed twice with 10 ml cold PBS (1X, pH 7.4). The fluid was collected as intestinal fluid in a 50 ml centrifuge tube. Both the harvested fluids were centrifuged at 3,200 x g, 4°C, for 15 min to separate solids from the fluids. The supernatants were retained as rat gastric fluid and rat intestinal fluid, respectively. Fluids were stored at -20°C until use.

Degradation was evaluated by measuring relative turbidity of the samples over time, as reported by Klinger and Landfester [22]. Microgels were suspended in trypsin solutions of varying concentration, PBS, SGF, SIF, or rat gastrointestinal fluids at various concentrations. 100 µl of each solution was added to a 96-well plate in triplicate, and the absorbance was measured at 500 nm in 5 minute intervals over 90 minutes using a Bio-Tek Synergy™ HT multi-mode plate reader (Winooski, VT). The temperature was controlled at 37°C and the plate underwent shaking for 3 seconds before each measurement.

Activity of the trypsin following incubation with particles and deactivation methods including addition of serum-containing cell culture media and 5 minutes incubation at 60°C, 70°C, or 80°C, was evaluated using a trypsin activity assay adapted from the protocol by Yanes et al. [23]. Briefly, degradation supernatant was combined with 1 mg/ml BAEE in PBS at a 1:9 sample:BAEE ratio by volume. Immediately after addition of the BAEE, absorbance at 253 nm was measured at the minimum interval (typically 40-50 seconds) for 5 minutes using a Bio-Tek Synergy™ HT multi-mode plate reader (Winooski, VT).

6.2.3.7 *In vitro* Cytotoxicity Study

Lines of L929 and RAW 264.7 cells were obtained from American Type Culture Collection (ATCC, Rockwell, MD). All cell lines were cultured in Dulbecco's modified Eagle medium (DMEM) (Mediatech, Herndon, VA) supplemented with 10% heat-inactivated HyClone™ Fetal Bovine Serum, USDA Tested (Fisher Scientific), 1% 200 mM L-glutamine solution (Mediatech), 100 U/ml penicillin, and 100 µg/ml streptomycin (Mediatech). Cytotoxicity studies were performed using DMEM without phenol red supplemented with 2% heat-inactivated HyClone™ Fetal Bovine Serum, USDA Tested (Fisher Scientific), 1% non-essential amino acids (Mediatech), 100 U/ml penicillin, and 100 µg/ml streptomycin (Mediatech). Cells were incubated at 37°C in a 5% CO₂ environment.

Cells were seeded at a density of 10,000 cells/well in a 96-well plate and allowed to incubate for 24 hours prior to the experiment. Microgels were degraded in 1.25 or 0.625 mg/ml trypsin in PBS at concentrations ranging from 1.3-6 mg/ml. Degradation took place at 37°C with shaking for at least 4 hours. Trypsin was deactivated by addition of 2X volume DMEM without phenol red containing 2% fetal bovine serum. Cells were

incubated with degraded microgels for 8 hours at 37°C and 5% CO₂. The cytotoxic effect of the microgels was evaluated using a CellTiter 96® Aqueous One Solution Cell Proliferation MTS Assay (Promega, Madison, WI). MTS assay was added to the wells and incubated for 90 minutes at the same conditions before absorbance measurements were made at 490 nm using a Bio-Tek Synergy™ HT multi-mode plate reader (Winooski, VT). Cytotoxicity is reported as ‘relative cell proliferation’, or normalization of the assay absorbance values to the average assay absorbance for cells incubated in only culture media.

5.2.3.8 Loading and Release Studies

Microgels were loaded by equilibrium partitioning post-synthesis with recombinant human insulin (Sigma). Microgels were incubated at 37°C for 4 hours in a 0.5 mg/mL insulin solution of pH ~5.5 at a ratio of 7:1 microgel:therapeutic by weight. The microgels were collected by centrifugation at 10,000 x g for 5 minutes then collapsed by resuspension in 0.5 N HCl. Microgels were separated from supernatant by centrifugation at 10,000 xg for 5 minutes. The loaded microgels were lyophilized and stored at -20°C for further studies. Protein loading was evaluated with a MicroBCA assay protein quantification assay (Pierce-Thermo, Rockford, IL).

Release studies were completed in SGF or dilute Trypsin-EDTA solution in 1X PBS buffer at 37°C at a microgel concentration of 0.6 mg/mL buffer. Samples were taken at 0, 5, 10, 15, 30, 60, and 90 minutes. Concentration of released protein was evaluated using the MicroBCA assay and a human insulin ELISA kit (Abnova, Taiwan).

6.3 RESULTS AND DISCUSSION

Synthesis of the uncrosslinked P(MAA-co-NVP) was optimized to a 1:3 (w/w) total monomer to solvent ratio after varying the ratio from 1:5 to 1:1; the optimization

was based on the ratio with the highest monomer content that yielded a solution with a workable viscosity as opposed to a solid or solution so viscous that it could not be easily purified or dissolved. Purification and lyophilization yielded white, fluffy polymer. It was noted that the pH of the solution prior to freeze drying and lyophilization affected the appearance and solubility; polymer lyophilized at pH ~4 appeared more granular and required prolonged mixing to go into aqueous solution, whereas polymer lyophilized at pH ~8 looked similar to cotton balls and dissolved easily in aqueous solutions. This is likely due to the phase transition of MAA from hydrophobic to hydrophilic due to its ionized state above pH 5.

Linear polymer lyophilized at pH ~8 was predominately used in the peptide crosslinking reactions due to its high solubility in aqueous conditions. Potentiometric titration was used to determine that the linear polymer was 45 mol% or 39 wt% MAA. Scheme 6.1 shows the mechanism of the EDC-NHS crosslinking reaction with the linear P(MAA-co-NVP). Upon dissolution of the polymer in the ethanol-water solution, the pH was adjusted to ~5 to favor the activation of the carboxylic acid groups by EDC and increase the stability of the active ester intermediate [24]. EDC was added at a molar ratio of 1:2 to the MAA groups on the linear chains, and NHS was added at a molar ratio of 1:1.8 to the EDC. Upon addition of the EDC and NHS the solution became turbid but no precipitation was evident. Both the EDC and NHS were dissolved in ethanol to limit instability due to hydrolysis.

After activation of the carboxylic acid groups, the pH was raised to ~7-8 to facilitate attack on the primary amines of the oligopeptide [24]. It was noted that without raising the pH, the crosslinking reaction would not proceed. Various polymer:EDC:NHS:peptide weight ratios, some of which are shown in Table 6.1, were tested to identify the formulation with the highest peptide incorporation and

reproducibility. All formulations with peptide content below a polymer:peptide ratio of ~3:1 failed to produce hydrogels. After testing at least 25 synthesis recipes, a best performing formulation of solvents, polymer, and EDC-NHS was chosen to be an ethanol-water mixture with a polymer:EDC:NHS:peptide weight ratio of 20:10:3.3:10.

Peptide was added at a molar ratio of 1:3.6 relative to the EDC; the free amine groups were in 1.4x excess relative to the theoretical maximum of activated carboxyl groups. Upon addition of the peptide solution the mixture was immediately turbid and precipitation of crosslinked polymer was evident. After reacting for at least 8 hours the crosslinked polymer typically resembled a hydrogel with an amorphous shape. The hydrogel was not broken vigorous shaking or mixing by vortex, indicating the mechanical integrity of the crosslinks.

During the washes to remove impurities the hydrogel typically swelled at least twice in volume, and following lyophilization it appeared as fluffy white chunks, as seen in Figure 6.1 (initial). The dried hydrogel was easily crushed into a powder consisting of particles <30 μm in size, shown in the SEM micrograph in Figure 6.2.

6.3.1 Fluorescamine Assay

The fluorescamine assay was used to quantify the amount peptide remaining in solution following the EDC-NHS crosslinking reaction. The fluorescamine reagent is commonly used as a fluorimetric assay of free amine content, thereby an indirect measurement of protein or peptide content [25]. A known concentration of peptide was used as the standard to obtain quantitative results. Assay of the reaction conditions minus peptide showed no background fluorescence, which is expected as the peptide is the sole source of free amines.

First, the fluorescamine assay was used to roughly optimize the ratio of linear polymer to peptide. The reaction efficiencies of a 1:1 and a 2:1 polymer:peptide weight ratio were compared as determined by peptide remaining in solution at the completion of the reaction. In the case of the 1:1 ratio, 16.6% of the peptide remained in solution. However, at the 2:1 ratio only 1.8% of the peptide remained in solution. As this was very satisfactory reaction efficiency, all subsequent reactions were carried out at the 2:1 polymer:peptide weight ratio.

The fluorescamine assay was also used to determine the effect of pH on reaction efficiency. According to the assay, only ~2-6% of the peptide remained in the supernatant following the crosslinking reactions at a polymer:peptide weight ratio of 2:1. The peptide incorporation was further affected by pH of the EDC-NHS reaction; nearly 98% of the peptide reacted when the carboxylic acid groups were activated at pH ~5, while about 93% of the peptide reacted following activation at a neutral pH. Therefore, pH of the reaction conditions was carefully monitored and adjusted to pH ~5 during the activation, then raised to pH ~7-8 prior to the addition of the primary amine groups.

6.3.2 FTIR Spectroscopy

FTIR spectroscopy of the linear polymer in high and low pH conditions was performed to confirm the presence of hydrogen bonding at low pH. As shown in Figure 6.3, the shift in the carbonyl stretching bands from 1680 cm^{-1} to 1725 cm^{-1} and 1640 cm^{-1} between the pH 8 and pH 4 conditions confirmed the presence of hydrogen bonding between the carboxyl groups of the MAA and the carbonyl of the NVP [9]³. The bands at 2500 cm^{-1} and 3000 cm^{-1} suggest intermolecular hydrogen bonding of the carboxyl

³ See also Section 5.3.2

groups on the MAA [26]. Additionally, the appearance of the band at 1560 cm^{-1} at pH 8 is characteristic of carboxylic groups in the ionized state [27], causing breaking of hydrogen bonds at high pH.

FTIR spectroscopy was also used to evaluate the composition of the peptide-crosslinked microgels before and after degradation. As shown in Figure 6.4, the characteristic bands of the carboxylic groups of MAA are present at 2900 cm^{-1} and 1560 cm^{-1} and the bands of carbonyl groups in MAA and NVP are present at 1640 cm^{-1} . Characteristic bands of the peptide that may be attributed to CN and NH₂ stretching appear at 1140 cm^{-1} and 800 cm^{-1} [27]. Incorporation of the peptide into the crosslinked gel was confirmed by the presence of these bands. Figure 6.5 shows that there was no discernable difference between the spectra of intact and degraded microgels. However, as demonstrated with the linear polymer, upon exposure to the low pH of the SGF the characteristic carbonyl bands were shifted compared to that in SIF, indicating the presence of hydrogen bonding within the microgels at low pH conditions. Interestingly, though, the characteristic peak of ionized carboxylic groups remained even in the low pH conditions of SGF, indicating that the hydrogels was not fully protonated and complexed. This could present issues in protecting the therapeutic from the harsh gastric environment.

6.3.3 Degradation

The peptide crosslink was designed with multiple arginine and lysine residues so that it would be targeted specifically by trypsin but would not be susceptible to attack by pepsin [17]. Trypsin is known to cleave at the C-terminal of arginine and lysine residues [28] and each peptide link has 4 possible cleavage sites as shown in Scheme 6.1.

First, degradation of the microgels was assessed visually in SGF containing the enzyme pepsin, SIF containing the enzyme trypsin, or PBS. As seen in Figure 6.1, the

hydrogel in trypsin solution is no longer visible after only 30 minutes. However, the hydrogel in the pepsin and PBS solutions are easily visible up to 4 hours of incubation. SEM was used to discern the morphology of partially degraded microgels, shown in Figure 6.6. The microgels were incubated in buffers for 90 minutes then flash frozen in liquid nitrogen and lyophilized to preserve the structure and morphology of the gels during swelling and degradation. Due to this process, salts crystals from the buffer solutions can be seen on the surface of the microgels. A microgel in SGF is shown in Figures 6.6A and 6.6D and a microgel in PBS is shown in Figures 6.6C and 6.6F; in both cases, the edges are crisp and a porous structure is easily discernable. A microgel in SIF is shown in Figures 6.6B and 6.6E, and in this case the edges are smooth and rounded and the structure is more collapsed rather than porous, as if it were melting, confirming the loss of structural integrity due to degradation of the crosslinks.

As the method of synthesis yields amorphous hydrogel pieces on the order of millimeters in size, gravimetric analysis of degradation over time is extremely difficult to execute. Thus, a different method of assessing degradation was sought. Turbidity is commonly used to evaluate the temperature-dependent phase transition and swelling of thermoresponsive polymers such as poly(N-isopropyl acrylamide) [29, 30], and Klinger and Landfester [31] showed that for photo-degradable poly(methyl methacrylate) particles the increase in hydrodynamic radius as a function of swelling and degradation correlated well with the decrease in turbidity.

Per the second report by Klinger and Landfester [22], change in relative turbidity could be used to evaluate degradation as a function of time. Klinger and Landfester attribute the reduction in turbidity during degradation to a loosening of the network, resulting in greater swelling of the gel therefore less contrast between the refractive

indices of the solvent and the polymer [31]. Mathematically, it can be explained by the following equation for turbidity as described by Lechner [32]:

$$\tau = \frac{\varphi Q_{ext}^3}{2d} \quad (6.1)$$

where φ is the volume fraction of the particles, Q_{ext} is the Mie extinction efficiency, and d is that particle diameter. In most cases, it is useful to make the substitution

$$\varphi = \frac{c}{\rho} \quad (6.2)$$

where c = mass concentration of the particles and ρ =density of the particles. Q_{ext} is a function of the ratio of refractive indices of the particles and solvent, n_p/n_0 , as well as the size of the particles, and decreases as the ratio n_p/n_0 decreases.

Therefore, it was hypothesized that as the enzymatically-degradable microgels swelled then degraded into smaller particles and linear polymer chains with minimal contrast between refractive indices of the polymer and solvent, the turbidity should decrease over time in correlation with the extent of degradation. Absorbance of the degrading microgel solutions was measured at an arbitrary value of 500 nm as the absorbance of the solutions plateaued in the 300-800 nm range. Measurements were made in 5 minute intervals over a period of at least 90 minutes. The absorbance value was first converted to percent transmittance using the following equation

$$I = 10^{(2-A)} \quad (6.3)$$

then to turbidity using the equation

$$\tau(t) = -\ln\left(\frac{I_t}{I_0}\right) \quad (6.4)$$

where I_t is transmittance of the sample at time t and I_0 is transmittance of pure solvent.

Finally, relative turbidity was calculated as

$$\tau_{rel} = \frac{\tau(t)}{\tau(t=0)} \quad (6.5)$$

and plotted as a function of time.

As hypothesized, upon incubation with trypsin solutions of various concentrations the turbidity of the microgel solutions decreased over 90 minutes, shown in Figure 6.7. Since the mass concentration of particles was held constant, it is logical that trypsin concentration was directly related to extent of reduction in relative turbidity; the higher the trypsin content, the greater the degradation.

Interestingly, when microgels were incubated in low trypsin concentrations or in PBS there was an initial increase in turbidity followed by decreasing turbidity or a plateau in the case of PBS. As the particles are expected to swell in PBS and swell then degrade in the trypsin, this behavior is incongruent with the explanation set forth by Klinger and Landfester [31], in which turbidity is expected to decrease with swelling of the particles. Looking at the relationship for turbidity established by Lechner in Eq. 6.1, turbidity is dependent upon particle size and concentration as well as the contrast between polymer and solvent refractive indices. This initial increase in turbidity may be attributed to the increase in size of the particles, which can increase turbidity due to light scattering. The imbibition of solvent by the swollen particles likely reduced the refractive index of the particles but was not sufficient to overcome the effect of the particle size contribution, particularly at this particle concentration. At approximately 30 minutes the particles in PBS reached equilibrium swelling, at which point the relative turbidity became constant. The point at which the degradation by trypsin was sufficient enough to overcome the effect of particle size and reduce the relative turbidity was dependent upon the concentration of trypsin, with the transition to decreasing relative turbidity happening sooner at higher trypsin concentrations where degradation is presumably happening on a faster timescale.

The degradation of the microgels during incubation with the rat gastrointestinal fluids versus trypsin solutions is shown in Figure 6.8. As in the previous case, the

relative turbidity of the microgels in PBS solution increased for the first ~30 minutes then was relatively constant over the remainder of the 4 hour incubation period. Relative turbidity of particle solutions at both the 0.3 and 0.6 mg/ml trypsin concentrations decreased to well below 10% by the end of the 4 hour incubation, though the solution with higher trypsin concentration arrived at a lower value in a shorter period of time. The relative turbidity of the particles incubated with gastric fluid was approximately constant for nearly 3 hours, at which time the evaporation of the fluid started to have an effect on the enzyme concentration, the absorbance path length, or both, and turbidity decreased slightly. Most encouraging, though, was the significant degradation of the microgels incubated in rat intestinal fluid. The relative turbidity steadily decreased across the 4 hour incubation period, arriving at a final reduction in relative turbidity of 85%. Though the degradation was not as rapid as the trypsin solutions, the intestinal fluid was significantly diluted during harvest so it is quite possible that the physiological trypsin concentration is higher, resulting in more rapid degradation *in vivo*. These results are extremely promising for oral drug delivery applications, as the degradation is specific to intestinal fluid and occurs on a timescale relevant to small intestinal residence time [33].

The activity of trypsin can be evaluated by spectrophotometric measurement using BAEE, an arginine-based trypsin substrate that absorbs at 253 nm upon cleavage by trypsin. Trypsin activity is correlated to rate of absorbance increase over the initial 5 minutes of the reaction, which reaches a plateau when the reaction is complete [34]. Due to the scale of the degradation reactions, the assay was adapted and optimized for a 96-well assay format on the microliter-scale as opposed to the previously reported milliliter-scale protocols.

Using the optimized reaction conditions for the 96-well assay, various degradation and trypsin deactivation conditions were evaluated to determine the trypsin

activity as a function of microgel concentration as well as determining an effective method of deactivating trypsin prior to exposure to cells. Microgel concentrations of 0, 1.5, 3, and 6 mg/ml were incubated with 0.6 mg/ml trypsin at 37°C for 90 minutes. In the first experiment, DMEM with 2% fetal bovine serum was added to the degradation solution at 0, 80, or 160 μ l amounts to quench the trypsin activity. As shown in Figure 6.9, the samples receiving no DMEM had a strong linear correlation in absorbance increase over time; as previously reported, the greater the slope of this linear fit the higher the trypsin activity [34]. Slope and R^2 values of the linear fit for each particle concentration are shown in Table 6.2, and it can be seen that trypsin activity is reduced in the presence of higher microgel concentrations. This confirms that trypsin activity is being consumed by the peptide crosslinks within the microgels, leading to the degradation of the microgels as desired. At all concentrations tested absorbance did not reach a plateau, meaning that trypsin was in excess relative to peptide crosslinks and could likely be used at a lower concentration to achieve degradation.

Therefore, in a subsequent study microgel concentration was held constant at 2 mg/ml and trypsin concentration was varied from 0.0375-0.6 mg/ml. As seen in Figure 6.10A, the lowest two trypsin concentrations of trypsin solutions containing no microgels have final absorbance values below that of the control, PBS, indicating no appreciable trypsin activity. Therefore, we can expect to see little degradation at those concentrations. As expected, samples taken after 90 minutes of incubation with microgels quickly reached a plateau during the trypsin assay, shown in Figure 6.10B, confirming low activity. Trypsin concentrations of 0.3 and 0.6 mg/ml were sufficient to maintain enough trypsin activity to degrade peptide crosslinks in the microgels. Further narrowing the range of trypsin concentrations, the activity assay was used to determine that trypsin concentrations down to 0.2 mg/ml maintained sufficient activity during degradation with

microgels (data not shown). Figure 6.10C demonstrates that the trypsin activity was effectively quenched by incubation at 70°C for 5 minutes.

Upon addition of DMEM containing serum, trypsin activity is entirely consumed by reaction with protein in the serum and the increase in absorbance due to reaction with BAEE is negligible. This is desirable for subsequent exposure to cells in later studies, as trypsin can have a negative impact on cell metabolism and behavior. However, the downside is that the microgel concentration is significantly diluted upon addition of the DMEM so initial degradation reactions must be highly concentrated.

In the next study, trypsin was deactivated by heating for a short amount of time. According to the literature, a 5 minute incubation period in temperatures ranging from 60-80°C should be sufficient to deactivate the trypsin [35]. Following the 90 minute degradation period in 0.6 mg/ml trypsin, samples at each microgel concentration were incubated at 60, 70, or 80°C for 5 minutes. The BAEE trypsin activity assay indicated that samples incubated at 60°C still contained some trypsin activity, as evidenced by the positive increase in absorbance over time shown in Figure 6.11A. However, the slope was much less than that of samples with active trypsin with values ranging from only 16-26 a.u./min compared to 64-80 a.u./min.

Samples incubated at 70°C and 80°C for 5 minutes had negligible trypsin activity, shown in Figure 6.11B. This method of deactivation could be advantageous to the addition of DMEM, as microgels remain concentrated and less material will be needed for subsequent studies. The effect of particles and inactivated trypsin on cell metabolism should be thoroughly investigated, though.

6.3.4 Cytotoxicity

Cytotoxicity studies were performed with various microgel concentrations to find the maximum concentration that L929 murine fibroblast and RAW 264.7 murine macrophage cells could withstand without disruption to metabolic activity. Microgels were incubated in 1.2 or 0.6 mg/ml trypsin solution for at least 4 hours to ensure degradation of the microgels; PBS buffer was used as a control. As trypsin can have negative effects on cell function [36], particularly antigen-presenting ability of macrophages [37], the trypsin was deactivated by the addition of excess cell media prior to the addition to cells. Cells were incubated with degraded microgel solutions for 8 hours to assess cytotoxic effect. Figures 6.12A and 6.12B show L929 and RAW 264.7 cell proliferation, respectively, relative to a cells incubated in normal media without microgels. Viability greater than 80% is considered acceptable in our evaluation. For all formulations and concentrations, cell proliferation is greater than 80% relative to the cells incubated in normal media. This was somewhat unexpected, as concentrations above 1.25 mg/ml of nondegradable particles with a similar formulation induced some cytotoxicity in human carcinoma cells [9]⁴. This supports the hypothesis that the size of the nondegradable particles posed a physical impediment of cellular activity due to the density of the sedimenting particles covering the cell monolayer. It was concluded that these degradation conditions and the degraded microgels within these concentrations posed minimal cytotoxic threat to these two cell lines.

6.3.5 Loading and Release

Insulin, a small therapeutic protein ~5.8 kDa, was used in loading and release studies as an oral delivery method for insulin has been widely investigated for many

⁴ See also Section 5.3.6

years. Protein concentration was measured in the superNAtant following the 4 hour loading period with microgels, then again in the superNAtant following collapse of the microgels in 0.5 N HCl. Protein that was likely surface loaded was lost during the HCl wash. However, a significant amount of protein remained loaded following the HCl wash, disproving the possibility of diffusion from the microgels in low pH conditions. Loading efficiencies were calculated as follows, where c_o is the initial protein concentration, c_f is the final protein concentration, $mass_o$ is the initial mass of protein in solution, $mass_f$ is the final mass of protein in solution, and $mass_p$ is the mass of polymer in solution:

$$Loading\ Efficiency = \frac{c_o - c_f}{c_o} * 100 \quad (6.6)$$

$$Weight\ Loading\ Efficiency = \frac{mass_o - mass_f}{mass_o - mass_f + mass_p} * 100 \quad (6.7)$$

The overall loading efficiency of the insulin, shown in Figure 6.13A, was ~41% and the weight loading efficiency of insulin was 5.7%, shown in Figure 6.13B. Though the loading and weight efficiencies leave room for improvement, they were comparable to those reported for similar hydrogel systems with large proteins [9, 11].

Release studies were carried out by incubating the microgels in SGF or SIF for 90 minutes, and samples were taken at 5, 10, 15, 30, 60 and 90 minutes. Unfortunately, the ELISA was unable to detect any insulin in the samples (data not shown). Since the standards created from the insulin loading solution were detected by the ELISA, the lack of detection in the release samples is either due to degradation or insolubility in the release conditions.

6.4 CONCLUSIONS

Synthesis of the linear polymer and crosslinked hydrogels was greatly affected by pH of the respective reaction solutions. The crosslinking reaction was most successful using linear polymer lyophilized at pH 8 in a two-part EDC-NHS linking reaction transitioned from pH 5 to pH 8. Incorporation of the peptide was consistently above 97% as determined by fluorescamine assay of the peptide remaining in solution, and incorporation was verified by IR spectra.

Proteolytic degradation of the peptide crosslinks upon incubation with trypsin solutions, SIF, and rat intestinal fluid was demonstrated by reduced relative turbidity as a function of time and trypsin concentration. In contrast, relative turbidity of the microgel solutions remained constant upon incubation in PBS, SGF, and rat gastric fluid, verifying that the microgels were not susceptible to degradation by the gastric enzyme pepsin. The degradable microgels induced negligible cytotoxic effects, even at high concentration, in both the degraded and nondegraded states. These studies confirm the biodegradable behavior of the peptide crosslinked hydrogel is highly suitable for intestinal delivery applications.

The P(MAA-co-NVP) polymer backbone demonstrated pH responsive behavior, swelling at neutral conditions and collapsing at low pH gastric conditions. However, complexation of the MAA groups at low pH was not complete, allowing some swelling at low pH conditions that could pose issues moving forward with oral delivery studies. Despite this potential drawback, the microgels were able to efficiently load the therapeutic protein insulin and retain the loaded protein in low pH conditions. Insulin release could not be determined due to instability in the release conditions. In conclusion, this work clearly demonstrates that the enzymatic response, relevant degradation

timescale, and high biocompatibility of this biodegradable microgel system endow it with significant potential as a vehicle for oral delivery of delicate therapeutics.

6.5 TABLES

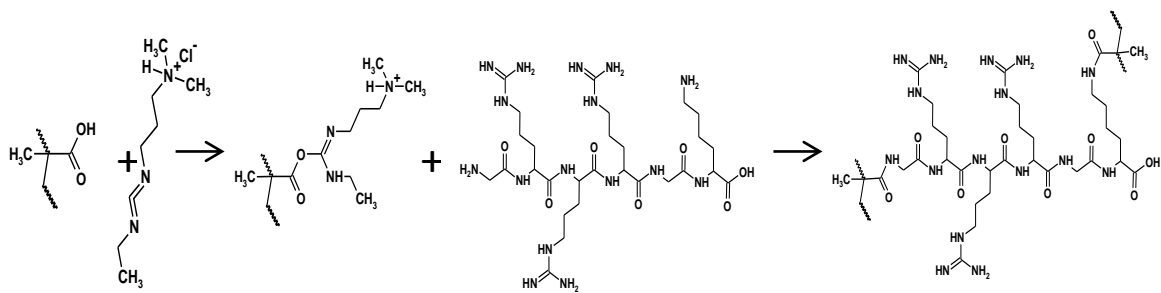
Trial	Polymer	EDC	NHS	Peptide	Result
1	26	10	3.3	1	Failed
2	53	10	3.3	1	Failed
3	53	10	3.3	1	Solubility issues
4	22	10	3.3	10	Hydrogel
5	10	10	3.3	10	Hydrogel
6	25	10	3.3	6.8	Hydrogel
7	22.5	10	3.3	6.8	Hydrogel
8	20	10	3.3	10	Hydrogel
9	17	10	3.3	10	Hydrogel

Table 6.1: Crosslinking reaction formulations (by weight ratio) and outcomes. The best performing formulation (Trial 8) is highlighted in yellow.

Microgel Concentration (mg/ml)	R²	Slope
6	0.89	51.1
3	0.99	64.4
1.5	0.99	68.3
0	0.99	80.7

Table 6.2: Linear parameters of the activity assay of 0.6 mg/ml trypsin incubated with various concentrations of P(MAA-co-NVP) microgels containing degradable crosslinks for 90 minutes (37°C, pH 7.4, N=3). As indicated by the high linear correlation, the trypsin remains active at the end of the incubation period, and the activity is a function of microgel concentration incubated with the trypsin as indicated by the slope of the fitted line.

6.6 FIGURES



Scheme 6.1: Peptide crosslinking reaction scheme. Carboxylic acid groups on the poly(methacrylic acid-co-*N*-vinylpyrrolidone) linear polymer are activated by EDC, then react with at least two of the five primary amine groups on the GRRRGK peptide to form a crosslinked hydrogel network.

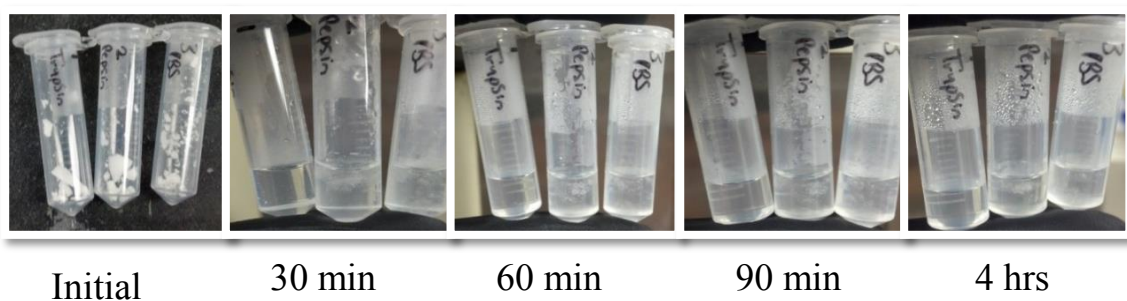


Figure 6.1: Visual indication of hydrogel degradation in SIF (trypsin), SGF (pepsin), or PBS over a 4 hour incubation period. After synthesis and lyophilization, the hydrogel is fluffy, white, and chunky in appearance (Initial). At only 30 minutes after addition of the various buffers, the hydrogel in SIF is no longer visible to the naked eye. Hydrogel incubated in SGF or PBS is still visible at the 4 hour time point.

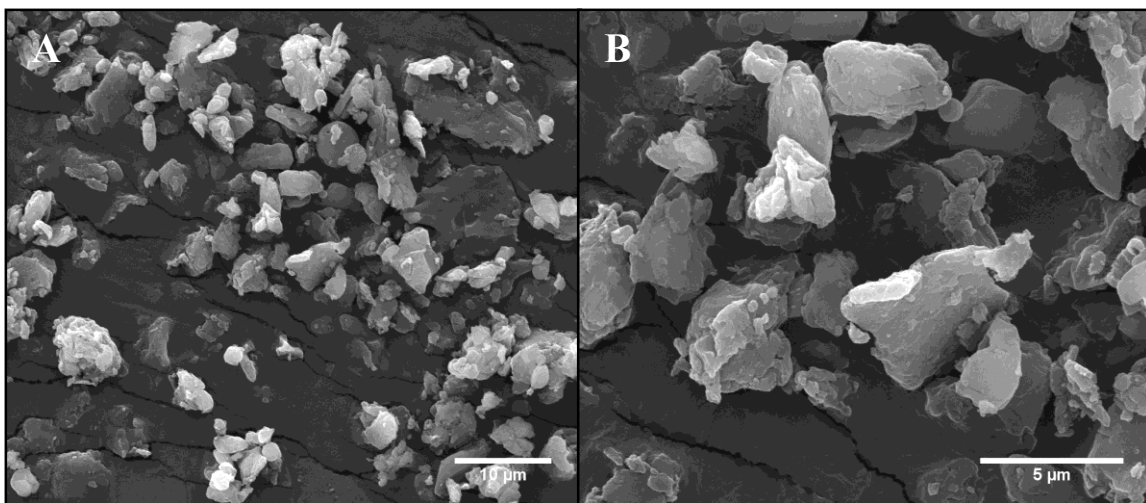


Figure 6.2: P(MAA-co-NVP) microgels with peptide crosslinks in the dry state, crushed and sieved to $<30\text{ }\mu\text{m}$. Particles were dusted onto a carbon-tape coated aluminum stub then coated with 10 nm Pt/Pd. A) scale bar = $10\text{ }\mu\text{m}$; B) scale bar = $5\text{ }\mu\text{m}$ (HV=15.00 kV, WD=9.6 mm).

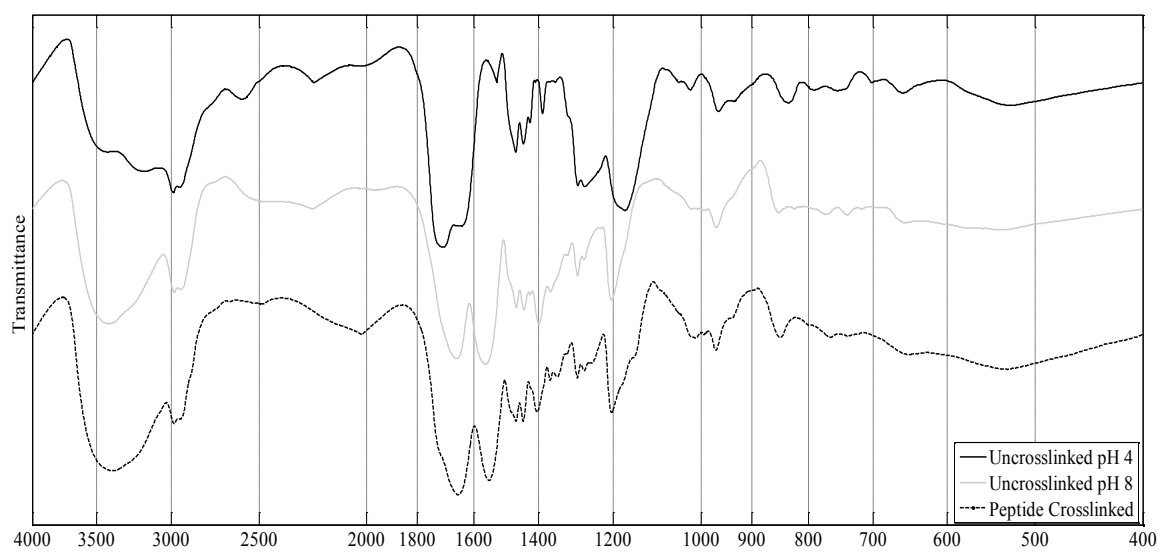


Figure 6.3: FT-IR spectra of uncrosslinked P(MAA-co-NVP) lyophilized at pH 4 or pH 8 and peptide crosslinked P(MAA-co-NVP) at neutral pH; samples were pressed in a KBr disk.

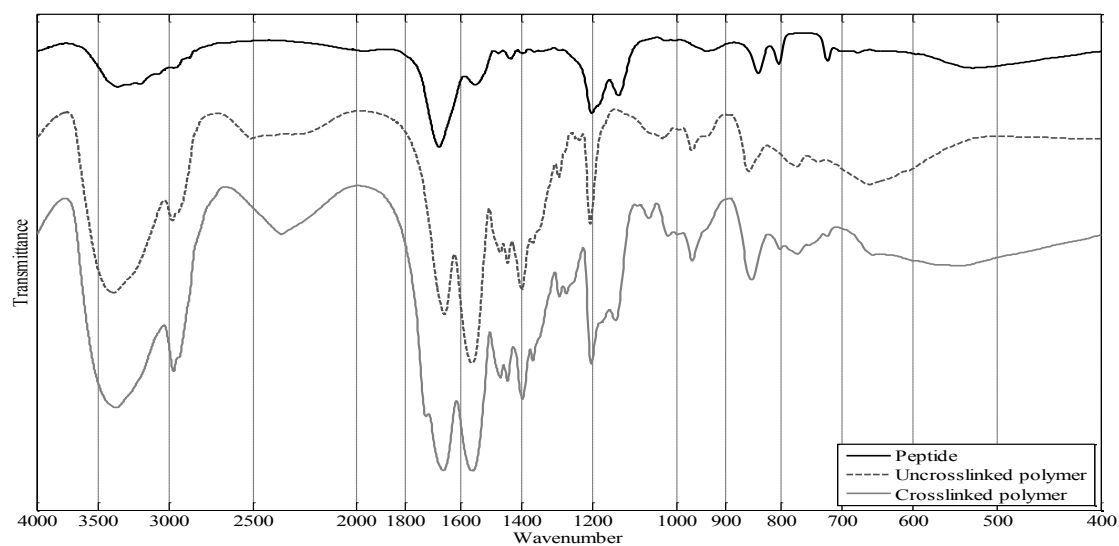


Figure 6.4: FT-IR spectra of GRRRGK peptide, uncrosslinked P(MAA-co-NVP) lyophilized at pH 8, and peptide crosslinked P(MAA-co-NVP) at neutral pH; samples were pressed in a KBr disk.

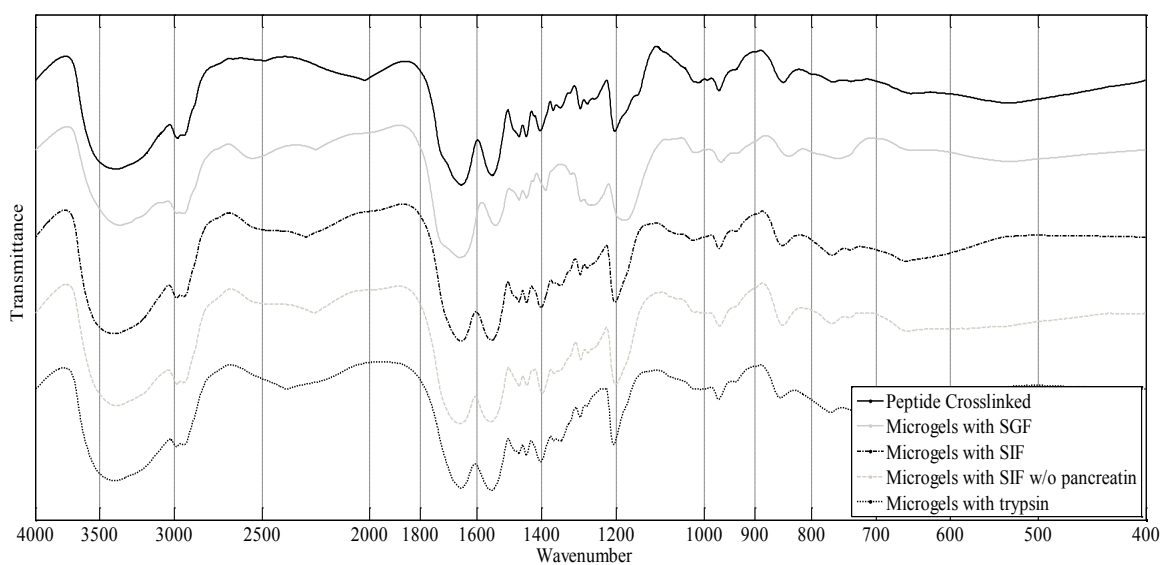


Figure 6.5: FT-IR spectra of peptide crosslinked P(MAA-co-NVP) at neutral pH and peptide crosslinked P(MAA-co-NVP) degradation products following incubation with SGF, SIF, SIF without pancreatin, or a trypsin solution; samples were lyophilized and pressed in a KBr disk.

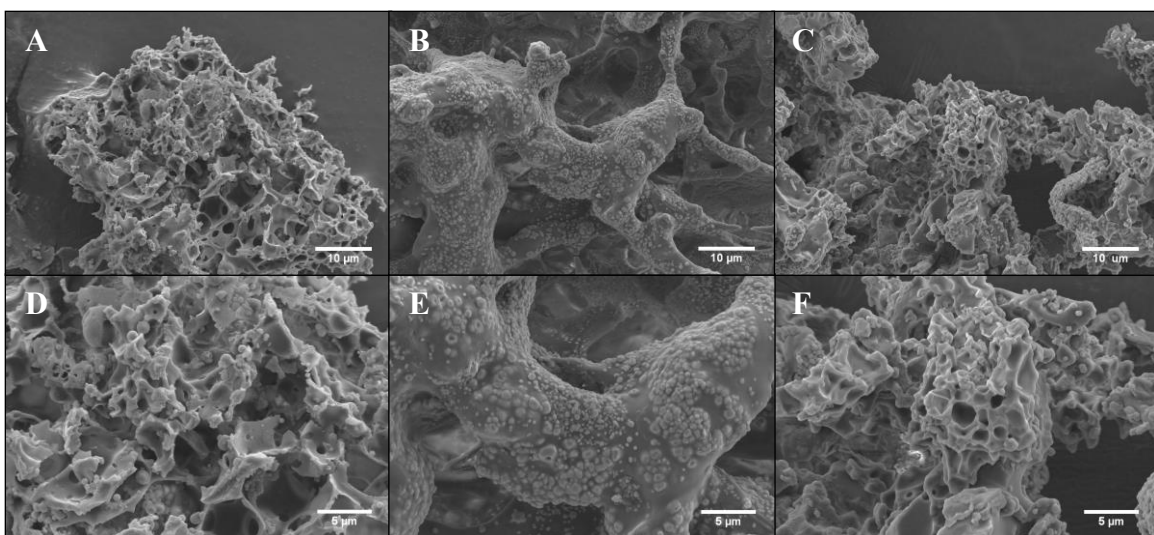


Figure 6.6: SEM micrographs of microgels after 90 minutes incubation in A) SGF (scale =10 μm); B) SIF (scale=10 μm); C) PBS (scale=10 μm); D) SGF (scale =5 μm); E) SIF (scale=5 μm); F) PBS (scale=5 μm); (EHT=5.00 kV, WD=15.6 mm). Following incubation, microgels were lyophilized and dusted onto a carbon-tape coated aluminum stub, then coated with 5 nm Pt/Pd.

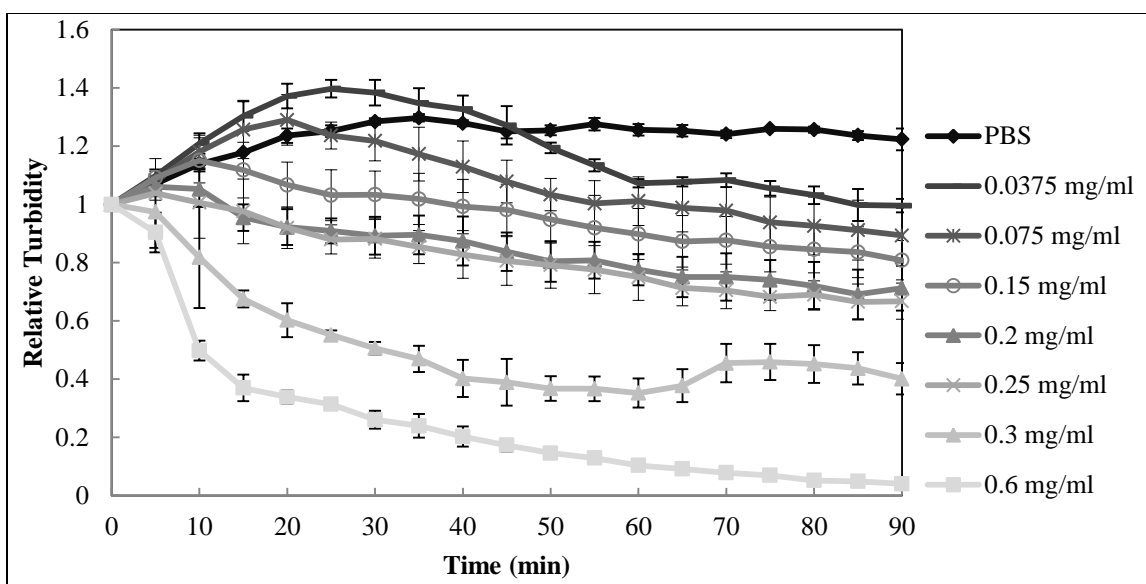


Figure 6.7: Relative turbidity over time of 2 mg/ml solutions of P(MAA-co-NVP) microgels with degradable crosslinks incubated in trypsin solutions ranging from 0-0.6 mg/ml trypsin in PBS (37°C, pH 7.4, N=3).

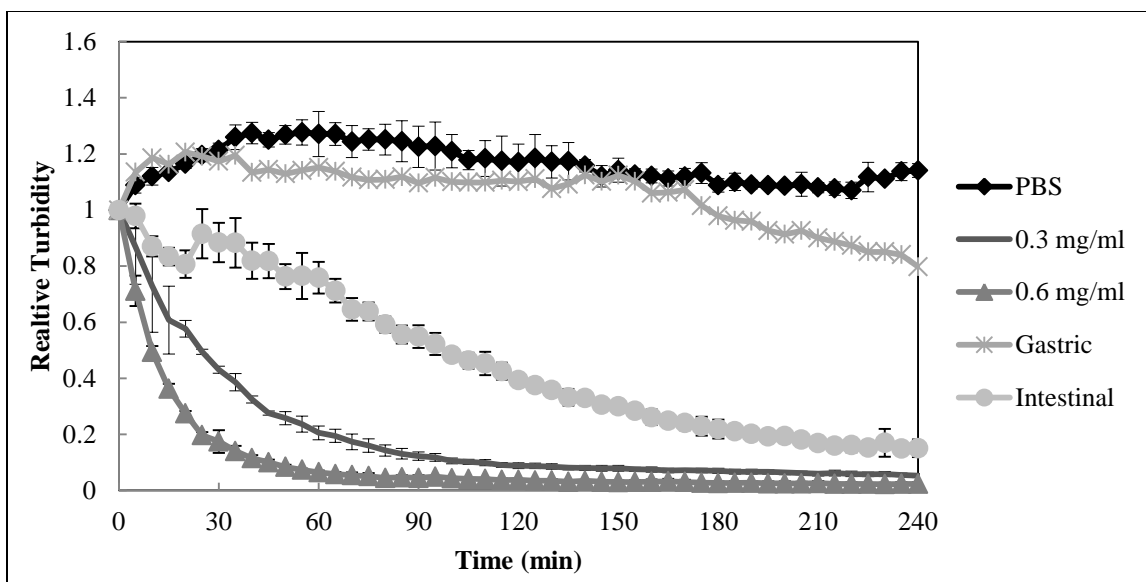


Figure 6.8: Relative turbidity over time of 2 mg/ml solutions of P(MAA-co-NVP) microgels with degradable crosslinks incubated in PBS, 0.3 mg/ml trypsin in PBS, 0.6 mg/ml trypsin in PBS, rat gastric fluid*, or rat intestinal fluid (37°C, pH 7.4, N=3). * Gastric fluid error bars intentionally not shown to simplify the plot; error is ± 0.24 on average in a consistent manner across the period of the study.

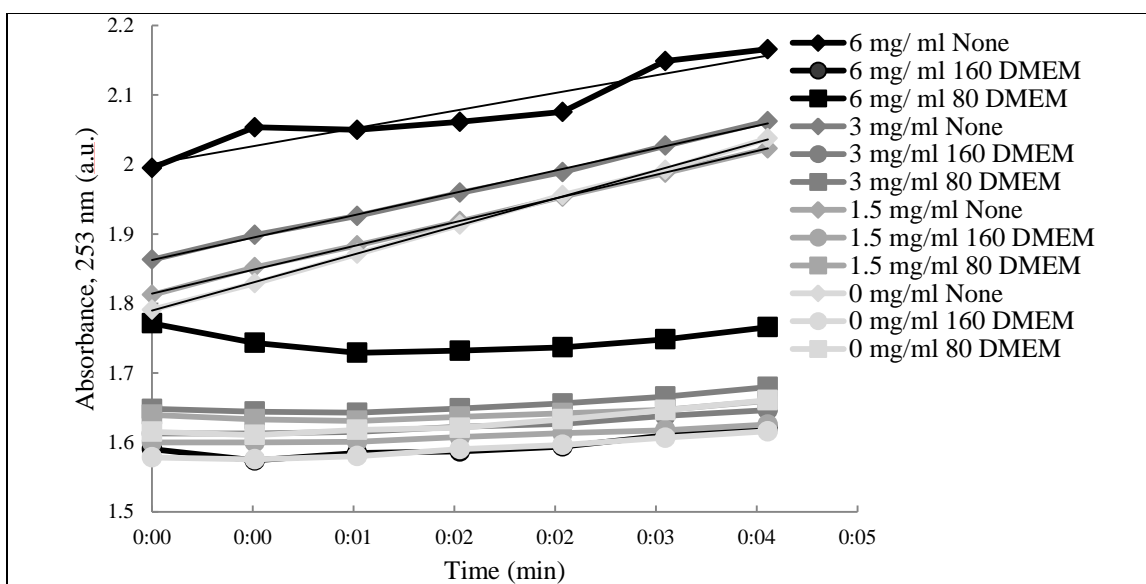


Figure 6.9: Activity assay of 0.6 mg/ml trypsin incubated with various concentrations of P(MAA-co-NVP) microgels containing degradable crosslinks for 90 minutes, and then deactivated with 0, 80, or 160 μ l DMEM (37°C, pH 7.4, N=3). Trypsin activity in the samples receiving no DMEM is evidenced by the strong linear correlation. Both volumes of DMEM were sufficient quench trypsin activity.

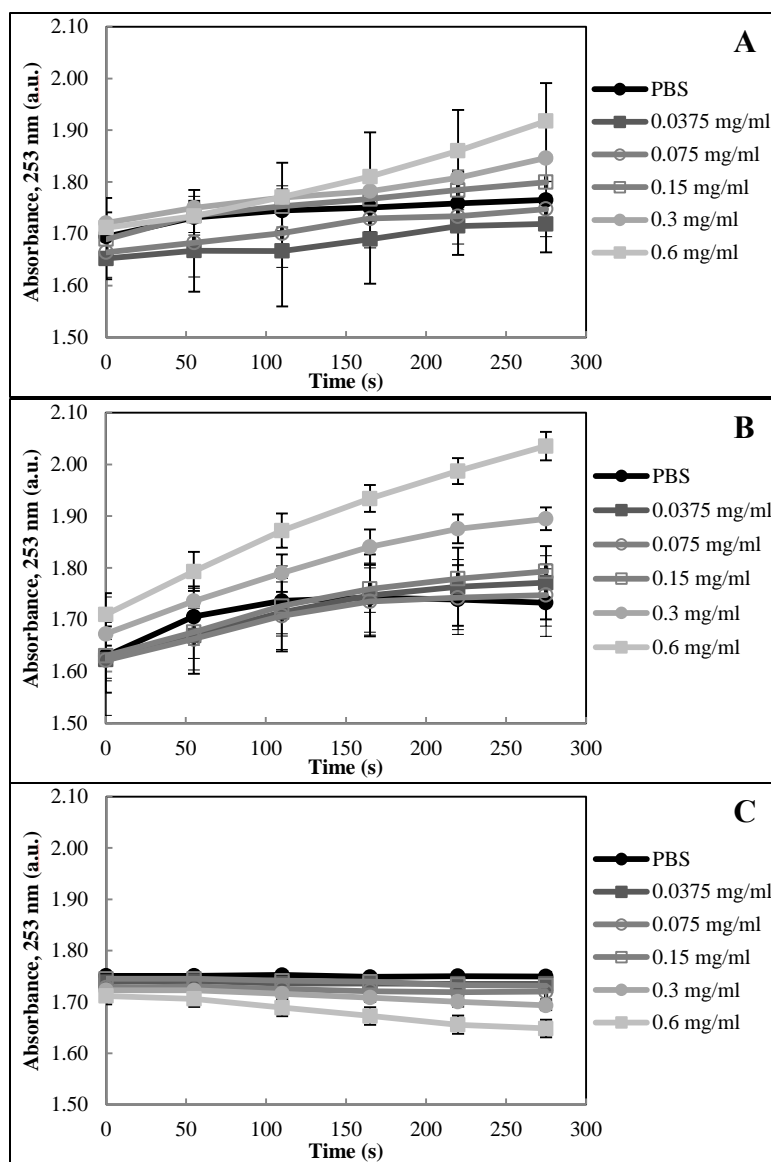


Figure 6.10: Activity assay of various trypsin concentrations incubated A) without microgels B) with 2 mg/ml P(MAA-co-NVP) microgels containing degradable crosslinks for 90 minutes, and C) deactivated at 70°C for 5 minutes (degradation at 37°C, pH 7.4, N=3).

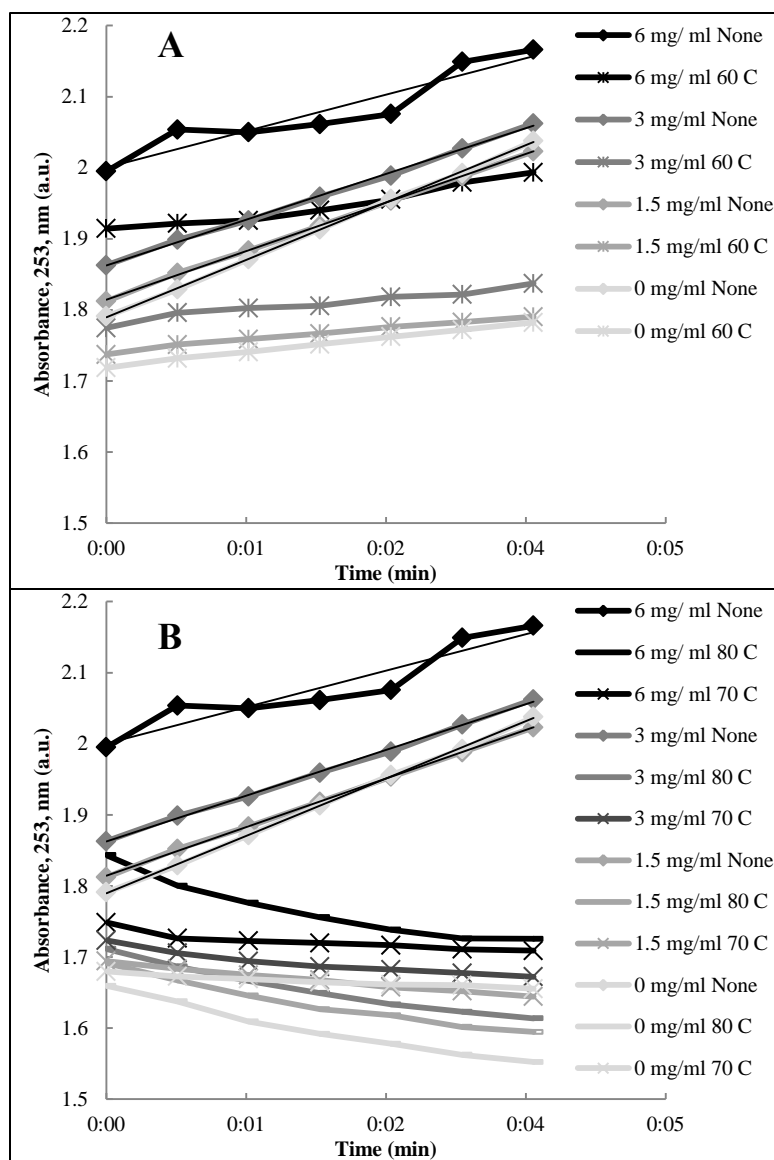


Figure 6.11: Activity assay of 0.6 mg/ml trypsin incubated with various concentrations of P(MAA-co-NVP) microgels containing degradable crosslinks for 90 minutes, and then deactivated with 5 minutes incubation at A) 60°C and B) 70°C or 80°C (degradation at 37°C, pH 7.4, N=3). Incubation at either 70°C or 80 °C was sufficient to deactivate trypsin.

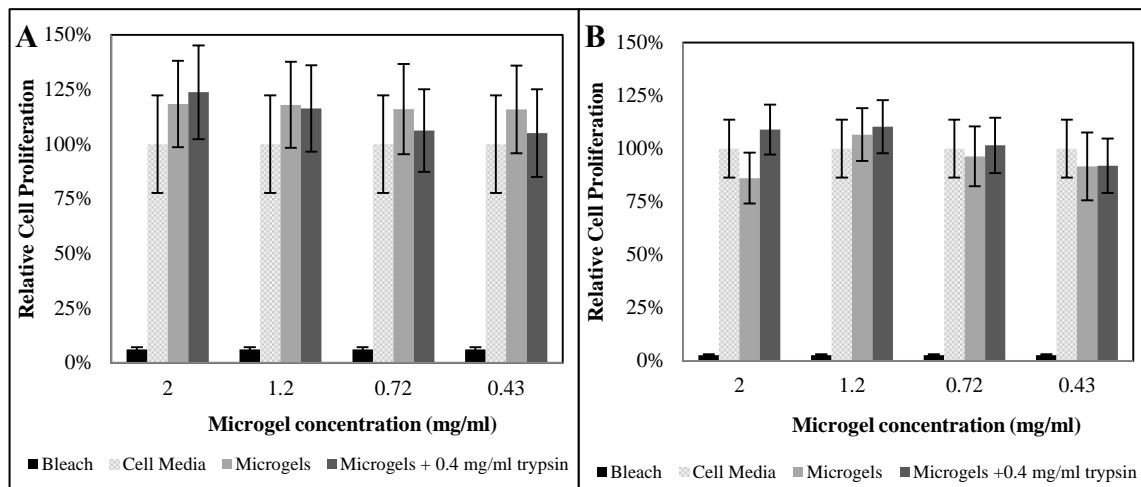


Figure 6.12: Evaluation of degraded microgel exposure effect on cell metabolism using an MTS cell proliferation assay (Promega). Microgels were incubated in PBS or 1.2 mg/ml trypsin in PBS for 90 minutes at 37°C, then the enzyme activity was quenched by addition of media with serum. Murine fibroblast L929 and murine macrophage RAW 264.7 cells were incubated with degraded microgel solutions ranging from 0.43-2 mg/mL in culture media for 8 h. Following removal of the microgel solutions, the MTS assay was allowed to incubate for 90 min. Cell proliferation is relative to the positive control (culture media only, patterned bar) (N=3).

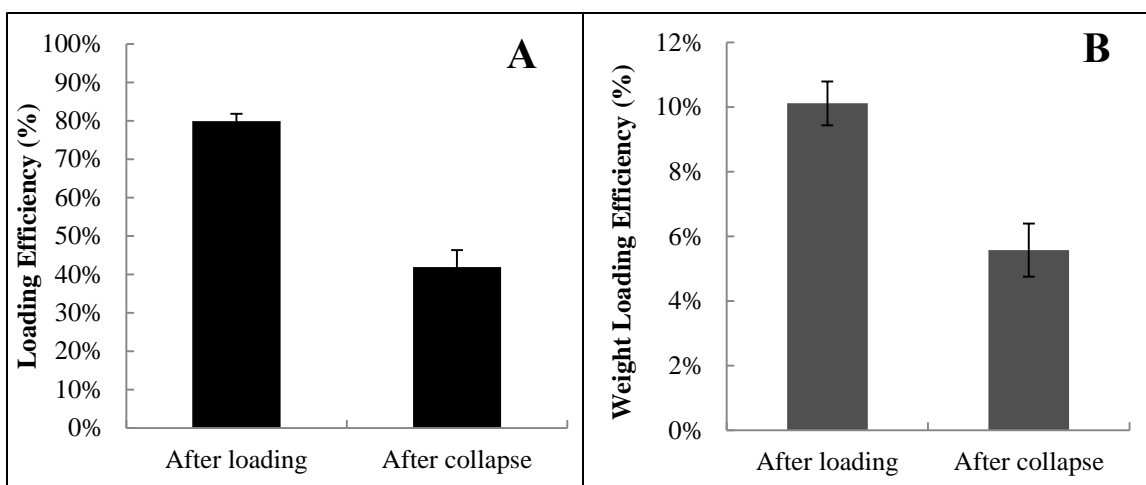


Figure 6.13: Loading efficiencies of degradable P(MAA-co-NVP) microgels with peptide crosslinker. Insulin (MW 5.8 kDa) was loaded into the microgels. Loading efficiency was based on amount of protein into microgels relative to initial amount in solution. Weight loading efficiency is weight of loaded protein relative to total weight of microgel and protein. Microgels were loaded over 4 hours at 37°C (N=3).

REFERENCES

- [1] Peppas, N.A., Hilt, J.Z., Khademhosseini, A., and Langer, R., *Hydrogels in biology and medicine: From molecular principles to bionanotechnology*. Adv Mater, 2006. **18**(11): p. 1345-1360.
- [2] Hoffman, A.S., *Environmentally sensitive polymers and hydrogels*. MRS Bulletin, 1991. **16**: p. 42-46.
- [3] Qiu, Y. and Park, K., *Envinronment-sensitive hydrogels for drug delivery*. Adv Drug Deliver Rev, 2001. **53**(3): p. 321-339.
- [4] Caldorera-Moore, M. and Peppas, N.A., *Micro- and nanotechnologies for intelligent and responsive biomaterial-based medical systems*. Adv Drug Deliver Rev, 2009. **61**(15): p. 1391-1401.
- [5] Holzapfel, B.M., Reichert, J.C., Schantz, J.-T., Gbureck, U., Rackwitz, L., Nöth, U., Jakob, F., Rudert, M., Groll, J., and Hutmacher, D.W., *How smart do biomaterials need to be? A translational science and clinical point of view*. Adv Drug Deliver Rev, 2013. **65**(4): p. 581-603.
- [6] Kost, J. and Langer, R., *Responsive polymeric delivery systems*. Adv Drug Deliver Rev, 2012. **64**: p. 327-341.
- [7] Torres-Lugo, M. and Peppas, N.A., *Preparation and characterization of p(maa-g-eg) nanospheres for protein delivery applications*. J Nanopart Res, 2002. **4**: p. 73-81.
- [8] Torres-Lugo, M. and Peppas, N.A., *Molecular design and in vitro studies of novel ph-sensitive hydrogels for the oral delivery of calcitonin*. Macromolecules, 1999. **32**: p. 6646-6651.
- [9] Knipe, J.M., Chen, F., and Peppas, N.A., *Multiresponsive polyanionic microgels with inverse ph responsive behavior by encapsulation of polycationic nanogels*. J Appl Polym Sci, 2014.
- [10] Lowman, A.M., Morishita, M., Kajita, M., Nagai, T., and Peppas, D.N.A., *Oral delivery of insulin using ph-responsiv complexation gels*. J Pharm Sci, 1999. **88**: p. 933-937.

- [11] Carr, D.A., Gomez-Burgaz, M., Boudes, M.C., and Peppas, D.N.A., *Complexation hydrogels for the oral delivery of growth hormone and salmon calcitonin*. Ind Eng Chem Res, 2010. **49**: p. 11991-11995.
- [12] Carr, D.A. and Peppas, N.A., *Assessment of poly(methacrylic acid-co-n-vinyl pyrrolidone) as a carrier for the oral delivery of therapeutic proteins using caco-2 and ht29-mtx cell lines*. J Biomed Mater Res A, 2009. **92A**: p. 504-512.
- [13] Glangchai, L.C., Caldorera-Moore, M., Shi, L., and Roy, K., *Nanoimprint lithography based fabrication of shape-specific, enzymatically-triggered smart nanoparticles*. J Controlled Release, 2008. **125**(3): p. 263-272.
- [14] Guo, D.-S., Wang, K., Wang, Y.-X., and Liu, Y., *Cholinesterase-responsive supramolecular vesicle*. J Am Chem Soc, 2012. **134**(24): p. 10244-10250.
- [15] Ulbrich, K., Strohalm, J., and Kopecek, J., *Polymers containing enzymatically degradable bonds. Iv. Hydrophilic gels cleavable by chymotrypsin*. Biomaterials, 1982. **3**: p. 150-154.
- [16] Subr, V., Duncan, R., and Kopecek, J., *Release of macromolecules from hydrophilic gels containing enzymatically degradable bonds*. J. Biomater. Sci. Polymer Edn, 1990. **1**: p. 261-278.
- [17] Vlieghe, P., Lisowski, V., Martinez, J., and Khrestchatisky, M., *Synthetic therapeutic peptides: Science and market*. Drug Discovery Today, 2010. **15**(1-2): p. 40-56.
- [18] Wanakule, P., Liu, G.W., Fleury, A.T., and Roy, K., *Nano-inside-micro: Disease-responsive microgels with encapsulated nanoparticles for intracellular drug delivery to the deep lung*. J Controlled Release, 2012. **162**: p. 429-437.
- [19] Thornton, P.D., Mart, R.J., and Ulijn, R.V., *Enzyme-responsive polymer hydrogel particles for controlled release*. Adv Mater, 2007. **19**(9): p. 1252-1256.
- [20] Pharmacopeia, T.U.S., *United states pharmacopeia 29 national formulary 24, in Reagents: Test Solutions*. 2006.
- [21] Yamagata, T., Morishita, M., Kavimandan, N.J., Nakamura, K., Fukuoka, Y., Takayama, K., and Peppas, N.A., *Characterization of insulin protection*

- properties of complexation hydrogels in gastric and intestinal enzyme fluids.* J Controlled Release, 2006. **112**(3): p. 343-349.
- [22] Klinger, D. and Landfester, K., *Enzymatic- and light-degradable hybrid nanogels: Crosslinking of polyacrylamide with acrylate-functionalized dextrans containing photocleavable linkers.* J Polym Sci, Part A: Polym. Chem, 2012. **50**(6): p. 1062-1075.
- [23] Yanes, O., Villanueva, J., Querol, E., and Aviles, F., *Enzymatic measurements for the detection of trypsin and carboxypeptidase a inhibitory activity.* 2007.
- [24] Hermanson, G.T., *Bioconjugate techniques.* 1996, San Diego, CA: Academic Press, Inc.
- [25] Bohlen, P., Stein, S., Dairman, W., and Udenfriend, S., *Fluorometric assay of proteins in the nanogram range.* Archives of Biochemistry and Biophysics, 1973. **155**: p. 213-220.
- [26] Lee, J.Y., Painter, P.C., and Coleman, M.M., *Hydrogen bonding in polymer blends. 4. Blends involving polymers containing methacrylic acid and vinylpyridine groups.* Macromolecules, 1988. **21**: p. 954-960.
- [27] Kolev, T., *Solid-state ir-ld spectroscopic and theoretical analysis of arginine-containing peptides.* Biopolymers, 2006. **83**: p. 39-45.
- [28] Olsen, J.V., *Trypsin cleaves exclusively c-terminal to arginine and lysine residues.* Mol Cell Proteomics, 2004. **3**(6): p. 608-614.
- [29] Xu, J., Ye, J., and Liu, S., *Synthesis of well-defined cyclic poly(n-isopropylacrylamide) via click chemistry and its unique thermal phase transition behavior.* Macromolecules, 2007. **40**: p. 9103-9110.
- [30] Qiu, X.-P., Tanaka, F., and Winnik, F.M., *Temperature-induced phase transition of well-defined cyclic poly(n-isopropylacrylamide)s in aqueous solution.* Macromolecules, 2007. **40**: p. 7069-7071.
- [31] Klinger, D. and Landfester, K., *Photo-sensitive pmma microgels: Light-triggered swelling and degradation.* Soft Matter, 2011. **7**: p. 1426-1440.

- [32] Lechner, M.D., *Influence of mie scattering on nanoparticles with different particle sizes and shapes: Photometry and analytical ultracentrifugation with absorption optics*. JouRNAI of the Serbian Chemical Society, 2005. **70**: p. 361-369.
- [33] Davis, S.S., Hardy, J.G., and Fara, J.W., *Transit of pharmaceutical dosage forms through the small intestine*. Gut, 1986. **27**: p. 886-892.
- [34] Schwert, G.W. and Takenaka, Y., *A spectrophotometric determination of trypsin and chymotrypsin*. Biochimica Et Biophysica Acta, 1955. **16**: p. 570-575.
- [35] Pace, J., *Lxviii. The inactivation of trypsin by heat*. Biochemical JouRNAI, 1930. **24**: p. i3.
- [36] Kaplan, J.G. and Bona, C., *Proteases as mitogens: The effect of trypsin and pronase on mouse and human lymphocytes*. Experimental Cell Research, 1974. **88**: p. 388-394.
- [37] Unanue, E.R., *Antigen-presenting function of the macrophage*. Annual Review of Immunology, 1984. **2**: p. 395-428.

Chapter 7: Biodegradable Microencapsulated Nanogels for Orally Delivered siRNA

7.1 INTRODUCTION

RNA interference, an endogenous mechanism for silencing specific genes [1], has exciting potential as a therapy for many diseases. In fact, there are approximately thirty recent or active clinical trials involving small interfering RNA (siRNA) therapy, but at least twenty of the studies utilize intravenous or injection-based methods of administration and none of the studies administer siRNA orally [2]. Oral delivery of siRNA would be particularly well-suited to treating diseases of the gastrointestinal (GI) tract, such as inflammatory bowel diseases, and intestinal absorption also offers a route to systemic delivery. However, there are many extracellular and intracellular barriers to oral siRNA delivery such as proteolytic degradation [3], harsh pH environments [4], and the necessity to achieve intracellular delivery and endosomal escape while maintaining the integrity of the siRNA [5, 6], making successful oral delivery of siRNA a daunting task.

The current strategies for oral delivery of siRNA to the intestine are relatively few in number, and they employ creative solutions that are only effective in a limited capacity. For example, Aouadi et al. [7] developed the first oral delivery system, in which a cationic core was loaded with layers of siRNA and additional polycationic polymer, and encapsulated in β 1,3-D-glucan microshells. The system was very potent, reducing target protein expression by up to 80%, but lacked specificity in targeting and delivery.

Amiji et al. [8, 9] developed a hybrid nanoparticle-in-microsphere oral delivery system to the intestinal mucosa in which FITC-gelatin nanoparticles were embedded in a poly(ϵ -caprolactone) matrix of less than 2-5 μ m in diameter,. Though it performed well *in vivo* its ability to withstand low pH conditions and prevent premature release of siRNA is questionable.

Thioketal nanoparticles were designed by Wilson et al. [10] to be degraded by reactive oxygen species produced by phagocytes at the site of inflammation in the intestine, thereby delivering siRNA to knockdown a well-known inflammatory cytokine as a treatment for inflammation. The highly specific release mechanism of this system is quite appealing for treating inflammatory diseases of the gastrointestinal tract, but is not translatable to disease models in which inflammation is not present. Laroui et al. [11] published a report on branched polyethyleneimine complexed with siRNA, loaded into polylactides, and covered with polyvinyl alcohol in a multi-step synthesis process. The particles were then encapsulated in alginate or chitosan for oral administration to mice, where they were effective in reducing the target protein expression.

These studies establish a solid foundation but leave significant room for improvement, particularly in terms of increasing delivery specificity, maintaining siRNA integrity, and increasing dosage efficacy. Consequently, there is great need to design an improved polymer carrier which can not only protect siRNA from harsh gastric conditions and target delivery to specific regions of diseased or healthy intestine, but can also facilitate cellular uptake and endosomal escape into the cytoplasm where RNAi occurs. One strategy to achieve this is by encapsulating polycationic nanogels within a biodegradable intestinal delivery vehicle.

To achieve this goal, *polycationic 2-(diethylamino)ethyl methacrylate-based nanogels* were encapsulated within an enzymatically-degradable poly(methacrylic acid-co-N-vinyl-2-pyrrolidone) hydrogel. Thus, the anionic hydrogel should protect the payload in gastric conditions but swell, degrade, and release the nanogels complexed with siRNA in intestinal conditions. Herein, the synthesis, biodegradation, siRNA loading, cellular uptake, cytotoxicity, and silencing efficiency of this novel microencapsulation system for oral siRNA delivery are described.

7.2 EXPERIMENTAL METHODS

7.2.1 Chemicals

Methacrylic acid (MAA), N-vinyl pyrrolidone (NVP), and Irgacure 184® (1-hydroxy-cyclohexyl-phenylketone) were obtained from Sigma-Aldrich (St. Louis, MO). 1-ethyl-3-(3-dimethylaminopropyl) carbodiimide hydrochloride (EDC) was obtained from Sigma Aldrich. N-hydroxysuccinimide (NHS) was obtained from Pierce Biotechnology, Inc. (Rockford, IL). The custom sequence oligopeptide GRRRGK was synthesized by CHI Scientific (Maynard, MA). All reagents were used as received. Purified pepsin from porcine gastric mucosa (≥ 2500 U/mg), pancreatin from porcine pancreas (4x USP specifications), Trypsin-EDTA solution (1X) and N α -benzoyl-L-arginine ethyl ester hydrochloride (BAEE) trypsin substrate were obtained from Sigma-Aldrich. 4-Chloro-7-nitrobenzofurazan (NBD-Cl, 98%) was obtained from Acros Organics (Geel, Belgium). All other solvents and buffers were purchased from Fisher Scientific (Waltham, MA). Polycationic 2-(diethylamino)ethyl methacrylate-based nanogels (~100 nm diameter) were synthesized by Forbes et al. [12] and tagged with a fluorescent molecule, NBD-Cl, by Forbes et al. [13].

7.2.2 Synthesis and Purification

7.2.2.1 *Synthesis of Linear Polymer*

P(MAA-co-NVP) linear polymer was synthesized by photoinitiated, free-radical polymerization. MAA and NVP were added at a 1:1 molar ratio to a 1:1 (w/w) deionized water and ethanol solution to yield a 1:3 (w/w) total monomer to solvent ratio. Photoinitiator Irgacure 184® was added at 1 wt% with respect to total monomer weight.

The mixture was homogenized by sonication then the round bottom flask was sealed with a rubber septum. The solution was purged with nitrogen for 20 minutes, then

the reaction was initiated with a Dymax BlueWave® 200 UV point source (Dymax, Torrington, CT) at 100mW/cm² intensity and allowed to polymerize for 30 minutes while stirring.

Following polymerization, the linear polymer was purified from unreacted monomer by addition of 1 N hydrochloric acid (HCl) to precipitate polymer, centrifugation, and resuspension in deionized water. After 3 wash cycles, the polymer solution was frozen in liquid nitrogen (LN₂) and lyophilized for at least 24 hours.

7.2.2.2 Synthesis of Peptide Crosslinked Gels

Linear P(MAA-co-NVP) was dissolved in a 1:1 (v/v) water:ethanol solution at a concentration of 50 mg/ml. EDC was dissolved in ethanol at a concentration of 50 mg/ml and NHS was dissolved in ethanol at a concentration of 16 mg/ml. The EDC and NHS solutions were added to the polymer solution at a ratio of 6:3:1 polymer:EDC:NHS by weight. The solution was mixed by vortex briefly, then allowed to react for ~3 min with shaking. Polycationic nanoparticles in a 10 mg/ml solution in ethanol were added at 10 wt% relative to the P(MAA-co-NVP) and the solution was briefly mixed by vortex. The pH was raised to ~8 by the addition of 1 N sodium hydroxide (NaOH), and then a volume of 100 mg/ml peptide in ethanol solution was added to achieve a 2:1 weight ratio of polymer:peptide. The mixture was allowed to react overnight with shaking then purified by 3 wash cycles with water and centrifugation at 10,000 x g for 5 minutes. Following the washes, the polymer was frozen in LN₂ and lyophilized for at least 24 hours.

After lyophilization, the polymer was milled into a fine power by crushing with mortar and pestle. The powder was sifted to the size ranges of 30-75 µm and less than 30 µm by ultraprecision ASTM sieves (Precision Eforming, Cortland, NY).

7.2.3 Cell Culture

Human colon adenocarcinoma Caco-2, murine fibroblast L929, and murine macrophage RAW 264.7 cells obtained from American Type Culture Collection (ATCC, Rockwell, MD). All cell lines were cultured in Dulbecco's modified Eagle medium (DMEM) (Mediatech, Herndon, VA) supplemented with 10% heat-inactivated HyClone™ Fetal Bovine Serum, USDA Tested (Fisher Scientific), 1% 200 mM L-glutamine solution (Mediatech), 100 U/ml penicillin, and 100 µg/ml streptomycin (Mediatech). Cytotoxicity studies were performed using DMEM without phenol red supplemented with 2% heat-inactivated HyClone™ Fetal Bovine Serum, USDA Tested (Fisher Scientific), 1% non-essential amino acids (Mediatech), 100 U/ml penicillin, and 100 µg/ml streptomycin (Mediatech) or OptiMEM® reduced serum media (no phenol red) (Life Technologies, Grand Island, NY). Transfection studies were completed in OptiMEM® reduced serum media (no phenol red). Cells were incubated at 37°C in a 5% CO₂ environment.

7.2.4 *In vitro* Cytotoxicity Study

Cells were seeded at a density of 10,000 cells/well in a 96-well plate and allowed to incubate for 24 hours prior to the experiment. Microgels were degraded in 0.3-1.25 mg/ml trypsin in phosphate buffered saline (PBS) at concentrations ranging from 1.3-6 mg/ml. Degradation took place at 37°C with shaking for 90 minutes or 4 hours. Trypsin was deactivated by addition of 2X volume DMEM without phenol red containing 2% fetal bovine serum or by incubation at 70°C for 5 minutes. Cells were incubated with degraded microgels for 18 hours at 37°C and 5% CO₂. The cytotoxic effect of the microgels was evaluated using a CellTiter 96® Aqueous One Solution Cell Proliferation MTS Assay or a CytoTox-ONE™ Homogeneous Membrane Integrity Assay (Promega, Madison, WI). In the case of the proliferation assay, MTS was added to the wells and

incubated for 90 minutes at the same conditions before absorbance measurements were made at 490 nm using a Bio-Tek Synergy™ HT multi-mode plate reader (Winooski, VT). In the case of the membrane integrity assay, 50 µl of the cell media from each well was combined with 50 µl of the assay solution in a black-walled 96-well plate, incubated at room temp for 10 minutes, then the fluorescence was measured at 530/560 (sensitivity=60) using a Bio-Tek Synergy™ HT multi-mode plate reader (Winooski, VT). Cytotoxicity is reported as 'relative cell proliferation' using the MTS assay and 'percent viability' using the membrane integrity assay.

7.2.5 siRNA Loading

Microgels containing NBD-labeled nanogels were loaded by equilibrium partitioning post-synthesis with Silencer® Select Negative Control No. 1 (Life Technologies), AllStars Mm/Rn Cell Death Control siRNA, AllStars Hs Cell Death Control siRNA, Negative Control siRNA (Qiagen, Hilden, Germany), or fluorescently labeled DyLight 647-labeled siRNA (Sense: DY647-UAAGGCUAUGAAGAGAUACUU (Thermo Scientific, Lafayette, CO). Microgels were incubated at a concentration of 12 mg/ml at 37°C for 1.5 hours in a 400 nM or 100 nM siRNA solution in nuclease-free PBS at pH ~5.5. Nuclease free 10X PBS was prepared by dissolving sodium chloride, potassium chloride, monobasic potassium phosphate, and sodium phosphate dibasic heptahydrate in water, treating with 0.1% v/v diethylpyrocarbonate (DEPC) overnight, and then autoclaving to remove DEPC. The microgels were collected by centrifugation at 10,000 x g for 5 minutes. The loaded microgels were stored at -20°C until further studies. siRNA loading was evaluated by Quant-iT™ RiboGreen® RNA Assay Kit (Invitrogen).

7.2.6 Microgel Degradation and siRNA Stability

7.2.6.1 Microgel Degradation

Microgels were degraded at various trypsin concentrations ranging from 0.2-1.2 mg/ml in 1X phosphate buffered saline solution (pH 7.4), simulated gastric fluid, simulated intestinal fluid, rat gastric fluid or rat intestinal fluid.

Simulated gastric fluid (SGF) and simulated intestinal fluid (SIF) were prepared according to USP 29 [14]. Briefly, SGF was prepared by dissolving 2 g of sodium chloride and 3.2 g of purified pepsin from porcine stomach mucosa was dissolved in ~800 ml deionized water. 7 ml of HCl was added, followed by enough water to make up to 1 L and the pH adjusted to 1.2. SIF was prepared by dissolving 6.8 g monobasic potassium phosphate in 250 ml deionized water, then 77 ml of 0.2 N NaOH was added while stirring. 500 ml additional water was added then 10 g pancreatin was mixed into the solution. The pH was adjusted to 6.8 using 0.2 N NaOH or HCl then the solution was made up to 1 L with water.

Gastrointestinal fluids were harvested from Sprague Dawley juvenile male rats (250-300 g) according to a protocol published by Yamagata et al. with some modifications [15]. Briefly, after sacrificing the rat the stomach was excised and ligated at both ends. A needle was inserted to inject 5 ml of pH 1.2 HCl-NaCl buffer (same as SGF minus pepsin) and the gastric contents were collected in a 50 ml centrifuge tube. Similarly, a ~20 cm section of the upper small intestine was cannulated and flushed twice with 10 ml cold PBS (1X, pH 7.4). The fluid was collected as intestinal fluid in a 50 ml centrifuge tube. Both the harvested fluids were centrifuged at 3,200 x g, 4°C, for 15 min to separate solids from the fluids. The supernatants were retained as rat gastric fluid and rat intestinal fluid, respectively. Protein content of the fluids was measured using a

NanoDrop 1000 spectrophotometer (Thermo Scientific, Wilimington, DE). Fluids were stored at -20°C until use.

Degradation was evaluated by measuring relative turbidity of the samples over time, as reported by Klinger and Landfester [16]. Microgels were suspended in trypsin solutions of varying concentration, PBS, SGF, SIF, or rat gastrointestinal fluids at various concentrations. 100 µl of each solution was added to a 96-well plate in triplicate, and the absorbance was measured at 500 nm in 5 minute intervals over 90 minutes using a Bio-Tek Synergy™ HT multi-mode plate reader (Winooski, VT). The temperature was controlled at 37°C and the plate underwent shaking for 3 seconds before each measurement.

Activity of the trypsin following incubation with particles and deactivation methods including addition of serum-containing cell culture media and 5 minutes incubation at 70°C was evaluated using a trypsin activity assay adapted from the protocol by Yanes et al. [17]. Briefly, degradation supernatant was combined with 1 mg/ml BAEE in PBS at a 1:9 sample:BAEE ratio by volume. Immediately after addition of the BAEE, absorbance at 253 nm was measured at the minimum interval (typically 40-50 seconds) for 5 minutes using a Bio-Tek Synergy™ HT multi-mode plate reader (Winooski, VT).

7.2.6.2 Evaluation of siRNA Stability by Polyacrylamide Gel electrophoresis

For polyacrylamide gel electrophoresis, samples were degraded in trypsin concentrations from 0.3-1.2 mg/ml for 90 min then the trypsin was deactivated with DMEM or heat. Samples were also incubated in rat gastric fluid, rat intestinal fluid, PBS, or SGF to determine release and stability of siRNA. Competitive polyanion assays were completed using solutions of heparin sodium salt from porcine intestinal mucosa (Sigma-

Aldrich) to competitively complex with the polycationic nanogels and promote siRNA dissociation from the nanogels. Ribonuclease A from bovine pancreas (RNase A) (Sigma-Aldrich) was used as a positive degradation control; siRNA was incubated in a 0.05 mg/ml RNase A solution for 90 minutes at 37°C. Samples were diluted 1:1 by volume with Novex® TBE-urea sample loading buffer (2X) (Life Technologies), denatured at 70°C for 3 min, and loaded into a Novex® TBE-urea denaturing polyacrylamide gel with 15% crosslinking (Life Technologies). The gel was run at constant 180V for 70 min in 1X Novex® TBE running buffer (Life Technologies). Following the run, the gel was stained with SYBR green II (Sigma-Aldrich) diluted 1:10,000 by volume in 1X TBE running buffer for 30 minutes with shaking, the gel was rinsed with DI water for 5 minutes with shaking, and then the gel was imaged with a Typhoon 9500 fluorescent imager using the SYBR green II filter, 50 µm pixel size, 500 pmt. (GE Life Sciences, Pittsburgh, PA).

7.2.7 Confocal Microscopy

Microgels were fluorescently labeled with TAMRA-cadaverine (Biotium) via EDC-NHS reaction. Briefly, 15 mg microgels were mixed with 1.25 mg of EDC and 1.25 mg NHS in 0.1 M MES buffer at pH 4.7. After a ~3 minute incubation period at room temperature, 15 µl of 0.5 mg/ml TAMRA-cadaverine solution was added and allowed to react for 2 hours at room temperature. The polymer was washed 5X by centrifugation at 10,000 x g for 5 minutes and resuspension in 1 ml DI water to remove unreacted fluorophore. The final wash was left overnight to allow the polymer to fully swell. The microgels were centrifuged again, the supernatant removed, and the remaining polymer flash-frozen in LN₂ followed by lyophilization. Fluorescent microgels were incubated in

PBS or trypsin at a concentration of 2 mg/ml for 90 minutes. Slides were prepared by mounting 10 μ l of particle solution on slides with ProLong® gold antifade reagent.

For cell uptake studies, coverslips (18 mm round, no. 1.5 thickness) were acid-washed overnight with 1 N HCl at 60°C, rinsed with ethanol/water mixtures with successively increasing volume ratios of ethanol, and then the coverslips were placed in a 12-well plate. RAW 274.6 cells were seeded in the wells at a density of 115,000 cells/well. Microgels containing NBD-labeled nanogels, with or without fluorescently labeled DY647 siRNA, were degraded at a concentration of 2.5 mg/ml in 0.6 mg/ml trypsin for 60 minutes then incubated at 70°C for 5 minutes to deactivate trypsin. 24 hours after plating the cells, the media was aspirated and replaced with 0.4 ml OptiMEM and 0.1 ml of degraded microgel solution. Lipofectamine 2000 (Life Technologies) loaded with fluorescently labeled DY647 siRNA was used as a positive control for siRNA delivery. Cells were incubated with the particles or Lipofectamine 2000 for 18 hours.

After the incubation period, the media was aspirated and the cells were washed 3X with cold Dulbecco's phosphate buffered saline (DPBS, Sigma-Aldrich), fixed with cold IC fixation buffer containing 4% paraformaldehyde (Life Technologies), and washed 3X with cold Hyclone™ Hank's balanced salt solution (HBSS, Fisher Scientific). In some cases, the cell membrane was stained with 1 μ g/ml AlexaFluor® 594 conjugated wheat germ agglutinin (Life Technologies) for 10 minutes then washed 2X with cold HBSS and once with cold, sterile DI water. ProLong® gold antifade reagent with or without DAPI stain (Life Technologies) was used to mount the coverslips on acid-washed slides. Slides were stored at -4°C until imaging.

Slides were imaged with Zeiss LSM 710 confocal microscope with 40x- and 63x-oil objectives. Sequential scanning was used to eliminate emission bleed-through between

channels. The pinhole was set to 1 AU in the green channel. The gain and offset for each channel were set using single stain controls, and were kept constant for the full series of images to allow image comparisons. Images were collected in 8 bit format with an average=4 to reduce noise, and all images underwent identical postprocessing ($\gamma = 0.7$ for red, blue, and green channels, $\gamma = 0.1.3$ for bright-field).

7.2.8 ImageStream Flow Cytometry

Microgels containing NBD-labeled nanogels and were incubated in PBS (pH 7.4) or 0.6 mg/ml trypsin solution at 1.5 mg/ml for 60 min then the trypsin was deactivated by incubation at 70°C for 5 minutes. Analysis of nanogel distribution and microgel degradation was conducted using Amnis ImageStream (Seattle, WA) imaging flow cytometer. Nanogels were excited with a 488 laser and detected in channel 2 (505-560 nm) and bright field images were collected in channel 4 (595-660 nm). At least 10,000 events were collected for analysis. Out-of-focus particles and debris were excluded from the analysis by gating the Gradient RMS feature in IDEAS® software; typically, events with Gradient RMS value <50 were considered out of focus. Fluorescence intensity in the green channel was gated to intensity values > 3000.

7.2.9 Cell Transfection

RAW 264.7 cells were seeded at 10,000 cells/well in 96-well cell culture plates for transfection studies. The RAW 264.7 cells were allowed to incubate approximately 48 hours and the Caco-2 cells approximately 24 hours, until they reached a confluence of about 50%.

After the appropriate cell growth period, microgels were loaded with siRNA for transfection studies using the same conditions described in Section 7.2.4. Microgels were loaded with AllStars Mm/Rn Cell Death Control siRNA, AllStars Hs Cell Death Control

siRNA, or Negative Control siRNA at a loading concentration of 400 nM. Microgels were degraded at a concentration of 3.5 or 2 mg/ml in 0.3 mg/ml trypsin in PBS at 37°C for 90 minutes. Nanoparticles were complexed with siRNA (AllStars Mm/Rn Cell Death Control siRNA, AllStars Hs Cell Death Control siRNA, or Negative Control siRNA) in 1X PBS pH 5.5 at 0.125 mg/mL nanoparticles and 400 nM siRNA for ~15 prior to addition to cells. siRNA (400 nM) was incubated with 2 µl Lipofectamine 2000 (positive control) in 78 µl OptiMEM for ~15 minutes prior to addition to cells.

The microgels were added to cells at a final concentration of 0.7 and 0.4 mg/mL in OptiMEM, nanoparticles were added to cells at a final concentration of 0.025 mg/ml in OptiMEM, and the Lipofectamine 2000 loading solution was added to cells at a 1:5 dilution in OptiMEM. Cells were incubated with particles for 48 hours, at which point the media was removed by aspiration and replaced with CellTiter 96® Aqueous One Solution Cell Proliferation MTS Assay (Promega). Cells were incubated with MTS solution for 90 minutes, and the absorbance at 490 and 690 nm was measured with a Bio-Tek Synergy™ HT multi-mode plate reader (Winooski, VT). The viability results for the AllStars Death and the Negative Control siRNA were compared by Student's t test (two-tailed, unequal variance) to check for statistically significant silencing. The silencing efficiency was evaluated using the absorbance of cells with death siRNA and cells with negative control siRNA as shown in Eq. 7.1:

$$\text{silencing efficiency} = 100 \times \left(1 - \frac{A_{\text{Death}}}{A_{\text{Negative}}} \right) \quad 7.1$$

7.3 RESULTS AND DISCUSSION

P(MAA-co-NVP) was synthesized and crosslinked with peptide as described in Section 6.3, the only difference being the addition of polycationic nanogels prior to the

addition of the peptide. The polycationic nanogels were added at 10 wt% with respect to polymer weight and appeared brown in color due to the conjugated fluorophore NBD-Cl. Prior to use in the microgels, NBD-Cl was reacted in excess to primary amines present in the nanogels to serve a dual purpose; first, to impart fluorescent detection of the nanogels, and second, to protect the primary amines from reacting during the EDC-NHS reaction with the peptide crosslink.

Upon addition of the peptide, the mixture was immediately turbid and precipitation of brown, crosslinked hydrogel was evident. After the reaction was complete, the hydrogel was washed by repeated centrifugation and resuspension in DI water to remove impurities. The superNAtant was retained from each wash to determine the incorporation efficiency of the nanogels. Following the washes, the hydrogel was frozen in LN₂ and lyophilized. The dry product appeared as fluffy brown chunks, and was easily crushed into a powder consisting of particles <30 µm in size.

7.3.1 Incorporation of Polycationic Nanogels

The fluorescence of the nanogels in the wash superNAtant was measured using a Bio-Tek Synergy™ HT multi-mode plate reader and compared to the fluorescence values of known concentrations of nanogels. It was determined that 30-40% of the nanogels were incorporated into the hydrogel, bringing the final weight ratio to 3-4% with respect to the polymer weight.

Incorporation of the polycationic nanogels was visualized using confocal laser scanning microscopy. The hydrogel particles were labeled with a TAMRA fluorophore that was reactive to carboxylic acid functional groups on the P(MAA-co-NVP). After purification, the particles were lyophilized and a known weight was resuspended in PBS (pH 7.4). Slides were prepared by dropping the particle solution onto a slide and fixing

the coverslips with ProLong® gold antifade reagent. Imaging of the particles confirmed the presence of the nanogels (green) within the P(MAA-co-NVP) particles (red), as seen in Figure 7.1. The porous structure of the hydrogels was also discernible in the bright field image, in Figure 7.1D. A Z-stack image, Figure 7.2, was obtained to verify the distribution of nanogels throughout the particle. Though the nanogels were throughout the particle, they did tend to be present in clusters or pockets, which is consistent with the method of crosslinking.

7.3.2 Degradation of Microgels with Nanogels

Degradation studies with SIF, SGF, trypsin, and PBS were completed to verify that incorporation of the nanogels did not affect degradation kinetics. As previously observed in hydrogels without nanogels⁵, the turbidity of the particle solutions could be used as a measure of degradation over time. Figure 7.3 shows the decrease in turbidity over time of 1.5-6 mg/ml microgels in 0.6 or 1.2 mg/ml trypsin. All concentrations plateaued at the lowest turbidity value within 90 minutes, which was approximately the same as microgels containing no nanogels. Therefore, it does not seem as if the nanogels significantly affect the degradation kinetics. However, as the relative turbidity plateaued at values of 18% and higher, it is possible that the nanogels prevent complete degradation of the microgels. This may be attributed to the reaction of some of the amine groups present in the nanogels during the EDC-NHS crosslinking reaction, effectively incorporating the nanogels as nondegradable crosslinks within the gel. While this is an undesirable side reaction that reduces the number of nanogels able to be released from the microgels, it is thought to be limited by the protection of the amine groups via NBD-Cl and is not prevalent enough to affect the ability of the microgels to degrade.

⁵ See Section 6.3.3

It was further noted that the initial change in turbidity over the first 20 minutes of exposure to trypsin was linear, as shown in Figure 7.4A (1.2 mg/ml trypsin) and Figure 7.4B (0.6 mg/ml trypsin). The corresponding microgel to trypsin ratio versus initial rate of turbidity decrease values were then plotted to determine the relationship. The fit was nearly linear, as shown in Figure 7.5 ($R^2=0.98$), and may be used to approximate degradation time of a known microgel to trypsin weight ratio.

Additionally, trypsin activity assays with BAEE were performed to ensure the quenching of trypsin activity prior to exposure to cells. Microgels were incubated with 1.2 mg/ml or 0.6 mg/ml trypsin in pH 7.4 PBS for 90 minutes at 37°C, and then subjected to deactivation by incubation at 70°C for 5 minutes or addition of 2X volume DMEM containing serum. Figure 7.6A shows the complete deactivation of 1.2 mg/ml trypsin by both heat and DMEM compared unadulterated trypsin solutions, and Figure 7.6B shows the same for 0.6 mg/ml trypsin solutions. Therefore, it was concluded that either was a satisfactory method of deactivating trypsin at concentrations at and below 1.2 mg/ml.

As further confirmation of nanogel incorporation as well as visualization of degradation on the micro-scale, microgels in various solutions were imaged with ImageStream flow cytometry. This equipment enabled the analysis of entire populations of microgels using parameters such as fluorescence intensity in a particular channel or particle size as detected by bright field imaging. It allowed real-time imaging and quantification of the change in particle size distribution during degradation.

Representative images obtained via ImageStream analysis of microgels incubated for 90 minutes in 1.2 mg/ml trypsin, 0.6 mg/ml trypsin, or pH 7.4 PBS are shown in Figure 7.7A, 7.7B, and 7.7C, respectively. Analysis of the microgel populations confirmed that at least 70% of the events detected had fluorescent intensities above a minimum threshold. Further, the events were gated to remove out-of-focus particles and

debris from further analysis. The images revealed distinct differences in the size and morphology of the microgels following incubation in the trypsin or PBS solutions; microgels exposed to trypsin are smaller in size and less porous in appearance than microgels exposed to only PBS. Additionally, the fluorescence intensity is very strong and dense in the trypsin samples, whereas it is more diffuse throughout the PBS samples. This could be an indication of formation of strongly fluorescent and highly compact complexes between nanogels and degraded hydrogel due to electrostatic binding, rather than diffusion of nanogels from the degradation hydrogel as desired.

The size distribution of the events was also plotted in histogram form to better quantify the change in size as a function of degradation. Figure 7.8 compares the histogram plots of microgels incubated in A) 1.2 mg/ml trypsin, B) 0.6 mg/ml trypsin, and c) PBS. It was observed that compared to the PBS control the size range of microgels was greatly reduced from a maximum of $2800\ \mu\text{m}^2$ to $600\ \mu\text{m}^2$ upon incubation in trypsin, as would be expected due to enzymatic degradation. Also convincing was the shift in median particle area from $163\ \mu\text{m}^2$ in PBS to $39\ \mu\text{m}^2$ in trypsin.

Similar results were obtained using ImageStream to visualize large populations of microgels incubated in SGF, SIF, or 1.2 mg/ml trypsin solution. Samples were run after 0, 15, 30, 60, and 120 minutes of incubation in each of the conditions. As before, events were gated by fluorescence intensity as well as gradient RMS, a metric used to gate for images in the focal plane. Figure 7.9 compares representative images of microgels in each of the solutions at time zero, and Figure 7.10 compares the histogram plots of the size distribution of events in each solution at time zero. The size distribution of microgels in SGF and SIF was much broader than that of microgels in trypsin, and again the fluorescence was more diffuse in particles incubated in SGF and SIF than in trypsin. The median microgel sizes were 54, 79, and $23\ \mu\text{m}^2$ in SGF, SIF, and trypsin, respectively.

Unfortunately, since it was not logistically possible to run the samples at exactly at time zero, some degradation had already occurred in the trypsin samples at the nominal time zero. Consequently there was a slight misrepresentation of the particle size and fluorescent intensity in the trypsin samples at the nominal time zero.

However, the size and fluorescence visualization of the microgels after 120 minutes of incubation was very indicative of the degradation over a longer period of time. Figure 7.11 shows representative images of the microgels in each condition and Figure 7.12 shows histogram plots of the corresponding microgel size distributions. It is apparent from the images that again the size, morphology, and fluorescence intensity of microgels exposed to SIF and trypsin had discernible differences from that of microgels incubated in SGF, a non-degrading buffer. The degraded particles were small in size and entirely fluorescent compared to their larger undegraded counterparts with diffuse clusters of fluorescence. The histogram plots confirm quantitatively that the size range decreased upon exposure to degrading buffers, and the median sizes were $65\ \mu\text{m}^2$ in SGF to 25 and $26\ \mu\text{m}^2$ in SIF and trypsin, respectively. Therefore, after 120 minutes of incubation in the buffers, the median size of the microgels in SGF did not decrease, as expected, while the median sizes of microgels exposed to SIF and trypsin did decrease due to degradation.

Figure 7.13 shows the median microgel size (μm^2) at each time point in each of the three buffers. It can be seen that median size of the particles incubated in SGF fluctuated over time, but did not follow a decreasing trend. The median size of particles incubated in SIF, on the other hand, gradually decreased over the 120 minute incubation period, as would be expected of microgels slowly degraded in the presence of a physiologically relevant concentration of trypsin. Microgels exposed to 1.2 mg/ml

trypsin, however, decreased in median size due to degradation by the time of the first measurement and did not degrade further over the 120 minute period.

7.3.3 Cytotoxicity of Degraded Microgels with Nanogels

As the degradation behavior of the microgels containing nanogels was consistent with a relevant timescale in simulated intestinal conditions, the next step was to ensure the cytocompatibility of the degraded and undegraded microgels in trypsin solutions of varying concentration. These studies were critical, as both polycationic polymers such as the nanogels [18] and active trypsin [19, 20], can have a detrimental effect on cell health and metabolism. Caco-2 human adenocarcinoma cells, often used to model the intestinal epithelium, and RAW 264.7 murine macrophage, used to model target cells for nanogel uptake, were used in these studies. Two cytotoxicity assays were used; the MTS cell proliferation assay was indicative of any changes to cell metabolism upon exposure to microgels, and the LDH membrane integrity assay was indicative of the viability of cells after exposure.

Microgels were incubated in 1.25 or 0.625 mg/ml trypsin solution for at least 4 hours to ensure degradation of the microgels; PBS buffer was used as a control. Trypsin was deactivated by the addition of excess cell media prior to the addition to Caco-2 cells. Cells were incubated with degraded microgel solutions for 18 hours to assess cytotoxic effect. Figures 7.14A and 7.14B show Caco-2 cell proliferation and viability, respectively, as a function of microgel and trypsin concentration relative to cells incubated in normal media without microgels. The cell proliferation was affected by the degraded microgels in a concentration-dependent manner; the highest concentration of 2 mg/ml induced an unacceptable amount of change in cell metabolism as measured by the MTS assay. However, all concentrations maintained very high cell viability after 18

hours of incubation. Thus, high concentrations of degraded microgels may affect the metabolism of Caco-2 cells, but they do not kill the cells.

A comprehensive study evaluating effect of trypsin concentration, culture medium, and trypsin concentration during degradation was performed in the RAW 264.7 cells. Microgels at a concentration of 2 mg/ml were degraded in 0.15, 0.2, 0.25, and 0.3 mg/ml trypsin for 90 minutes at 37°C, and then the trypsin was deactivated by incubation at 70°C for 5 minutes. The microgels were then added to the cells at a final concentration of 1 mg/ml or 0.4 mg/ml in OptiMEM or 1 mg/ml in DMEM. Two different culture media were tested as the OptiMEM is a reduced-serum medium, and the presence of serum is thought to negatively impact cellular uptake and transfection by nanoparticles. Therefore, it was hypothesized that increased uptake of nanoparticles with inherently cytotoxic cationic functional groups may be more disruptive to the cell metabolism or cell membrane.

Figure 7.15 shows the results of the MTS cell proliferation assay following incubation of the RAW 264.7 cells with the degraded microgels for 18 hours. Absorbance at 490 nm is relative to that of cells exposed only to culture medium for the 18 hour incubation period. In all three exposure conditions, undegraded microgels in PBS were slightly less disruptive to cell metabolism than degraded microgels, suggesting that degradation of the microgel matrix does cause increased cellular exposure to the potentially cytotoxic polycationic nanogels within.

Figure 7.15A shows that the 1 mg/ml microgel concentration in OptiMEM did have an effect on cellular metabolism, as the relative absorbance was reduced below 50% at all trypsin concentrations. Also important to note is that cells exposed to the deactivated trypsin without microgels also experienced a reduction in relative

absorbance, indicating the negative effect of high trypsin concentrations on cell metabolism.

Figure 7.15B indicates that the same microgel concentration in serum-containing DMEM resulted in less effect on cell metabolism due to the degraded microgels, as the relative absorbance of trypsin with and without microgels was approximately the same. This could be due to the serum content causing nonspecific protein binding to the nanogels, resulting in a reduction in both cytotoxicity and cellular uptake. It is important to note, though, that this concentration of microgels did result in a 30% reduction in absorbance relative to the control cells incubated in DMEM only. Therefore, this microgel concentration still significantly affects cell metabolism.

Finally, Figure 7.15C shows the results of the MTS assay of RAW 264.7 cells incubated with 0.4 mg/ml degraded microgels in OptiMEM culture medium. As expected, the lower microgel concentration resulted in less disruption of cell metabolism relative to cells exposed only to OptiMEM, with a decrease in relative absorbance of only ~25% across all trypsin concentrations. There was also little difference in relative absorbance between cells incubation deactivated trypsin alone or deactivated trypsin with degraded microgels.

The results from the LDH assay, shown in Figure 7.16, mirror the results from the MTS assay, with the only notable exception being a much more pronounced effect of 1 mg/ml degraded microgels in DMEM on membrane integrity, shown in Figure 7.16B. Interestingly, this negative effect was a function of microgel:trypsin ratio, with ratios likely resulting in less degradation being less detrimental to cell viability. In fact, undegraded microgels in PBS were significantly less toxic at 70% viability than microgels incubated in the lowest trypsin concentration, at 40% viability. This strongly

suggests that the degradation products or release of nanogels from degraded microgels has a detrimental effect on cell membrane viability at this concentration.

At the reduced concentration of 0.4 mg/ml in OptiMEM shown in Figure 7.16C, however, cell viability is quite high at >80% for all conditions tested. In subsequent cell transfection studies, these conditions were used to induce minimal toxic effect as a result of microgels or degradation conditions.

7.3.4 siRNA Loading

Loading studies were conducted with the Silencer® Select Negative Control No. 1 scrambled sequence siRNA at 1000 nM or 400 nM to evaluate the ability of the microgels to load siRNA. Microgels were incubated with the siRNA at a particle concentration of 12 mg/ml in pH 5.5 PBS for up to 4 hours at room temperature with agitation. The loading pH was selected as both the microgels and nanogels are partially charged at this condition, facilitating swelling of the hydrogel networks to allow increased diffusion of siRNA to complex with the positively charged nanogels. Following incubation, the microgel/siRNA solutions were centrifuged to separate loaded microgels from siRNA remaining in solution. Afterwards, the siRNA content in the supernatant was measured with the Quant-iT™ RiboGreen® RNA Assay Kit.

Loading efficiencies were calculated as follows, where c_o is the initial molar siRNA concentration, c_f is the final molar siRNA concentration, and c_p is the mass concentration of polymer in solution:

$$\text{Loading Efficiency} = \frac{c_o - c_f}{c_o} * 100 \quad (7.2)$$

$$\text{Weight Loading Efficiency} = \frac{\text{moles}_o - \text{moles}_f}{\text{mass}_p} \quad (7.3)$$

Representative weight and loading efficiencies of the scrambled siRNA are shown in Figure 7.17. This scrambled siRNA sequence achieved weight efficiencies of 0.06 and 0.02 nmol siRNA/mg polymer and loading efficiencies of 75% and 59% in 1000 nM and 400 nM siRNA loading concentrations, respectively. The weight and loading efficiencies were highest in the loading solution with the greater siRNA concentration, as would be expected due to the greater concentration gradient acting as a diffusional driving force. In general for a variety of siRNAs tested, weight efficiencies ranged from 0.02-0.11 nmol siRNA/mg polymer, and loading efficiencies ranged from 59-90%. The variation in loading efficiency was attributed to batch-to-batch variability in the microgels as well as differences in siRNA sequences. Incubation time for loading did not greatly affect efficiencies, and consequently the loading period was reduced to 1.5 hours to limit degradation of siRNA by hydrolysis.

The loading efficiencies were consistently lower than those achieved with nanogels alone [21], but this was to be expected due to the increased complexity of diffusion through the microgel matrix as well as the possibility of unfavorable electrostatic repulsion between the polyanionic P(MAA-co-NVP) and negatively charged siRNA. Overall, the results indicate that these concerns are not prohibitive to loading siRNA into the microgels as significant loading of the siRNA was achieved.

7.3.5 Microgel Degradation and siRNA Stability

As siRNA is quite susceptible to degradation by proteases [3], there was concern that the stability and integrity of the siRNA could be compromised during the trypsin-induced degradation of the microgels. Therefore, the stability of the siRNA following incubation in various conditions was evaluated by polyacrylamide gel electrophoresis (PAGE), as has been reported previously in the literature [22]. PAGE separates molecules

by electrophoretic mobility, which is a function of the size, conformation and charge of the molecule. Thus, it is widely used to determine the stability of various biological molecules including proteins, RNA, and DNA.

In the case of denaturing PAGE, as was utilized in the studies herein, the higher order structure of the siRNA was denatured by exposure to urea, limiting the dependence of electrophoretic mobility to size and charge alone. In this way, the degradation of siRNA in various conditions was examined. Microgels with nanogels loaded with siRNA, nanogels complexed with siRNA, and siRNA alone were incubated in 0.3 mg/ml trypsin in PBS, rat intestinal fluid, rat gastric fluid, PBS, or SGF for 90 minutes at 37°C followed by 5 minutes incubation at 70°C to deactivate trypsin. Microgels were incubated at a concentration of 5 mg/ml, nanogels at a concentration of 0.4 mg/ml, and siRNA at a concentration of 400 nM. Figure 7.18A shows the image of the gel; it was noted that the samples incubated with trypsin showed signs of significant siRNA degradation, evidenced by the smaller molecular weight bands in lanes 1, 6, and 11. However, it was positive that at least some of the siRNA remained stable in rat intestinal fluid and PBS (lanes 2, 7, 12 and 4, 9, 14, respectively), conditions where siRNA degradation is undesirable. As expected, rat gastric and SGF conditions resulted in noticeable siRNA degradation (lanes 3, 8, 13 and 5, 10, 15, respectively). Few concrete assertions can be made regarding siRNA release from the degraded microgels and nanogels other than the fact that it is taking place, as evidenced by the bands corresponding to the stable siRNA band in lane 14.

The same siRNA-loaded samples incubated in the various conditions were then incubated in 0.5 mg/ml heparin in OptiMEM to better evaluate release of siRNA in the various conditions. Heparin was used as a competitive polyanion to induce dissociation of the siRNA from the polycationic nanogels, as other researchers have reported [23, 24].

Figure 7.18B shows the image of the gel of the samples after incubation with heparin. Again, it was observed that free, undegraded siRNA was present in all samples with the exception of the samples incubated at high trypsin concentration. The presence of heparin did not seem to increase dissociation of the siRNA. Of course, it is impossible to say conclusively whether or not the free siRNA increased upon incubation with heparin without extracting and quantifying siRNA in the gel, but it was determined that the effort required to quantify the siRNA was not justified in this experiment. The presence of free, undegraded siRNA following incubation in physiologically relevant proteolytic conditions was confirmed, and this proof-of-concept was sufficient for these studies.

Looking for closely at the effect of trypsin on siRNA stability, siRNA, siRNA complexed with nanogels, and microgels with nanogels loaded with siRNA were degraded in 0.6 mg/ml trypsin for 1 hour at 37°C, and then the trypsin was deactivated by incubation at 70°C for 5 minutes. One set was added to PBS an identical set was added to a 0.5 mg/ml heparin solution to promote dissociation of siRNA. As a control, siRNA was incubated in 0.05, 0.1, and 0.5 mg/ml Ribonuclease A to fully degrade the siRNA.

Figure 7.19A shows the PAGE results. Intact siRNA bands were clearly shown in lanes 1 (without heparin) and 5 (with heparin), though some bands of degraded siRNA were also present. Faint bands of intact siRNA were present in the nanogel samples (lanes 2 and 6) as well as in one of the degraded microgel samples (lanes 4 and 8). Again, it seemed as if heparin had no effect on the amount of free siRNA. It was unexpected that only one of the microgel samples contained intact siRNA, it is possible that the sample in lanes 3 and 7 was contaminated with an RNase. The bands of siRNA fully degraded by RNase can be seen in lane 9; the higher concentrations of RNase degraded the siRNA to such an extent that it ran off the gel and was no longer detectable.

To verify that the degradation observed in all samples was not due to the incubation temperature or pH at which the siRNA was incubated, siRNA alone was incubated on ice, at room temperature followed by 90°C for 5 minutes, pH 5.5 PBS at 37°C, pH 8.5 PBS at 37°C, with microgels at loading conditions, and in 1.2 or 0.6 mg/ml trypsin with and without particles at 37°C. As shown in Figure 7.19B, only the siRNA exposed to trypsin, with or without microgels, experienced degradation. This confirms that the high trypsin activity was the culprit behind the degraded siRNA and not hydrolysis at elevated temperature.

While it was encouraging that some free, intact siRNA was released from microgels and nanogels, the amount of siRNA degraded by trypsin was disconcerting. Fortunately, the concentrations of trypsin used in these studies are much higher than physiologically relevant trypsin levels. As demonstrated in rat intestinal fluid, the ability of these microgel systems to deliver intact siRNA in physiological or *in vivo* conditions may be much greater than these studies project.

7.3.6 Confocal Microscopy to Verify InteRNAIization

Confocal laser scanning laser microscopy was used to verify cellular inteRNAIization of nanogels from degraded microgels. Microgels containing fluorescently tagged nanogels were incubated in 0.6 mg/ml trypsin for 90 minutes to degrade the microgel matrix and allow release of the nanogels. Following degradation, the samples were incubated at 70°C for 5 minutes to deactivate the trypsin and the degraded microgels were added to cells at a final concentration of 0.5 mg/ml in OptiMEM. The cells were incubated for 18 hours with the degraded particles then fixed, stained with fluorescently labeled wheat germ agglutinin, a cell membrane marker, then extensively washed and mounted onto slides with ProLong® gold antifade reagent

containing DAPI nuclear stain. Nanogels alone were used for comparison, as the cellular internalization of the nanogels has been previously documented [13]. All images were representative of the entire cell population; in each condition tested, the cells were at approximately 60% confluence and appeared to be in good health as determined by the bright field images.

Figure 7.20 shows the fluorescent and bright field images of RAW 264.7 cells incubated with A) nanogels and B) degraded microgels containing nanogels. In both cases, comparison of the artificially-colored green in the third panel with the bright field images in the fifth panel as well as the fluorescent overlay in the fourth panel indicated the presence of nanogels in proximity to the nuclei of cells, suggesting internalization. Interesting to note is the high prevalence of micron-size particles with green fluorescence both near and around the cells in the degraded microgel samples; this lends credibility to the working theory that upon degradation the nanogels do not completely release from the microgel matrix. Rather, they may be electrostatically bound with degraded microgel products in a highly fluorescent complex that is microns in size.

To verify internalization of nanogels, Z-stack images through the cells were taken. An orthogonal view of the Z-stacks, shown in Figure 7.21, confirmed the presence of the nanogels within the artificially-colored red cell membranes. Within the orthogonal view, the main panel displays the x-y plane, the bottom panel displays the x-z plane, and the right panel displays the z-y plane. In both the cells with nanogels, Figure 7.21A, and the cells with degraded microgels and nanogels, Figure 7.21B, the nanogels were localized within the cells membranes, which was likely indicative of endosomal compartmentalization. In the case of the degraded microgels with nanogels, at least some of the potentially electrostatically-bound nanogel complexes were still able to be

internalized by cells. Therefore, the complexation does not entirely prohibit internalization, but may affect efficacy and siRNA delivery.

With the goal of getting a better idea of the electrostatic interactions between the microgels, nanogels, and siRNA, all three of which are charged species, microgels and nanogels loaded with DY 647-siRNA were also degraded and incubated with RAW 264.7 cells in the same manner. Figure 7.22 shows images of cells incubated with A) degraded microgels containing nanogels and siRNA; B) nanogels complexed with siRNA; and C) TAMRA-labeled microgels with nanogels and siRNA. Again, in all three cases the fluorescence of the nanogels in relation to the bright field image suggests that cellular uptake of the nanogels may be occurring. Additionally, the fluorescence of the siRNA is in good spatial agreement with the nanogel fluorescence, indicating complexation between the two species. As before, the relatively large clusters of degraded microgel and nanogels are visible around the cells in the bright field images of A and C, and there is associated fluorescence of each of the charged molecules corresponds to these clusters. This strongly suggests complexation between microgels, nanogels, and siRNA, but it is impossible to conclude whether or not the complexes are still capable of transfection and gene silencing from microscopy images alone.

7.3.7 Transfection of Murine Macrophage and Human Adenocarcinoma Cells

Transfection conditions were determined by the best cytotoxicity, degradation, and siRNA stability results. RAW 264.7 murine macrophage and Caco-2 human adenocarcinoma cells were incubated with siRNA and degraded microgels (0.4 and 0.7 mg/ml), undegraded microgels (0.7 mg/ml), nanogels (0.025 mg/ml), commercially available transfection agent Lipofectamine 2000, or naked siRNA. Both cell lines were treated identically, with the exception of mouse and human variant AllStars Death

siRNA. Silencing was measured by an MTS assay of cell proliferation relative to that of scrambled siRNA controls. Experiments were run in quadruplicate and were repeated across two sets of each cell line.

As shown in Figure 7.23, similar gene silencing was obtained in both the A) RAW 264.7 and B) Caco-2 cell lines. At all concentrations and conditions tested, the microgels were unable to achieve greater than 20% silencing, and in some instances the variation between experiments was quite large. In fact, in the RAW cells the silencing by the degraded microgels with nanogels was significantly less than the silencing by nanogels with siRNA (T-test, $p < 0.05$). Silencing efficiency was of a similar magnitude in the Caco-2 cells, but none of the samples performed significantly better than the others in this cell line.

Though the nanogels were able to achieve a significant silencing efficiency in the RAW 264.7 cells, the percentage is still much less than what has been previously reported of these particles [13], so it is possible that the experimental conditions are not conducive to high transfection and silencing. It is much more likely, however, that the electrostatic interactions between P(MAA-co-NVP), the nanogels, and the siRNA are complicating transfection and silencing. Additionally, as the MTS assay is a measure of cell metabolism rather than cell death, it may not be the ideal assay to evaluate silencing efficiency. It was used in these studies to allow for direct comparison to the previous work by Forbes and Peppas [13].

However, a positive aspect of the transfection studies was that the viability of the cells exposed only to the various hydrogel particles (no siRNA) was consistently at or greater than 60%. Toxicity of transfection agents is a continual challenge in delivering siRNA, and fortunately neither the nanogels nor the degradable microgels containing nanogels induced very high levels of toxicity during transfection. Also encouraging was

the repeatability of these results in separate studies; though well-to-well variability was high for a few samples, the magnitude of average silencing efficiency and viability was consistent from study to study as well as across cell lines, making the results more credible.

7.4 CONCLUSIONS

Nanogels were encapsulated in enzymatically-degradable P(MAA-co-NVP) microgels via a facile crosslinking reaction. Nanogel incorporation and distribution was confirmed by fluorescent spectroscopy and confocal microscopy. Enzyme-specific degradation of the microgels was evaluated by decrease in relative turbidity over time as well as ImageStream flow cytometry; the degradation timescale was relevant to intestinal residence time and the degradation products induced minimal cytotoxic effects at low concentrations.

siRNA was efficiently loaded into the microgel systems due to equilibrium partitioning and charge interactions. However, the siRNA did experience reduced stability following incubation in the microgel degradation conditions, particularly at high trypsin concentrations. Despite the attack by trypsin on the siRNA, a detectable amount was released from the microgel system and escaped degradation, especially in the physiologically relevant buffers, which is promising for future *in vivo* applications.

Cellular uptake of nanogels released from degraded microgels was confirmed in RAW 264.7 cells by confocal microscopy. Both ImageStream analysis and confocal microscopy suggest that electrostatic complexation is occurring between the negatively charged degraded P(MAA-co-NVP) and positively charged nanogels, but some of the complexes, free nanogels, or both are internalized by the cells. However, the ability of the system to induce gene silencing is somewhat disappointing, perhaps due to loss of

siRNA stability upon incubation with trypsin or due to electrostatic interactions interfering with the delivery. Though the ability of the system to induce gene silencing is somewhat disappointing, the transfection efficiencies are consistent across both Raw 264.7 and Caco-2 cell lines.

Future work on this system should focus on tuning the charge densities of the nanogels and microgel encapsulation system to limit electrostatic binding. The performance of this system should also be evaluated *in vivo* or in conditions more closely resembling *in vivo* to verify the biodegradability and silencing efficiency; it is possible that a greater portion of the siRNA will remain stable at physiological trypsin concentrations, and competing charged molecules in the intestinal environment may decrease the electrostatic binding via competitive dissociation.

7.5 FIGURES

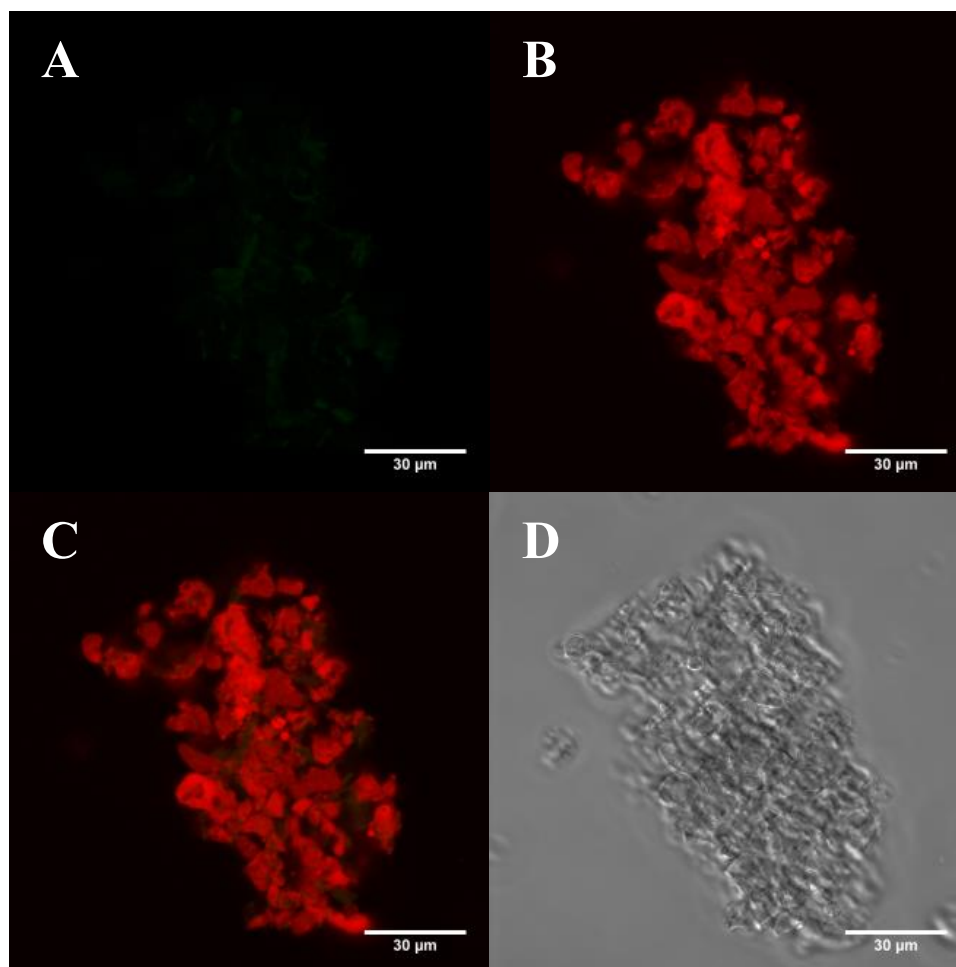


Figure 7.1: Image of P(MAA-co-NVP) microgel crosslinked by degradable peptide and encapsulating polycationic nanogels taken by confocal laser scanning microscopy. A) Nanogels labeled with NBD-Cl (green); B) P(MAA-co-NVP) microgel matrix labeled with TAMRA-cadaverine (red); C) green and red overlay showing nanogel distribution in microgel; D) bright field image of microgel. (Scale bar = 30 μm)

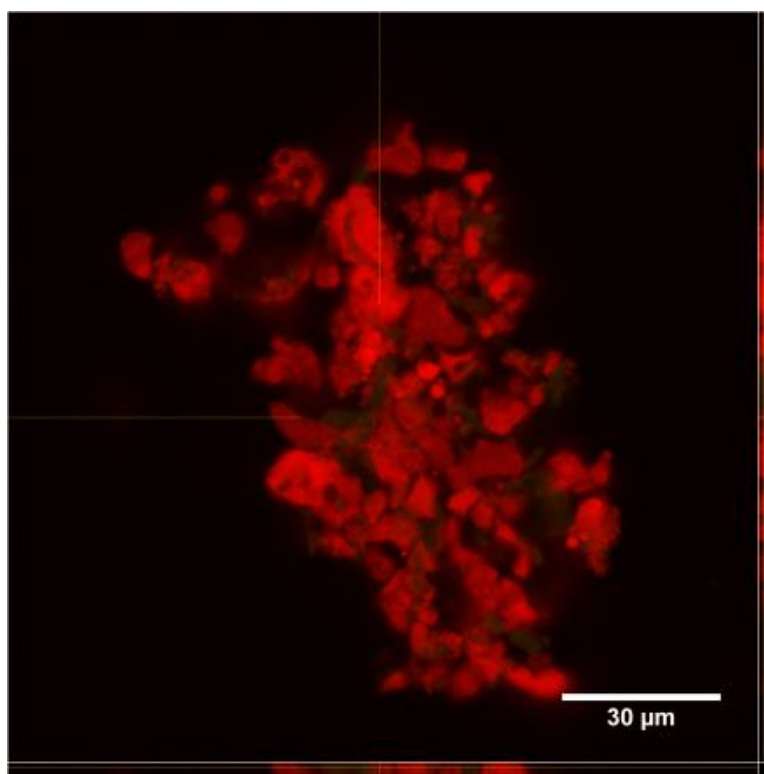


Figure 7.2: Orthogonal view of Z-stack image of P(MAA-co-NVP) microgel crosslinked by degradable peptide and encapsulating polycationic nanogels taken by confocal laser scanning microscopy. Nanogels labeled with NBD-Cl (green) in P(MAA-co-NVP) microgel matrix labeled with TAMRA-cadaverine (red). (Scale bar = 30 μm)

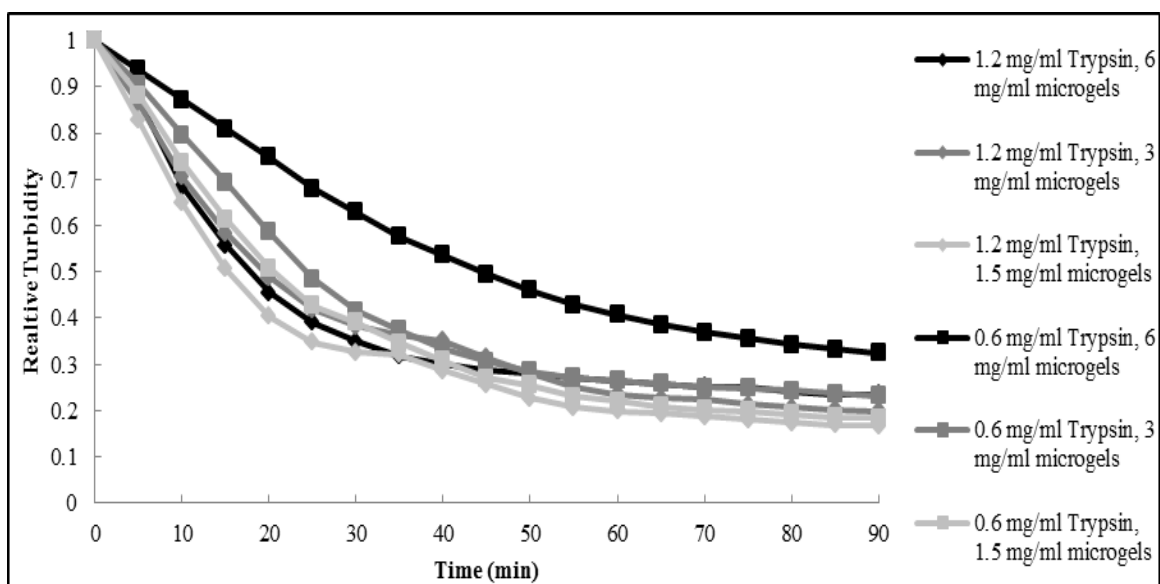


Figure 7.3: Relative turbidity over time of various concentrations of P(MAA-co-NVP) microgels with degradable crosslinks encapsulating nanogels during incubation in 0.6 and 1.2 mg/ml trypsin in PBS (37°C, pH 7.4, N=3).

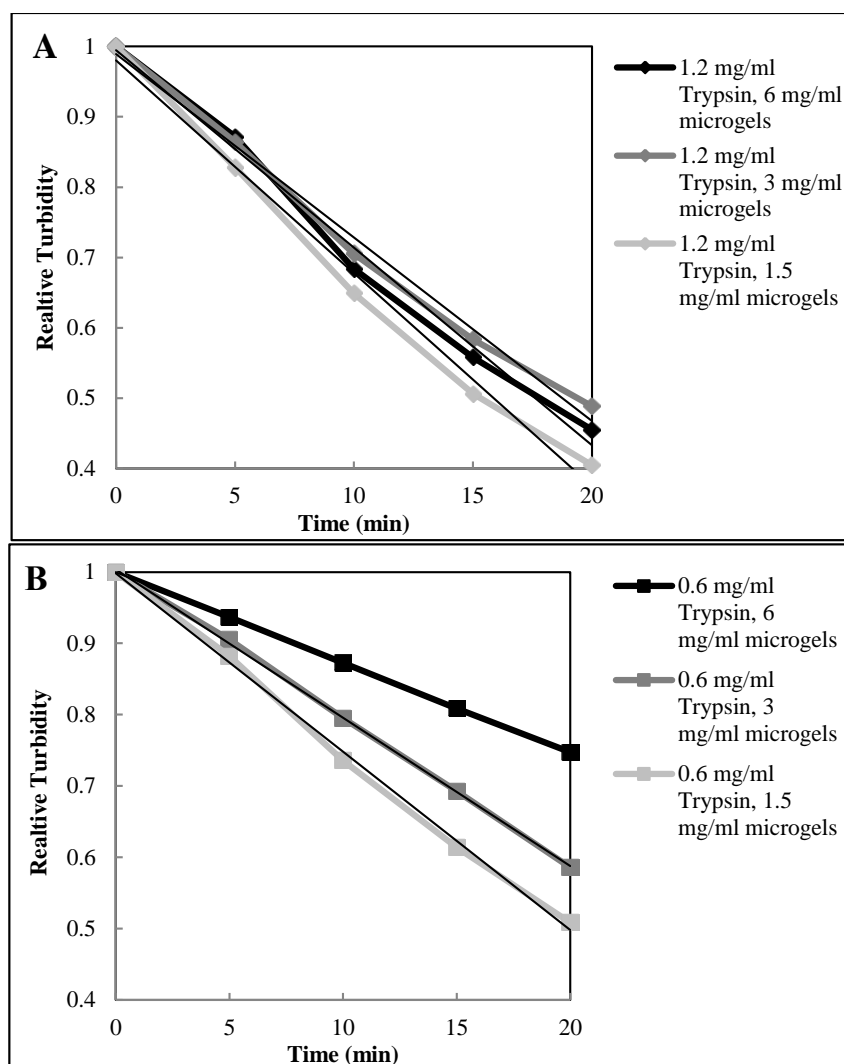


Figure 7.4: Relative turbidity over the first 20 minutes of incubation of trypsin with various concentrations of P(MAA-co-NVP) microgels with degradable crosslinks encapsulating nanogels; A) 1.2 mg/ml trypsin; B) 0.6 mg/ml trypsin in PBS (37°C, pH 7.4, N=3). Initial decrease in relative turbidity was fitted with a linear fit ($R^2 > 0.98$).

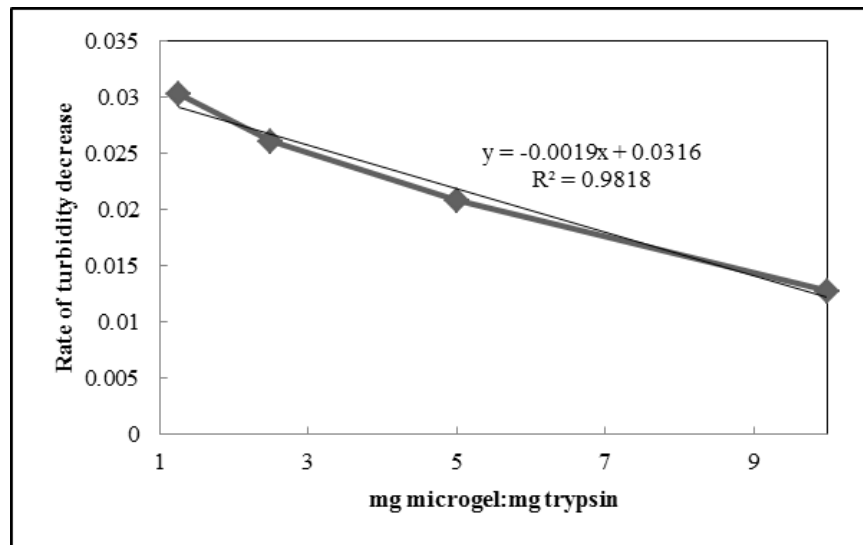


Figure 7.5: The microgel:trypsin weight ratio versus initial rate of turbidity decrease was correlated with a linear fit ($R^2=0.98$). The relationship may be used to approximate degradation time of a known microgel:trypsin weight ratio.

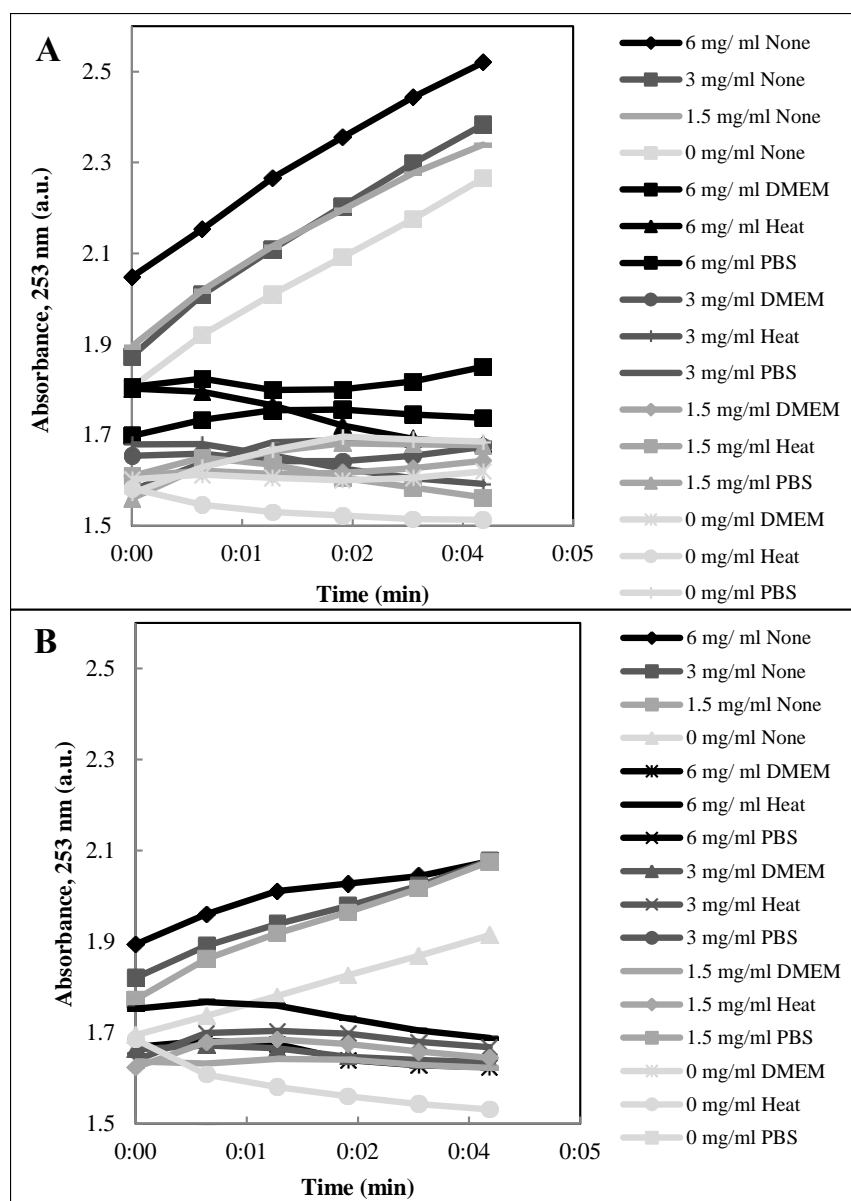


Figure 7.6: BAEE activity assay of A) 1.2 mg/ml trypsin; B) 0.6 mg/ml trypsin incubated with various concentrations of P(MAA-co-NVP) microgels containing degradable crosslinks for 90 minutes, and then deactivated by 5 minutes incubation at 70°C or addition of 2X volume of DMEM (degradation at 37°C, pH 7.4, N=3).

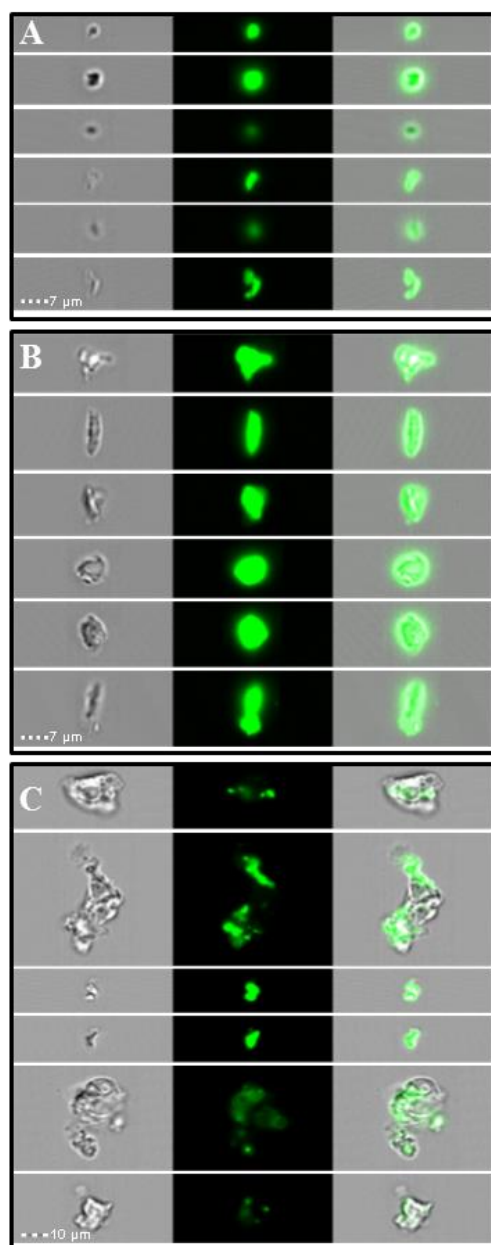


Figure 7.7: Representative images obtained via ImageStream analysis of microgels encapsulating fluorescent nanogels incubated for 90 minutes in A) 1.2 mg/ml trypsin (scale bar = 7 μm), B) 0.6 mg/ml trypsin (scale bar = 7 μm), or C) pH 7.4 PBS (scale bar = 10 μm). Left: bright field, middle: green channel (nanogels), right: overlay.

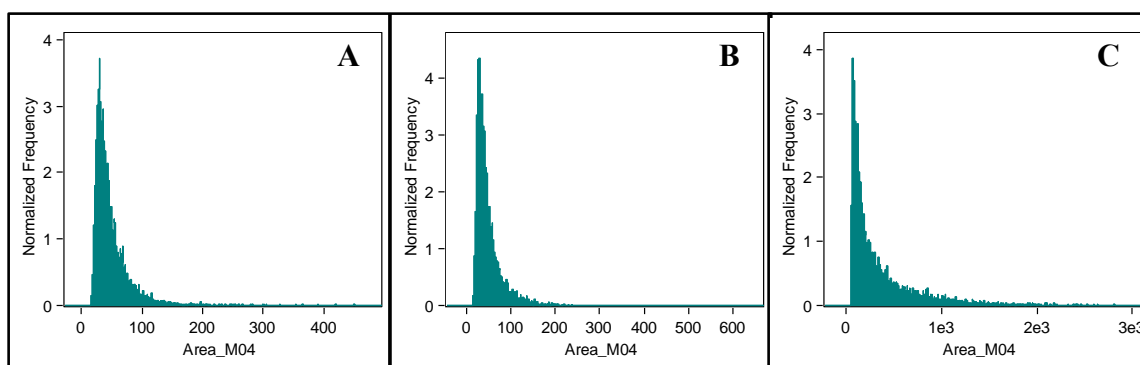


Figure 7.8: Histogram plots of particle size (μm^2) obtained by ImageStream analysis of microgels encapsulating fluorescent nanogels incubated for 90 minutes in A) 1.2 mg/ml trypsin, B) 0.6 mg/ml trypsin, or C) pH 7.4 PBS.

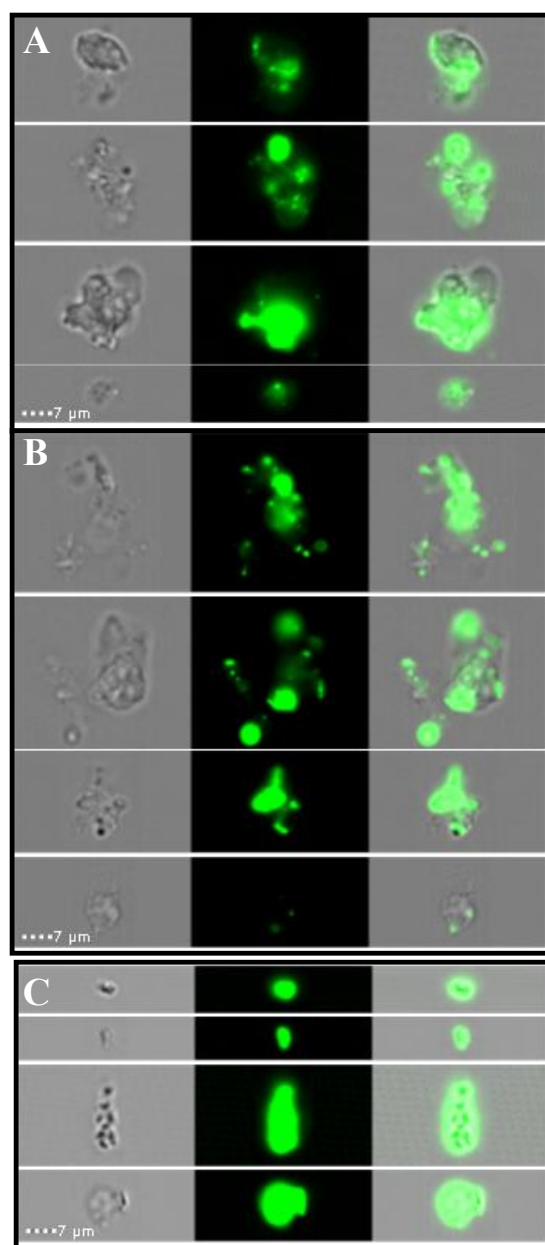


Figure 7.9: Representative images obtained via ImageStream analysis of microgels encapsulating fluorescent nanogels incubated for ~0 minutes in A) SGF (scale bar = 7 μm), B) SIF (scale bar = 7 μm), or C) 0.6 mg/ml trypsin (scale bar = 7 μm). Left: bright field, middle: green channel (nanogels), right: overlay.

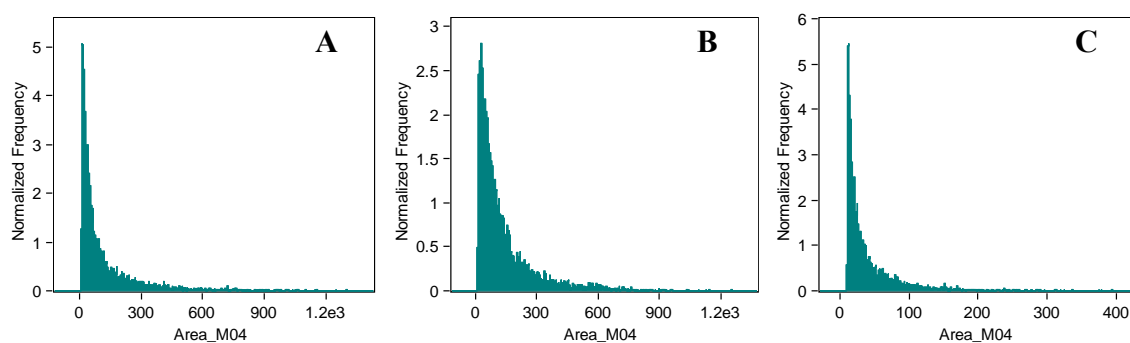


Figure 7.10: Histogram plots of particle size (μm^2) obtained by ImageStream analysis of microgels encapsulating fluorescent nanogels incubated for ~ 0 minutes in A) SGF, B) SIF, or C) 0.6 mg/ml trypsin.

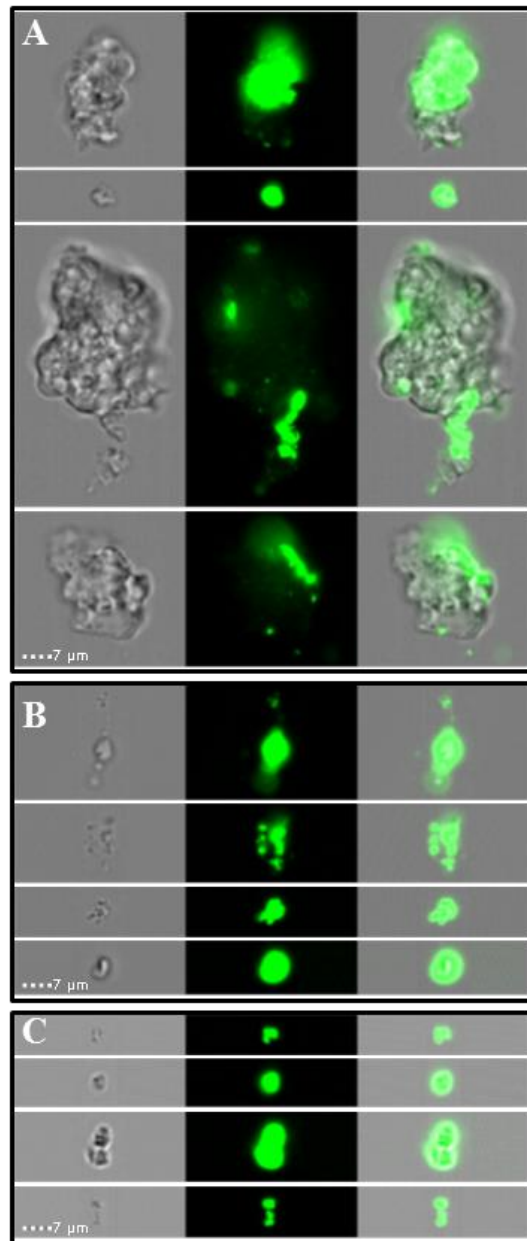


Figure 7.11: Representative images obtained via ImageStream analysis of microgels encapsulating fluorescent nanogels incubated for 120 minutes in A) SGF (scale bar = 7 μm), B) SIF (scale bar = 7 μm), or C) 0.6 mg/ml trypsin (scale bar = 7 μm). Left: bright field, middle: green channel (nanogels), right: overlay.

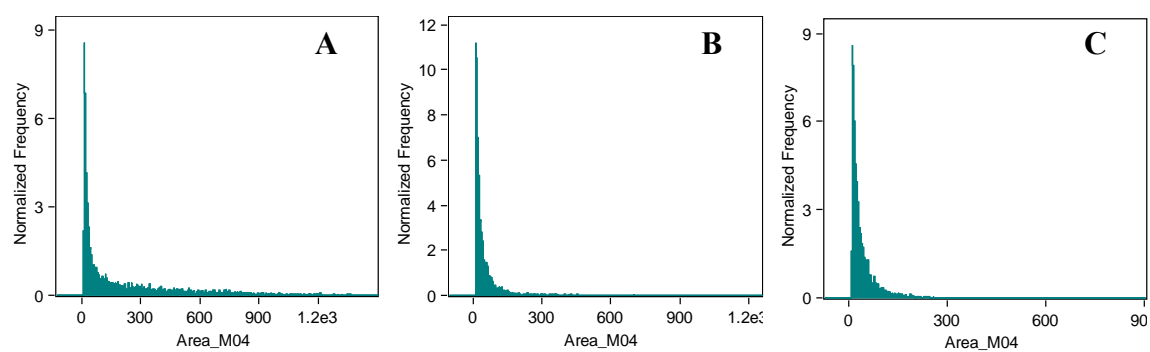


Figure 7.12: Histogram plots of particle size (μm^2) obtained by ImageStream analysis of microgels encapsulating fluorescent nanogels incubated for 120 minutes in A) SGF, B) SIF, or C) 0.6 mg/ml trypsin.

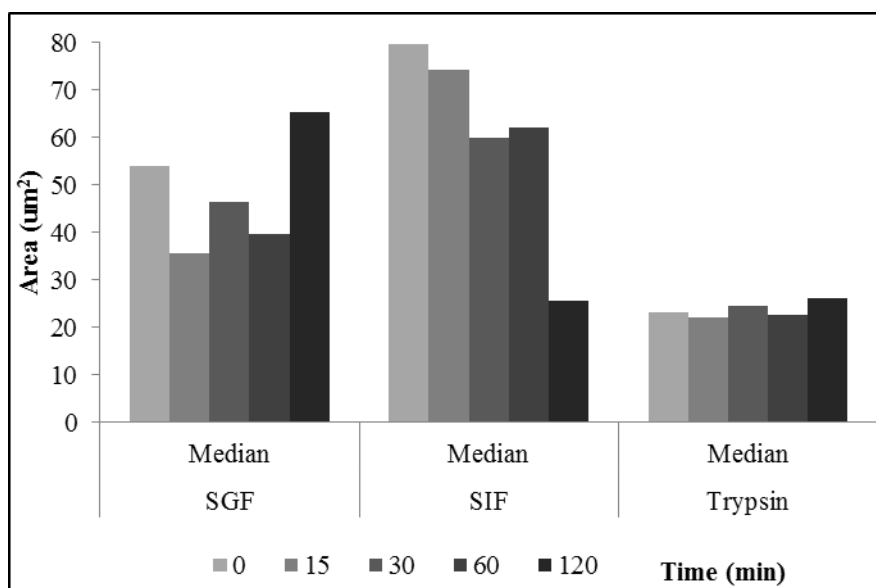


Figure 7.13: Median particle size (μm^2) values obtained by ImageStream analysis of microgels encapsulating fluorescent nanogels at various time points during the 120 minute degradation period.

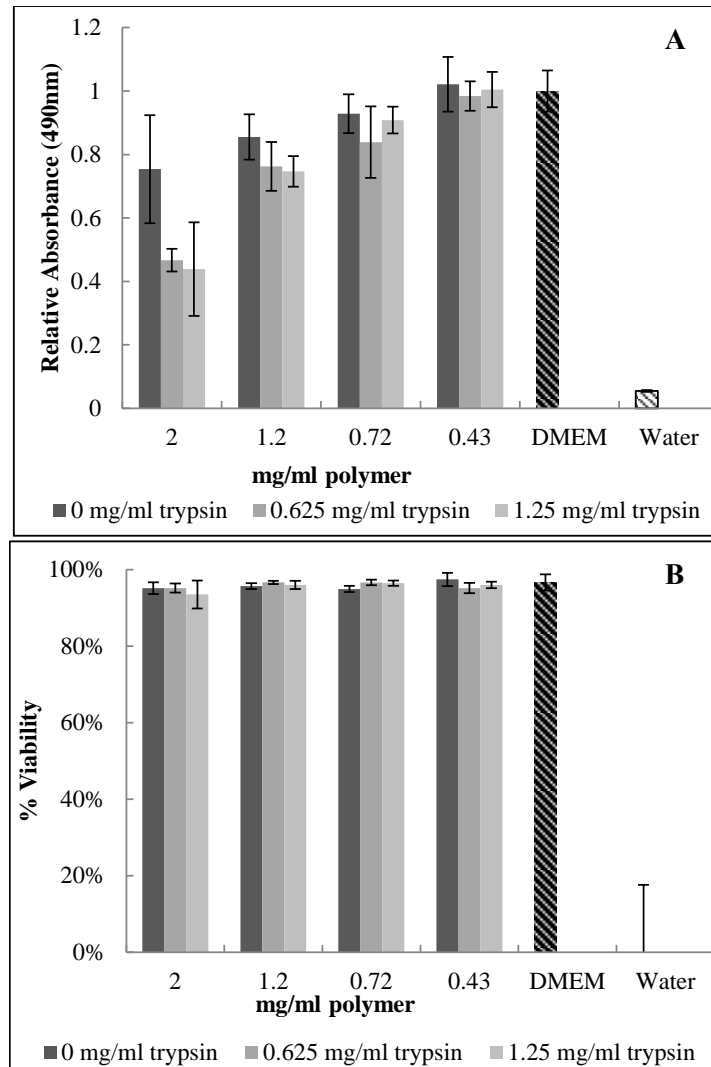


Figure 7.14: Evaluation of degraded microgel and trypsin exposure effect on cell metabolism using a A) MTS cell proliferation assay (Promega) and B) LDH membrane integrity assay (Promega). Microgels were incubated in PBS or various trypsin concentrations for 4 hours at 37°C, then the trypsin was deactivated by 2X addition of DMEM. Human adenocarcinoma Caco-2 cells were incubated with degraded microgel solutions at various concentrations for 18 hours. Following microgel incubation, the MTS and LDH assays were used to evaluate cytotoxicity. (N=3).

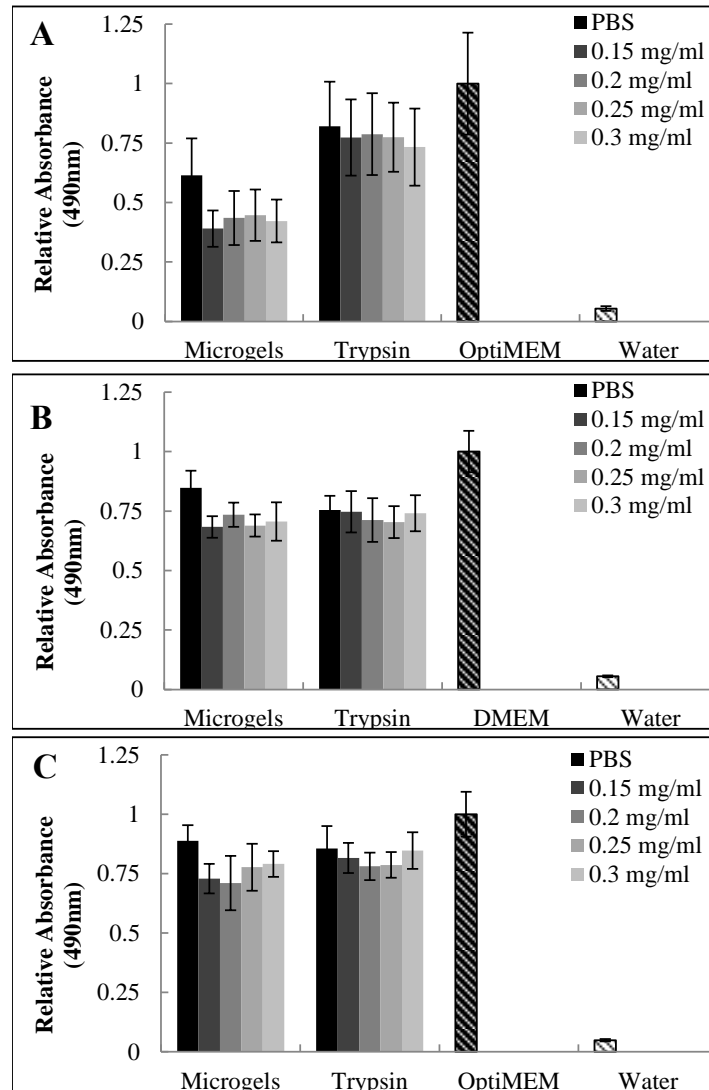


Figure 7.15: Evaluation of degraded microgel and trypsin exposure effect on cell metabolism using a MTS cell proliferation assay (Promega). Microgels were incubated in PBS or various trypsin concentrations for 90 minutes at 37°C, then the trypsin was deactivated by incubation at 70°C for 5 minutes. Murine macrophage RAW 264.7 cells were incubated with degraded microgel solutions at A) 1 mg/ml in OptiMEM; B) 1 mg/ml in DMEM; or C) 0.4 mg/ml in OptiMEM for 18 hours. Following microgel incubation, the MTS assay was allowed to incubate for 90 min. Absorbance at 490 nm is relative to the positive control (culture media only, patterned bar) (N=3).

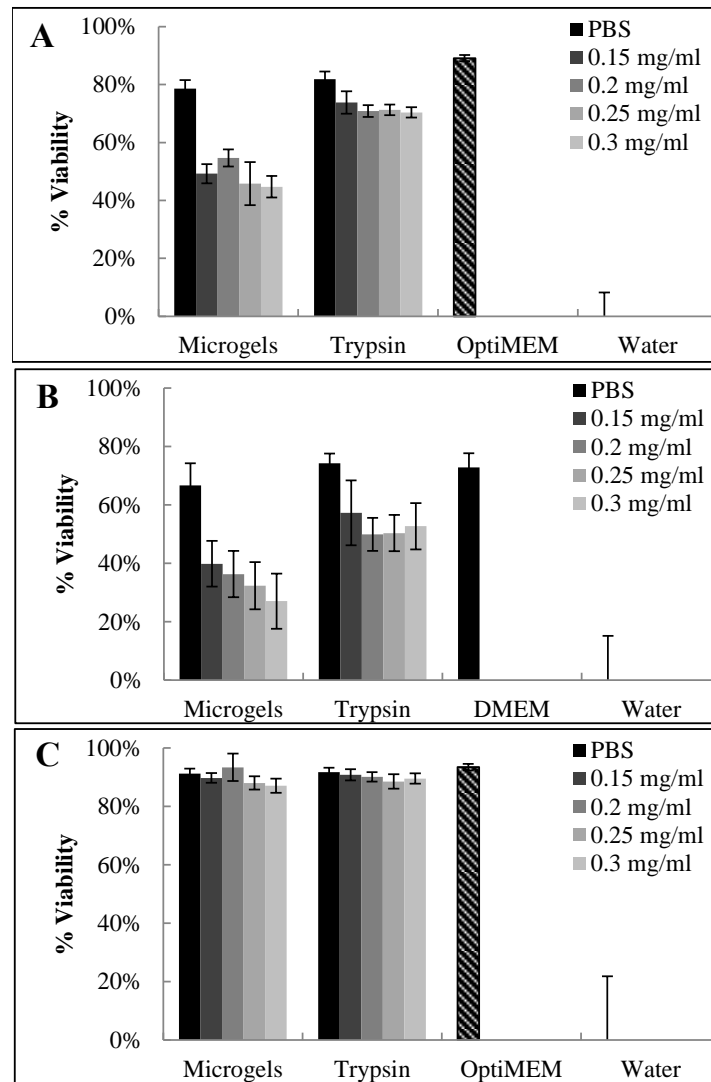


Figure 7.16: Evaluation of degraded microgel and trypsin exposure effect on cell metabolism using a LDH membrane integrity assay (Promega). Microgels were incubated in PBS or various trypsin concentrations for 90 minutes at 37°C, then the trypsin was deactivated by incubation at 70°C for 5 minutes. Murine macrophage RAW 264.7 cells were incubated with degraded microgel solutions at A) 1 mg/ml in OptiMEM; B) 1 mg/ml in DMEM; or C) 0.4 mg/ml in OptiMEM for 18 hours. Following microgel incubation, the LDH assay was used to evaluate cell viability (N=3).

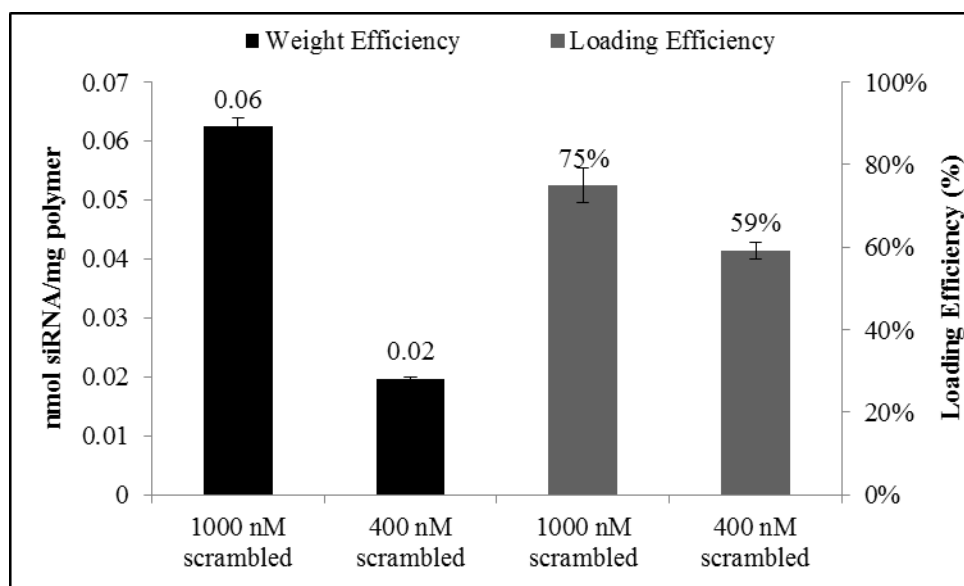


Figure 7.17: Representative siRNA loading efficiencies of degradable P(MAA-co-NVP) microgels with peptide crosslinker and encapsulated polycationic nanogels. Loading efficiency was based on amount of siRNA in microgels relative to initial amount in solution. Weight loading efficiency is moles of siRNA relative to the weight of microgels. Microgels were loaded over 4 hours at room temperature (N=3).

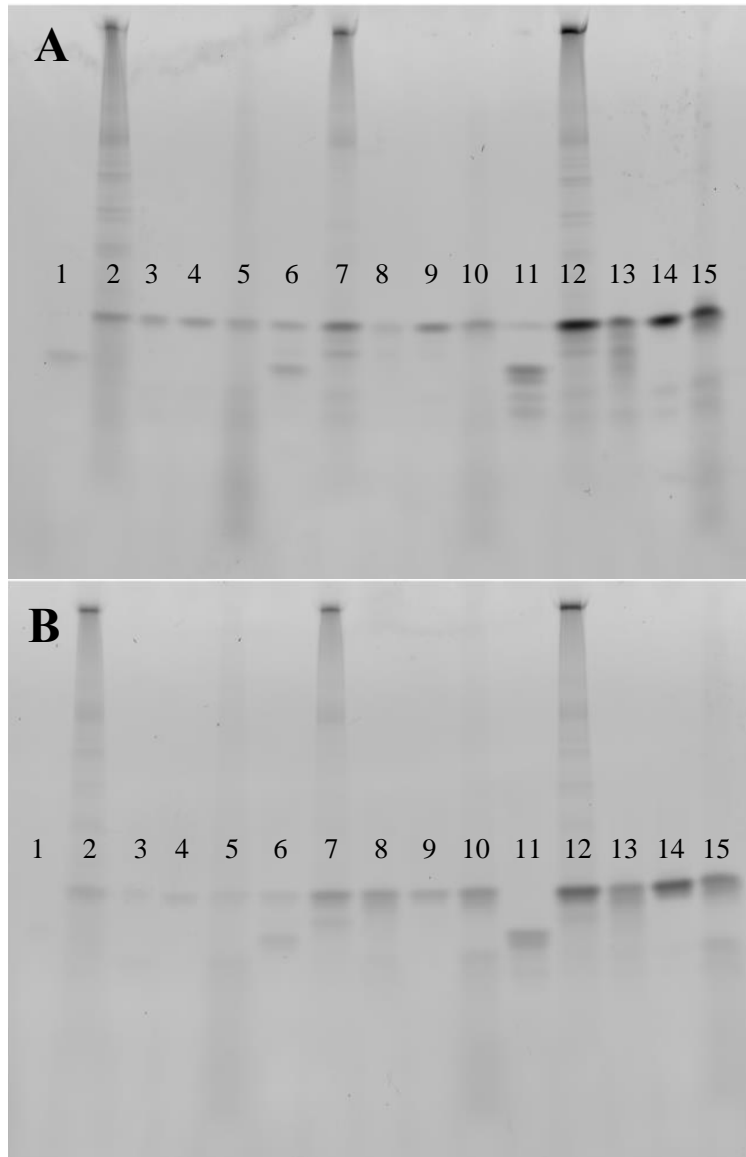


Figure 7.18: PAGE evaluation of siRNA degradation after siRNA-loaded microgels were incubated in 1) 0.3 mg/ml trypsin; 2) rat intestinal fluid; 3) rat gastric fluid; 4) PBS; or 5) SGF; siRNA-complex nanogels incubated with 6) 0.3 mg/ml trypsin; 7) rat intestinal fluid; 8) rat gastric fluid; 9) PBS; or 10) SGF; or siRNA incubated with 11) 0.3 mg/ml trypsin; 12) rat intestinal fluid; 13) rat gastric fluid; 14) PBS; or 15) SGF. Solutions were run A) immediately after incubation in the buffers or B) after an additional 15 minute incubation with heparin solution.

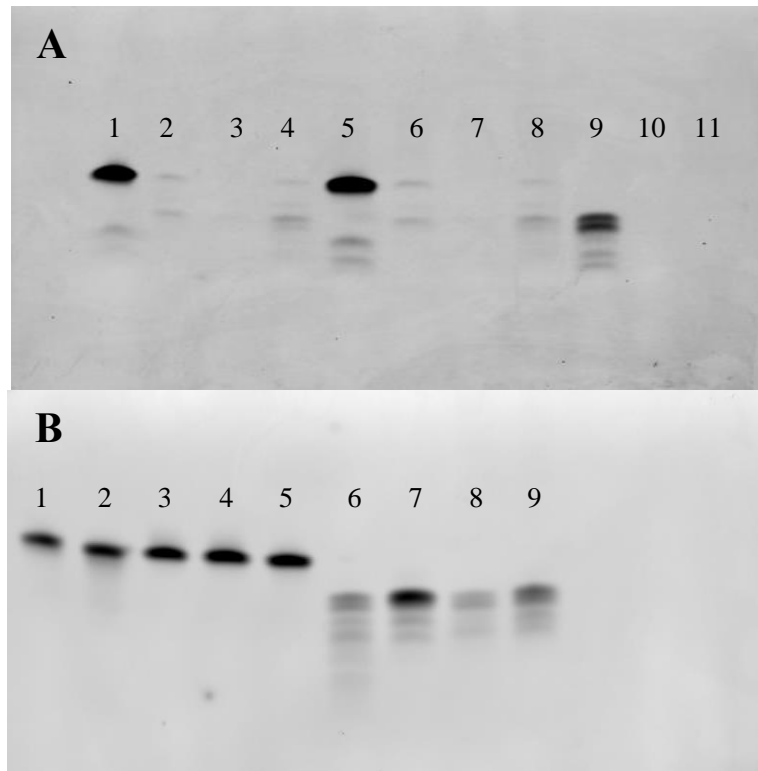


Figure 7.19: A) PAGE evaluation of siRNA degradation after 1) siRNA-loaded microgels; 2) siRNA and nanogels; 3) microgels with nanogels and siRNA; and 4) microgels with nanogels and siRNA were incubated with 0.6 mg/ml trypsin for 90 minutes; after 5) siRNA-loaded microgels; 6) siRNA and nanogels; 7) microgels with nanogels and siRNA; and 8) microgels with nanogels and siRNA were incubated with 0.6 mg/ml trypsin for 90 minutes followed by 15 minutes incubation with heparin; and 9-10) incubation of siRNA with different concentrations RNase.

B) PAGE evaluation of siRNA degradation after 1) siRNA on ice; 2) siRNA at room temperature; 3) siRNA in pH 5.5 PBS; 4) siRNA in pH 8.5 PBS; 5) siRNA loaded with microgels; 6) siRNA in 1.2 mg/ml trypsin; 7) siRNA in 0.6 mg/ml trypsin; 8) siRNA and microgels in 1.2 mg/ml trypsin; 9) siRNA and microgels in 0.6 mg/ml trypsin.

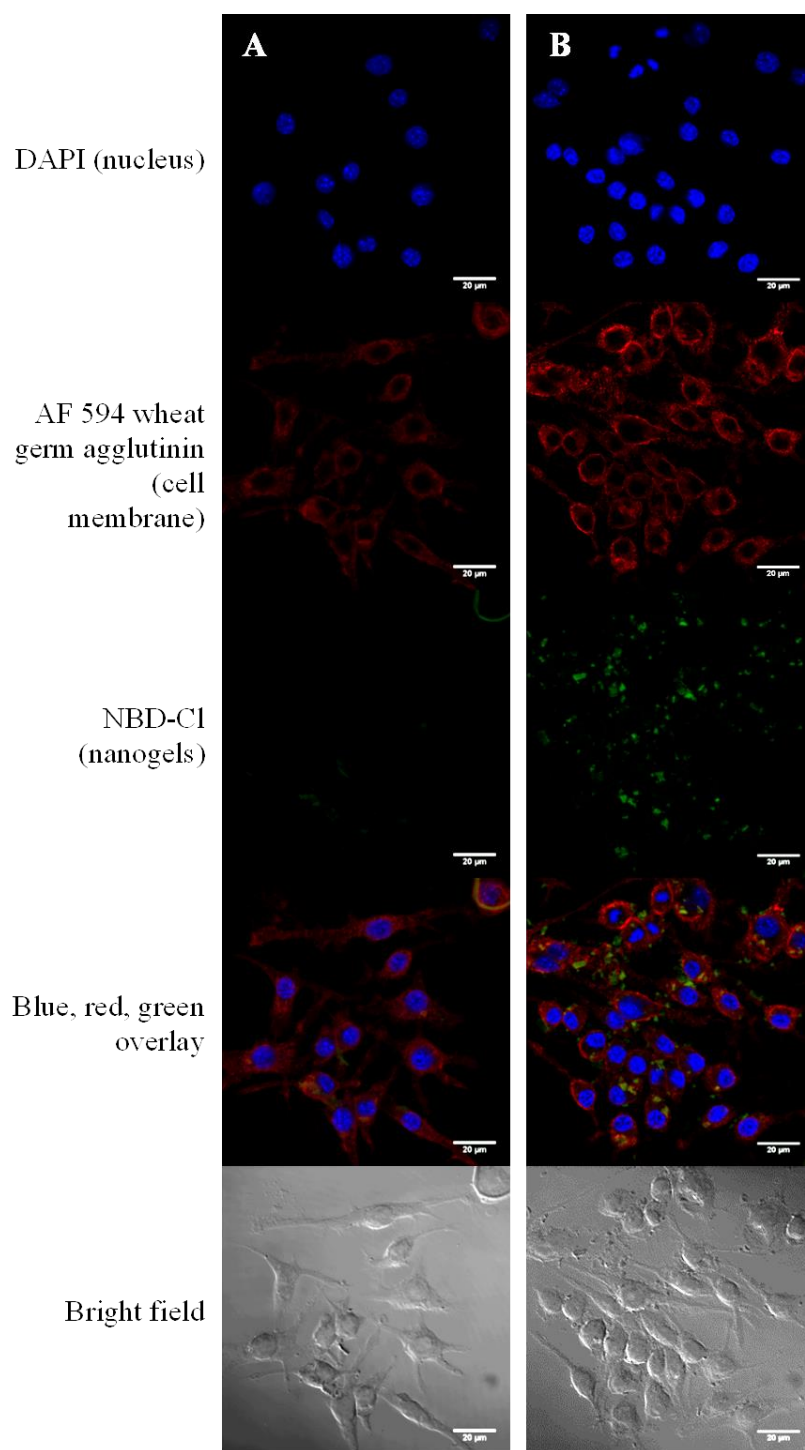


Figure 7.20: Confocal laser scanning microscopy fluorescent and bright field images of RAW 264.7 cells incubated with A) nanogels and B) degraded microgels containing nanogels (Scale bar = 20 μm).

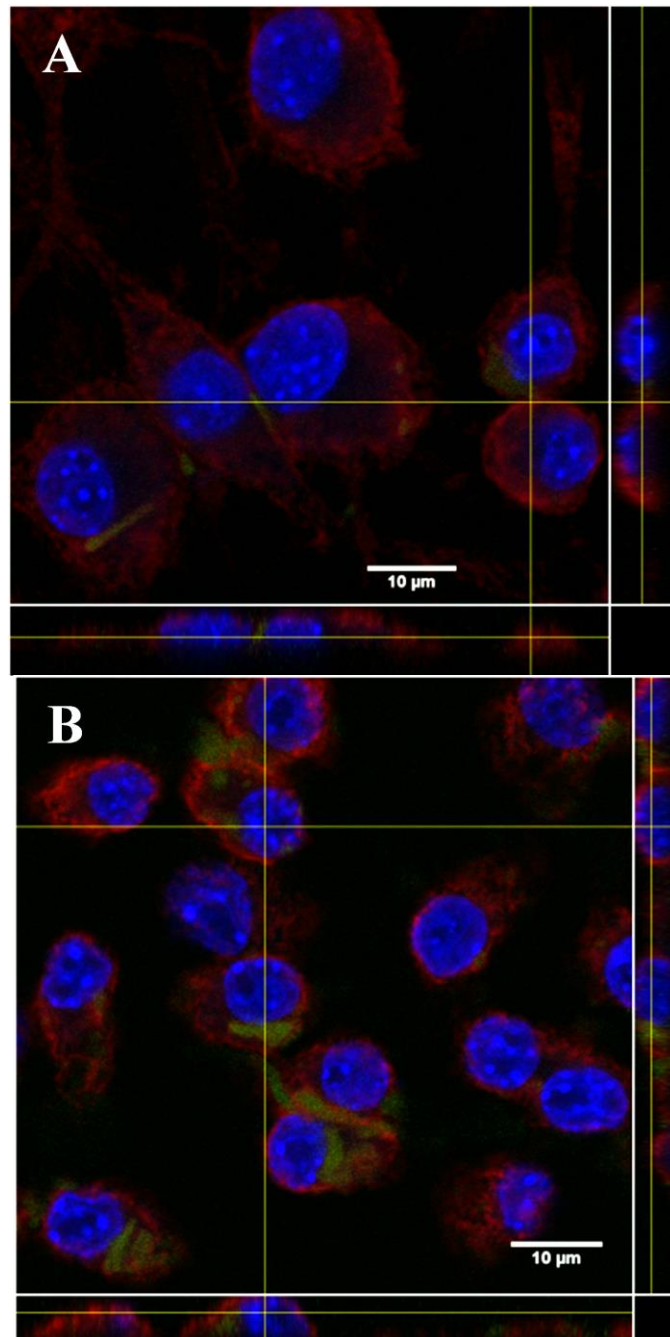


Figure 7.21: Confocal laser scanning microscopy fluorescent Z-stack orthogonal images of RAW 264.7 cells incubated with A) nanogels and B) degraded microgels containing nanogels (Scale bar = 10 μm).

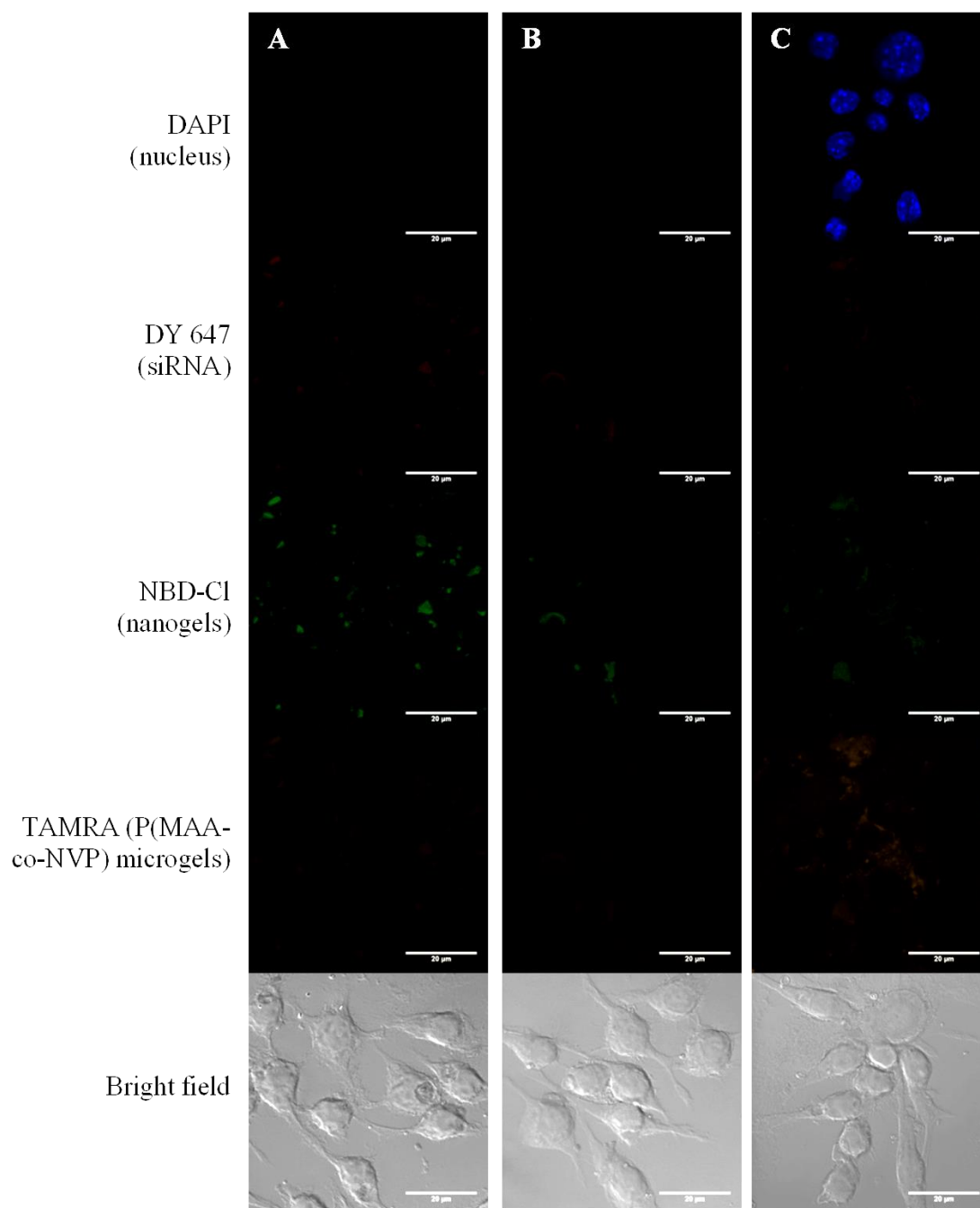


Figure 7.22: Confocal laser scanning microscopy fluorescent and bright field images of RAW 264.7 cells incubated with A) degraded microgels with fluorescently-tagged nanogels and fluorescently-tagged siRNA; B) fluorescently-tagged nanogels with fluorescently tagged siRNA; and C) fluorescently-tagged degraded microgels containing fluorescently-tagged nanogels and fluorescently-tagged siRNA (Scale bar = 20 µm).

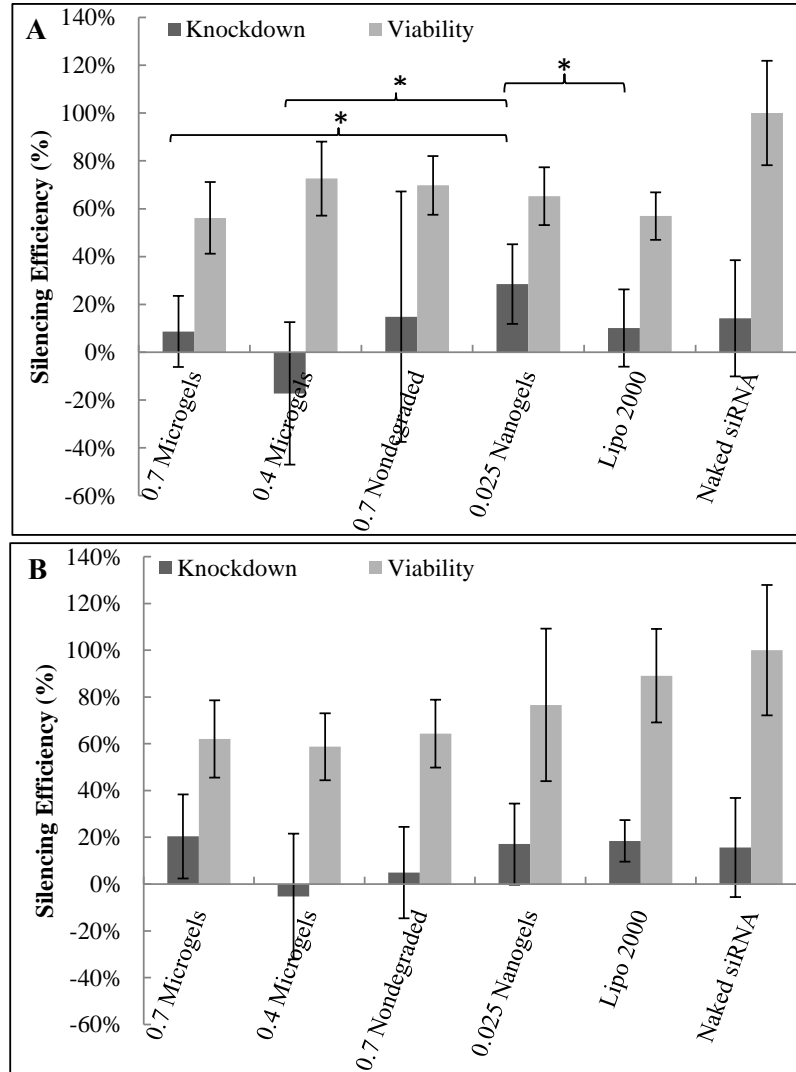


Figure 7.23: Gene knockdown by degraded and undegraded microgels containing nanogels, nanogels, commercially available Lipofectamine 2000, or naked siRNA. AllStars Death and Negative Control (Qiagen) were used, and MTS cell proliferation assay was used to quantify silencing efficiency (N=4, * $p < 0.05$).

REFERENCES

- [1] Kim, D.H. and Rossi, J.J., *Strategies for silencing human disease using RNA interference*. Nature Reviews Genetics, 2007. **8**(3): p. 173-184.
- [2] *Clinicaltrials.Gov*. 2012.
- [3] Fattal, E. and Bochot, A., *State of the art and perspectives for the delivery of antisense oligonucleotides and siRNA by polymeric nanocarriers*. Int. J. Pharm., 2008. **364**(2): p. 237-248.
- [4] Bouchie, A., *Companies in footrace to deliver RNAi*. Nat Biotechnol, 2012. **30**(12): p. 1154-1157.
- [5] Whitehead, K.A., Langer, R., and Anderson, D.G., *Knocking down barriers: Advances in siRNA delivery*. Nat. Rev. Drug Discovery, 2009. **8**(2): p. 129-138.
- [6] Schiffelers, R.M., Woodle, M.C., and Scaria, P., *Pharmaceutical prospects for RNA interference*. Pharm Res, 2003. **21**: p. 1-7.
- [7] Aouadi, M., Tesz, G.J., Nicoloro, S.M., Wang, M., Chouinard, M., Soto, E., Ostroff, G.R., and Czech, M.P., *Orally delivered siRNA targeting macrophage map4k4 suppresses systemic inflammation*. Nature, 2009. **458**(7242): p. 1180-1184.
- [8] Bhavsar, M.D. and Amiji, M.M., *Development of novel biodegradable polymeric nanoparticles-in-microsphere formulation for local plasmid DNA delivery in the gastrointestinal tract*. AAPS PharmSciTech, 2008. **9**(1): p. 288-294.
- [9] Bhavsar, M.D., Tiwari, S.B., and Amiji, M.M., *Formulation optimization for the nanoparticles-in-microsphere hybrid oral delivery system using factorial design*. J Controlled Release, 2006. **110**(2): p. 422-430.
- [10] Wilson, D.S., Dalmaso, G., Wang, L., Sitaraman, S.V., Merlin, D., and Murthy, N., *Orally delivered thioketal nanoparticles loaded with TNF-alpha-siRNA target inflammation and inhibit gene expression in the intestines*. Nat Mater, 2010. **9**: p. 923-928.

- [11] Laroui, H., Theiss, A.L., Yan, Y., Dalmasso, G., Nguyen, H.T.T., Sitaraman, S.V., and Merlin, D., *Functional TNF- α gene silencing mediated by polyethyleneimine/TNF- α siRNA nanocomplexes in inflamed colon*. Biomaterials, 2011. **32**(4): p. 1218-1228.
- [12] Forbes, D.C., Creixell, M., Frizzell, H., and Peppas, N.A., *Polycationic nanoparticles synthesized using ARGET ATRP for drug delivery*. Eur J Pharm Biopharm, 2013. **84**(3): p. 472-478.
- [13] Forbes, D.C. and Peppas, N.A., *Polymeric nanocarriers for siRNA delivery to murine macrophages*. Macromol Biosci, 2014. **14**(8): p. 1096-1105.
- [14] Pharmacopeia, T.U.S., *United states pharmacopeia 29 national formulary 24*, in *Reagents: Test Solutions*. 2006.
- [15] Yamagata, T., Morishita, M., Kavimandan, N.J., Nakamura, K., Fukuoka, Y., Takayama, K., and Peppas, N.A., *Characterization of insulin protection properties of complexation hydrogels in gastric and intestinal enzyme fluids*. J Controlled Release, 2006. **112**(3): p. 343-349.
- [16] Klinger, D. and Landfester, K., *Enzymatic- and light-degradable hybrid nanogels: Crosslinking of polyacrylamide with acrylate-functionalized dextrans containing photocleavable linkers*. J Polym Sci, Part A: Polym. Chem, 2012. **50**(6): p. 1062-1075.
- [17] Yanes, O., Villanueva, J., Querol, E., and Aviles, F., *Enzymatic measurements for the detection of trypsin and carboxypeptidase a inhibitory activity*. 2007.
- [18] Fischer, D., Li, Y., Ahlemeyer, B., Krieglstein, J., and Kissel, T., *In vitro cytotoxicity testing of polycations: Influence of polymer structure on cell viability and hemolysis*. Biomaterials, 2003. **24**: p. 1121-1131.
- [19] Kaplan, J.G. and Bona, C., *Proteases as mitogens: The effect of trypsin and pronase on mouse and human lymphocytes*. Experimental Cell Research, 1974. **88**: p. 388-394.
- [20] Unanue, E.R., *Antigen-presenting function of the macrophage*. Annual Review of Immunology, 1984. **2**: p. 395-428.

- [21] Forbes, D.C. and Peppas, N.A., *Polycationic nanoparticles for siRNA delivery: Comparing ARGET ATRP and UV-initiated formulations*. ACS Nano, 2014. **8**: p. 2908-2917.
- [22] Hickerson, R.P., Vlassov, A.V., Wang, Q., Leake, D., Ilves, H., Gonzalez-Gonzalez, E., Contag, C.H., Johnston, B.H., and Kaspar, R.L., *Stability study of unmodified siRNA and relevance to clinical use*. Oligonucleotides, 2008. **18**: p. 345-354.
- [23] Moret, I.s., Peris, J.E., Guillem, V.M., Benet, M., Revert, F., Dasi, F., Crespo, A., and Alino, S.F., *Stability of pei-DNA and dotap-DNA complexes: Effect of alkaline ph, heparin and serum*. J Controlled Release, 2001. **76**(169-181).
- [24] Zelphati, O. and Francis C. Szoka, J., *Mechanism of oligonucleotide release from cationic liposomes*. P Natl Acad Sci USA, 1996. **93**: p. 11493-11498.

Chapter 8: Conclusions and Recommendations for Future Research

8.1 CONCLUSIONS

RNA interference mediated by siRNA holds great promise as a treatment for many diseases that are associated with aberrant gene expression. However, to date many of the siRNA-based therapies that have made it to the clinical trial stage are administered via injection, and the oral administration route has yet to be successfully utilized. This is attributed to the diverse and plentiful challenges facing oral delivery of siRNA: degradation by proteases, extreme pH conditions, short half-life in circulation, relatively large size and negative charge, and lysosomal degradation. Thus, a carrier that has the ability to load siRNA via electrostatic complexation, protect the delicate siRNA during transit through the gastrointestinal tract, deliver the siRNA to the small intestine, and facilitate cellular uptake and endosomal escape is needed to overcome these challenges.

Polymers with pH responsive behavior are well-poised to meet these challenges. Polycationic nanogels have been developed in the Peppas lab and their ability to bind siRNA, cross the cell membrane, and induce gene silencing has been demonstrated [1-3]. On the other hand, anionic hydrogels have been widely used to deliver drugs and protein therapeutics to the small intestine. Thus, a combination of polymers with inverse pH responsive behavior may be able to meet the requirements as a carrier for orally delivered siRNA.

The goal of this work was to develop, synthesize, and characterize an anionic hydrogel material capable of encapsulating and releasing polycationic nanogels to deliver siRNA. Two major approaches were explored, one with nondegradable crosslinkers and one with biodegradable, biomolecule-based crosslinkers. Both approaches utilized poly(methacrylic acid-co-*N*-vinylpyrrolidone), an anionic polymer that is protonated and

collapsed at low pH conditions, but ionized and swollen at high pH conditions, making it suitable for oral drug delivery applications.

Formulations with two different nondegradable crosslinking agents, tetra(ethylene glycol) dimethacrylate (TEGDMA) and poly(ethylene glycol) dimethacrylate (n=400) (PEGDMA), and varying cationic nanogel incorporation were synthesized by UV-initiated bulk free radical polymerization. Nanogel incorporation within the microgels was confirmed by fluorescent microscopy. The pH responsive swelling behavior of the different formulations indicated that hydrogels with the shorter TEGDMA crosslinking agent experienced higher weight swelling ratios with increased nanogel content while the swelling of the PEGDMA gels were not dependent upon nanogel content. As the PEGDMA formulations exhibited consistent and favorable pH responsive swelling behavior independent of nanogel encapsulation, a protein and a small molecule model therapeutic were successfully loaded into the PEGDMA microgels with and without nanogels. The release efficiencies of both the model therapeutics were lower than expected, and nanogel content did not affect loading or release efficiency. The major issue with this system, however, was its inability to release the encapsulated nanogels. Without the release of the nanogels, siRNA has a low probability of cellular uptake and endosomal escape.

This prompted a redesign of the anionic P(MAA-co-NVP) microgel system to incorporate a biodegradable crosslinker that is responsive to enzymes present in different regions of the intestine. Linear P(MAA-co-NVP) was first synthesized by UV-initiated solution polymerization, paying close attention to the charge state of the polymer after purification. The crosslinking reaction was most successful using linear polymer lyophilized at pH 8 in a two-part EDC-NHS linking reaction transitioned from pH 5 to pH 8. Incorporation of the peptide was consistently above 97% as determined by

fluorescamine assay of the peptide remaining in solution, and incorporation was verified by IR spectra. Nanogels were incorporated simply by addition to the solution just prior to the EDC-NHS crosslinking reaction, and the encapsulation of nanogels was confirmed by fluorescence spectroscopy and microscopy.

Proteolytic degradation of the peptide-crosslinked microgels, both with and without nanogels, during incubation with trypsin solutions, simulated intestinal fluid (SIF), and rat intestinal fluid was demonstrated by reduced relative turbidity as a function of time and trypsin concentration. In contrast, relative turbidity of the microgel solutions remained constant upon incubation in phosphate buffered saline pH 7.4 (PBS), simulated gastric fluid (SGF), and rat gastric fluid, verifying that degradation was specific to the intestinal enzyme trypsin. The relative turbidity of nearly all trypsin and microgel concentrations tested reached a plateau within 90 minutes, indicating complete degradation. The microgels in SIF and rat intestinal fluid, on the other hand, required up to 4 hours to fully degrade, but this is still a relevant time scale for intestinal delivery. ImageStream flow cytometry was used to further analyze and quantify microgel degradation; over two hours in SIF, the median size of the microgels decreased by 68% whereas the median size of microgels in SGF actually increased by 20%.

The degradable microgels induced a cytotoxic effect in a concentration-dependent manner in both the degraded and nondegraded states, but at low concentrations the changes in cell metabolism were tolerable. The cell viability after 8-18 hours of exposure to microgel concentrations less than 0.4 mg/ml was consistently greater than 90% as measured by an LDH membrane integrity assay. These trends were consistent for formulations with and without nanogels, though the toxicity of the cationic nanogels became apparent at a concentration of 1 mg/ml of microgels. These studies confirm that

the biodegradable behavior and biocompatibility of the peptide crosslinked hydrogel was highly suitable for intestinal delivery applications.

The P(MAA-co-NVP) polymer backbone retained its pH responsive behavior after the crosslinking reaction. Despite potential concerns of incomplete complexation at low pH conditions, the microgels were able to load the therapeutic protein insulin with about 40% loading efficiency as well as retain the loaded protein in low pH conditions.

Similarly, siRNA was loaded into the microgel systems containing polycationic nanogels by equilibrium partitioning and charge interactions with the nanogels with 60-80% efficiency, depending on the type and concentration of siRNA. However, the siRNA experienced some degradation during incubation in simulated intestinal conditions, particularly at high trypsin concentrations, used to degrade the microgels. Despite the attack by trypsin on the siRNA, nondegraded siRNA was released from the microgel system, especially in the more physiologically relevant buffers, as detected by polyacrylamide gel electrophoresis.

Cellular uptake of nanogels released from degraded microgels was confirmed in RAW 264.7 murine macrophage cells by confocal microscopy. Both ImageStream analysis and confocal microscopy suggest that electrostatic complexation is occurring between the negatively charged degraded P(MAA-co-NVP) and positively charged nanogels, but some of the complexes, free nanogels, or both are still internalized by the cells. Despite the internalization of nanogels, the ability of the delivery system to induce gene silencing in RAW 264.7 and Caco-2 human adenocarcinoma cells was somewhat disappointing, at less than 20% silencing efficiency and significantly less than the silencing efficiency attained by the nanogels alone in RAW 264.7 cells. This may be due to loss of siRNA stability upon incubation in intestinal conditions and/or electrostatic interactions interfering with release nanogels and siRNA. Though the ability of the

system to induce gene silencing was somewhat disappointing, the transfection efficiencies were consistent and repeatable across both RAW 264.7 and Caco-2 cell lines, making the results credible and reducing concerns about variability within the microgel composition.

This work demonstrates that polycationic nanogels can be encapsulated in anionic P(MAA-co-NVP) microgels via two different synthesis methods, but a biodegradable crosslinker is necessary to release the nanogels from the matrix. The trypsin-degradable GRRRGK peptide was incorporated as a crosslinker via facile EDC-NHS reaction with P(MAA-co-NVP). The ability of this microgel encapsulation system to degrade in response to a specific enzyme on a relevant timescale, induce minimal cytotoxicity, load siRNA, deliver a detectable amount of viable siRNA, and release nanogels for cellular uptake endow it with significant potential as a vehicle for oral delivery of siRNA that should be further studied and improved.

8.2 RECOMMENDATIONS FOR FUTURE RESEARCH

Future work on this system could be directed toward tuning the charge densities of the nanogels and the microgel encapsulation system to limit electrostatic binding. This may be achieved by changing the molar ratio of MAA:NVP or the weight incorporation of nanogels in the microgels.

Transfection with the improved systems may be executed to determine the effect of charge interactions on silencing efficiency. Transfection conditions such as trypsin concentration during degradation, microgel concentration, during transfection, transfection media, and transfection duration should also be further optimized to decrease electrostatic interactions, limit siRNA degradation, and increase silencing efficiency.

Different gene targets could be explored, as various siRNAs and cell models may react to the microgel systems differently. Some gene targets that are common in the literature and for which siRNAs are commercially available are GAPDH, a ubiquitous gene that maintains normal cell metabolism, and TNF- α [4-6], a cytokine overexpressed in inflammatory diseases.

Further, the performance of this microgel system should be evaluated *in vivo* or at least in more physiologically accurate cell model conditions to verify the biodegradability and silencing efficiency; it is possible that a greater portion of the siRNA will remain stable at physiological trypsin concentrations, and competing charged molecules in the intestinal environment may decrease the electrostatic binding via competitive dissociation. It would be of interest to use the microgels to deliver anti-TNF- α siRNA orally to a dextran sodium sulfate-induced colitis mouse model [4, 5] or evaluate systemic knockdown of TNF- α via epithelial permeation in an *in vitro* or *in vivo* model [7, 8].

REFERENCES

- [1] Liechty, W.B., Scheuerle, R.L., and Peppas, N.A., *Tunable, responsive nanogels containing t-butyl methacrylate and 2-(t-butylamino)ethyl methacrylate*. Polym, 2013. **54**(15): p. 3784-3795.
- [2] Forbes, D.C. and Peppas, N.A., *Polymeric nanocarriers for siRNA delivery to murine macrophages*. Macromol Biosci, 2014. **14**(8): p. 1096-1105.
- [3] Forbes, D.C. and Peppas, N.A., *Polycationic nanoparticles for siRNA delivery: Comparing ARGET ATRP and UV-initiated formulations*. ACS Nano, 2014. **8**: p. 2908-2917.
- [4] Kriegel, C. and Amiji, M., *Oral TNF- α gene silencing using a polymeric microsphere-based delivery system for the treatment of inflammatory bowel disease*. J Controlled Release, 2011. **150**(1): p. 77-86.
- [5] Wilson, D.S., Dalmasso, G., Wang, L., Sitaraman, S.V., Merlin, D., and Murthy, N., *Orally delivered thioketal nanoparticles loaded with TNF- α -siRNA target inflammation and inhibit gene expression in the intestines*. Nat Mater, 2010. **9**: p. 923-928.
- [6] Laroui, H., Theiss, A.L., Yan, Y., Dalmasso, G., Nguyen, H.T.T., Sitaraman, S.V., and Merlin, D., *Functional TNF α gene silencing mediated by polyethyleneimine/TNF α siRNA nanocomplexes in inflamed colon*. Biomaterials, 2011. **32**(4): p. 1218-1228.
- [7] He, C., Yin, L., Tang, C., and Yin, C., *Multifunctional polymeric nanoparticles for oral delivery of TNF- α siRNA to macrophages*. Biomaterials, 2013. **34**(11): p. 2843-2854.
- [8] He, C., Yin, L., Tang, C., and Yin, C., *Trimethyl chitosan-cysteine nanoparticles for systemic delivery of TNF- α siRNA via oral and intraperitoneal routes*. Pharm Res, 2013. **30**(10): p. 2596-2606.

Appendix A: Emulsion Polymerization of Poly(methacrylic acid-co-*N*-vinyl-2-pyrrolidone) Particles

A.1 INTRODUCTION

Design parameters of an effective oral delivery vehicle for small interfering RNA (siRNA) include ability to transverse the digestive tract, cross the cell membrane, and escape into the cell cytosol, all while maintaining the bioactivity of the easily-degraded siRNA. Anionic hydrogels have been shown to have suitable properties for oral delivery of delicate proteins[1, 2], and may have utility in as part of a composite hydrogel system to deliver encapsulated siRNA to the site of cell uptake.

Emulsion polymerizations consist of monomer droplets dispersed in a nonsolvent continuous phase and are stabilized by surfactants at concentrations above the critical micelle concentration. Upon addition of the initiator to the dispersant phase, free radicals diffuse into the surfactant micelles to initiate polymerization within the micelles [3]. Thus, emulsion polymerizations have the advantage of using micelle size to control the size of the resulting latex particles [4].

A typical emulsion employs an aqueous dispersant phase with hydrophobic monomers. Hydrophilic monomers such as methacrylic acid (MAA) require an inverse emulsion, or water-in-oil (W/O) emulsion. The hydrophilic-lipophilic balance (HLB), or the ratio of hydrophilic to lipophilic groups present on a surfactant or in a surfactant system [5], is a critical aspect of a successful inverse emulsion [6]. Additionally, monomers with acid functional groups, such as methacrylic acid, introduce stability issues into the emulsion [7].

The aim of this work was the development of a novel inverse emulsion photopolymerization to synthesize hydrophilic, pH-responsive anionic poly(methacrylic

acid-co-*N*-vinyl-2-pyrrolidone) hydrogel particles that may be used as part of a composite hydrogel system for the oral delivery of siRNA to the gastrointestinal tract.

A.2 EXPERIMENTAL METHODS

A.2.1 Chemicals

Methacrylic acid (MAA and *N*-vinyl-2-pyrrolidone (NVP) were obtained from Sigma-Aldrich (St. Louis, MO). Poly(ethylene glycol) (400) dimethacrylate (PEGDMA) was purchased from Polysciences, Inc. (Warrington, PA). TweenTM 80 (poly[ethylene glycol](80) sorbitan monooleate) or TweenTM 20 (poly[ethylene glycol](20) sorbitan monooleate) and SpanTM 80 (sorbitan monooleate) were obtained from Sigma Aldrich. Mineral oil was obtained from Thermo-Fisher. Irgacure 184[®] (1-hydroxy-cyclohexyl-phenylketone) was purchased from Sigma-Aldrich. All reagents were used as received.

A.2.2 Emulsion Polymerization

Inverse emulsion compositions were based on emulsion recipes reported by Kriwet et al. [4] and consisted of 25% (w/w) hydrophilic phase, 5% (w/w) monomer, 2-5 % (w/w) surfactant, and the remainder was mineral oil. MAA:NVP molar ratio was held constant at 1:1, and PEGDMA was added at 1 mol% with respect to total monomer content.

First, the mineral oil and surfactants TweenTM 80 (poly[ethylene glycol](80) sorbitan monooleate) or TweenTM 20 (poly[ethylene glycol](20) sorbitan monooleate) and SpanTM 80 (sorbitan monooleate) were combined to form the continuous phase. The monomers and sodium hydroxide (1 N) were added to water to form the hydrophilic phase. The hydrophilic phase was then be added to the lipophilic phase while stirring, followed by the addition of 1 wt % Irgacure[®] 184 with respect to the total monomer content.

The phases were emulsified using a Misonix Ultrasonicator (Misonix, Inc., Newtown, CT) at 90 W for 10 seconds on/10 seconds off for a total of 20 minutes, transferred to a round bottom flask, then bubbled with nitrogen for 20 minutes to remove the free radical scavenger oxygen. Polymerization was initiated with a Dymax BlueWave® 200 UV point source (Dymax, Torrington, CT) for a period of time proportional to the volume of the emulsion (i.e., 3 hours for 100 ml reaction volume) with constant stirring. Following polymerization, the latex particles were extracted from the emulsion by precipitation with 2-propanol and further purified by washes with acetone, followed by dialysis against DI water in 12-14 kDa MWCO dialysis tubing (Spectrum Labs, Rancho Dominguez, CA) for 10 days. The polymer particles were then lyophilized and stored in a desiccator at room temperature.

A.2.3 Emulsion Characterization

Emulsion stability was evaluated by using a Bio-Tek Synergy™ HT multi-mode plate reader (Winooski, VT) to measure the UV/VIS absorbance spectra of the emulsions over time, as changes in turbidity indicate instability. Emulsions were screened in a high-throughput manner in 96-well plates.

SEM samples were prepared by drop-casting polymer solutions at concentrations of 1-2.5 mg/mL in water onto carbon-tape covered aluminum stubs. After drying, the samples were coated with 10-12 nm of Pt/Pd coating using a Cressington 208 Benchtop sputter coater (Watford, England). Scanning electron microscopy images were obtained using an FEI Quanta 650 FEG scanning electron microscope (Hillsboro, OR). SEM micrographs were used to evaluate the stability of the emulsion during polymerization as well as the size and morphology of the resulting particles.

Dynamic light scattering (DLS) measurements were made using a Malvern Zetasizer Nano ZS (Worcestershire, UK) to determine the size and zeta potential of the polymer particles as a function of pH. Particles were run at a concentration of 0.5 mg/mL in water.

A.3 RESULTS AND DISCUSSION

Surfactants, surfactant ratios, and the degree of neutralization (DN) of MAA were varied within the ranges shown in Table A.1 to evaluate the effect on emulsion stability. Emulsions were examined visually over time to detect any coalescence, flocculation, creaming, or Ostwald ripening that could be indicative of instability. Additionally, the absorbance spectra of the emulsions were measured over time to correlate turbidity to stability. Emulsions that changed in turbidity or showed any of the aforementioned characteristics of instability were deemed unstable.

Figure A.1 shows representative images of emulsions at time=0 and time=60. The emulsion formulation on the left, E61, remained turbid over 60 minutes and showed no signs of separation, indicating good stability. Emulsions 62-65, however, either changed in turbidity, coalesced, or both, indicating instability. Figure A.2 shows that the absorbance measurements were in good agreement with the visual observations, with the absorbance values dropping in the unstable emulsions.

The emulsion compositions were recorded on a teRNArY phase diagram to determine regions of stability. For Span 80:Tween 20 formulations with 2 wt% surfactant, 75:25-50:50 Span:Tween ratio, and 40-80% DN, no distinct region of stability was present, as seen in Figure A.3. At 3 wt% surfactant, 75:25-50:50 Span:Tween ratio, and 40-80% DN, a region of stability was observed at or near 50:50 Span:Tween ratio and did not depend on DN in this region, as shown in Figure A.5. Corresponding

absorbance spectra are shown in Figures A.4 and A.6, and it can be seen that there was a clear division in absorbance spectra between stable and unstable emulsions with 2 wt% surfactant, but the absorbance spectra were less conclusive in the 3 wt% surfactant emulsions.

Overall, emulsions prepared with Span 80 and Tween 80 were more stable than emulsions prepared with Span 80 and Tween 20. For Span 80:Tween 80 formulations with 2 wt% surfactant, 75:25-50:50 Span:Tween ratio, and 40-80% DN, nearly all the emulsions were stable over 60 minutes, as seen in Figure A.7. The same was true for emulsions with 3 wt% surfactant, 75:25-50:50 Span:Tween ratio, and 40-80% DN, as shown in Figure A.9. Additionally, the corresponding absorbance spectra, shown in Figures A.8 and A.10, were in 100% agreement with visual observations of emulsion stability, demonstrated by the distinct differences in absorbance values.

Based on these results, a surfactant amount of 2 wt% and Span 80:Tween 80 of 75:25 was chosen as the best performing emulsion conditions. This ratio of surfactant has an HLB of approximately 6.9, which is just above the range of 3-6 recommended for inverse emulsions [8]. The degree of neutralization of MAA was next varied from 40-80% and the resulting polymer was further characterized. At the end of the polymerization, some sediment was present in the emulsions with the two lowest DN, indicating instability of the product. This was verified by SEM, shown in Figure A.11.

To verify the pH-responsive behavior of the polymer particles, DLS was used to measure the zeta potential and Z-average size of particles from the 2 wt% and Span 80:Tween 80 of 75:25 emulsion with the highest DN, 80%. As shown in Figure A.12, there was an inverse relationship between zeta potential and Z-average size of the particles as the pH increased from 2 to 8. It should be noted that accurate size

measurements could not be obtained below pH 4, as the particles were protonated at low pH and prone to aggregation due to hydrogen bonding.

A.4 CONCLUSIONS

Best-performing co-surfactant systems and W/O emulsion compositions were determined to achieve a stable photoemulsion polymerization for synthesis of hydrophilic P(MAA-co-NVP) hydrogel particles. A high-throughput method was developed to screen emulsion stability over time of 96 formulations at once using absorbance measurements obtained from a plate reader; correlation to visual observations of stability was 100% for Span 80:Tween 80 formulations. Particles were able to be extracted from the emulsion and purified. The pH-response and zeta potential of the polymer indicated that it may be a suitable material to be used in a composite hydrogel system for oral delivery applications.

A.5 TABLES

Parameter	Range Tested
Dual surfactant system	Span 80, Tween 20 Span 80, Tween 80
Ratio of Tween:Span	0:100 - 50:50
Surfactant amount (relative to entire weight of emulsion)	2-5%
Degree of Neutralization (DN) (Moles NaOH relative to moles of MAA)	40-80%

Table A1: Parameters varied to determine effect on emulsion stability.

A.5 FIGURES

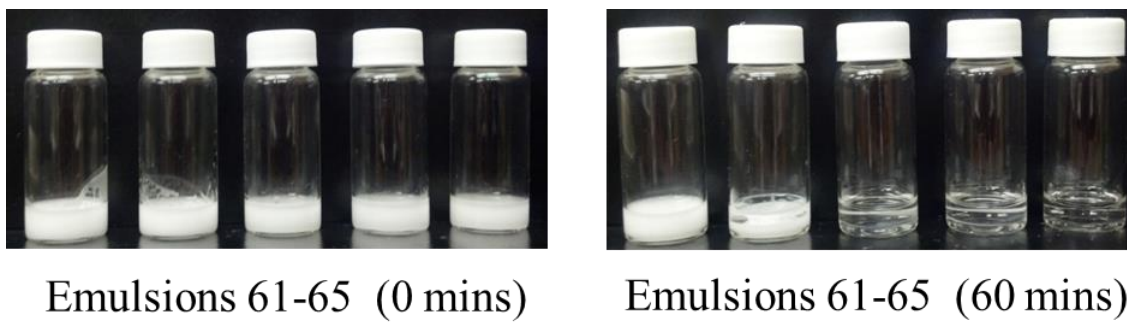


Figure A.1: Representative images of emulsions at time=0 and time=60 minutes.

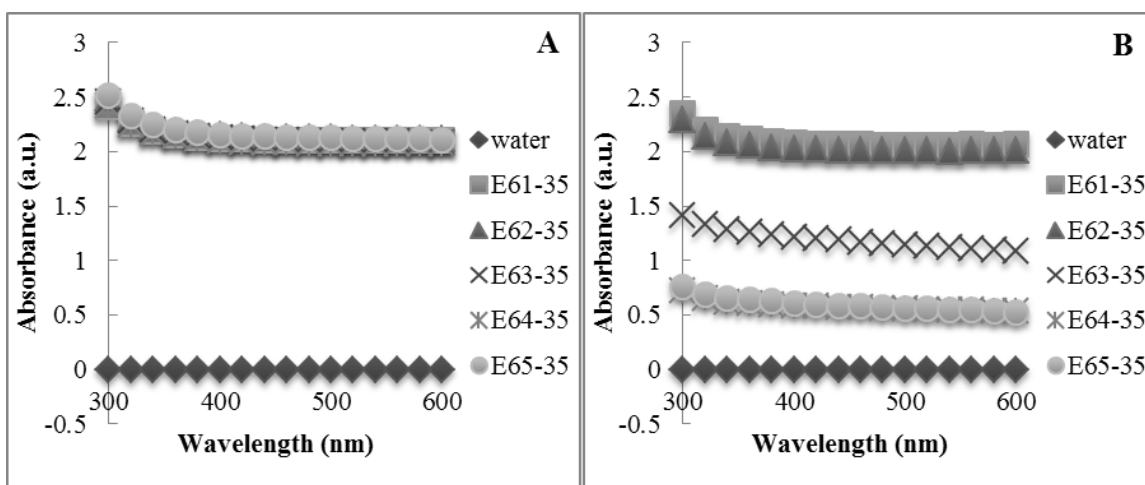


Figure A.2: Absorbance spectra of emulsions at A) time=0 and B) time=60 minutes.

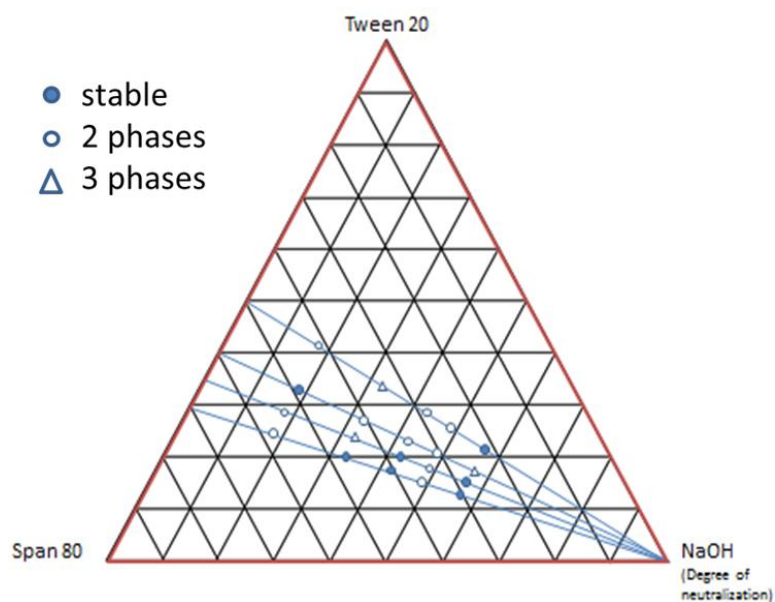


Figure A.3: TeRNArY phase plot of emulsions with 2 wt% Span 80/Tween 20 co-surfactant system.

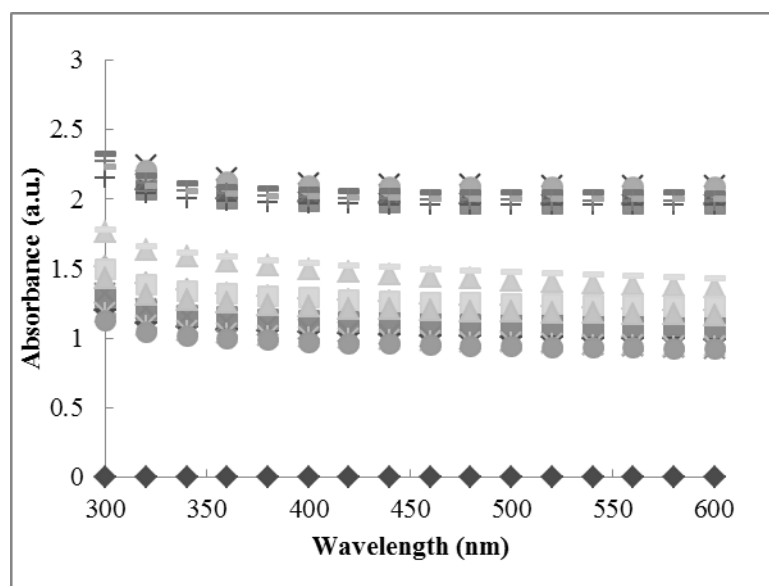


Figure A.4: Absorbance spectra of emulsions with 2 wt% Span 80/Tween 20 co-surfactant system.

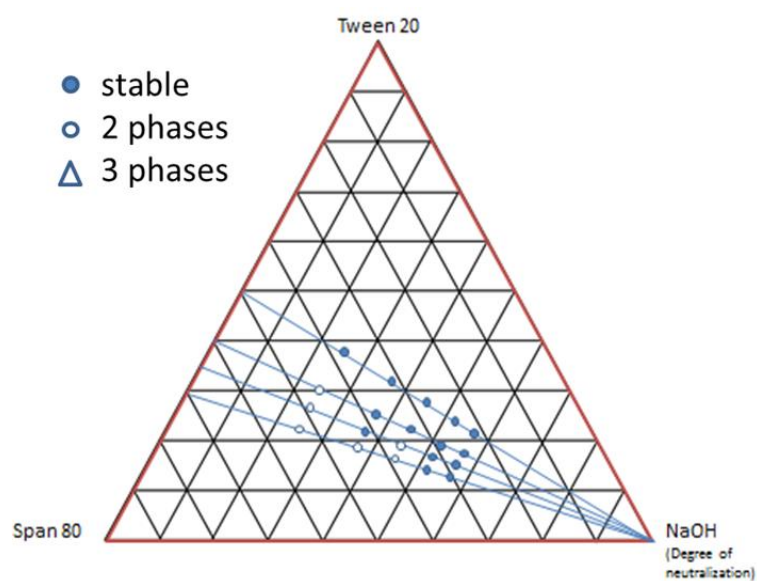


Figure A.5: TeRNArY phase plot of emulsions with 3 wt% Span 80/Tween 20 co-surfactant system.

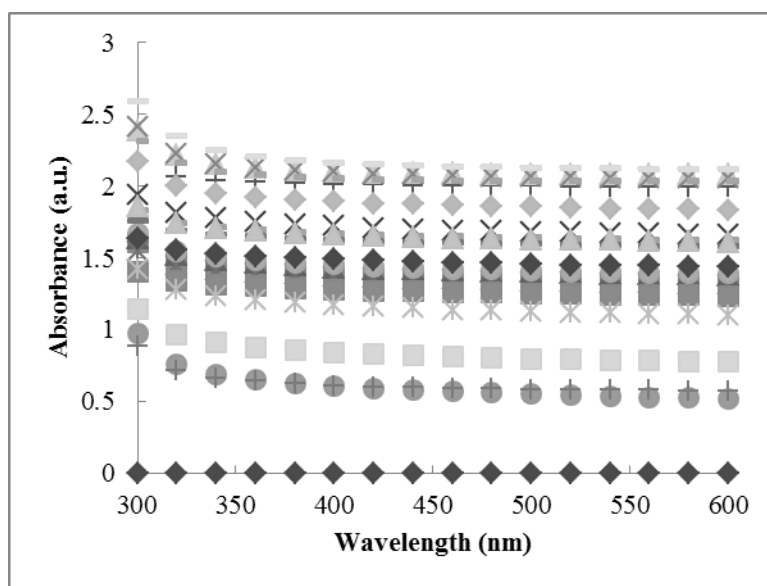


Figure A.6: Absorbance spectra of emulsions with 3 wt% Span 80/Tween 20 co-surfactant system.

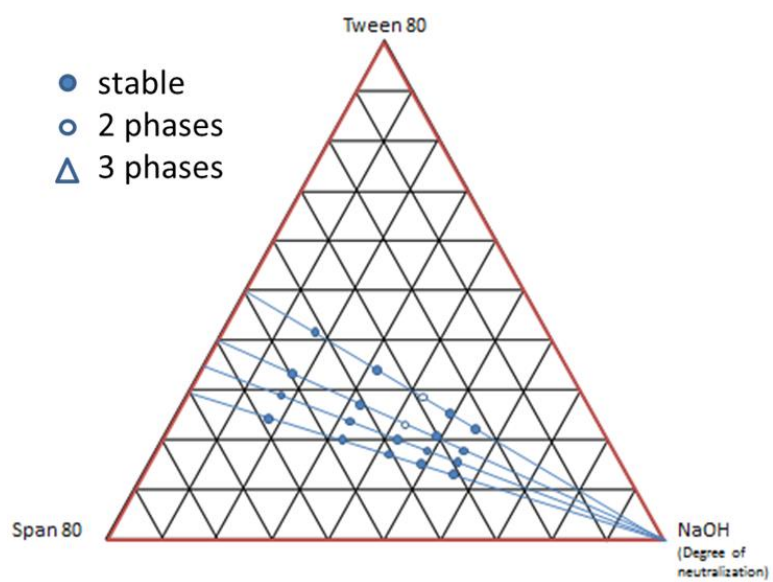


Figure A.7: TeRNArY phase plot of emulsions with 2 wt% Span 80/Tween 80 co-surfactant system.

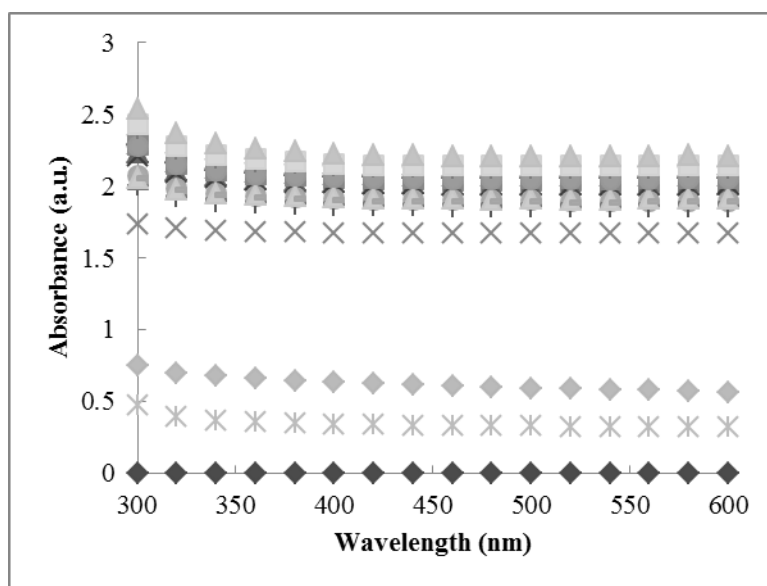


Figure A.8: Absorbance spectra of emulsions with 2 wt% Span 80/Tween 80 co-surfactant system.

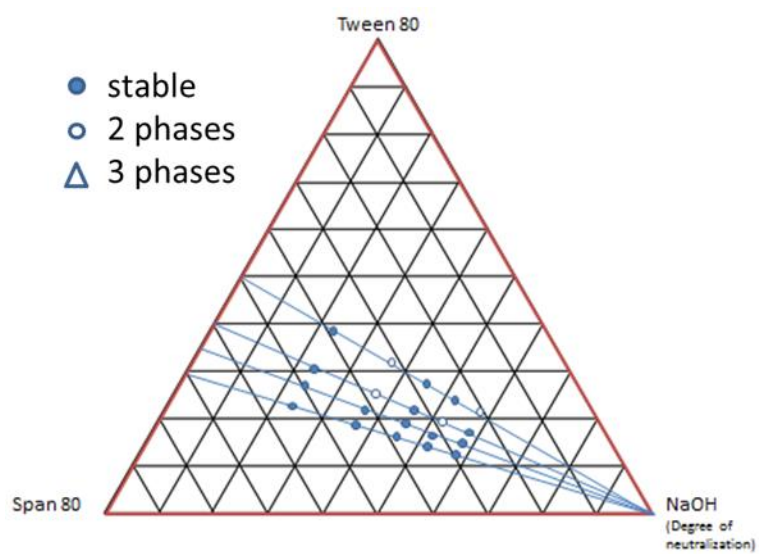


Figure A.9: TeRNArY phase plot of emulsions with 3 wt% Span 80/Tween 80 co-surfactant system.

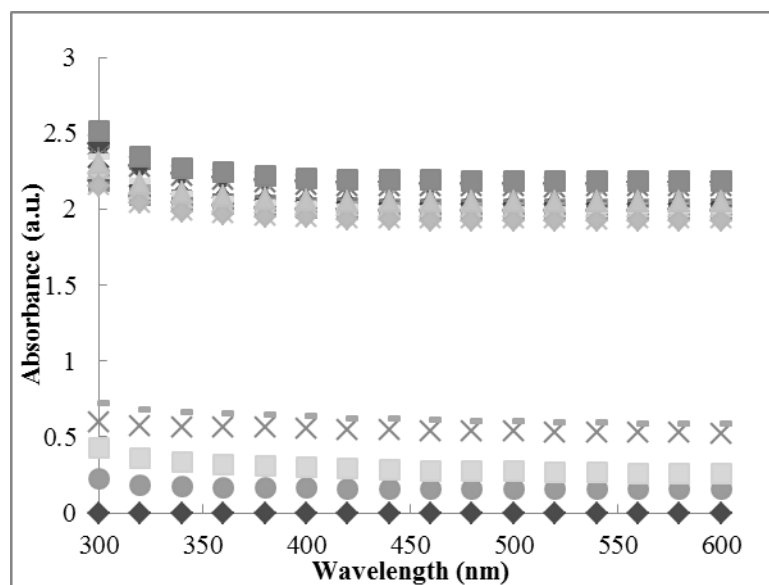


Figure A.10: Absorbance spectra of emulsions with 2 wt% Span 80/Tween 80 co-surfactant system.

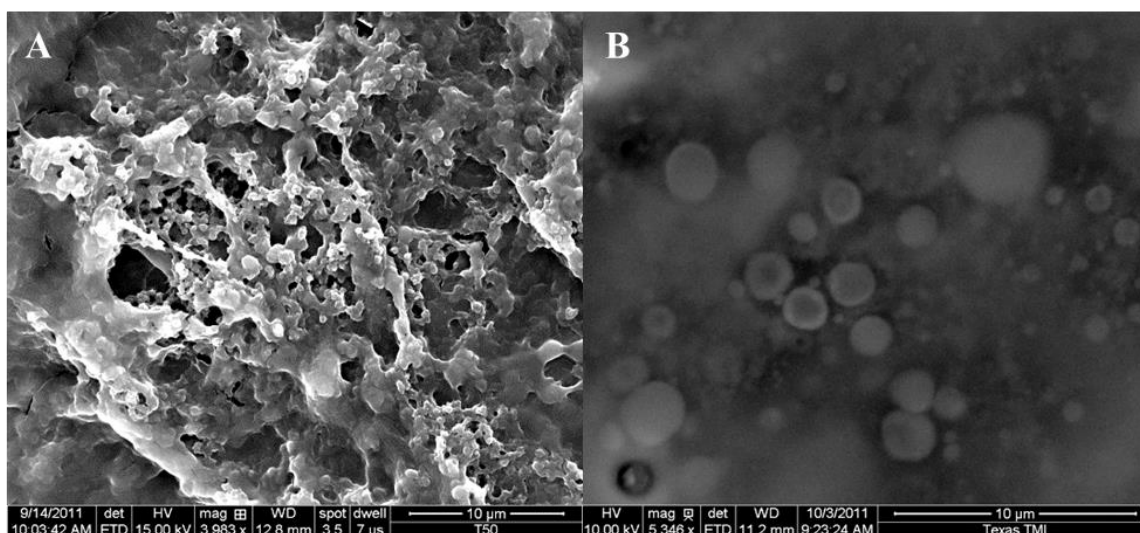


Figure A.11: SEM micrographs of particles from A) an unstable emulsion with low DN and B) a stable emulsion with high DN. (Scale bar= 10 µm).

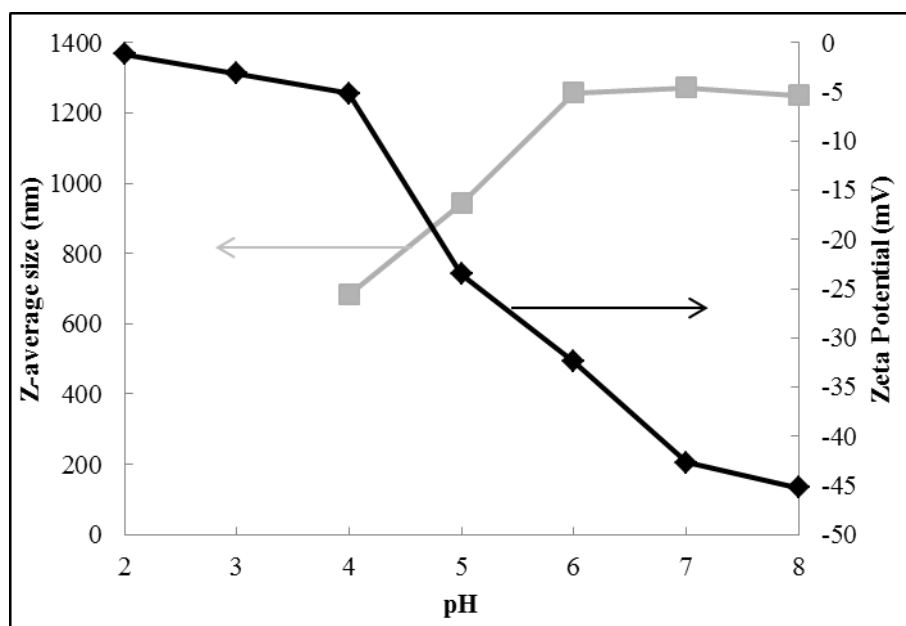


Figure A.12: Z-average size and zeta potential measurements made using DLS of P(MAA-co-NVP) particles synthesized via a stable emulsion polymerization (0.5 mg/ml in water).

REFERENCES

- [1] Lowman, A.M., Morishita, M., Kajita, M., Nagai, T., and Peppas, D.N.A., *Oral delivery of insulin using ph-responsive complexation gels*. J Pharm Sci, 1999. **88**: p. 933-937.
- [2] Carr, D.A., Gomez-Burgaz, M., Boudes, M.C., and Peppas, D.N.A., *Complexation hydrogels for the oral delivery of growth hormone and salmon calcitonin*. Ind Eng Chem Res, 2010. **49**: p. 11991-11995.
- [3] Van Der Hoff, B.M.E., *Kinetics of emulsion polymerization*. 1962. **34**: p. 6-31.
- [4] Kriwet, B., Walter, E., and Kissel, T., *Synthesis of bioadhesive poly(acrylic acid) nano- and microparticles using an inverse emulsion polymerization method for the entrapment of hydrophilic drug candidates*. J Controlled Release, 1998. **56**: p. 149-158.
- [5] Griffin, W.C., *Calculation of HLB values of non-ionic surfactants*. JouRNAl of the Society of Cosmestic Chemists, 1954. **5**: p. 249-256.
- [6] Williams, J.M., *High internal phase water-in-oil emulsions: Influence of surfactants and cosurfactants on emulsion stability and foam quality*. Langmuir, 1991. **7**: p. 1370-1377.
- [7] Plochocka, K. and Chuang, J.-C., *Inverse emulsion crosslinked polyacrylic acid of controlled pH*. 1993, ISP Investments Inc.: US.
- [8] Chern, C.-S., *Principles and applications of emulsion polymerization*. 2008, Hoboken, NJ: John Wiley & Sons, Inc.

Appendix B: Abbreviations

AGO-2	argonaute-2
ARGET	activator regenerated by electron transfer
ATRP	atom transfer radical polymerization
AuCM	cysteamine-modified gold nanoparticles
BAEE	N α -benzoyl-L-arginine ethyl ester hydrochloride
BSA	bovine serum albumin
CD	celiac disease
CdSe	cadmium selenide
β -CD	β -cyclodextrin
DEPC	diethylpyrocarbonate
DLS	dynamic light scattering
DMEM	Dulbecco's modified Eagle medium
DN	degree of neutralization
EDC	1-ethyl-3-(3-dimethylaminopropyl) carbodiimide hydrochloride
FRET	fluorescent resonance energy transfer
FTIR	Fourier transform infrared spectroscopy
GeRP	β -1,3-D-glucan-encapsulated siRNA particle
GFD	gluten-free diet
GI	gastrointestinal
HA	hyaluronic acid
HCl	hydrochloric acid
HLA	human leukocyte antigen
HLB	hydrophilic-lipophilic balance

IBD	inflammatory bowel disease
IL-6	interleukin-6
IPN	interpenetrating polymer network
KGM	konjac glucomannan
L-Arg	L –arginine
LN2	liquid nitrogen
LPS	lipopolysaccharide
MAA	methacrylic acid
MMC	migrating myoelectric complex
mRNA	messenger RNA
MTX	methotrexate
MWCO	molecular weight cut-off
NaOH	sodium hydroxide
NBD-Cl	4-chloro-7-nitrobenzofurazan
NHS	N-hydroxysuccinimide
NiMOS	nanoparticle-in-microsphere
NVP	N-vinyl-2-pyrrolidone
P(MAA-co-NVP)	poly(methacrylic acid-co-N-vinylpyrrolidone)
PAAD	poly(acrylic acid) derivatives
PAGE	polyacrylamide gel electrophoresis
PASP	poly(aspartic acid)
PBS	phosphate buffered saline
PCL	poly(ϵ -caprolactone)
PDEAEMA	poly[2-(diethylamino) ethyl methacrylate]
PEG	poly(ethylene glycol)

PEGDMA	poly(ethylene glycol) dimethacrylate
pEGFP	enhanced green fluorescent protein
PEI	polyethyleneimine
PGA	poly(glutamic acid)
PLL	poly(L-lysine)
PMAA	poly(methacrylic acid)
QD	quantum dot
RNA	ribonucleic acid
RNAi	RNA interference
RNAse A	ribonuclease A
RT-PCR	reverse transcription- polymerase chain reaction
SEM	scanning electron microscopy
SGF	simulated gastric fluid
SIF	simulated intestinal fluid
siRNA	small interfering RNA
TBAEMA	2-(tert-butylamino)ethyl methacrylate
TBMA	tert-butyl methacrylate
TEGDMA	tetra(ethylene glycol) dimethacrylate
TGA	thermal gravimetric analysis
TKN	thioketal nanoparticle
TMC-Cys	trimethyl chitosan-cysteine conjugate
TNF- α	tumor necrosis factor- α
W/O	water-in-oil
ZnS	zinc sulfide

Appendix C: Publications, Presentations and Coursework

C.1 PUBLICATIONS

1. **Knipe, J.M.** and Peppas, N.A. "Microencapsulated Nanogels for siRNA Delivery," In Preparation.
2. **Knipe, J.M.**, Chen, F., and Peppas, N.A. "Enzymatically Degradable Hydrogels for Site-Specific Intestinal Delivery," In Preparation.
3. **Knipe, J.M.** and Peppas, N.A. "Multi-responsive Hydrogels for Drug Delivery and Tissue Engineering Applications," *Regenerative Biomaterials*, Accepted.
4. **Knipe, J.M.**, Chen, F., and Peppas, N.A. "Multi-responsive polyanionic microgels with inverse pH-responsive behavior by encapsulation of polycationic nanogels," *JouRNal of Applied Polymer Science*, 131, **2014**, 40098-40105.
5. **Knipe, J.M.**, Peters, J.T., and Peppas, N.A. "Theranostic agents for gene delivery and spatiotemporal imaging," *Nano Today*, 8, **2013**, 21-38.

C.2 PRESENTATIONS

1. **Knipe, J.M.**, Chen, F., and Peppas, N.A. "Enzymatically Degradable Microgels for the Oral Delivery of siRNA," *Biomedical Engineering Society Annual Meeting*, San Antonio, TX. October 24, 2014. (Accepted.)
2. **Knipe, J.M.**, Chen, F., Khot, S., and Peppas, N.A. "Microencapsulated Nanogel System for the Oral Delivery of siRNA," *American Association of Pharmaceutical Scientists Annual Meeting*, San Antonio, TX. November 11, 2013. (Poster.)
3. **Knipe, J.M.**, Chen, F., Khot, S., and Peppas, N.A. "Biodegradable microencapsulated nanogel system for the oral delivery of siRNA," *WE13 Annual*

- Conference of The Society of Women Engineers*, Baltimore, MD. October 24, 2013. (Oral presentation and poster.)
4. **Knipe, J.M.** and Peppas, N.A. "Microencapsulated polymeric systems for the oral delivery of siRNA," *Biomaterials Day of the Society for Biomaterials*, Austin, TX. May 31, 2013.
 5. **Knipe, J.M.** and Peppas, N.A. "Microencapsulated polymeric systems for the oral delivery of siRNA," *Graduate and Industry Networking Event*, Austin, TX. February 27, 2013.
 6. **Knipe, J.M.**, Pham, T.N, and Peppas, N.A. "Nanoscale Anionic Hydrogel Prepared by Emulsion Polymerization for Oral Delivery of siRNA," *AIChE Annual Meeting*, Pittsburgh, PA. November 1, 2012. (Oral presentation.)
 7. **Knipe, J.M.** and Peppas, N.A. "Synthesis and Characterization of Composite Hydrogel Particles for Oral Delivery of siRNA," *Biomedical Engineering Society Annual Meeting*, Atlanta, GA. October 25, 2012. (Oral presentation.)
 8. **Knipe, J.M.** and Peppas, N.A. "Synthesis and Characterization of Composite Hydrogel Particles for Oral Delivery of Small Interfering RNA," *Biomaterials Day of the Society for Biomaterials*, Houston, TX. July 27, 2012.

C.3 COURSEWORK

1. CHE 381N FLUID FLOW AND HEAT TRANSFER
2. CHE 381P ADV ANALYSIS FOR CHEM ENGINEER
3. CHE 387K ADVANCED THERMODYNAMICS
4. CHE 392 POLYMER SCIENCE
5. CH 392N PHYS CHEM OF MACROMOLEC SYSTEM
6. CHE 384 ADV ENGINEERING BIOMATERIALS
7. CHE 384 MASS TRANSFER IN POLYMERS
8. LEB 380 14-INTELLECTUAL PROPERTY

References

- Abraham, C. and Cho, J.H., Inflammatory bowel disease. *N Engl J Med*, 2009. 361: p. 2066-2078.
- Agami, R., Rnai and related mechanisms and their potential use for therapy. *Current Opinion in Chemical Biology*, 2002. 6: p. 829-834.
- Aigner, A., Applications of RNA interference: Current state and prospects for siRNA-based strategies in vivo. *Appl Microbiol Biot*, 2007. 76(1): p. 9-21.
- Akinc, A., Thomas, M., Klibanov, A.M., and Langer, R., Exploring polyethylenimine-mediated DNA transfection and the proton sponge hypothesis. *The JouRNaI of Gene Medicine*, 2005. 7(5): p. 657-663.
- Ameres, S.L., Martinez, J., and Schroeder, R., Molecular basis for target RNA recognition and cleavage by human risc. *Cell*, 2007. 130(1): p. 101-112.
- Annabi, N., Tamayol, A., Uquillas, J.A., Akbari, M., Bertassoni, L.E., Cha, C., Camci-Unal, G., Dokmeci, M.R., Peppas, N.A., and Khademhosseini, A., 25th anniversary article: Rational design and applications of hydrogels in regenerative medicine. *Adv Mater*, 2014. 26(1): p. 85-124.
- Aouadi, M., Tesz, G.J., Nicoloro, S.M., Wang, M., Chouinard, M., Soto, E., Ostroff, G.R., and Czech, M.P., Orally delivered siRNA targeting macrophage map4k4 suppresses systemic inflammation. *Nature*, 2009. 458(7242): p. 1180-1184.
- Atkinson, H. and Chalmers, R., Delivering the goods: Viral and non-viral gene therapy systems and the inherent limits on cargo DNA and inteRNAI sequences. *Genetica*, 2010. 138(5): p. 485-498.
- Bajpai, A.K., Shukla, S.K., Bhanu, S., and Kankane, S., Responsive polymers in controlled drug delivery. *Prog Polym Sci*, 2008. 33(11): p. 1088-1118.

- Ballarín-González, B., Dagnaes-Hansen, F., Fenton, R.A., Gao, S., Hein, S., Dong, M., Kjems, J., and Howard, K.A., Protection and systemic translocation of siRNA following oral administration of chitosan/siRNA nanoparticles. *Mol Ther Nucleic Acids*, 2013. 2(3): p. e76.
- Barker, N., van de Wetering, M., and Clevers, H., The intestinal stem cell. *Gene Dev*, 2008. 22(14): p. 1856-1864.
- Barrow, L., Spiller, R.C., and Wilson, C.G., Pathological influences on colonic motility: Implications for drug delivery. *Adv Drug Deliver Rev*, 1991. 7: p. 201-218.
- Bartlett, D.W., Insights into the kinetics of siRNA-mediated gene silencing from live-cell and live-animal bioluminescent imaging. *Nucleic Acids Res*, 2006. 34(1): p. 322-333.
- Bhavsar, M.D. and Amiji, M.M., Development of novel biodegradable polymeric nanoparticles-in-microsphere formulation for local plasmid DNA delivery in the gastrointestinal tract. *AAPS PharmSciTech*, 2008. 9(1): p. 288-294.
- Bhavsar, M.D., Tiwari, S.B., and Amiji, M.M., Formulation optimization for the nanoparticles-in-microsphere hybrid oral delivery system using factorial design. *J Controlled Release*, 2006. 110(2): p. 422-430.
- Bianco, G. and Gehlen, M.H., Synthesis of poly(n-vinyl-2-pyrrolidone) and copolymers with methacrylic acid initiated by the photo-fenton reaction. *J Photochem Photobiol A*, 2002. 149: p. 115-119.
- Biju, V., Anas, A., Akita, H., Shibu, E.S., Itoh, T., Harashima, H., and Ishikawa, M., Fret from quantum dots to photodecompose undesired acceptors and report the condensation and decondensation of plasmid DNA. *ACS Nano*, 2012. 6: p. 3776-3788.
- Blanchette, J., Kavimandan, N., and Peppas, N., Principles of transmucosal delivery of therapeutic agents. *Biomed Pharmacother*, 2004. 58(3): p. 142-151.

- Blanchette, J. and Peppas, N.A., Oral chemotherapeutic delivery: Design and cellular response. *Ann Biomed Eng*, 2005. 33(2): p. 142-149.
- Bohlen, P., Stein, S., Dairman, W., and Udenfriend, S., Fluorometric assay of proteins in the nanogram range. *Archives of Biochemistry and Biophysics*, 1973. 155: p. 213-220.
- Boirivant, M. and Cossu, A., Inflammatory bowel disease. *Oral Dis*, 2012. 18(1): p. 1-15.
- Bouchie, A., Companies in footrace to deliver RNAi. *Nat Biotechnol*, 2012. 30(12): p. 1154-1157.
- BOUSSIF, O., LEZOUALC'H, F., ZANTA, M.A., MERGNY, M.D., SCHERMAN, D., DEMENEIX, B., and BEHR, J.-P., A versatile vector for gene and oligonucleotide transfer into cells in culture and in vivo: Polyethylenimine. *P Natl Acad Sci USA*, 1995. 92: p. 7297-7301.
- Braun, G.B., Pallaoro, A., Wu, G., Missirlis, D., Zasadzinski, J.A., Tirrell, M., and Reigh, N.O., Laser-activated gene silencing via gold nanoshell-siRNA conjugates. *ACS Nano*, 2009. 3: p. 2007-2015.
- Caldorera-Moore, M. and Peppas, N.A., Micro- and nanotechnologies for intelligent and responsive biomaterial-based medical systems. *Adv Drug Deliver Rev*, 2009. 61(15): p. 1391-1401.
- Caldorera-Moore, M.E., Liechty, W.B., and Peppas, N.A., Responsive theranostic systems: Integration of diagnostic imaging agents and responsive controlled release drug delivery carriers. *Acc. Chem. Res.*, 2011. 44: p. 1061-1070.
- Carr, D.A., Gomez-Burgaz, M., Boudes, M.C., and Peppas, D.N.A., Complexation hydrogels for the oral delivery of growth hormone and salmon calcitonin. *Ind Eng Chem Res*, 2010. 49: p. 11991-11995.
- Carr, D.A. and Peppas, N.A., Molecular structure of physiologically-responsive hydrogels controls diffusive behavior. *Macromol Biosci*, 2009. 9: p. 497-505.

- Carr, D.A. and Peppas, N.A., Assessment of poly(methacrylic acid-co-n-vinyl pyrrolidone) as a carrier for the oral delivery of therapeutic proteins using caco-2 and ht29-mtx cell lines. *J Biomed Mater Res A*, 2009. 92A: p. 504-512.
- Casadei, M.A., Pitarresi, G., Calabrese, R., Paolicelli, P., and Giammona, G., Biodegradable and ph-sensitive hydrogels for potential colon-specific drug delivery: Characterization and in vitro release studies. *Biomacromolecules*, 2008. 9: p. 43-49.
- Chapel, J.P. and Berret, J.F., Versatile electrostatic assembly of nanoparticles and polyelectrolytes: Coating, clustering and layer-by-layer processes. *Curr Opin Colloid Interface Sci*, 2012. 17(2): p. 97-105.
- Chen, A.A., Derfus, A.M., Khetani, S.R., and Bhatia, S.N., Quantum dots to monitor RNAi delivery and improve gene silencing. *Nucleic Acids Res.*, 2005. 33(22): p. e190-e190.
- Cheng, R., Meng, F., Deng, C., Klok, H.-A., and Zhong, Z., Dual and multi-stimuli responsive polymeric nanoparticles for programmed site-specific drug delivery. *Biomaterials*, 2013. 34(14): p. 3647-3657.
- Cheng, Y., Nada, A.A., Valmikinathan, C.M., Lee, P., Liang, D., Yu, X., and Kumbar, S.G., In situ gelling polysaccharide-based hydrogel for cell and drug delivery in tissue engineering. *J Appl Polym Sci*, 2014. 131: p. 39934-39945.
- Chern, C.-S., Principles and applications of emulsion polymerization. 2008, Hoboken, NJ: John Wiley & Sons, Inc.
- Clinicaltrials.Gov. 2012.
- Colombo, P., Conte, U., Gazzaniga, A., Maggi, L., Sangalli, M.E., Peppas, N.A., and Manna, A.L., Drug release modulation by physical restrictions of matrix swelling. *Int J Pharm*, 1990. 63: p. 43-48.

- Cone, R.A., Barrier properties of mucus. *Adv Drug Deliver Rev*, 2009. 61(2): p. 75-85.
- Cummings, J.H. and Macfarlane, G.T., The control and consequences of bacterial fermentation in the human colon. *J Appl Bacteriol*, 1991. 70: p. 443-459.
- Davis, S.S., Hardy, J.G., and Fara, J.W., Transit of pharmaceutical dosage forms through the small intestine. *Gut*, 1986. 27: p. 886-892.
- Derfus, A.M., Chen, A.A., Min, D., Ruoslahti, E., and Bhatia, S.N., Targeted quantum dot conjugates for siRNA delivery. *Bioconjugate Chem.*, 2007. 18: p. 1391-1396.
- Deshpande, A.A., Rhodes, C.T., Shah, N.H., and Malick, A.W., Controlled-release drug delivery systems for prolonged gastric residence: An overview. *Drug Dev Ind Pharm*, 1996. 22: p. 531-539.
- Dijk-Wolthuis, W.N.E.v., Franssen, O., Talsma, H., Steenbergen, M.J.v., Bosch, J.J.K.-v.d., and Hennink, W.E., Synthesis, characterization, and polymerization of glycidyl methacrylate derivatized dextran. *Macromolecules*, 1995. 28: p. 6317-6322.
- Dijk-Wolthuis, W.N.E.v., Franssen, O., Talsma, H., Steenbergen, M.J.v., Bosch, J.J.K.-v.d., and Hennink, W.E., Degradation and release behavior of dextran-based hydrogels. *Macromolecules*, 1997. 30: p. 4639-4645.
- Döring, A., Birnbaum, W., and Kuckling, D., Responsive hydrogels – structurally and dimensionally optimized smart frameworks for applications in catalysis, micro-system technology and material science. *Chem Soc Rev*, 2013. 42(17): p. 7391.
- Dorsett, Y. and Tuschl, T., SiRNAs: Applications in functional genomics and potential as therapeutics. *Nat Rev Drug Discovery*, 2004. 3(4): p. 318-329.
- Dressman, J.B., Berardi, R.R., Dermentzoglou, L.C., Russell, T.L., Schmaltz, S.P., Barnett, J.L., and Jarvenpaa, K.M., Upper gastrointestinal pH in young, healthy man and women. *Pharm Res*, 1990. 7: p. 756-761.

- Duan, H. and Nie, S., Cell-penetrating quantum dots based on multivalent and endosome-disrupting surface coatings. *J. Am. Chem. Soc.*, 2007. 129: p. 3333-3338.
- Edlund, U. and Albertsson, A.-C., Degradable polymer microspheres for controlled drug delivery. *Adv Polym Sci*, 2002. 157: p. 67-112.
- Egami, M., Haraguchi, Y., Shimizu, T., Yamato, M., and Okano, T., Latest status of the clinical and industrial applications of cell sheet engineering and regenerative medicine. *Archives of Pharmacal Research*, 2013. 37(1): p. 96-106.
- Elbashir, S.M., Harborth, J., Lendeckel, W., Yalcin, A., Weber, K., and Tuschl, T., Duplexes of 21-nucleotide RNAs mediate RNA interference in cultured mammalian cells. *Nature* 2001. 411: p. 494-498.
- Ensign, L.M., Cone, R., and Hanes, J., Oral drug delivery with polymeric nanoparticles: The gastrointestinal mucus barriers. *Adv Drug Deliver Rev*, 2012. 64(6): p. 557-570.
- Evans, K.E. and Sanders, D.S., Celiac disease. *Gastroenterol Clin N*, 2012. 41(3): p. 639-650.
- Fasano, A. and Catassi, C., Current approaches to diagnosis and treatment of celiac disease: An evolving spectrum. *Gastroenterology*, 2001. 120(3): p. 636-651.
- Fattal, E. and Bochot, A., State of the art and perspectives for the delivery of antisense oligonucleotides and siRNA by polymeric nanocarriers. *Int. J. Pharm.*, 2008. 364(2): p. 237-248.
- Fire, A., Xu, S.Q., Montgomery, M.K., Kostas, S.A., Driver, S.E., and Mello, C.C., Potent and specific genetic interference by double-stranded RNA in *caenorhabditis elegans*. *Letters to Nature*, 1998. 391: p. 806-811.
- Firestone, B.A. and Siegel, R.A., Kinetics and mechanisms of water sorption in hydrophobic, ionizable copolymer gels. *J Appl Polym Sci*, 1991. 43(5): p. 901-914.

- Fischer, D., Li, Y., Ahlemeyer, B., Krieglstein, J., and Kissel, T., In vitro cytotoxicity testing of polycations: Influence of polymer structure on cell viability and hemolysis. *Biomaterials*, 2003. 24: p. 1121-1131.
- Fisher, O.Z., Kim, T., Dietz, S.R., and Peppas, N.A., Enhanced core hydrophobicity, functionalization and cell penetration of polybasic nanomatrices. *Pharm Res*, 2009. 26(1): p. 51-60.
- Fisher, O.Z. and Peppas, N.A., Polybasic nanomatrices prepared by uv-initiated photopolymerization. *Macromolecules*, 2009. 42(9): p. 3391-3398.
- Fleige, E., Quadir, M.A., and Haag, R., Stimuli-responsive polymeric nanocarriers for the controlled transport of active compounds: Concepts and applications. *Adv Drug Deliver Rev*, 2012. 64(9): p. 866-884.
- Forbes, D.C., Creixell, M., Frizzell, H., and Peppas, N.A., Polycationic nanoparticles synthesized using ARGET ATRP for drug delivery. *Eur J Pharm Biopharm*, 2013. 84(3): p. 472-478.
- Forbes, D.C. and Peppas, N.A., Oral delivery of small RNA and DNA. *J. Controlled Release*, 2012. 162(2): p. 438-445.
- Forbes, D.C. and Peppas, N.A., Differences in molecular structure in cross-linked polycationic nanoparticles synthesized using ARGET ATRP or uv-initiated polymerization. *Polym*, 2013. 54(17): p. 4486-4492.
- Forbes, D.C. and Peppas, N.A., Polycationic nanoparticles for siRNA delivery: Comparing ARGET ATRP and uv-initiated formulations. *ACS Nano*, 2014. 8: p. 2908-2917.
- Forbes, D.C. and Peppas, N.A., Polymeric nanocarriers for siRNA delivery to murine macrophages. *Macromol Biosci*, 2014. 14(8): p. 1096-1105.

- Foss, A.C., Goto, T., Morishita, M., and Peppas, N.A., Development of acrylic-based copolymers for oral insulin delivery. *Eur J Pharm Biopharm*, 2004. 57(2): p. 163-169.
- Friend, D.R., New oral delivery systems for treatment of inflammatory bowel disease. *Adv Drug Deliver Rev*, 2005. 57(2): p. 247-265.
- Galaev, I.Y. and Mattiasson, B., 'Smart' polymers and what they could do in biotechnology and medicine. *Trends Biotechnol*, 1999. 17: p. 335-340.
- Gao, T., Ye, Q., Pei, X., Xia, Y., and Zhou, F., Grafting polymer brushes on graphene oxide for controlling surface charge states and templated synthesis of metal nanoparticles. *J Appl Polym Sci*, 2013. 127(4): p. 3074-3083.
- Gao, X., He, C., Xiao, C., Zhuang, X., and Chen, X., Biodegradable pH-responsive polyacrylic acid derivative hydrogels with tunable swelling behavior for oral delivery of insulin. *Polym*, 2013. 54(7): p. 1786-1793.
- Gecse, K., Roka, R., Ferrier, L., Leveque, M., Eutamene, H., Cartier, C., Ait-Belgnaoui, A., Rosztoczy, A., Izbeki, F., Fioramonti, J., Wittmann, T., and Bueno, L., Increased faecal serine protease activity in diarrhoeic ibs patients: A colonic luminal factor impairing colonic permeability and sensitivity. *Gut*, 2008. 57(5): p. 591-599.
- GeRNAndt, J. and Hansson, P., Core-shell separation of a hydrogel in a large solution of proteins. *Soft Matter*, 2012. 8(42): p. 10905.
- Ghosh, P.B. and Whitehouse, M.W., 7-chloro-4-nitrobenzo-2-oxa-1,3-diazole: A new fluorogenic reagent for amino acids and other amines. *Biochem. J.*, 1968. 108: p. 155.
- Gil, E. and Hudson, S., Stimuli-responsive polymers and their bioconjugates. *Prog Polym Sci*, 2004. 29(12): p. 1173-1222.

- Gitlin, L., Karelsky, S., and Andino, R., Short interfering RNA confers intracellular antiviral immunity in human cells. *Nature*, 2002. 418: p. 430-434.
- Glangchai, L.C., Caldorera-Moore, M., Shi, L., and Roy, K., Nanoimprint lithography based fabrication of shape-specific, enzymatically-triggered smart nanoparticles. *J Controlled Release*, 2008. 125(3): p. 263-272.
- Gran, M.L., Metal-polymer nanoparticulate systems for exteRNAlly-controlled delivery, in *Chemical Engineering*. 2010, The University of Texas at Austin: Austin.
- Griffin, W.C., Calculation of hlb values of non-ionic surfactants. *JouRNAl of the Society of Cosmestic Chemists*, 1954. 5: p. 249-256.
- Gu, Z., Dang, T.T., Ma, M., Tang, B.C., Cheng, H., Jiang, S., Dong, Y., Zhang, Y., and Anderson, D.G., Glucose-responsive microgels integrated with enzyme nanocapsules for closed-loop insulin delivery. *ACS Nano*, 2013. 7: p. 6758-6766.
- Guo, D.-S., Wang, K., Wang, Y.-X., and Liu, Y., Cholinesterase-responsive supramolecular vesicle. *J Am Chem Soc*, 2012. 134(24): p. 10244-10250.
- Gyenes, T., Torma, V., Gyarmati, B., and Zrínyi, M., Synthesis and swelling properties of novel ph-sensitive poly(aspartic acid) gels. *Acta Biomater*, 2008. 4(3): p. 733-744.
- Haeberlin, B. and Friend, D.R., Anatomy and physiology of the gastrointestinal tract: Implications for colonic drug delivery, in *Oral colon-specific drug delivery*, D.R. Friend, Editor. 1992, CRC Press, Inc.: Boca Raton, FL. p. 1-43.
- Han, L.-H., Lai, J.H., Yu, S., and Yang, F., Dynamic tissue engineering scaffolds with stimuli-responsive macroporosity formation. *Biomaterials*, 2013. 34(17): p. 4251-4258.
- Hao, L., Patel, P.C., Alhasan, A.H., Giljohann, D.A., and Mirkin, C.A., Nucleic acid-gold nanoparticle conjugates as mimics of microRNA. *Small*, 2011. 7(22): p. 3158-3162.

- He, C., Yin, L., Tang, C., and Yin, C., Multifunctional polymeric nanoparticles for oral delivery of TNF- α siRNA to macrophages. *Biomaterials*, 2013. 34(11): p. 2843-2854.
- He, C., Yin, L., Tang, C., and Yin, C., Trimethyl chitosan-cysteine nanoparticles for systemic delivery of TNF- α siRNA via oral and intraperitoneal routes. *Pharm Res*, 2013. 30(10): p. 2596-2606.
- Hermanson, G.T., *Bioconjugate techniques*. 1996, San Diego, CA: Academic Press, Inc.
- Hickerson, R.P., Vlassov, A.V., Wang, Q., Leake, D., Ilves, H., Gonzalez-Gonzalez, E., Contag, C.H., Johnston, B.H., and Kaspar, R.L., Stability study of unmodified siRNA and relevance to clinical use. *Oligonucleotides*, 2008. 18: p. 345-354.
- Ho, B.-C., Lee, Y.-D., and Chin, W.-K., Thermal degradation of polymethacrylic acid. *J Polym Sci, Part A: Polym. Chem*, 1992. 30: p. 2389-2397.
- Ho, Y.-P., Chen, H.H., Leong, K.W., and Wang, T.-H., Evaluating the intracellular stability and unpacking of DNA nanocomplexes by quantum dots-fret. *J. Controlled Release*, 2006. 116(1): p. 83-89.
- Hoffman, A.S., Environmentally sensitive polymers and hydrogels. *MRS Bulletin*, 1991. 16: p. 42-46.
- Hoffman, A.S., Hydrogels for biomedical applications. *Adv Drug Deliver Rev*, 2002. 43: p. 3-12.
- Hoffman, A.S., Stimuli-responsive polymers: Biomedical applications and challenges for clinical translation. *Adv Drug Deliver Rev*, 2013. 65(1): p. 10-16.
- Holzapfel, B.M., Reichert, J.C., Schantz, J.-T., Gbureck, U., Rackwitz, L., Nöth, U., Jakob, F., Rudert, M., Groll, J., and Hutmacher, D.W., How smart do biomaterials need to be? A translational science and clinical point of view. *Adv Drug Deliver Rev*, 2013. 65(4): p. 581-603.

- Houghton, S.E. and McCarthy, C.F., The isolation, partial characterization, and subfractionation of human intestinal brush borders. *Gut*, 1973. 14: p. 529-534.
- Hovgaard, L. and Brondsted, H., Dextran hydrogels for colon-specific drug delivery. *J Controlled Release*, 1995. 36: p. 159-166.
- Huschka, R., Barhoumi, A., Liu, Q., Roth, J.A., Ji, L., and Halas, N.J., Gene silencing by gold nanoshell-mediated delivery and laser-triggered release of antisense oligonucleotide and siRNA. *ACS Nano*, 2012. 6: p. 7681-7691.
- Huschka, R., Neumann, O., Barhoumi, A., and Halas, N.J., Visualizing light-triggered release of molecules inside living cells. *Nano Lett.*, 2010. 10(10): p. 4117-4122.
- Hutvagner, G., A microRNA in a multiple-turnover RNAi enzyme complex. *Science*, 2002. 297(5589): p. 2056-2060.
- Jeong, B. and Gutowska, A., Lessons from nature: Stimuli-responsive polymers and their biomedical applications. *Trends Biotechnol*, 2002. 20(7): p. 305-311.
- Jeong, S., Choi, S.Y., Park, J., Seo, J.-H., Park, J., Cho, K., Joo, S.-W., and Lee, S.Y., Low-toxicity chitosan gold nanoparticles for small hairpin RNA delivery in human lung adenocarcinoma cells. *J. Mater. Chem.*, 2011. 21(36): p. 13853.
- Jiang, H.L. and Zhu, K.J., Comparison of poly(aspartic acid) hydrogel and poly(aspartic acid)/gelatin complex for entrapment and pH-sensitive release of protein drugs. *J Appl Polym Sci*, 2006. 99(5): p. 2320-2329.
- Jung, J., Solanki, A., Memoli, K.A., Kamei, K.-i., Kim, H., Drahl, M.A., Williams, L.J., Tseng, H.-R., and Lee, K., Selective inhibition of human brain tumor cells through multifunctional quantum-dot-based siRNA delivery. *Angew. Chem., Int. Ed. Engl.*, 2010. 49(1): p. 103-107.

- Kamei, N., Morishita, M., Chiba, H., Kavimandan, N.J., Peppas, N.A., and Takayama, K., Complexation hydrogels for intestinal delivery of interferon β and calcitonin. *J Controlled Release*, 2009. 134(2): p. 98-102.
- Kaplan, J.G. and Bona, C., Proteases as mitogens: The effect of trypsin and pronase on mouse and human lymphocytes. *Experimental Cell Research*, 1974. 88: p. 388-394.
- Kavimandan, N., Losi, E., and Peppas, N., Novel delivery system based on complexation hydrogels as delivery vehicles for insulin–transferrin conjugates. *Biomaterials*, 2006. 27(20): p. 3846-3854.
- Kayitmazer, A.B., Seeman, D., Minsky, B.B., Dubin, P.L., and Xu, Y., Protein–polyelectrolyte interactions. *Soft Matter*, 2013. 9(9): p. 2553.
- Khalil, I.A., Uptake pathways and subsequent intracellular trafficking in nonviral gene delivery. *Pharmacological Reviews*, 2006. 58(1): p. 32-45.
- Khan, M.Z.I., Prebeg, Z., and Kurjakovic, N., A pH-dependent colon targeted oral delivery system using methacrylic acid copolymers i. Manipulation of drug release using eudragit 1100-55 and eudragit s100 combinations. *J Controlled Release*, 1999. 58: p. 215-222.
- Kharkar, P.M., Kiick, K.L., and Kloxin, A.M., Designing degradable hydrogels for orthogonal control of cell microenvironments. *Chem Soc Rev*, 2013. 42(17): p. 7335.
- Kim, E.Y., Schulz, R., Swantek, P., Kunstman, K., Malim, M.H., and Wolinsky, S.M., Gold nanoparticle-mediated gene delivery induces widespread changes in the expression of innate immunity genes. *Gene Ther.*, 2011. 19(3): p. 347-353.
- Kim, S. and Healy, K.E., Synthesis of injectable poly(n-isopropylacrylamide-co-acrylic acid) hydrogels with proteolytically degradable crosslinks. *Biomacromolecules*, 2003. 4: p. 1214-1223.

- Klein, S., Zolk, O., Fromm, M.F., Schrödl, F., Neuhuber, W., and Krysch, C., Functionalized silicon quantum dots tailored for targeted siRNA delivery. *Biochem. Biophys. Res. Commun.*, 2009. 387(1): p. 164-168.
- Klinger, D. and Landfester, K., Photo-sensitive pmma microgels: Light-triggered swelling and degradation. *Soft Matter*, 2011. 7: p. 1426-1440.
- Klinger, D. and Landfester, K., Enzymatic- and light-degradable hybrid nanogels: Crosslinking of polyacrylamide with acrylate-functionalized dextrans containing photocleavable linkers. *J Polym Sci, Part A: Polym. Chem*, 2012. 50(6): p. 1062-1075.
- Knipe, J.M., Chen, F., and Peppas, N.A., Multiresponsive polyanionic microgels with inverse pH responsive behavior by encapsulation of polycationic nanogels. *J Appl Polym Sci*, 2014.
- Knipe, J.M., Peters, J.T., and Peppas, N.A., Theranostic agents for intracellular gene delivery with spatiotemporal imaging. *Nano Today*, 2013. 8(1): p. 21-38.
- Koetting, M.C. and Peppas, N.A., pH-responsive poly(itaconic acid-co-N-vinylpyrrolidone) hydrogels with reduced ionic strength loading solutions offer improved oral delivery potential for high isoelectric point-exhibiting therapeutic proteins. *Int J Pharm*, 2014. 471(1-2): p. 83-91.
- Kolev, T., Solid-state IR-1D spectroscopic and theoretical analysis of arginine-containing peptides. *Biopolymers*, 2006. 83: p. 39-45.
- Kost, J. and Langer, R., Responsive polymeric delivery systems. *Adv Drug Deliver Rev*, 2012. 64: p. 327-341.
- Kriegel, C. and Amiji, M., Oral TNF- α gene silencing using a polymeric microsphere-based delivery system for the treatment of inflammatory bowel disease. *J Controlled Release*, 2011. 150(1): p. 77-86.

- Kriegel, C. and Amiji, M.M., Dual TNF- α /cyclin d1 gene silencing with an oral polymeric microparticle system as a novel strategy for the treatment of inflammatory bowel disease. *Clin Trans Gastroenterol*, 2011. 2(3): p. e2.
- Kriegel, C., Attarwala, H., and Amiji, M., Multi-compartmental oral delivery systems for nucleic acid therapy in the gastrointestinal tract. *Adv Drug Deliver Rev*, 2013. 65(6): p. 891-901.
- Kriwet, B., Walter, E., and Kissel, T., Synthesis of bioadhesive poly(acrylic acid) nano- and microparticles using an inverse emulsion polymerization method for the entrapment of hydrophilic drug candidates. *J Controlled Release*, 1998. 56: p. 149-158.
- Kurisawa, M. and Yui, N., Dual-stimuli-responsive drug release from interpenetrating polymer network-structured hydrogels of gelatin and dextran. *J Controlled Release*, 1998. 54: p. 191-200.
- Laroui, H., Theiss, A.L., Yan, Y., Dalmasso, G., Nguyen, H.T.T., Sitaraman, S.V., and Merlin, D., Functional TNF α gene silencing mediated by polyethyleneimine/TNF α siRNA nanocomplexes in inflamed colon. *Biomaterials*, 2011. 32(4): p. 1218-1228.
- Lechner, M.D., Influence of mie scattering on nanoparticles with different particle sizes and shapes: Photometry and analytical ultracentrifugation with absorption optics. *JouRNAl of the Serbian Chemical Society*, 2005. 70: p. 361-369.
- Lee, H., Kim, I.-K., and Park, T.G., Intracellular trafficking and unpacking of siRNA/quantum dot-pei complexes modified with and without cell penetrating peptide: Confocal and flow cytometric fret analysis. *Bioconjugate Chem.*, 2010. 21: p. 289-295.
- Lee, J.Y., Painter, P.C., and Coleman, M.M., Hydrogen bonding in polymer blends. 4. Blends involving polymers containing methacrylic acid and vinylpyridine groups. *Macromolecules*, 1988. 21: p. 954-960.

- Lee, M.-Y., Park, S.-J., Park, K., Kim, K.S., Lee, H., and Hahn, S.K., Target-specific gene silencing of layer-by-layer assembled gold-cysteamine/siRNA/pe/-ha nanocomplex. *ACS Nano*, 2011. 5: p. 6138-6147.
- Lee, S.C., Kwon, I.K., and Park, K., Hydrogels for delivery of bioactive agents: A historical perspective. *Adv Drug Deliver Rev*, 2013. 65(1): p. 17-20.
- Lehr, C.-M., Poelma, F.G.J., Junginger, H.E., and Tukker, J.J., An estimate of turnover time of intestinal mucus gel layer in the rat in situ loop. *Int J Pharm*, 1991. 70: p. 235-240.
- Lesuffleur, T., Porchet, N., Aubert, J.-P., Swallow, D., Gum, J.R., S.Kim, Y., Real, F.X., and Zweibaum, A., Differential expression of the human mucin genes *muc1* to *muc5* in relation to growth and differentiation of different mucus-secreting ht-29 cell populations. *J Cell Sci*, 1993. 106: p. 771-783.
- Li, J.-M., Zhao, M.-X., Su, H., Wang, Y.-Y., Tan, C.-P., Ji, L.-N., and Mao, Z.-W., Multifunctional quantum-dot-based siRNA delivery for hpv18 e6 gene silence and intracellular imaging. *Biomaterials*, 2011. 32(31): p. 7978-7987.
- Li, S., Liu, Z., Ji, F., Xiao, Z., Wang, M., Peng, Y., Zhang, Y., Liu, L., Liang, Z., and Li, F., Delivery of quantum dot-siRNA nanoplexes in sk-n-sh cells for bace1 gene silencing and intracellular imaging. *Mol. Ther. Nucleic Acids*, 2012. 1(4): p. e20.
- Li, Y., Duan, X., Jing, L., Yang, C., Qiao, R., and Gao, M., Quantum dot-antisense oligonucleotide conjugates for multifunctional gene transfection, mRNA regulation, and tracking of biological processes. *Biomaterials*, 2011. 32(7): p. 1923-1931.
- Liang, Z., Liu, Y., Li, X., Wu, Q., Yu, J., Luo, S., Lai, L., and Liu, S., Surface-modified gold nanoshells for enhanced cellular uptake. *J Biomed Mater Res A*, 2011. 98A(4): p. 479-487.
- Liechty, W.B., Kryscio, D.R., Slaughter, B.V., and Peppas, N.A., Polymers for drug delivery systems. *Annu Rev Chem Biomol Eng*, 2010. 1(1): p. 149-173.

- Liechty, W.B., Scheuerle, R.L., and Peppas, N.A., Tunable, responsive nanogels containing t-butyl methacrylate and 2-(t-butylamino)ethyl methacrylate. *Polym*, 2013. 54(15): p. 3784-3795.
- Liu, J., Argonaute2 is the catalytic engine of mammalian RNAi. *Science*, 2004. 305(5689): p. 1437-1441.
- Liu, J., Chen, G., Guo, M., and Jiang, M., Dual stimuli-responsive supramolecular hydrogel based on hybrid inclusion complex (hic). *Macromolecules*, 2010. 43(19): p. 8086-8093.
- Loftus, E.V., Kane, S.V., and Bjorkman, D., Short-term adverse effects of 5-aminosalicylic acid agents in the treatment of ulcerative colitis. *Aliment Pharm Therap*, 2004. 19(2): p. 179-189.
- Loría-Bastarrachea, M.I., Herrera-Kao, W., Cauich-Rodríguez, J.V., Cervantes-Uc, J.M., Vázquez-Torres, H., and Ávila-Ortega, A., A tg/ftir study on the thermal degradation of poly(vinyl pyrrolidone). *J Therm Anal Calorim*, 2010. 104(2): p. 737-742.
- Lowman, A.M., Morishita, M., Kajita, M., Nagai, T., and Peppas, D.N.A., Oral delivery of insulin using ph-responsive complexation gels. *J Pharm Sci*, 1999. 88: p. 933-937.
- Lowman, A.M. and Peppas, N.A., Analysis of the complexation/decomplexation phenomena in graft copolymer networks. *Macromolecules*, 1997. 30: p. 4959-4965.
- Lv, H., Zhang, S., Wang, B., Cui, S., and Yan, J., Toxicity of cationic lipids and cationic polymers in gene delivery. *J Controlled Release*, 2006. 114(1): p. 100-109.
- Lv, L.-P., Landfester, K., and Crespy, D., Stimuli-selective delivery of two payloads from dual responsive nanocontainers. *Chem Mater*, 2014. 26(11): p. 3351-3353.

- MacDonald, T.T. and Pender, S.L.F., Proteolytic enzymes in inflammatory bowel disease. *Inflamm Bowel Dis*, 1998. 4: p. 157-164.
- Marambio, O.G., Pizarro, G.d.C., Jeria-Orell, M., and Geckeler, K.E., Swelling behavior and metal ion retention from aqueous solution of hydrogels based onn-1-vinyl-2-pyrrolidone andn-hydroxymethylacrylamide. *J Appl Polym Sci*, 2009. 113(3): p. 1792-1802.
- Martinez, J., Patkaniowska, A., Urlaub, H., Luhrmann, R., and Tuschl, T., Single-stranded antisense siRNAs guide target RNA cleavage in RNAi. *Cell*, 2002. 110: p. 563-574.
- Martins, A.M., Alves, C.M., Kurtis Kasper, F., Mikos, A.G., and Reis, R.L., Responsive and in situ-forming chitosan scaffolds for bone tissue engineering applications: An overview of the last decade. *J Mater Chem*, 2010. 20(9): p. 1638.
- McCaffrey, A.P., Meuse, L., Pham, T.-T.T., Conklin, D.S., Hannon, G.J., and Kay, M.A., Rna interference in adult mice. *Nature*, 2002. 418: p. 38-39.
- McLeod, A.D., Dextran prodrugs for colon-specific drug delivery, in *Oral colon-specific drug delivery*, D.R. Friend, Editor. 1992, CRC Press, Inc.: Boca Raton, FL. p. 213-231.
- Merdan, T., Kopecek, J., and Kissel, T., Prospects for cationic polymers in gene and oligonucleotide therapy against cancer. *Adv Drug Deliver Rev*, 2002. 54: p. 715-758.
- Moran, N., First gene therapy approved. *Nat Biotechnol*, 2012. 30(12): p. 1153-1153.
- Moret, I.s., Peris, J.E., Guillem, V.M., Benet, M., Revert, F., Dasi, F., Crespo, A., and Alino, S.F., Stability of pei–DNA and dotap–DNA complexes: Effect of alkaline ph, heparin and serum. *J Controlled Release*, 2001. 76(169-181).
- Morishita, M., Goto, T., Nakamura, K., Lowman, A.M., Takayama, K., and Peppas, N.A., Novel oral insulin delivery systems based on complexation polymer

- hydrogels: Single and multiple administration studies in type 1 and 2 diabetic rats. *J Controlled Release*, 2006. 110(3): p. 587-594.
- Morishita, M., Goto, T., Peppas, N.A., Joseph, J.I., Torjman, M.C., Munsick, C., Nakamura, K., Yamagata, T., Takayama, K., and Lowman, A.M., Mucosal insulin delivery systems based on complexation polymer hydrogels: Effect of particle size on insulin enteral absorption. *J Controlled Release*, 2004. 97(1): p. 115-124.
- Motornov, M., Roiter, Y., Tokarev, I., and Minko, S., Stimuli-responsive nanoparticles, nanogels and capsules for integrated multifunctional intelligent systems. *Prog Polym Sci*, 2010. 35(1-2): p. 174-211.
- Mrsny, R.J., Drug absorption in the colon: A critical review, in *Oral colon-specific drug delivery*, D.R. Friend, Editor. 1992, CRC Press, Inc.: Boca Raton, FL. p. 45-84.
- Muzzarelli, R.A.A., Greco, F., Busilacchi, A., Sollazzo, V., and Gigante, A., Chitosan, hyaluronan and chondroitin sulfate in tissue engineering for cartilage regeneration: A review. *Carbohydrate Polymers*, 2012. 89(3): p. 723-739.
- Nakamura, K., Murray, R.J., Joseph, J.I., Peppas, N.A., Morishita, M., and Lowman, A.M., Oral insulin delivery using p(maa-g-eg) hydrogels: Effects of network morphology on insulin delivery characteristics. *J Controlled Release*, 2004. 95(3): p. 589-599.
- Ng, C.-T., Dheen, S.T., Yip, W.-C.G., Ong, C.-N., Bay, B.-H., and Lanry Yung, L.-Y., The induction of epigenetic regulation of prosl gene in lung fibroblasts by gold nanoparticles and implications for potential lung injury. *Biomaterials*, 2011. 32(30): p. 7609-7615.
- Nguyen, L.H., Kudva, A.K., Guckert, N.L., Linse, K.D., and Roy, K., Unique biomaterial compositions direct bone marrow stem cells into specific chondrocytic phenotypes corresponding to the various zones of articular cartilage. *Biomaterials*, 2011. 32(5): p. 1327-1338.
- Niidade, T. and Huang, L., Gene therapy progress and prospects: Nonviral vectors. *Gene Ther.*, 2002. 9(24): p. 1647-1652.

- Novina, C.D., Murray, M.F., Dykxhoorn, D.M., Beresford, P.J., Riess, J., Lee, S.-K., Collman, R.G., Lieberman, J., Shankar, P., and Sharp, P.A., SiRNA-directed inhibition of hiv-1 infection. *Nature Medicine*, 2002.
- Nugent, S.G., Kumar, D., Rampton, D.S., and Evans, D.F., Intestinal luminal ph in inflammatory bowel disease: Possible determinants and implications for therapy with aminosalicylates and other drugs. *Gut*, 2001. 48: p. 571-577.
- Oberle, R.L. and Amidon, G.L., The influence of variable gastric emptying and intestinal transit rates on the plasma level curve of cimetidine; an explanation for the double peak phenomenon. *J Pharmacokinet Biopharm*, 1987. 15: p. 529-544.
- Olsen, J.V., Trypsin cleaves exclusively c-terminal to arginine and lysine residues. *Mol Cell Proteomics*, 2004. 3(6): p. 608-614.
- Pace, J., Lxviii. The inactivation of trypsin by heat. *Biochemical JouRNAI*, 1930. 24: p. i3.
- Patel, P.C., Hao, L., Au Yeung, W.S., and Mirkin, C.A., Duplex end breathing determines serum stability and intracellular potency of siRNA–au nps. *Mol. Pharm.*, 2011. 8(4): p. 1285-1291.
- Patell, M.K., Enteric coated tablet and process for making. 1988, Bristol-Myers Company: United States.
- Pecot, C.V., Calin, G.A., Coleman, R.L., Lopez-Berestein, G., and Sood, A.K., Rna interference in the clinic: Challenges and future directions. *Nat Rev Cancer*, 2010. 11(1): p. 59-67.
- Pekel, N., Sahiner, N., Guven, O., and Rzaev, Z.M.O., Synthesis and characterization of n-vinylimidazole-ethyl methacrylate copolymers and determination of monomer reactivity ratios. *Eur Polym J*, 2001. 37: p. 2443-2451.

- Peppas, N.A., Hydrogels and drug delivery. *Curr Opin Colloid Interface Sci*, 1997. 2(5): p. 531-537.
- Peppas, N.A., Bures, P., Leobandung, W., and Ichikawa, H., Hydrogels in pharmaceutical formulations. *Eur J Pharm Biopharm*, 2000. 50: p. 27-46.
- Peppas, N.A. and Byrne, M.E., New biomaterials for intelligent biosensing, recognitive drug delivery and therapeutics. *Bull. Gattefossé*, 2003. 96: p. 23-25.
- Peppas, N.A., Hilt, J.Z., Khademhosseini, A., and Langer, R., Hydrogels in biology and medicine: From molecular principles to bionanotechnology. *Adv Mater*, 2006. 18(11): p. 1345-1360.
- Peppas, N.A. and Klier, J., Controlled release by using poly(methacrylic acid-g-ethylene glycol) hydrogels. *J Controlled Release*, 1991. 16: p. 203-214.
- Peppas, N.A., Wood, K.M., and Blanchette, J.O., Hydrogels for oral delivery of therapeutic proteins. *Expert Opin. Biol. Ther.*, 2004. 4: p. 1-7.
- Pérez, R.A., Won, J.-E., Knowles, J.C., and Kim, H.-W., Naturally and synthetic smart composite biomaterials for tissue regeneration. *Adv Drug Deliver Rev*, 2013. 65(4): p. 471-496.
- Pharmacopeia, T.U.S., United states pharmacopeia 29 national formulary 24, in Reagents: Test Solutions. 2006.
- Plochocka, K. and Chuang, J.-C., Inverse emulsion crosslinked polyacrylic acid of controlled ph. 1993, ISP Investments Inc.: US.
- Podolsky, D.K., Inflammatory bowel disease. *N Engl J Med*, 2002. 347: p. 417-429.
- Polacco, G., Cascone, M.G., Petarca, L., and Peretti, A., Thermal behaviour of poly(methacrylic acid)/poly(n-vinyl-2-pyrrolidone) complexes. *Eur Polym J*, 2000. 36: p. 2541-2544.

- Qi, L. and Gao, X., Quantum dot-amphipol nanocomplex for intracellular delivery of real-time imaging of siRNA. *ACS Nano*, 2008. 2: p. 1403-1410.
- Qian, J., Jiang, L., Cai, F., Wang, D., and He, S., Fluorescence-surface enhanced raman scattering co-functionalized gold nanorods as near-infrared probes for purely optical in vivo imaging. *Biomaterials*, 2011. 32(6): p. 1601-1610.
- Qiu, X.-P., Tanaka, F., and Winnik, F.M., Temperature-induced phase transition of well-defined cyclic poly(n-isopropylacrylamide)s in aqueous solution. *Macromolecules*, 2007. 40: p. 7069-7071.
- Qiu, Y. and Park, K., Environment-sensitive hydrogels for drug delivery. *Adv Drug Deliver Rev*, 2001. 53(3): p. 321-339.
- Quadir, M.A., Martin, M., and Hammond, P.T., Clickable synthetic polypeptides—routes to new highly adaptive biomaterials. *Chem Mater*, 2014. 26(1): p. 461-476.
- Rand, T.A., Biochemical identification of argonaute 2 as the sole protein required for RNA-induced silencing complex activity. *P Natl Acad Sci USA*, 2004. 101(40): p. 14385-14389.
- Rand, T.A., Petersen, S., Du, F., and Wang, X., Argonaute2 cleaves the anti-guide strand of siRNA during risc activation. *Cell*, 2005. 123(4): p. 621-629.
- Reynolds, J.L., Law, W.C., Mahajan, S.D., Aalinkeel, R., Nair, B., Sykes, D.E., Yong, K.-T., Hui, R., Prasad, P.N., and Schwartz, S.A., Nanoparticle based galectin-1 gene silencing, implications in methamphetamine regulation of hiv-1 infection in monocyte derived macrophages. *J. Neuroimmune Pharmacol.*, 2012. 7(3): p. 673-685.
- Robbins, P.D. and Ghivizzani, S.C., Viral vectors for gene therapy. *Pharmacol. Ther.*, 1998. 80: p. 35-47.

- Russell, T.L., Berardi, R.R., Barnett, J.L., Dermentzoglou, L.C., Jarvenpaa, K.M., Schmaltz, S.P., and Dressman, J.B., Upper gastrointestinal pH in seventy-nine healthy, elderly, north american men and women. *Pharm Res*, 1993. 10: p. 187-196.
- Ryther, R.C.C., Flynt, A.S., Phillips, J.A., and Patton, J.G., SiRNA therapeutics: Big potential from small RNAs. *Gene Ther*, 2004. 12(1): p. 5-11.
- Satarkar, N.S., Biswal, D., and Hilt, J.Z., Hydrogel nanocomposites: A review of applications as remote controlled biomaterials. *Soft Matter*, 2010. 6(11): p. 2364.
- Schiffelers, R.M., Woodle, M.C., and Scaria, P., Pharmaceutical prospects for RNA interference. *Pharm Res*, 2003. 21: p. 1-7.
- Schoener, C.A., Hutson, H.N., and Peppas, N.A., pH-responsive hydrogels with dispersed hydrophobic nanoparticles for the oral delivery of chemotherapeutics. *J Biomed Mater Res A*, 2013. 101A(8): p. 2229-2236.
- Schuppan, D., Current concepts of celiac disease pathogenesis. *Gastroenterology*, 2000. 119(1): p. 234-242.
- Schwert, G.W. and Takenaka, Y., A spectrophotometric determination of trypsin and chymotrypsin. *Biochimica Et Biophysica Acta*, 1955. 16: p. 570-575.
- Selvin, P.R., The renaissance of fluorescence resonance energy transfer. *Nat. Struct. Mol. Biol.*, 2000. 7: p. 730-734.
- Serra, L., Domenech, J., and Peppas, N., Design of poly(ethylene glycol)-tethered copolymers as novel mucoadhesive drug delivery systems. *Eur J Pharm Biopharm*, 2006. 63(1): p. 11-18.
- Sery, T.W. and Hehre, E.J., Degradation of dextrans by enzymes of intestinal bacteria. *J Bacteriol*, 1956. 71: p. 373-380.

- Shaheen, S.M., Akita, H., Yamashita, A., Katoono, R., Yui, N., Biju, V., Ishikawa, M., and Harashima, H., Quantitative analysis of condensation/decondensation status of pdna in the nuclear sub-domains by qd-fret. *Nucleic Acids Res.*, 2011. 39(7): p. e48-e48.
- Sharpe, L.A., Daily, A.M., Horava, S.D., and Peppas, N.A., Therapeutic applications of hydrogels in oral drug delivery. *Expert Opin Drug Deliv*, 2014. 11(6): p. 901-915.
- Shuey, D.J., McCallus, D.E., and Giordano, T., Rnai: Gene-silencing in therapeutic intervention. *Drug Discovery Today*, 2002. 7: p. 1040-1046.
- Siegel, R.A., Stimuli sensitive polymers and self regulated drug delivery systems: A very partial review. *J Controlled Release*, 2014.
- Silva, J.M., Hammond, S.M., and Hannon, G.J., Rna interference: A promising approach to antiviral therapy? *Trends Mol Med*, 2002. 8: p. 505-508.
- Simon, G.L. and Gorbach, S.L., The human intestinal microflora. *Digest Dis Sci*, 1986. 31: p. 147S-162S.
- Sinha, V.R. and Kumria, R., Polysaccharides in colon-specific drug delivery. *Int J Pharm*, 2001. 224: p. 19-38.
- Slaughter, B.V., Khurshid, S.S., Fisher, O.Z., Khademhosseini, A., and Peppas, N.A., Hydrogels in regenerative medicine. *Adv Mater*, 2009. 21(32-33): p. 3307-3329.
- Smeds, K.A. and Grinstaff, M.W., Photocrosslinkable polysaccharides for in situ hydrogel formation. *JouRNAI of Biomedical Materials Research*, 2001. 54: p. 115-121.
- Smedt, S.C.D., Demeester, J., and Hennink, W.E., Cationic polymer based gene delivery systems. *Pharm Res*, 2000. 17: p. 113-126.

- Sørensen, D.R., Leirdal, M., and Sioud, M., Gene silencing by systemic delivery of synthetic siRNAs in adult mice. *JouRNAI of Molecular Biology*, 2003. 327(4): p. 761-766.
- Soutschek, J., Akinc, A., Bramlage, B., Charisse, K., Constien, R., Donoghue, M., Elbashir, S., Geick, A., Hadwiger, P., Harborth, J., John, M., Kesavan, V., Lavine, G., Pandey, R.K., Racie, T., Rajeev, K.G., Rohl, I., Toudjarska, I., Wang, G., Wuschko, S., Bumcrot, D., Koteliensky, V., Limmer, S., Manoharan, M., and Vornlocher, H.-P., Therapeutic silencing of an endogenous gene by systemic administration of modified siRNAs. *Nature*, 2004. 432: p. 173-178.
- Squier, C.A. and Kremer, M.J., Biology of oral mucosa and esophagus. *J Natl Cancer Inst Monogr*, 2001. 29: p. 7-15.
- Stevenson, M., Therapeutic potential of RNA interference. *New England JouRNAI of Medicine*, 2004. 351: p. 1772-1777.
- Stuart, M.A.C., Huck, W.T.S., Genzer, J., Müller, M., Ober, C., Stamm, M., Sukhorukov, G.B., Szleifer, I., Tsukruk, V.V., Urban, M., Winnik, F., Zauscher, S., Luzinov, I., and Minko, S., Emerging applications of stimuli-responsive polymer materials. *Nat Mater*, 2010. 9: p. 101-113.
- Subr, V., Duncan, R., and Kopecek, J., Release of macromolecules from hydrophilic gels containing enzymatically degradable bonds. *J. Biomater. Sci. Polymer Edn*, 1990. 1: p. 261-278.
- Takeshita, F. and Ochiya, T., Therapeutic potential of RNA interference against cancer. *Cancer Science*, 2006. 97(8): p. 689-696.
- Tan, W.B., Jiang, S., and Zhang, Y., Quantum-dot based nanoparticles for targeted silencing of her2/neu gene via RNA interference. *Biomaterials*, 2007. 28(8): p. 1565-1571.
- Temtem, M., Barroso, T., Casimiro, T., Mano, J.F., and Aguiar-Ricardo, A., Dual stimuli responsive poly(n-isopropylacrylamide) coated chitosan scaffolds for controlled

- release prepared from a non residue technology. *J Supercrit Fluids*, 2012. 66: p. 398-404.
- Thelen, K., Coboeken, K., Willmann, S., Burghaus, R., Dressman, J.B., and Lippert, J., Evolution of a detailed physiological model to simulate the gastrointestinal transit and absorption process in humans, part 1: Oral solutions. *J Pharm Sci*, 2011: p. n/a-n/a.
- Thoma, K. and Bechtold, K., Enteric coated hard gelatin capsules, Capsugel, Editor. p. 1-17.
- Thornton, P.D., Mart, R.J., and Ulijn, R.V., Enzyme-responsive polymer hydrogel particles for controlled release. *Adv Mater*, 2007. 19(9): p. 1252-1256.
- Tokarev, I. and Minko, S., Stimuli-responsive porous hydrogels at interfaces for molecular filtration, separation, controlled release, and gating in capsules and membranes. *Adv Mater*, 2010. 22(31): p. 3446-3462.
- Tokareva, I., Minko, S., Fendler, J.H., and Hutter, E., Nanosensors based on responsive polymer brushes and gold nanoparticle enhanced transmission surface plasmon resonance spectroscopy. *J Am Chem Soc*, 2004. 126: p. 15950-15951.
- Torres-Lugo, M. and Peppas, N.A., Molecular design and in vitro studies of novel pH-sensitive hydrogels for the oral delivery of calcitonin. *Macromolecules*, 1999. 32: p. 6646-6651.
- Torres-Lugo, M. and Peppas, N.A., Preparation and characterization of p(maa-g-eg) nanospheres for protein delivery applications. *J Nanopart Res*, 2002. 4: p. 73-81.
- Tuesca, A., Nakamura, K., Morishita, M., Joseph, J., Peppas, N., and Lowman, A., Complexation hydrogels for oral insulin delivery: Effects of polymer dosing on in vivo efficacy. *J Pharm Sci*, 2008. 97(7): p. 2607-2618.

- Ulbrich, K., Strohalm, J., and Kopecek, J., Polymers containing enzymatically degradable bonds. Iv. Hydrophilic gels cleavable by chymotrypsin. *Biomaterials*, 1982. 3: p. 150-154.
- Unanue, E.R., Antigen-presenting function of the macrophage. *Annual Review of Immunology*, 1984. 2: p. 395-428.
- Vader, W., The hla-dq2 gene dose effect in celiac disease is directly related to the magnitude and breadth of gluten-specific t cell responses. *P Natl Acad Sci USA*, 2003. 100(21): p. 12390-12395.
- Van Der Hoff, B.M.E., Kinetics of emulsion polymerization. 1962. 34: p. 6-31.
- Vlieghe, P., Lisowski, V., Martinez, J., and Khrestchatisky, M., Synthetic therapeutic peptides: Science and market. *Drug Discovery Today*, 2010. 15(1-2): p. 40-56.
- Wanakule, P., Liu, G.W., Fleury, A.T., and Roy, K., Nano-inside-micro: Disease-responsive microgels with encapsulated nanoparticles for intracellular drug delivery to the deep lung. *J Controlled Release*, 2012. 162: p. 429-437.
- Weinbaum, S., Tarbell, J.M., and Damiano, E.R., The structure and function of the endothelial glycocalyx layer. *Annu Rev Biomed Eng*, 2007. 9(1): p. 121-167.
- Welsch, N., Becker, A.L., Dzubiella, J., and Ballauff, M., Core-shell microgels as “smart” carriers for enzymes. *Soft Matter*, 2012. 8(5): p. 1428.
- West, J.L. and Hubbell, J.A., Polymeric biomaterials with degradation sites for proteases involved in cell migration. *Macromolecules*, 1999. 32: p. 241-244.
- White, E.M., Yatvin, J., Grubbs, J.B., Bilbrey, J.A., and Locklin, J., Advances in smart materials: Stimuli-responsive hydrogel thin films. *J Polym Sci, Part B: Polym Phys*, 2013. 51(14): p. 1084-1099.

- Whitehead, K.A., Langer, R., and Anderson, D.G., Knocking down barriers: Advances in siRNA delivery. *Nat. Rev. Drug Discovery*, 2009. 8(2): p. 129-138.
- Williams, J.M., High internal phase water-in-oil emulsions: Influence of surfactants and cosurfactants on emulsion stability and foam quality. *Langmuir*, 1991. 7: p. 1370-1377.
- Wilson, D.S., Dalmasso, G., Wang, L., Sitaraman, S.V., Merlin, D., and Murthy, N., Orally delivered thioketal nanoparticles loaded with TNF- α -siRNA target inflammation and inhibit gene expression in the intestines. *Nat Mater*, 2010. 9: p. 923-928.
- Wood, K.M., Stone, G.M., and Peppas, N.A., Wheat germ agglutinin functionalized complexation hydrogels for oral insulin delivery. *Biomacromolecules*, 2008. 9: p. 1293-1298.
- Wu, G.Y. and Wu, C.H., Receptor-mediated in vitro gene transformation by a soluble DNA carrier system. *The Journal of Biological Chemistry*, 1987. 262: p. 4429-4432.
- Wu, Y., Ho, Y.-P., Mao, Y., Wang, X., Yu, B., Leong, K.W., and Lee, L.J., Uptake and intracellular fate of multifunctional nanoparticles: A comparison between lipoplexes and polyplexes via quantum dot mediated Förster resonance energy transfer. *Mol. Pharm.*, 2011. 8(5): p. 1662-1668.
- Wurster, D.E. and Lindlof, J.A., Apparatus for the encapsulation of discrete particles. 1965, Wisconsin Alumni Research Foundation: United States. p. 5.
- Xiao, B. and Merlin, D., Oral colon-specific therapeutic approaches toward treatment of inflammatory bowel disease. *Expert Opin Drug Deliv*, 2012. 9: p. 1393-1407.
- Xiao, L., Isner, A.B., Hilt, J.Z., and Bhattacharyya, D., Temperature responsive hydrogel with reactive nanoparticles. *J Appl Polym Sci*, 2013. 128(3): p. 1804-1814.

- Xu, J., Ganesh, S., and Amiji, M., Non-condensing polymeric nanoparticles for targeted gene and siRNA delivery. *Int J Pharm*, 2012. 427(1): p. 21-34.
- Xu, J., Ye, J., and Liu, S., Synthesis of well-defined cyclic poly(n-isopropylacrylamide) via click chemistry and its unique thermal phase transition behavior. *Macromolecules*, 2007. 40: p. 9103-9110.
- Xu, Q., Huang, W., Jiang, L., Lei, Z., Li, X., and Deng, H., Kgm and pmaa based ph-sensitive interpenetrating polymer network hydrogel for controlled drug release. *Carbohydrate Polymers*, 2013. 97(2): p. 565-570.
- Yamagata, T., Morishita, M., Kavimandan, N.J., Nakamura, K., Fukuoka, Y., Takayama, K., and Peppas, N.A., Characterization of insulin protection properties of complexation hydrogels in gastric and intestinal enzyme fluids. *J Controlled Release*, 2006. 112(3): p. 343-349.
- Yanes, O., Villanueva, J., Querol, E., and Aviles, F., Enzymatic measurements for the detection of trypsin and carboxypeptidase a inhibitory activity. 2007.
- Yang, J., Chen, J., Pan, D., Wan, Y., and Wang, Z., Ph-sensitive interpenetrating network hydrogels based on chitosan derivatives and alginate for oral drug delivery. *Carbohydrate Polymers*, 2013. 92(1): p. 719-725.
- Yang, Y. and Urban, M.W., Self-healing polymeric materials. *Chem Soc Rev*, 2013. 42(17): p. 7446.
- Yezhelyev, M.V., Qi, L., O'Regan, R.M., Nie, S., and Gao, X., Proton-sponge coated quantum dots for siRNA delivery. *J. Am. Chem. Soc.*, 2008. 130: p. 9006-9012.
- Yigit, C., Welsch, N., Ballauff, M., and Dzubiella, J., Protein sorption to charged microgels: Characterizing binding isotherms and driving forces. *Langmuir*, 2012. 28(40): p. 14373-14385.
- Yuan, F., Thiele, G.M., and Wang, D., Nanomedicine development for autoimmune diseases. *Drug Dev Res*, 2011. 72(8): p. 703-716.

- Zelphati, O. and Francis C. Szoka, J., Mechanism of oligonucleotide release from cationic liposomes. *P Natl Acad Sci USA*, 1996. 93: p. 11493-11498.
- Zhang, B., Zhang, Y., Mallapragada, S.K., and Clapp, A.R., Sensing polymer/DNA polyplex dissociation using quantum dot fluorophores. *ACS Nano*, 2011. 5: p. 129-138.
- Zhang, J., He, C., Tang, C., and Yin, C., TeRNArY polymeric nanoparticles for oral siRNA delivery. *Pharm Res*, 2013. 30(5): p. 1228-1239.
- Zhang, S., Zhao, B., Jiang, H., Wang, B., and Ma, B., Cationic lipids and polymers mediated vectors for delivery of siRNA. *J Controlled Release*, 2007. 123(1): p. 1-10.
- Zhao, X., Yin, L., Ding, J., Tang, C., Gu, S., Yin, C., and Mao, Y., Thiolated trimethyl chitosan nanocomplexes as gene carriers with high in vitro and in vivo transfection efficiency. *J Controlled Release*, 2010. 144(1): p. 46-54.
- Zhu, X., Lu, P., Chen, W., and Dong, J., Studies of uv crosslinked poly(n-vinylpyrrolidone) hydrogels by ftir, raman and solid-state nmr spectroscopies. *Polym*, 2010. 51(14): p. 3054-3063.

Vita

Jennifer M. Knipe, originally from Martinsburg, WV, received her B.S. as an Honors scholar in chemical engineering from West Virginia University in May 2010. As an undergraduate researcher at WVU, she worked under Dr. David Klinke in collaboration with Dr. Christopher Cuff to identify and model the differentiation program of dendritic cells. During her senior year, she also worked as a project management intern in the Project Management Center at the U.S. Department of Energy National Energy and Technology Laboratory. After graduating from WVU, Jennifer joined the McKetta Department of Chemical Engineering at The University of Texas at Austin as a National Science Foundation Graduate Research Fellow. During her tenure at UT-Austin, she was also a recipient of the P.E.O. Scholar Award. Jennifer completed her Ph.D. research under the direction of Dr. Nicholas Peppas.

Permanent address: jennifer.knipe@utexas.edu

This dissertation was typed by the author.